Dissertation zur Erlangung des Doktorgrades

der Fakultät für Chemie und Pharmazie

an der Ludwig-Maximilians-Universität München

InterAKTion with FKBPs

Modulation of the Akt/mTOR pathway by FKBPs

Anne-Katrin Fabian

aus Stendal, Deutschland

2013

Erklärung

Diese Dissertation wurde im Sinne von § 7 der Promotionsordnung vom 28. November 2011 von Herrn Prof. Dr. Christoph W. Turck betreut und von Herrn Prof. Dr. Christoph W. Turck vor der Fakultät für Chemie und Pharmazie vertreten.

Eidesstattliche Versicherung

Diese Dissertation wurde eigenständig und ohne unerlaubte Hilfe erarbeitet.

München, den 12.04.2013

………………………………………….

Anne-Katrin Fabian

Dissertation eingereicht am 12.04.2013

1. Gutachter: Prof. Dr. C. W. Turck
2. Gutachter: Prof. Dr. R. Beckmann

Mündliche Prüfung am 25.07.2013

This work was performed at the Max Planck Institute of Psychiatry in the research group "Chemical Genomics" under the supervision of Dr. Felix Hausch

Publications

Parts of this work are published or submitted for publication:

Fabian, A.-K., März, A. M., Neimanis, S., Biondi, R., Kozany, C., Hausch, F., *InterAKTions with FKBPs - Mutational and Pharmacological Exploration*. PLoS One, 2013. **8**(2): p. e57508

März, A. M., **Fabian, A.-K.**, Kozany, C., Bracher, A., Hausch, F., *Large FK506-binding Proteins shape the Pharmacology of Rapamycin.* Mol Cell Biol, 2013. **33**(7): p. 1357-67

Wang, Y., Kirschner, A., **Fabian, A.-K.**, Gopalakrishnan, R., Kress, C., Hoogeland, B., Koch, U., Kozany, C., Bracher, A., Hausch, F., *Increasing Ligand Efficiency by Conformational Control*. 2013, manuscript in review

General publications:

Fabian, A.-K., *INR-Werte selbst bestimmen – Messgeräte zur Blutgerinnungskontrolle*, PZ Prisma, 2010. (1): p. 49-57

Fabian, A.-K., *Die Rolle des Apothekers in der Antikoagulanzientherapie – Erfahrungen und Beispiele aus Deutschland und den USA*. PZ Prisma, 2009. (3): p. 159-166

Richter, U., **Fabian, A.-K.**, Rahfeld, B., Dräger, B., *Overexpression of tropinone reductase alters alkaloid composition in Atropa belladonna root cultures*. Journal of Experimental Botany, 2005. **56**(412): p. 645-652

Poster presentations

"Large FK506-binding proteins contribute to the pharmacology of rapamycin"
März, A. M., **Fabian, A.-K.**, Kozany, C., Bracher, A., Hausch, F.
Biochemical Society Focused Meeting - Talks about TORCs: Recent advances in target of rapamycin signaling, London, March 14th – 15th 2013

"Insights into Akt-FKBP Interactions"

Fabian, A.-K., Kozany, C., März, A. M., Hausch, F.

MPI summer symposium, Munich, July 25th 2012

Oral presentations

"Biochemical insights into InterAKTions of FKBPs"

MPI Institute seminar, February 2nd 2012

General Awards

Förderpreis Pharmazeutische Betreuung 2008

_____

Table of contents

Table of contents

Table of contents

_____

1. Introduction

1.1 FKBPs and their versatile biological functions

FK506-binding proteins (FKBPs) belong to the highly conserved group of immunophilins and display peptidyl-prolyl-cis-trans isomerase (PPIase) activity [1, 2]. After discovery of cyclophilins in the 1980s, which are named for their high affinity to Cyclosporine A [3, 4] another unrelated PPIase was found and named FKBP [1, 5]. Most peptide bonds in folded proteins are found in *trans* conformation, whereas 6% of all Xaa-Pro peptide bonds show a *cis* conformation [6]. FKBPs are involved in the energetically hindered isomerization of these Xaa-Pro peptide bonds in order to fold proteins. Binding of a peptide substrate in the hydrophobic pocket of FKBP and stabilization of the transition state by hydrogen bonds accelerates the isomerization process [6]. Independent of their PPIase function some FKBPs act as chaperones where they recognize non-native proteins, prevent unwanted inter- and intramolecular interactions and influence the partitioning between unproductive and productive folding steps [7]. In addition to their role in protein maturation, the diverse members of the FKBP protein family bind tightly to the natural compounds FK506 and rapamycin. In complex with FKBPs FK506 induces an inhibitory ternary complex with the Ca^{2+} - and calmodulin-dependent protein phosphatase calcineurin [8, 9]. Complex formation leads to inhibition of dephosphorylation of the transcription factor NF-AT, which normally induces IL-2 expression and thereby promotes T-cell activation [10]. Contrary, the complex formed by FKBP12 and rapamycin inhibits the mechanistic target of rapamycin (mTOR), a protein kinase that regulates growth and cell cycle progression [11-13]. Therefore both natural compounds are used as immunosuppressants.

Recently it was shown that other FKBPs can substitute the effects of FKBP12 [14]. Since immunophilin ligands have been shown to have neuroprotective activities [15, 16] FKBPs were proposed as likely targets for mediating this neurotrophic activity, although there is disagreement as to their specific mechanism [17-20].

FKBPs are named according to their molecular mass, which range from 12 to 135 kDa [21]. While FKBP12, as the archetype of the family only consists of one FK506 binding domain (FK1) [22], which harbors the described PPIase activity, others have additional domains, such as the TPR domain, which enables these FKBPs to interact with the co-chaperone Hsp90 [23, 24]. The overall structure of FK domains consists of an antiparallel five-stranded β-sheet wrapped around a central α-helix [22, 25]. FKBP13 contains an additional C terminal ER recognition sequence [26, 27]. The TPR domain of the higher molecular weight FKBPs is

a helical structure consisting of three units of 34 aa. A single TPR unit consists of two consecutive α-helices of 12-15 residues each crossing to an angle of approximately 20°. An additional seventh helix that extends beyond the final TPR motif contains a putative calmodulin-binding site in FKBP38, FKBP51 and FKBP52 [24, 28, 29].
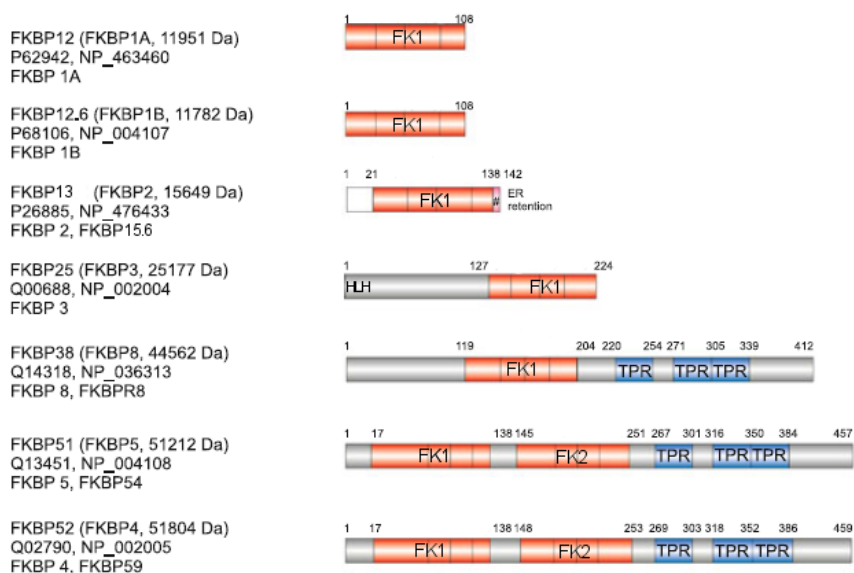
Figure 1.1: Domain structure of important human FKBPs
Gene names and the size of the unprocessed proteins are shown in brackets. In the second row, the accession numbers of UniProtKB/Swiss-Prot database and NCBI Reference Sequence are given. The third row shows alternative protein names. FK1=FK506 binding domain FK1, FK2=FK506 binding domain 2, TPR=Tetratricopeptide domain, HLH=Helix-Loop-Helix domain, modified after Schiene-Fischer [21]

In the following sections the FKBPs, used throughout this thesis will be further characterized.

1.1.1 FKBP12 and FKBP12.6 – small, but important

FKBP12 is ubiquitous expressed in almost all human tissues [30]. Human FKBP12 was shown to bind rapamycin with a Kd of 0.2 nM [31] and FK506 with a Kd of 0.4 nM by forming a ternary complex with TOR or calcineurin [8, 32]. It was further identified as accessory protein of the skeletal muscle ryanodine receptor 1 (RyR1) calcium release channel and the inositol-1,4,5-triphosphate receptor (IP$_3$R) suggesting a biological significance as regulator of Ca^{2+} signaling [33-35]. Also the receptor serine/threonine protein kinase TGF-β receptor 1 [36] and the epidermal growth factor receptor (EGFR) form an FKBP12 target since FKBP12 was shown to inhibit EGFR auto-phosphorylation [37].

The deposition of the microtubule-associated tau proteins into neurofibrillary tangles and impaired processing of the Amyloid Precursor Protein (APP) to β-amyloid (Aβ) are hallmarks of Alzheimer's disease. FKBP12 was found to associate with the tau [38] and the intracellular

_____

domain of APP [39]. In a mouse model which brain specific lacks FKBP12 mTOR signaling was enhanced and this was connected to enhanced long-term potentiation (LTP) and long term memory formation (LTM) [40]. In contrast Aβ1-42 induced inhibition of mTOR signaling and LTP was prevented in FKBP12 knockout mice supporting an involvement of FKBP12 in the pathology of alzheimer's disease [41]. Recently it was shown in a cellular assay that of all FKBPs abundant in the brain FKBP12 was the most prominent in accelerating α-synuclein fibril formation as a common feature in Parkinson's disease [42].

FKBP12.6 shares 85% sequence identity with FKBP12 and it is similar effective to enable FK506-dependent inhibition of calcineurin *in vitro* as FKBP12 [29, 43]. However, in contrast to FKBP12 FKBP12.6 was shown to regulate ryanodine receptor 2 (RyR2) function in the heart whereas FKBP12 is involved in regulating cardiac voltage-gated sodium channels [44].

1.1.2 FKBP51, FKBP52 – opposite effects

FKBP51 was initially isolated from murine T cells [45] and murine adipocytes [46], where it is involved in adipocyte differentiation. In general it is expressed in many human tissues some-times even in molar excess compared to FKBP12 [30]. FKBP51 is a multidomain protein with two FK506 binding domains (FKBD) of which only the FK1 domain shows PPIase activity and binding affinity to immunosuppressants [28].

One of the best-characterized properties of FKBP51 is its function as a co-chaperone of Hsp90/Hsp70 mediated by the TPR domain of FKBP51 [23, 47]. FKBP51 is a negative regu-lator of hormone binding affinity of the glucocorticoid receptor. The first indications pointing in this direction came from studies in new world primates, including squirrel monkeys which show markedly elevated FKBP51 levels of a highly potent isoform leading to reduced hor-mone binding affinity [48-50]. As a compensation these species are marked by high levels of circulating cortisol [51, 52]. Although less potent than squirrel monkey FKBP51, human FKBP51 can also modify steroid receptor activity [48, 53]. In intact cells, FKBP51 was shown to slow down the nuclear translocation of the GR, possibly by blocking FKBP52-mediated recruitment to the dynactin motor complex [54]. Mechanistically it seems that the Hsp90-binding but not PPIase activity of FKBP51 is necessary for its inhibitory effect on glucocorti-coid receptor binding affinity [55]. The expression of FKBP51 is strongly increased by corti-costeroids [56] indicating that FKBP51 attenuates cortisol responses in hormone-conditioned tissues as part of a negative feedback mechanism [53, 57]. This seems to be particularly important in the regulation of the HPA (hypothalamic-pituitary-adrenal) axis, one of the main regulators of stress response. Deregulation of the HPA axis caused by reduced glucocorti-coid receptor sensitivity was found to be common in depressed patients leading to the corti-

_____

costeroid receptor hypothesis of depression [58]. Indeed, polymorphisms within the FKBP51 encoding gene *FKBP5* were found to be associated with increased recurrence of depressive episodes and improved patient's response to antidepressive treatment [59-61]. Several research groups have shown a protective effect of FKBP51 knockout or knockdown on stress endocrinology and stress-coping behavior [62-64]. Taken together the results of these studies implicate an important role of FKBP51 in HPA axis deregulation and suggest that drug targeting of this protein might be beneficial for treatment of patients suffering from depression and anxiety disorders.

Beside their regulating role in steroid hormone receptor signaling a novel role for Hsp90 and associated co-chaperones in folding and aggregation disorders has emerged. FKBP51 was found to stabilize tau. *In vitro* FKBP51 stabilizes microtubules with tau in a reaction depending on the PPIase activity of FKBP51 which was shown with a PPIase deficient mutant (F130A) [65].

The emerging role of FKBP51 in cancer is increasingly being recognized, both as a biomarker for tumor progression and as a possible target for cancer therapy. Initially FKBP51 was found to be overexpressed in idiopathic myelofibrosis (IMF) megakaryocytes where it prevented apoptosis of malignant cells possibly by a NF-κB driven mechanism [66]. By mapping the protein interaction network of the TNF-α/NF-κB pathway it was later demonstrated that FKBP51 co-purifies with IKKα, IKKε, TGF-β activated kinase (TAK1) and mitogen activated protein kinase kinase (MEKK1) pointing to an essential role for FKBP51 in the overall signaling process of NF-κB activation [67]. Several studies shared evidence for pro-apoptotic or apoptotic effects of the prototypic FKBP ligand rapamycin through regulation of signal transduction of the of NF-κB pathway [68-70]. FKBP51 down-modulation was shown to sensitize melanoma cells to apoptosis caused by ionizing radiation, again revealing FKBP51 to counteract apoptotic processes [71]. It should be especially noted that FKBP51 is overexpressed in several prostate cancer cell lines and tissues where it promotes androgen receptor activity [72-74]. In contrast to the elevated FKBP51 levels in the above studies, Pei *et al.* [75] found FKBP51 protein levels to be decreased in pancreatic cancer samples. Furthermore, FKBP51 was shown to act as a scaffold protein for the phosphatase PHLPP, thereby negatively regulating the kinase Akt [75]. In a pancreatic cancer xenograft model the positive correlation between the expression of FKBP51 and the response to chemotherapeutics was confirmed *in vivo* [76]. However, diverging results have been reported from several other tumor tissues [77]. Nevertheless, the enhancement of the PHLPP-mediated Akt dephosphorylation, e.g. via FKBP51, could be an option to sensitize susceptible cancer cells to chemotherapy.

_____

FKBP52 shares 55 % identity (alignment by PRALINE (see section 3.13) with FKBP51 and was originally characterized in 1992 as a protein with three clearly distinguishable domains that are arranged like in FKBP51 [78-80]. Again, one active PPIase pocket located within the FK1 domain and a TPR domain is present. The TPR domain enables FKBP52 to interact with Hsp90. In contrast to FKBP51 FKBP52 is a positive regulator of the glucocorticoid receptor [81], progesterone receptor [82] and androgen receptor [83], but not the estrogen receptor or mineralocorticoid receptor [81]. The specific ability of FKBP52 to promote steroid hormone receptor activity is dependent on a region called proline rich loop overhanging the PPIase pocket but independent of PPIase activity [84]. Biochemically FKBP52 was shown to replace FKBP51 in the Hsp90/GR complex after hormone-binding, indicating a preference for FKBP52 for activated steroid hormone receptors [85-87]. Furthermore, FKBP52 but not FKBP51 binds via its PPIase domain to the motor protein dynein that is connected to microtubule and accelerates the translocation of activate steroid hormone receptors from the cytoplasm to the nucleus [88, 89]. The switch of bound FKBP51 with FKBP52 seems to be a crucial step during receptor activation [85].

The current model of steroid receptor translocation is depicted in Figure 1.2 (modified after [90] by Y. Wang, MPI of Psychiatry).
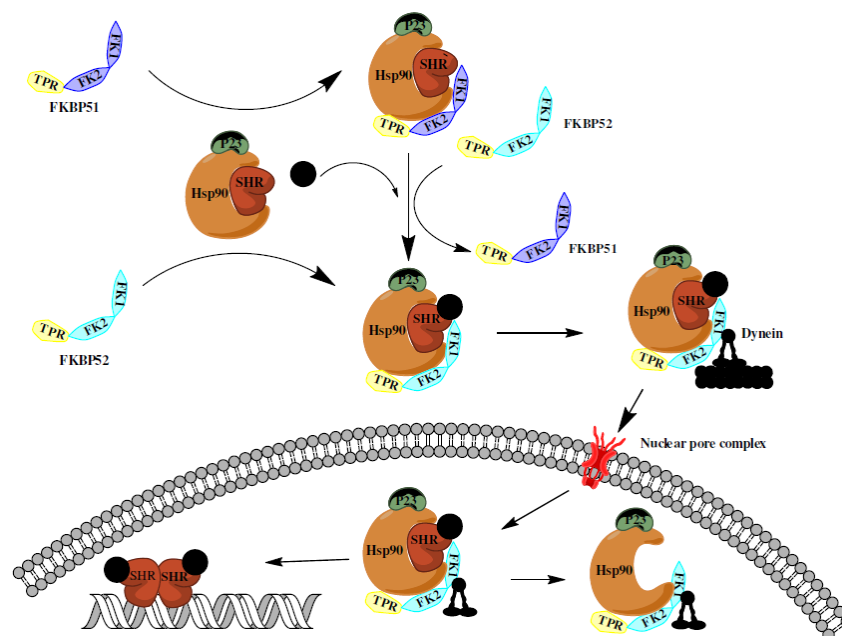
Figure 1.2: Current model of steroid hormone receptor translocation
FKBP51 enters the Hsp90-dimer-steroid-hormone receptor complex (SHR) by binding to the C-terminus of Hsp90 via its TPR domain. The complex is stabilized by the p23 cochaperone, bringing the FKBP FK1 domain into contact with the receptor ligand binding domain to directly influence hormone binding affinity. Upon steroid binding, the SHR heterocomplex exchanges FKBP51 for FKBP52, which is able to interact with dynein. The whole SHR–chaperone complex translocates through the nuclear pore complex followed by receptor transformation, binding of the steroid-activated receptor to hormone response elements and gene transcription regulation.

The physiological importance of FKBP52 on steroid receptor function is highlighted in *FKBP4* knockout mice. Male *FKBP4* knockout mice display several developmental defects in reproductive tissue consistent with androgen resistance [83, 91]. Female *FKBP4* knockout mice are infertile due to failure of embryo implantation in the uterus caused by progesterone resistance [82, 92, 93]. Furthermore these mice suffer from increased cell proliferation, inflammation and angiogenesis leading to endometriotic lesions, consistent with the finding that woman suffering from endometriosis show reduced FKBP52 expression [94]. Finally, a state of glucocorticoid resistance was observed in mice heterozygous for FKBP52 ablation after four weeks of high fat diet combined with a higher susceptibility to hyperglycemia and hyperinsulinemia [95].

Using RNAi to investigate possible causes of tau-induced neurodegeneration Kraemer *et al.* [96] found *FKBP4* RNAi to worsen the phenotype in a *Caenorhabditis elegans* model of human tauopathies [96]. Indeed FKBP52 seems to have opposing effects to FKBP51: Microtubule assembly formation of purified rat brain tubulin caused by addition of human recombinant tau was prevented in the presence of purified recombinant FKBP52, indicating an "anti-tau" activity of FKBP52 *in vitro* [97]. Moreover, FKBP52 expression levels were found to be abnormally low in post mortem analyzed frontal cortex of Alzheimer's disease patients as compared to controls [98] and FKBP52 prevented tau-accumulation in cellular models [97]. Currently it is not known wheather the FKBP52 induced neuroprotection against tauopathies is linked to degradation processes of modified tau proteins or changes in tau accumulation and to which extend Hsp90 is involved [99]. Nevertheless, activating FKBP52 or inhibiting FKBP51 may be novel therapeutic strategies for tauopathies in the future.

Another aspect should be mentioned: Gold *et al.* proposed FKBP inhibitors to promote neurite outgrowth in an FKBP52/Hsp90 dependent mode of action [100]. Indeed, the balance between FKBP51 and FKBP52 seems to play a key role during the early mechanism of neuronal differentiation [101].

1.1.3 FKBP25 – the mysterious

FKBP25 has an FK1 binding domain in common with other FKBPs but it differs in its ligand binding characteristics: The FK1 domain shows PPIase activity which is preferentially blocked by rapamycin with a Kd of 0.9 nM compared to the inhibitory effect of FK506 with a Kd of 160 nM [102, 103]. Investigations by Liang *et al.* suggested structurally differences in the 50S loop region, flexibility of the 40S loop insertion and a substitution of one residue in the hydrophobic ligand-binding pocket as possible cause for rapamycin selectivity [104].

Furthermore FKBP25 possesses a strongly hydrophilic N-terminal domain with no recognizable homology to any known protein [102, 105]. This domain embodies a helix-loop-helix (HLH) motif. An exclusive feature in FKBP25 is its nuclear translocation sequence consisting of four lysines [103]. Indeed FKBP25 is abundant in the nucleus [106], where it was found to be phosphorylated by serine/threonine kinase casein kinase II. The tight interaction with casein kinase II implied that FKBP25 might play a role in ribosome biogenesis and cell replication [107]. Furthermore FKBP25 was demonstrated to bind to the N-terminus of histone deacetylases (HDAC1 and HDAC2) and to the transcription factor YY1 modifying its binding capability [108]. In extracts from porcine brains analyzed with native 2D electrophoresis followed by MALDI-TOF FKBP25 was associated with the high-mobility group (HMG) protein II, which is also crucial for transcription of some genes and the GTP binding protein Rab 5. The latter interaction depends on FKBP25 phosphorylation [109]. It was demonstrated that FKBP25 is negatively regulated by the tumor suppressor protein p53 [110]. In turn FKBP25 seems to induce p53 activation and proteasome dependent down-regulation of p53's counterpart MDM2 [111]. Weather the PPIase domain is necessary for the above mentioned protein-protein interactions has not been investigated so far.

1.2 FKBP ligands

1.2.1 Immunosuppressive immunophilin ligands

The natural occurring prototypic ligands of immunophilins are the clinically used immunosuppressants cyclosporine A (CsA), FK506 and rapamycin (Figure 1.3).

Interestingly and most remarkably all three compounds impart a gain-of-function on their immunophilin partners but they affect different signaling pathways in T-lymphocytes.
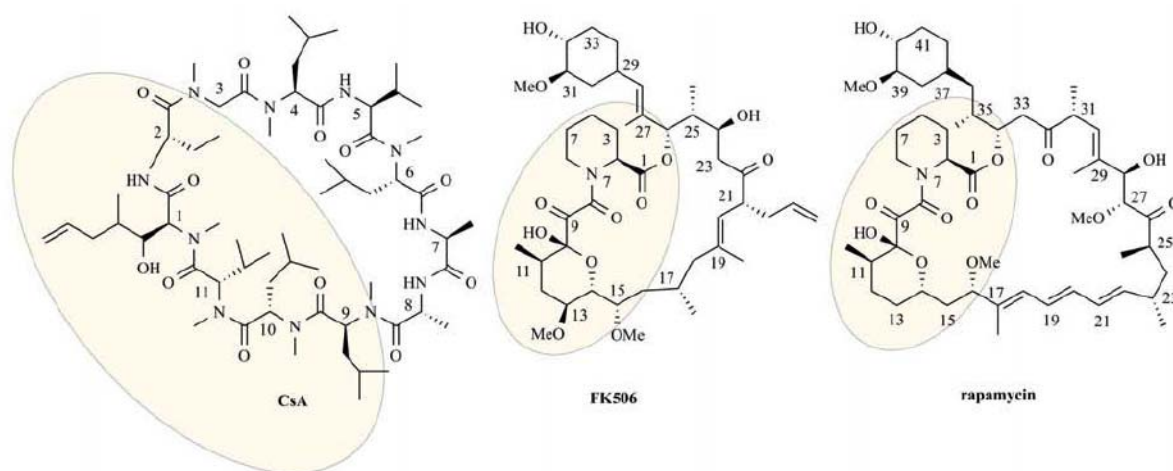
Figure 1.3: Immunosuppressive immunophilins [112]
Highlighted are the immunophilin-binding domains (Cyp for CsA, FKBP for FK506 and rapamycin); Aminoacids 3-7 of CsA, atoms 19-22 and 27-33 of FK506: calcineurin binding domain; Atoms 15-27 and 34-46 of rapamycin: mTOR binding domain

Cyclosporine A as the first immunophilin ligand to be discovered binds to the class of cyclophilins (Cyp). A ternary complex is formed with the phosphatase calcineurin (CN) [8]. In this heterocomplex calcineurin is unable to dephosphorylate its substrate nuclear factor of activated T-cells (NF-AT) which is necessary for T-cell activation and IL-2 expression [113]. In 1983 Cyclosporine A was FDA approved as trade brand Sandimmune® being first drug used to prevent allograft rejections in humans. It was further shown to to be effective in a variety of human autoimmune diseases, including psoriasis, nephrotic syndrome, type I diabetes, and sight-threatening uveitis [114].

FK506 (also: Tacrolimus) was first isolated from *Streptomyces tsucubaensis* and its target, the FKBP protein family was termed thereafter. Just as Cyp-CsA the FKBP-FK506 complex binds to and allosterically inhibits calcineurin leading to the same immunosuppressive effect as described before [113]. The immunosuppressive action of FK506 is mainly thought to be mediated by FKBP12 and partially by FKBP12.6 and FKBP51 [115, 116]. FK506 was FDA

approved as medication after organ transplantation to prevent allograft rejections as Pro-graf® in 1994. Additionally FK506 is used for treatment of various inflammatory diseases, such as contact eczema, hand dermatitis and psoriasis [117].

Rapamycin (also: Sirolimus) was isolated from *Streptomyces hygroscopicus* in the 1970s and was named after the location where this strain was isolated, the Easter Island (Rapa Nui) [118-120]. First, its fungicidal activity was discovered [121] later rapamycin was shown to be effective against transplanted tumors [122] and to have immunosuppressive action [123]. In organ transplantation experiments with animals it was demonstrated that rapamycin reduces allograft rejections [124]. In 1999 rapamycin was approved as Rapamune® for this indication. Furthermore the compounds anti-inflammatory and anti-proliferative effects are used in eluting stents to prevent restenosis in patients suffering from vascular obliterations [125].

Mechanistically rapamycin was thought to bind exclusively to FKBP12. The rapamy-cin/FKBP12 heterocomplex inhibits the serine/threonine protein kinase mTOR (mechanistic target of rapamycin) and allosteric inhibition of the latter results in a blockade of various downstream signaling pathways involved in the control of translation of proteins crucial for cell cycle progression [126, 127]. Thus the alteration of mTOR signaling by rapamycin has commanded great interest in the oncologic field [128, 129].

1.2.2 Unspecific non-immunosuppressive immunophilin ligands

Chronic rapamycin treatment was shown to enhance life span from yeast to mice [130-134]. In addition it might also improve the quality of life in the elderly as it was shown to improve the cognitive and behavioral deficits in several animal models of neurodegenerative diseases such as Alzheimer's, Parkinson's and Huntington's disease [135-139]. Another interesting observation was that FK506, rapamycin and CsA have additionally neuroprotective and neu-rotrophic effects [16]. However, the chronic use of these agents for diverse indications is lim-ited by the suppression of immune response, being an inacceptable side effect. Therefore especially the finding that the neuroprotective and neurotrophic effects were partially inde-pendent of calcineurin or mTOR inhibition, lead to tremendous efforts to identify immunophil-in ligands without immunosuppressive properties [112]. Compounds of this type used for ex-periments throughout this thesis are introduced below:

Antascomicin B was first isolated from a *Micromonospora* strain, which originated from a soil sample from china. Its ability to bind FKBP12 is in the same range as that of FK506 or rapamycin [140]. In 2005 Brittain *et al.* presented the total synthesis of Antascomicin B [141].

FK1706 is a semi-synthetic derivative of FK506, where the effector domain required for cal-cineurin binding was abolished. The compound shows significant neurotrophic effects, which

were shown to be putatively assigned to be mediated by FKBP52 and the Ras/Raf/mitogen-activated protein kinase signaling pathway, suggesting the potential of this compound to be used to treat a variety of neurological disorders [142]. A small phase I clinical trial didn't give any hints for drug induced discontinuations within the two-week time period. Thus the compound seems to be tolerated for an extended time period in humans [143].

The compounds of the YW serie were synthesized by Y. Wang at the MPI of Psychiatry [144]. The small molecule compounds were designed to improve the pharmacokinetic profile.
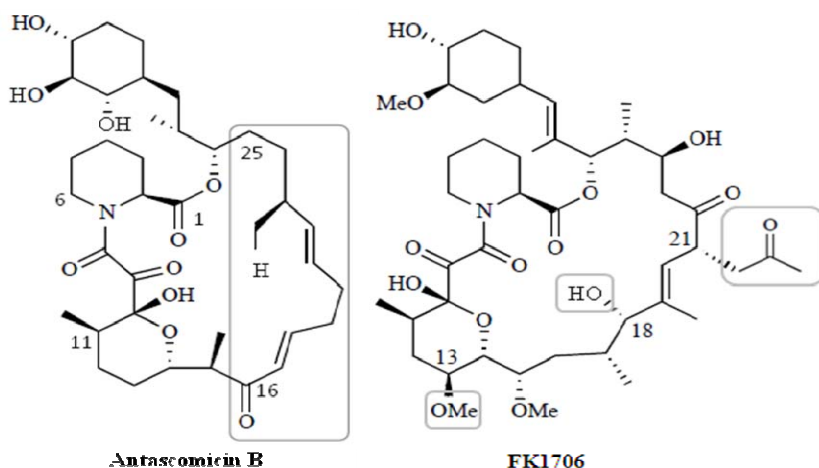
Figure 1.4: Examples of unselective non-immunosuppressive immunophilins [112]
Antascomicin B and FK1706 derived from natural products. Highlighted are modifications compared to rapamycin and FK506

1.2.3 Selective non-immunosuppressive immunophilin ligands

Due to strong off-target effects and lack of selectivity there is a high demand not only for non-immunosuppressive but also for selective inhibitors for FKBPs, which can be used to investigate the roles of individual FKBPs in mammalian systems and finally for development of medications targeting an FKBP subgroup in a certain tissue.

1.2.3.1 FKBP12-selective immunophilin ligands

Biricodar is a synthetic FKBP ligand still based on the dicarbonyl pipecolyl-scaffold derived from rapamycin and FK506. Biricodar binds to FKBP12 almost as tightly as to FK506 and FK1706 but discriminates more strongly against the larger FKBP51 and FKBP52 (> 500 fold selectivity for FKBP12) [145]. The compound also binds to p-glycoprotein (MDR1) [146] and has been investigated in several clinical trials as a chemo-sensitizing adjuvant, where it seemed to be well tolerated even with steady-state serum levels up to 10 μM [147].

Compound 44 (cmpd44)/GR591 was synthesized by R. Gopalakrishnan at the MPI of Psychiatry. The compound structurally differs from Biricodar by having a pipecolate sulfonamide moiety. Compound 44 is highly selective for FKBP12 as it binds to FKBP12 with an IC_{50} of 3 nM but to FKBP51 and FKBP52 with an IC_{50} of 2 µM and 3.1 µM, respectively [148].
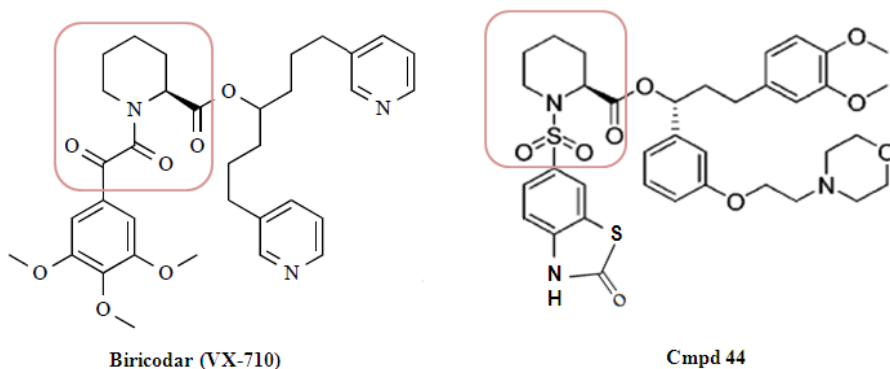
Figure 1.5: Examples of non-immunosuppressive immunophilins selective for FKBP12 [112, 148]
Biricodar and compound 44 are synthetic FKBP ligands. The conserved pipecolyl moiety is shaded.

1.2.3.2 FKBP51-selective immunophilin ligands

Based on the corticosteroid receptor hypothesis of depression [58] as introduced in section 1.1.2 our research group aimed to identify selective inhibitors for FKBP51. These compounds could be able to displace FKBP51 from the Hsp90/glucocorticoid-receptor-complex and thereby might restore physiologic glucocorticoid sensitivity leading to a reduction of circulating cortisol.

The compound **SG537**, synthesized by S. Gaali at the MPI of Psychiatry has a >10 000 fold selectivity for FKBP51 compared to FKBP52, the antagonist of FKBP51 in steroid receptor signaling [149].

1.3   The serine/threonine kinase Akt

Akt (also called PKB) was first described as the cellular homolog of the product of the *v-akt* oncogene [150]. In 1991 evidence was growing that this *act* gene codes for a ser-ine/threonine kinase [151-153] and classifies as a member of the AGC kinase superfamily, which share a highly conserved catalytic domain. Besides the three highly homologous Akt isoforms Akt1/PKBα, Akt2/PKBβ and Akt3/PKB this class includes among others the p70 ribosomal S6 kinase (S6K) , the serum- and glucocorticoid-inducible kinase (SGK), the Pro-tein kinase C related kinase (PRK) and finally the protein kinases A, G and C, where the name of the class derived from [154].

Although the three isoforms show broad tissue distribution [155], Akt1 is the most ubiquitous-ly expressed. Akt2 is expressed at a lower level than Akt1 except in insulin-responsive tis-sues where it predominates [156, 157] and Akt3 expression is the lowest, except in testes and brain [158, 159].

1.3.1   Structure of Akt and its regulation

Each Akt isoform is characterized by an N-terminal pleckstrin homology (PH) domain, an kinase lobe and a carboxy-terminal lobe, which also includes the hydrophobic motif (HM). This motif is characteristic for most AGC kinase family members [160].

Akt is a major kinase downstream of phosphoinositol-3-kinase (PI3K). Upon activation of receptor tyrosine kinases by ligands such as growth factors or insulin, auto-phosphorylation of tyrosine residues on the intracellular portion of the receptor leads to recruitment of PI3K. PI3K converts phophatidylinositol-4,5-bisphosphate (PIP2) to phophatidylinositol-3,4,5-triphosphate (PIP3), thereby affecting the structure of Akt and recruiting it via its PH domain from the cytosol to the plasma membrane [161]. Here, PDK1 phosphorylates the activation loop (T308) and thereby activates Akt [162]. In addition, phosphorylation of the hydrophobic motif (HM) at S473 by mTORC2 (mechanistic target of rapamycin complex 2) [163] is a cru-cial step for maximal activation [164]. mTORC2 comprises six different proteins, several of which are common to mTORC1 as well (section 1.4): mTOR; rapamycin insensitive compan-ion of mTOR (rictor); mammalian stress-activated protein kinase interacting protein (mSIN1); protein observed with Rictor-1 (Protor-1, also known as PRR5); mammalian lethal with Sec13 protein 8 (mLST8, also known as GβL) and DEP-domain-containing mTOR-interacting protein (DEPTOR) [165]. Constitutive Phosphorylation on T450 occurs during translation and is required for Akt integrity [166].

Figure 1.6 shows the structure and important features of Akt.

A

inactive   active

B


```
  1  MNEVSVIKEG WLHKRGEYIK TWRPRYFLLK SDGSFIGYKE RPEAPDQTLP
 51  PLNNFSVAEC QLMKTERPRP NTFVIRCLQW TTVIERTFHV DSPDEREEWM
101  RAIQMVANSL KQRAPGEDPM DYKCGSPSDS STTEEMEVAV SKARAKVTMN
151  DFDYLKLLGK GTFGKVILVR EKATGRYYAM KILRKEVIIA KDEVAHTVTE
201  SRVLQNTRHP FLTALKYAFQ THDRLCFVME YANGGELFFH LSRERVFTEE
251  RARFYGAEIV SALEYLHSRD VVYRDIKLEN IMLDKDGHIK IT DFG LCKEG
301  ISDGATMK T F CGTPEYLAPE VLEDNDYGRA VDWWGLGVVM YEMMCGRLPF
351  YNQDHERLFE LILMEEIRFP RTLSPEAKSL LAGLLKKDPK QRLGGGPSDA
401  KEVMEHRFFL SINWQDVVQK KLLPPFKPQV TSEVDTRYFD DEFTAQSITI
451  T PPDRYDSLG LLELDQRTHF PQF S YSAFRE EKDLLMSLFV SLILFSDFSS
501  LKSHSFSSNF ILLSFSSLKK
```

Figure 1.6: Structure of Akt/PKB

A 3D-structure of inactive (PDB code 1GZK) and active (PDB code 1O6K) recombinant Akt kinase domain ▨ . In activated Akt the αB- and αC helices of the N-lobe, together with the activation segment and the hydrophobic motif ▨ become ordered. Thereby catalytic residues become aligned leading to a conformational change in the DFG motif ▨ , which is involved in nucle-otide binding. **B** amino acid sequence of Akt2 (PH domain ▨ , kinase domain ▨ and hydrophobic motif ▨) and the structure of all three Akt isoforms. Highlighted are the DFG motif ▨ and important phosphorylation sites ▨ .

Akt is on one hand activated via phosphorylation but needs on the other hand tight regulation which is achieved by dephosphorylation. Protein phosphatase PP2A has been shown to dephosphorylate Akt at Thr308 [167, 168]. However, it should be noted that Akt, which is bound to the chaperone Hsp90 seems to be protected from dephosphorylation by PP2A

[169]. PHLPP (PH domain leucine-rich repeat protein phosphatase) is the phosphatase known to inactivate Akt (S473) [170]. Thereby PHLPP2 dephosphorylates Akt1 and Akt 3 whereas the highly homologues PHLPP1 dephosphorylates Akt2 and also Akt 3 [171].

1.3.2 Akt in health and disease

Akt constitutes an important node in diverse signaling cascades and plays an essential role in cell survival, growth, migration, proliferation, polarity, metabolism, cell cycle progression, muscle and cardiomyocyte contractility as well as angiogenesis [172].

1.3.2.1 Akt in protein synthesis, proliferation and cell survival

Over 100 substrates [173] are phosphorylated by activated Akt independent of the cellular localization. By phosphorylating the protein BAD [174], the transcription factor FOXO [175] and the pro-caspase-9 [176], Akt inhibits proapoptotic processes and promotes cell survival. Akt also activates NF-κB via regulating IκB kinase (IKK), thus results in transcription of pro-survival genes [177]. The same is achieved by Akt mediated activation of the E3 ubiquitin ligase MDM2, [178] which results in translocation of MDM2 to the nucleus where it degrades the tumor suppressor protein p53 thereby inhibiting its function.

Phosphorylation of the tumor suppressor proteins TSC2 [179] and PRAS40 [180] leads to their inhibition thereby activating mTORC1 signaling and promoting cell growth via promotion of ribosomal protein biosynthesis. By Akt-mediated phosphorylation of the cyclin-dependent kinase inhibitors p27^{Kip1} [181], Myt 1 [182] and several others cell cycle progression is accelerated. Deregulation of these tightly regulated processes can be observed in several cancers [183]. The Akt transforming mutation (E17K), which leads to a constitutive attachment of Akt to the cell membrane was identified in 8% of human breast, 6% of colorectal, and 2% of ovarian cancers [184].

The Akt signaling axis also actively engages with the migratory process in motile cells, including metastatic cancer cells. Thus Akt is involved in cell migration and invasion, epithelial-mesenchymal transition, and finally cancer metastasis [185]. Akt is involved in angiogenesis, which can further promote cancer development [186, 187].
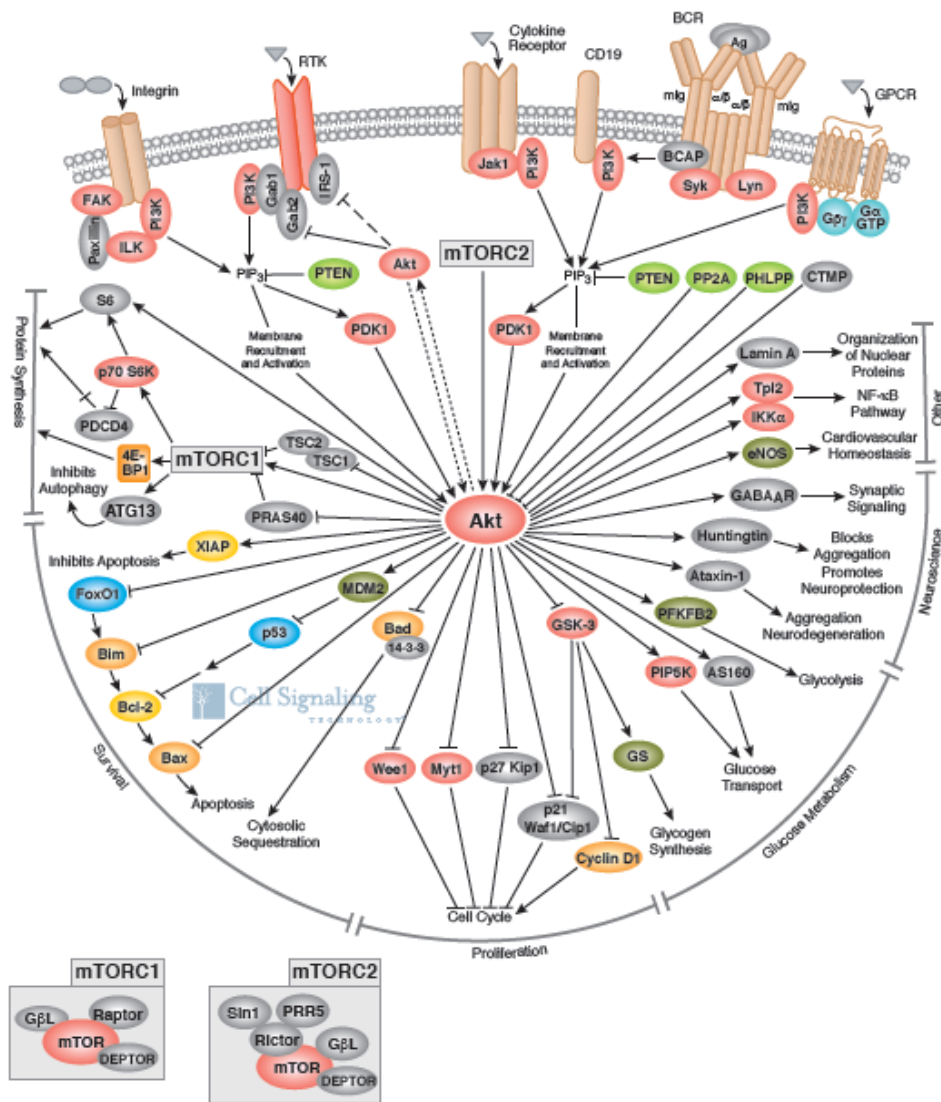
Figure 1.7: Upstream effectors and downstream targets of Akt (picture adapted from Cell Signaling Technology, Inc. (www.cellsignal.com)

1.3.2.2 Akt in metabolism

Insulin rapidly and persistently activates Akt leading to a manifold cell type specific influence on metabolism [188].

The first target of Akt, that was discovered was the constitutively active glycogen synthase 3 kinase (GSK-3), which is inhibited upon Akt phosphorylation [189, 190]. By inhibition of GSK-3β Akt increases the activity of the eukaryotic initiation factor 2B (eIF2B), a multimeric guanine-nucleotide exchange factor that facilitates the conversion of inactive eIF2-GDP to active eIF2-GTP, thus being a critical step for initiation of translation and thereby protein synthesis [191]. Akt mediated inhibition of GSK-3 leads to the activation of glycogen synthase [192], thereby promoting glycogen synthesis.

Besides effects mediated by GSK, Akt promotes increased cellular glucose metabolism by stimulating the localization of the glucose transporter Glut1 and Glu4 to the plasma membrane, thus facilitating increased glucose uptake [193, 194].

In addition, Akt increases glycolytic metabolism by stimulating the activity of hexokinase [195, 196] and phosphofructokinase [197], both rate-limiting enzymes of the glycolytic pathway.

An important pathway, which has impact on several metabolic processes, is the mTOR pathway, which will be focused on in section 1.4.

Finally, Akt activity is required for the antilipolytic action of insulin mediated by activation of phosphodiesterase-3B (PDE-3B) [198]. Mechanistically activation of PDE-3B leads to increased hydrolysis of cAMP, resulting in reduced activity of protein kinase A (PKA) and thereby depletion of hormone-sensitive lipase (HSL) and other target enzymes involved in lipolysis. In addition to this antilipolytic action, it was shown in a murine adipocyte cell line that insulin also seems to promote lipid storage by activation of lipogenesis via regulation of the lipogenic enzyme acetyl-CoA-carboxylase (ACC) by AMP activated protein kinase (AMPK) [199].

Akt's impact on metabolism is inextricably linked to its effects on cell growth and survival and Akt hyperactivation is believed to be associated with altered glucose metabolism observed in tumor cells. It was shown that proliferating cancer cells preferentially use aerobic glycolysis to support growth, a metabolic alteration called "Warburg effect" [200-202].

1.3.2.3 Akt in neurobiology

Akt controls different aspects of neuron function and neurodegeneration: First, it can regulate neurite outgrowth by several target proteins, such as GSK-3 and mTOR or NF-κB [203].

Second, the ligand-gated chloride ion channel γ-aminobutyric acid A (GABA$_A$) was identified as a direct Akt substrate *in vitro* and *in vivo*. The GABA$_A$ receptor mediates synaptic transmission at most inhibitory synapses in the mammalian brain. Akt mediated phosphorylation increases the number of GABA$_A$ receptors on the plasma membrane surface, which increases the efficacy of receptor mediated inhibition of GABAergic synapses [204].

Third, Akt was shown to directly or indirectly phosphorylate substrates involved in neurodegenerative diseases such as Huntington's disease [205], spinocerebellar ataxia type 1 (SCA1) [206], Alzheimer's disease [207] and schizophrenia [208, 209]. The phosphorylation of the protein huntingtin by Akt results in blockage of aggregation promoting neuroprotection. Most strikingly, an altered form of full length Akt was observed in patients suffering from Huntington's disease [205, 206]. In addition, Kaspar *et al.* found that stimulation of the Akt path-

way by insulin growth factor 1 (IGF-1) prolongs the lifespan in a mouse model for amyotrophic lateral sclerosis (ALS) [210].

Finally, Akt and GSK-3 have been associated with the action of psychiatric drugs. Specifically, the effects of lithium, valproate, olanzapine, clozapine but also haloperidol and fluoxetine are partially mediated by Akt and GSK-3 [211].

1.3.2.4 Severe limitations in mice lacking Akt

The importance of Akt signaling was demonstrated very clearly by knockout experiments in mice: **Akt2-/- mice** have a normal body mass, but display a profound diabetic phenotype including insulin resistance and hyperglycemia. This phenotype is accompanied by the loss of pancreatic β-cells [212, 213].

Akt1-/- mice experience defects in both fetal and postnatal growth, and these persisted into adulthood. Moreover, increased rates of apoptosis were observed. Generally these mice had increased neonatal mortality. However, in striking contrast to Akt2 null mice, Akt1 deficient mice are normal with regard to glucose tolerance and insulin-stimulated disposal of blood glucose [214, 215].

Akt3 knockout mice are characterized by impairment in brain development but are otherwise healthy [216].

Double knockout experiments indicated that some Akt isoforms are redundant; others seem to fulfill specific tasks. Particularly Akt1 seems be indispensable since it is exclusively involved in proliferation, differentiation, and early development [217].

1.4   Focus on PI3K/Akt/mTOR pathway

mTOR signaling mediated by mTORC1 is associated with cellular growth and proliferation in response to a variety of environmental cues, such as growth factors and nutrient availability (including aminoacids), as well as immune regulatory signals [218]. Of the numerous Akt targets reported, mTORC1 appears to be the master regulator of protein biosynthesis, which will be focused on in this section (Figure 1.8).
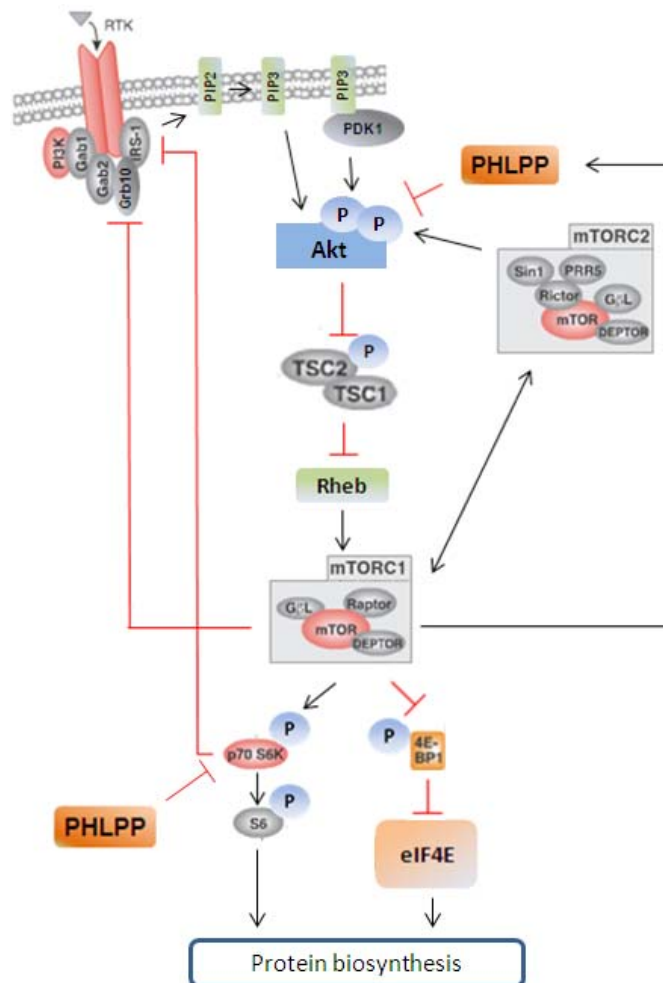
Figure 1.8: Simplified representation of the PI3K/Akt/mTOR signaling pathway with focus on the downstream signals S6K and 4E-BP1

Upon activation of the insulin receptor by hormone binding, Akt is phosphorylated as described in section 1.3.1. Akt kinase then directly phosphorylates the tumor suppressor proteins tuberous sclerosis protein 1 and 2 (TSC1/2) at several positions which lead to inhibition of TSC1/TSC2 [219, 220]. The proteins TSC1 (also known as Hamartin) and TSC2 (also known as Tuberin) form a functional complex in which TSC1 mainly fulfills stabilizing func-

tions whereas TSC2 acts as GTPase activating protein (GAP) for the small regulatory GTPase Rheb (Ras-homolog enriched in brain). TSC2 activates the intrinsic GTPase of Rheb and converts it to its inactive GDP bound state [221, 222]. The loss of the inhibitory effects of TSC protein leads to excessive cell growth and tumor formation, phenotypes that can be observed in the disease Tuberous Sclerosis [223]. Upon de-activation of TSC by phosphorylation of Akt, the active, GTP bound Rheb interacts with mTORC1 to promote signaling [224]. mTORC1 has four components (compare with mTORC2 – section 1.3.1): mTOR, which is the catalytic subunit of the complex; the regulatory associated protein of mTOR (Raptor); mLST8 (GβL) and DEPTOR [165]. Additionally, Akt activation by growth factors can activate mTORC1 in a TSC1/2-independent manner by promoting phosphorylation and thereby dissociation of the protein proline rich Akt substrate 40 kDa (PRAS40) from mTORC1 [180, 225, 226]. Physiologically, PRAS40 interacts with mTOR via Raptor and thereby competes with other substrates for binding to mTOR [227, 228].

Activated mTORC1 stimulates biosynthesis of ribosomes and translation of proteins via its substrates 4E-BP1 and S6Kinase.

The described processes entail significant energy consumption and the energy status of the cell is signaled to mTORC1 through AMP-activated protein kinase (AMPK), a master sensor of intracellular energy status [229]. By sensing energy depletion (low ATP:ADP) AMPK is activated and phosphorylates TSC2 thereby reducing mTORC1 activity via Rheb [230, 231]. Additionally, AMPK can reduce mTORC1 activity in response to energy depletion by direct phosphorylation of Raptor [232].

The active mTORC1 phosphorylates **4E-BP1** (PHAS-I) at its multiple phosphorylation sites resulting in its dissociation from eukaryotic initiation factor 4E (eIF4E), which in turn initiates cap-dependent translation [233]. For regulation via growth signals (especially insulin) four phosphorylation sites seem to be crucial (T37, T46, S65, T70) which are phosphorylated by mTORC1 in a strictly hierarchical manner: first the residues T37 and T46, creating the basis for phosphorylation of T70 [234] and finally S65 [235] resulting in total loss of eIF4E binding.

The second well studied target of mTORC1 is the serine/threonine protein kinase S6Kinase. The AGC kinase family member **S6K1** is present in mammalian cells in two isoforms, which are produced from the same transcript by differential translation and similar regulation [236]. S6K1L (p85 S6K) is characterized by an N-terminal extension that contains signals for nuclear localization, while the small isoform S6K1S (p70 S6K) is localized in the cytoplasm [237]. S6K2, a second S6K is highly identical to S6K1, especially within the catalytic and the autoinhibitory domain [238]. Both, S6K1 and S6K2, are expressed ubiquitously in mammalian tissues. S6K is activated by phosphorylation at multiple serine and threonine residues within the C-terminal regulatory domain and the kinase domain. First T389 is phosphorylated by mTORC1. This phosphor-threonine serves as adapter for the kinase PDK1 leading

to phosphorylation at position T229 within the catalytic activation loop [239]. The nucleo-cytoplasmatic shuttling of S6K seems to be mediated by phosphorylation events as well [240]. S6K regulates several effector proteins by direct phosphorylation, among them ribosomal proteins (S6, eIF-4B and eIF2k) [241, 242], transcription factors (CREB) and proteins involved in cell survival (BAD1, PDCD4, MDM2) [243].

After successful activation of S6Kinase the Akt signaling pathway is dampened by S6K1 dependent negative feedback inhibition [244]. S6K directly phosphorylates the insulin receptor substrate 1 (IRS-1), thereby hindering the scaffold function between the insulin receptor and PI3K, a process which is enhanced by degradation of IRS-1 [245]. This auto-regulatory process within the PI3K/Akt/mTORC1 signaling pathway is crucial for the fine-tuning of insulin sensitivity. There are several other feedback loops such as mTORC1 induced stabilization of the IRS adapter protein Grb10, which inhibits productive interaction of IRS with a key phosphotyrosine in the insulin receptor [246]; inhibition of mTORC2 by S6K1-mediated phosphorylation of rictor and mTORC1 mediated transcriptional upregulation of the phosphatidylinositol phosphatase and tensin homologue (PTEN) by the transcription factor hypoxia inducible factor 1 (HIF1α) [247]. Furthermore, expression of the phosphatase PHLPP is regulated by mTORC1 [248].

1.5 Pharmacological modulation of the PI3K/Akt/mTOR pathway

Receptor tyrosine kinase amplifications, mutations or silencing of the tumor suppressor PTEN and/or mutations within PI3K are the most common alterations which lead to upregulation of the PI3K/AKT signaling axis causing tumor genesis [249].

With Imatinib (Gleevec®) the first tyrosine kinase inhibitor was approved by the EMA against chronic myelogenous leukemia followed by the rapamycin analogues ("Rapalogues") temsirolimus (Torisel®) and everolimus (Afinitor®) for treatment of kidney cell carcinomas. However most of the PTEN- , PI3K-, Akt- and mTOR inhibitors are still in clinical trial phases I/II or III [250]. In addition, mTOR/PI3K dual specific inhibitors as well as combinatory therapies are promising [250, 251]. In research, modulators of the PI3K/Akt/mTOR pathway serve as valuable tools to get further insights into the complex mechanism of regulation of this important pathway.

1.5.1 Rapamycin – an "old acquaintance" connecting FKBPs, Akt and mTOR

A general anti-proliferative effect of the immunosuppressive drug rapamycin (see section 1.2.1) was first observed in a panel of different cancer lines under cell culture conditions [252], defining rapamycin as the first selective mTOR inhibitor [253]. To increase bioavailability and compound concentration in the target organs the "Rapalogues" were developed. Temsirolimus was additionally EMA approved against mantle cell lymphoma, while everolimus was recently approved as medication for advanced breast cancer and pancreatic neuroendocrine tumors.

The molecular mechanism of rapamycin was thought to be the induction of a ternary complex with mTOR and the obligatory accessory protein FKBP12. After acute treatment with rapamycin mTORC1 binds directly to FKBP12/rapamycin leading to a reduction of the kinase activity of mTORC1 [253]. In contrast, mTORC2 does not bind the rapamycin/FKBP12 complex, suggesting that the FRB domain is not accessible on mTORC2. However under conditions of prolonged rapamycin treatment rapamycin/FKBP12 was shown to reduce intact mTORC2 in some cell types, presumably as newly synthesized or turned over free mTOR molecules are sequestered [254]. Theoretically, the inhibition of the assembly of mTORC2 should lead to a decreased phosphorylation of Akt S473. This was not observed in every cell type and in some cell types phosphorylation was even shown to be increased [254]. This can be explained by a negative feedback loop from mTOR or p70S6K to Akt.

1.5.2 Akt inhibitors – more than one strategy

The majority of the described Akt inhibitors are competitive with ATP. AT7867 as a member of this class inhibits Akt1/2/3 and p70 S6 kinase with an IC_{50} of 32 nM/17 nM/47 nM and 85 nM, respectively [255, 256]. The compound binds and stabilizes the activated 'PH out' conformation of Akt (PDB code 2UW9) [255]. The occupation of the ATP binding site causes stabilization of a conformation in which the phosphorylated sites are protected from dephosphorylation by phosphatases, thus resulting in hyperphosphorylation and locking in a non-functional state [257, 258].

Inhibitor VIII was the first commercialized PH domain dependent allosteric Akt1/Akt2 inhibitor binding to Akt1 with an IC_{50} of 58 nM and to Akt2 with an IC_{50} of 210 nM [259]. The compound intercalates between the PH and the kinase domain of Akt and locks the latter in a closed inactive conformation (PDB code 3O96) with reduced phosphorylation at position S473 and T308 [260, 261]. The next generation allosteric compound derived from Akt inhibitor VIII (MK-2206) is currently evaluated in phase III clinical studies.

The most clinically advanced Akt inhibitor is the alkylphospholipid perifosine in phase III of clinical trials, where single agent activity was shown in sarcomas and Waldenström macroglobulinemia [250]. Phase III combination clinical trials are ongoing in colorectal cancer and multiple myeloma [262]. Based on its structure perifosine is incorporated into the cell membranes were it interferes with lipid-based signal transduction [263]. Additionally, the PH domain of all Akt isoforms seems to be a target, thereby preventing Akt activation [250]. Chemical structures of some Akt inhibitors are depicted in Figure 1.9.

AT7867 **Inhibitor VIII** **Perifosine**

Figure 1.9: Chemical structure of Akt inhibitors with different mechanisms of action

2. Aim of the project

Recently it was shown that FKBP51 acts as a scaffold protein mediating the interaction between PHLPP and Akt1 or Akt2, respectively [75]. In a pancreatic cancer xenograft model the positive correlation between the expression of FKBP51 and the response to chemotherapeutics was confirmed *in vivo* [76]. However, diverging results have been reported from several other tumor tissues [77]. Nevertheless, the enhancement of the PHLPP-mediated Akt dephosphorylation, e.g. via FKBP51, could be an option to sensitize susceptible cancer cells to chemotherapy. However, to implement this strategy pharmacologically, a much better biochemical understanding of the Akt/FKBP51/PHLPP interaction is required. The aim of this study was thus to get an improved insight into the interaction of FKBP51 and Akt.

Central questions were: Is there a direct FKBP51/Akt interaction? Which domains are involved and what activation status of Akt is obligatory? Is the interaction restricted to human FKBP51? Can other AGC kinases bind to FKBPs as well?

Further we aimed to investigate possible effects of different chemical modulators such as FKBP inhibitors and Akt inhibitors on Akt/FKBP interaction and downstream signaling. This is crucial in order to exclude and/or understand possible unwanted side effects of future medication.

Additionally there were hints from previous studies [14] showing that the immunosuppressive compound rapamycin exerts its effects not only by binding to FKBP12 but also by interaction with larger paralogs like FKBP51. Therefore it was asked if FKBP12 could be replaced by larger FKBPs in functional assays. These alternative FKBP/rapamycin/mTOR complexes would contain additional functional domains that could be relevant for the complex, cell-type specific effects of rapamycin. New insights could provide additional data supporting a rationale for FKBP subtype-selective rapamycin analogues, which could specifically target tissues that express a certain FKBP subtype.

3. Materials

3.1 Oligonucleotide primers

For amplification and cloning of the FKBP nucleotide sequences the following oligonucleotide primers Sigma-Aldrich (St. Louis, MO, USA) were used together with the indicated vectors:

Name	Sequence (5'-3')	Amplificat and Sequence	Cloning strategy
51-KpnI-Start-FK2-fwd	ACCA<u>GGTACC</u>**ATGTTT GAAGATGGAGGCATT ATCCG**	Human FKBP51 ΔFK1 (NM_004117) aa 141-457+FLAG tag	Amplification from pcDNA3 FKBP51FLAG and introduction in pcDNA3 with KpnI and EcoRI → pcDNA3FKBP51 ΔFK1FLAG
FLAG-Stop-EcoRI-rev	TTTTTT<u>GAATTC</u>*TCACT TGTCATCGTCGTCCTT GTAGTC*		
KpnI-FKBP51-fwd	GGCC<u>GGTACC</u>**ATGAC TACTGATGAAGGTGC CAAG**	Human FKBP51 FK1 (NM_004117) aa 1-140+FLAG tag	Amplification from pcDNA3 FKBP51FLAG and introduction in pcDNA3 with KpnI and EcoRI → pcDNA3 FKBP51FK1FLAG
FK1-FLAG-Stop-EcoRI-rev	TTTTT<u>GAATTC</u>TCA*CTT GTCATCGTCGTCCTTG TAGTC***CTCTCCTTTGA AATCAAGGAGC**		
Kpn-51-Start-TPR-fwd	CCGA<u>GGTACC</u>**ATGGA TACCAAAGAAAAATT GGAGCAG**	Human FKBP51 ΔFK1FK2 (NM_004117) aa 259-457+FLAG tag	Amplification from pcDNA3 FKBP51FLAG and introduction in pcDNA3 with KpnI and EcoRI →pcDNA3 FKBP51ΔFK1FK2FLAG
Flag-Stop-EcoRI-rev	TTTTTT<u>GAATTC</u>TCA*CT TGTCATCGTCGTCCTT GTAGTC*		
EcoRI-FKBP51-fwd	CCCG<u>GAATTC</u>ACC**ATGACTACTGATG AAGGTGCCAA**	Human FKBP51 FK1 (NM_004117) aa 1-140+FLAG tag	Amplification from prk5 FKBP51FLAG and intro-duction in pRK5 with EcoRI and BamH1→pRK5FKBP51 FK1FLAG
FK1-FLAG-Stop-BamH1-rev	TTTTT<u>GGATCC</u>TCA*CT TGTCATCGTCGTCCTT GTAGTC***CTCTCCTTTG AAATCAAGGAGC**		

Table 3.1: Oligonucleotide primers and cloning strategies used for generation of FKBP plasmids
The restriction sites are underlined, coding sequences are bold, tags are italic.

Materials

The following primers were used for introduction of Akt1 point mutations:

name	Sequence (5'-3')	Cloning strategy
Akt1 T450A-fwd	CCAGATGATCACCATC**G**CACCACCTGACCAAGA	Base exchange to pCMV5HA_Akt1T450A
Akt1 T450A-rev	TCTTGGTCAGGTGG<u>TG**C**</u>GATGGTGATCATCTGG	
Akt1 T450D-fwd	GGCCCAGATGATCACCATC<u>**GAT**</u>CCACCTGACCAAGATGACA	Base exchange to pCMV5HA_Akt1T450D
Akt1 T450D-rev	TGTCATCTTGGTCAGGTGG<u>**ATC**</u>GATGGTGATCATCTGGGCC	
PKBα T308A sense	GGTGCCACCATGAAG<u>**G**CC</u>TTTTGCGGCACAC	Base exchange to pCMV5HA_Akt1T308A
PKBα T308A antisense	GTGTGCCGCAAAA<u>GG**C**</u>CTTCATGGTGGCACC	
PKBα T308D sense	CGGTGCCACCATGAAG<u>**GA**C</u>TTTTGCGGCACACCT	Base exchange to pCMV5HA_Akt1T308D
PKBα T308D antisense	AGGTGTGCCGCAAAA<u>G**TC**</u>CTTCATGGTGGCACCG	
PKBa S473A sense	CTTCCCCCAGTTC<u>**G**CC</u>TACTCGGCCAG	Base exchange to pCMV5HA_Akt1S473A
PKBa S473A antisense	CTGGCCGGAGTA<u>GG**C**</u>GAACTGGGGGAAG	
PKBa S473D sense	CACTTCCCCCAGTTC<u>**GA**C</u>TACTCGGCCAGCAG	Base exchange to pCMV5HA_Akt1S473D
PKBa S473D antisense	CTGCTGGCCGAGTA<u>G**TC**</u>GAACTGGGGGAAGTG	

Table 3.2: Oligonucleotide primers to generate Akt1 point mutations
The tripletts coding for the changed aminoacids are underlined, the changed bases are shown in bold.

3.2 Expression vectors

name	resistance	Expression	Strategy/provider
pProEx-Hta (4779 bP)	Ampicilin	Expression of proteins with N terminal hexahistidine tag in E. coli	Invitrogen (Karlsruhe)
pProEx-Hta_FKBP12	Ampicillin	FKBP12 with N-terminal hexahistidin tag	[14, 264]
pProEx-Hta_FKBP12.6	Ampicillin	FKBP12.6 with N-terminal hexahistidin tag	[14, 264]
pProEx-Hta_FKBP13	Ampicillin	FKBP13 with N-terminal hexahistidin tag	[14, 264]
pProEx-Hta_FKBP25	Ampicillin	FKBP25 with N-terminal hexahistidin tag	[14, 264]
pProEx-Hta_FKBP51_FLAG	Ampicillin	FKBP51 with N-terminal hexahistidin tag and C-terminal FLAG tag	[14, 264]
pProEx-Hta_FKBP52_FLAG	Ampicillin	FKBP52 with N-terminal hexahistidin tag	[14, 264]
pProEx-Hta_Cyp40_FLAG	Ampicillin	Cyp40 with N-terminal hexahistidin tag and C terminal FLAG tag	[265]
pProEx-Hta_FKBP51FK1	Ampicillin	FKBPFK1 with N-terminal hexahistidin tag(aa 1-140)	C. Kozany, (MPI of Psychiatry, Munich)
pProEx-Hta_FKBP51ΔFK1	Ampicillin	FKBPΔFK1 with N-terminal hexahistidin tag (aa 143–457)	C. Kozany, (MPI of Psychiatry, Munich)

Table 3.3: Plasmids used for protein expression in bacteria I

name	resistance	Expression	Strategy/provider
pProEx-Hta_FKBP51TPR (pProEx-Hta_FKBP51ΔFKΔFK2)	Ampicillin	FKBP51TPR with N-terminal hexahistidin tag (aa257-457)	V. Kupfer, (MPI of Psychiatry, Munich)
pProEx-Hta_ FKBP51FK1^{F67L}	Ampicillin	FKBPFK1 with N-terminal hexahistidin tag(aa 1-140) and point mutation F67L	V. Kupfer, (MPI of Psychiatry, Munich)
pProEx-Hta_ FKBP51FK1^{F67I}	Ampicillin	FKBPFK1 with N-terminal hexahistidin tag(aa 1-140) and point mutation F67I	V. Kupfer, (MPI of Psychiatry, Munich)
pProEx-Hta_ FKBP51FK1^{F67M}	Ampicillin	FKBPFK1 with N-terminal hexahistidin tag(aa 1-140) and point mutation F67M	V. Kupfer, (MPI of Psychiatry, Munich)
pProEx-Hta_ FKBP51FK1^{F67A}	Ampicillin	FKBPFK1 with N-terminal hexahistidin tag(aa 1-140) and point mutation F67A	V. Kupfer, (MPI of Psychiatry, Munich)
pProEx-Hta_ FKBP51FK1^{F67G}	Ampicillin	FKBPFK1 with N-terminal hexahistidin tag(aa 1-140) and point mutation F67G	V. Kupfer, (MPI of Psychiatry, Munich)
pProEx-Hta_ FKBP51FK1^{F67S}	Ampicillin	FKBPFK1 with N-terminal hexahistidin tag(aa 1-140) and point mutation F67S	V. Kupfer, (MPI of Psychiatry, Munich)
pProEx-Hta_ FKBP51FK1^{F67T}	Ampicillin	FKBPFK1 with N-terminal hexahistidin tag(aa 1-140) and point mutation F67T	V. Kupfer, (MPI of Psychiatry, Munich)
pProEx-Hta_ FKBP51FK1^{I122V}	Ampicillin	FKBPFK1 with N-terminal hexahistidin tag(aa 1-140) and point mutation I122V	V. Kupfer, (MPI of Psychiatry, Munich)
pProEx-Hta_ FKBP51FK1F^{130Y}	Ampicillin	FKBPFK1 with N-terminal hexahistidin tag(aa 1-140) and point mutation F130Y	V. Kupfer, (MPI of Psychiatry, Munich)

Table 3.3: Plasmids used for protein expression in bacteria II

name	resistance	Expression	Strategy/provider
pProEx-Hta_FKBP51F67V_FLAG	Ampicillin	FKBP51FD67DV with N-terminal hexahistidin tag and C-terminal FLAG tag	C. Kozany, (MPI of Psychiatry, Munich)
pProEx-Hta_FKBP51FD67DV_FLAG	Ampicillin	FKBP51FD67DV with N-terminal hexahistidin tag and C-terminal FLAG tag (PPIase inactive mutant)	V. Kupfer , (MPI of Psychiatry, Munich)
pProEx-Hta _smFKBP51_FLAG	Ampicillin	Squirrel monkey FKBP51 with N terminal hexa-histidine and C-terminal FLAG tag	A. Kirschner (MPI of Psychiatry, Munich)
pProEx-Hta_FKBP51ΔFK1_FLAG	Ampicillin	FKBPΔFK1 with N-terminal hexahistidin tag (aa 143-457) and C –termanal FLAG tag	C. Kozany, (MPI of Psychiatry, Munich)

Table 3.3: Plasmids used for protein expression in bacteria III

name	resistance	Expression	Strategy/provider
pcDNA3	Ampicilin		Invitrogen (Karlsruhe)
pcDNA3_FLAG_FKBP51	Ampicillin	FKBP51 with N-terminal FLAG tag	[14]
pcDNA3_FLAG_FKBP52	Ampicillin	FKBP52 with N-terminal FLAG tag	[14]
pcDNA3_FLAG_FKBP12	Ampicillin	FKBP12 with N-terminal FLAG tag	[14]
pcDNA3_FLAG_FKBP12.6	Ampicillin	FKBP12.6 with N-terminal FLAG tag	[14]
pcDNA3_FLAG_FKBP25	Ampicillin	FKBP25 with N-terminal FLAG tag	[14]
pcDNA3_HA_PHLPP2	Ampicillin	PHLPP2 with N-terminal HA tag	Addgene (Cambridge, MA, USA) #22403
pcDNA3_HA_PHLPP1	Ampicillin	PHLPP1 with N-terminal HA tag	Addgene (Cambridge, MA, USA) #22404
pcDNA3_HA_PHLPP1ΔC	Ampicillin	PHLPP1 with N-terminal HA tag (aa 1-1202)	Addgene (Cambridge, MA, USA) #22931
pcDNA3_HA_PHLPP1ΔPH	Ampicillin	PHLPP1 with N-terminal HA tag (aa 127-1205)	Addgene (Cambridge, MA, USA) #22930

Table 3.4: Plasmids used for protein expression in eukaryotic cells I

name	resistance	Expression	Strategy/provider
pcDNA3_FKBP51ΔFK1_FLAG	Ampicillin	FKBP51 ΔFK1 with C terminal FLAG tag (aa 141- 457)	Amplified with 51-KpnI-Start-FK2-fwd and FLAG-Stop-EcoRI-rev
pcDNA3_FKBP51 ΔFK1FK2_FLAG	Ampicillin	FKBP51 ΔFK1 FK2 with C terminal FLAG tag (aa 259-457)	Amplified with Kpn-51-Start-TPR-fwd and FLAG-Stop-EcoRI-rev
pcDNA3_FKBP51FK1_FLAG	Ampicillin	FKBP51 FK1 with C terminal FLAG tag (aa 1-140)	Amplified with Kpn-FKBP51-fwd and FK1-FLAG-Stop-EcoRI-rev
pcDNA3_FLAG_FKBP12_mut_siRNA	Ampicillin	FKBP12 with silent mutations in RNAi recognition sequence, for expression in SH-SY5Y_shFKBP12	A. März (MPI of Psychiatry, Munich)
pRK5-SV40Pur-MCS	Ampicillin	-	[54, 266]
pRK5_FKBP52_FLAG	Ampicillin	FKBP52 with C terminal FLAG tag	[54, 266]
pRK5_FKBP51_FLAG	Ampicillin	FKBP51 with C terminal FLAG tag	[54, 266]
pRK5_FKBP51FK1_FLAG	Ampicillin	FKBP51FK1 with C-terminal FLAG tag (aa 1-140)	amplified with EcoRI-FKBP51-fwd and FK1-FLAG-Stop-BamH1-rev
pRK5_FKBP51ΔCBD_FLAG	Ampicillin	FKBP51ΔCBD with C terminal FLAG tag	RG Rein, (MPI of Psychiatry, Munich)

Table 3.4: Plasmids used for protein expression in eukaryotic cells II

name	resistance	Expression	Strategy/provider
pRK5_FKBP51TPR_mut_FLAG	Ampicillin	FKBP51$^{K352A/R356A}$ with C terminal FLAG tag (prevents interaction with Hsp90)	[266]
pRK5_FKBP51^{FD67DV}	Ampicillin	FKBP51^{FD67DV} with C-terminal FLAG tag (PPIase inactive mutant)	A. Kirschner (MPI of Psychiatry, Munich)
pCMV5.HA_PKBα	Ampicillin	PKBα with N terminal HA tag	P. Cron/B. Hemmings (FMI, Basel, Switzerland))
pCMV5.HA_PKBα^{T308A}	Ampicillin	PKBα with N terminal HA tag and T308A exchange	base exchange by point mutation
pCMV5.HA_PKBα^{T308D}	Ampicillin	PKBα with N terminal HA tag and T308D exchange	base exchange by point mutation
pCMV5.HA_PKBα^{S473A}	Ampicillin	PKBα with N terminal HA tag and S473A exchange	P. Cron/B. Hemmings (FMI, Basel, Switzerland)
pCMV5.HA_PKBα^{S473D}	Ampicillin	PKBα with N terminal HA tag and S473D exchange	base exchange by point mutation
pCMV5.HA_PKBα$^{T308A/S473A}$	Ampicillin	PKBα with N terminal HA tag and T308A/S473A exchange	base exchange by point mutation
pCMV5.HA_PKBα$^{T308D/S473A}$	Ampicillin	PKBα with N terminal HA tag and T308D/S473A exchange	base exchange by point mutation
pCMV5.HA_PKBα$^{T308D/S473D}$	Ampicillin	PKBα with N terminal HA tag and 308AD/S473D exchange	P. Cron/B. Hemmings (FMI, Basel, Switzerland)

Table 3.4: Plasmids used for protein expression in eukaryotic cells III

name	resistance	Expression	Strategy/provider
pCMV5.HA_PKBα^{T450A}	Ampicillin	PKBα with N terminal HA tag and T450A exchange	base exchange by point mutation
pCMV5.HA_PKBα^{T450D}	Ampicillin	PKBα with N terminal HA tag and T450D exchange	Base exchange by point mutation
pCMV5.HA_PKBα$^{T450A/S473D}$	Ampicillin	PKBα with N terminal HA tag and T450A/S473D exchange	base exchange by point mutation
pCMV5.HA_PKBα$^{T450D/S473D}$	Ampicillin	PKBα with N terminal HA tag and T450D/S473D exchange	base exchange by point mutation
pRK7_HA_S6K	Ampicillin	N terminal HA tagged S6 Kinase	Addgene (Cambridge, MA, USA) #8984
HA_Aκτ2	Ampicillin	N terminal HA tagged Akt2	[75]
pEBG2T-PKBα^{S473D}	Ampicillin	PKBα with N-terminal GST tag and S473D exchange	[267]
pEBG2T-PKBαΔPH^{S473D}	Ampicillin	PKBα (N terminal 177 aa deleted) with N-terminal GST tag And S473D exchange (hydrophobic motif)	[267]
pEBG2T-PKBαΔPH	Ampicillin	PKBα (N terminal 177 aa deleted) with N-terminal GST tag	[267]
pEBG2T-SGK_^{S422D}	Ampicillin	SGK (N terminal 61 aa deleted) with N terminal GST tag and hydrophobic motif mutation	[267]
pEBG2T-SGK	Ampicillin	SGK (N terminal 61 aa deleted) with N terminal GST tag	[267]

Table 3.4:Plasmids used for protein expression in eukaryotic cells IV

3.3 Antibodies

3.3.1 Primary antibodies

For protein detection in immunoblotting experiments, the following primary antibodies were diluted in buffered protein solution (BSA or milk powder):

Antibody	Antigen	Species	Dilution factor and used solution	Manufacturer, cat#
αActin	C-terminual sequence of human Actin	IgG, polyclonal, from goat	1:3000 in 5% (w/v)milk powder in TBS-T BSA	Santa Cruz Biotechnology (Santa Cruz, CA, USA)
αAkt kinase (pan)	C-terminal sequence of mouse Akt	IgG, monoclonal, from rabbit	1:1000 in 5% (w/v) milk powder in TBS-T	Cell Signaling (Danvers, MA, USA) #4685
αAkt (phospho S473)	Peptide around phospho S473	IgG, monoclonal, from rabbit	1:1000 in 5% (w/v) BSA in TBS-T	Cell Signaling (Danvers, MA, USA) #4058
αCyclophilin 40 (Cyclophilin D)	epitope corresponding to amino acids 186-370 mapping at the C-terminus of Cyclophilin D of human origin	IgG, polyclonal, from rabbit	1:1000 in 5% (w/v) milk powder in TBS-T	Santa Cruz Biotechnology (Santa Cruz, CA, USA) #H-185
αFFI	FK1 domain of FKBP51	IgG, polyclonal, from mouse	1:2000 in 5% (w/v) milk powder in TBS-T	[81]
αFKBP12	aa 1-13 of human FKBP12	IgG, polyclonal, from rabbit	1:1000 in 5% (w/v) milk powder in TBS-T	Abcam (Cambridge, UK) # ab2918
αFKBP12.6	aa 1-81 FKBP12.6	IgG1, monoclonal, from mouse	1:500 in 5% (w/v) milk powder in TBS-T	Abcam (Cambridge, UK) #ab58075
αFKBP25	Peptide from aa1-100	IgG, polyclonal, from rabbit	1:1000 in 5% (w/v) milk powder in TBS-T	Abcam (Cambridge, UK) #ab16654
αFKBP51	Peptide from aa 407-457	IgG, polyclonal, from rabbit	1:5000 in 5% (w/v) milk powder in TBS-T	Bethyl Laboratories (Montgomery, TX, USA)#A301-430

Table 3.5: Primary antibodies used in immunoblotting and their properties I

Antibody	Antigene	Species	Dilution factor and used solution	Manufacturer, cat#
αFKBP52	Peptide from aa 400-440	IgG, polyclonal, from rabbit	1:5000 in 5% (w/v) milk powder in TBS-T	Bethyl Laboratories (Montgomery, TX, USA)#A301-427A
αFLAG-HRP	DYKDDDDK	IgG, monoclonal, from mouse	1:10000 in 5% (w/v) milk powder in TBS-T	Sigma-Aldrich (Saint Louis, MO, USA) #A8592
αFLAG	DYKDDDDK	IgG, polyclonal, from rabbit	1:5000 in 5% (w/v) milk powder in TBS-T	Abcam (Cambridge, UK) #ab1162
αFoxO1	corresponding to carboxy-terminal residues of human FoxO1	IgG, monoclonal, from rabbit	1:1000 in 5% (w/v) BSA in TBS-T	Cell Signaling (Danvers, MA, USA) #2880
αFoxO1 (phosphoS256)	residues around Ser256 of human FoxO1	IgG, polyclonal from rabbit	1:1000 in 5% (w/v) BSA in TBS-T	Cell Signaling (Danvers, MA, USA) #9461
αGSK-3β	Not specified	IgG1, monoclonal from rabbit	1:1000 in 5% (w/v) BSA in TBS-T	Cell Signaling (Danvers, MA, USA) #9336
αGSK-3β (phosphoS9)	residues around Ser9 of human GSK3ß	IgG1, polyclonal from rabbit	1:1000 in 5% (w/v) BSA in TBS-T	Cell Signaling (Danvers, MA, USA) #9315
αGST	schistosomal GST	IgG, polyclonal from goat	1:5000 in 5% (w/v) milk powder in TBS-T 1:2000	GE Healthcare (Chalfont St Giles, GB)
αHA-HRP	YPYDVPDYA	IgG1, monoclonal, from rat	1:5000 in 5% (w/v) milk powder in TBS-T	Roche Diagnostics (Mannheim) #12013819001
αHA	YPYDVPDYA	IgG1, monoclonal, from mouse	1:1000 in 5% (w/v) milk powder in TBS-T	Roche Diagnostics (Mannheim) #11583816001

Table 3.5: Primary antibodies used in immunoblotting and their properties II

Antibody	Antigene	Species	Dilution factor and used solution	Manufacturer, cat#
αPHLPP1	region between residue 1150 and the C-terminus (residue 1205) of human PHLPP	IgG, polyclonal, from rabbit,	1:1000 in 5% (w/v) milk powder in TBS-T	Bethyl Laboratories (Montgomery, TX, USA) #A300-660A
αPHLPP2	Peptide from aa 1275-1323 of human PHLPP2	IgG, polyclonal, from rabbit,	1:1000 in 5% (w/v) milk powder in TBS-T	Bethyl Laboratories (Montgomery, TX, USA) #A300-661A
αSGK1	Peptide from aa 300 - 400 of human SGK1	IgG, polyclonal, from rabbit	1:1000 in 5% (w/v) milk powder in TBS-T	Abcam (Cambridge, UK) # ab43606

Table 3.5: Primary antibodies used in immunoblotting and their properties III

3.3.2 Secondary antibodies

The following secondary antibodies were used in immunoblotting experiments:

Name	Conjugation	IgG subtype from species	Dilution factor and used solution	Manufacturer
Mouse IgG	Horseradish peroxidase	Polyclonal, IgG, H&L, from goat	1:3500 in 5% (w/v) milk powder in TBS	Abcam (Cambridge, UK) #ab6885
Rabbit IgG	Horseradish peroxidase	Polyclonal, IgG, H&L, from goat	1:3500 in 5% (w/v) milk powder in TBS	Abcam (Cambridge, UK) #ab6721
Goat IgG	Horseradish peroxidase	Polyclonal, IgG, H&L, from donkey	1:3500 in 5% (w/v) milk powder in TBS	Abcam (Cambridge, UK) #ab6789

Table 3.6: Secondary antibodies used in immunoblotting experiments

3.4 Bacterial strains

While *Escherichia coli* strain DH5α was used especially for cloning of PCR products and for preparation of plasmid DNA, the strain BL21(DE3) is suitable for heterologous protein expression. The strains were purchased from Invitrogen (Karlsruhe) and display the following genotypes:

Strain	Genotype
DH5α	F' Phi80dlacZ ΔM15 Δ(lacZYA-argF)U169 deoR recA1 endA1 hsdR17(rK-mK+)phoA supE44 lambda- thi-1
BL21(DE3)pLysS	F–, *ompT*, *hsd*S$_B$ (r$_B$–, m$_B$–), *dcm*, *gal*, λ(DE3), pLysS, Cm^r.

Table 3.7: Bacterial strains used for cloning and expression experiments

3.5 Mammalian cell lines

The following mammalian cell lines were used:

Name	Description	Origin	Provided by	ATCC No.
HeLa	cervix adenocarcinoma cells	*H. sapiens*	Dr. T. Rein (MPI of Psychiatry, Munich)	CCL-2
HEK293	embryonic kidney cells	*H. sapiens*	Dr. T. Rein (MPI of Psychiatry, Munich)	CRL-1573
HEK293-T	embryonic kidney cells, transfected with SV40 T-antigen	*H. sapiens*	Dr. T. Rein (MPI of Psychiatry, Munich)	CRL-11268
MEF	embryonic fibroblast cells	*M. musculus*	Marc Cox (University of Texas, TX, USA)	CRL-2991

Table 3.8: Mammalian cell lines used for different experiments I

Name	Description	Origin	Provided by	ATCC No.
MEF51-/-	embryonic fibroblast cells, FKBP51 deficient	*M. musculus*	Marc Cox (University of Texas, TX, USA)	-
MEF52-/-	embryonic fibroblast cells, FKBP52 deficient	*M. musculus*	Marc Cox University of Texas, TX, USA)	-
SU.86.86	ductal carcinoma (pancreas)	*H.sapiens*	Kong Bo (TU Munich, Munich)	CRL-1837
SH-SY5Y	neuroblastoma cells	*H. sapiens*	Dr. M. Gerard (University of Leuven, Leuven, BE)	CRL-2266
SH-SY5Y-shFKBP12 (SH-SY5Y-12KD)	neuroblastoma cells, FKBP12 knock down	*H. sapiens*	Dr. M. Gerard (University of Leuven, Leuven, BE) [20]	-

Table 3.8: Mammalian cell lines used for different experiments II

3.6 Media and additives for cell culture

The following media and additives were used to maintain mammalian cell culture:

Name	Contains:	Used for	Manufacturer
Ampuwa sterile water			Fresenius-Kabi (Bad Homburg)
Dulbecco's Modified Eagle Medium	4.5 g/l glucose, L-glutamine, sodium pyruvate, phenol red	HeLa, HEK, SU.86.86	Gibco-Invitrogen (Karlsruhe)
Dulbecco's Modified Eagle Medium	4.5 g/l glucose, L-glutamine, sodium pyruvate	MEF, MEF51-/-, MEF52-/-	Gibco-Invitrogen (Karlsruhe)
Dulbecco's Modified Eagle Medium+GLUTAMAX	4.5 g/l glucose, L-alanyl-L-glutamine, phenol red	SH-SY5Y SH-SY5Y-shFKBP12	Gibco-Invitrogen (Karlsruhe)
Dulbecco's Phosphate Buffered Saline		all cell lines	Gibco-Invitrogen (Karlsruhe)
Heat Inactivated Fetal Calf Serum (FCS)		all cell lines	Gibco-Invitrogen (Karlsruhe)

Table 3.9: Media and additives used for cell culture experiments I

Name	Contains:	Used for	Manufacturer
Opti_MEM		Transfection with Lipofectamine LTX	Gibco-Invitrogen (Karlsruhe)
Sodium pyruvate	100x	SH-SY5Y	Gibco-Invitrogen (Karlsruhe)
Penicillin/ Strepomycin	5000 U/ml Penicillin, 5000 U/ml streptomycin	all cell lines, except SH-SY5Y, SH-SY5Y-shFKBP12	Gibco-Invitrogen (Karlsruhe)
Poly-D-Lysine	1 mg/ml	for homogeneous time resolved FRET assays	Merck-Millipore (Billerica, MA, USA)
Hygromycin	50 mg/ml	SH-SY5Y-shFKBP12	Gibco-Invitrogen (Karlsruhe)
Gentamicin	10 mg/ml	SH-SY5Y, SH-SY5Y-shFKBP12	PAA Laboratories GmbH (Cölbe)
MEM non-essential amino acid solution 100 x		SH-SY5Y, SH-SY5Y-shFKBP12	Gibco-Invitrogen (Karlsruhe)
0.25% Trypsin-EDTA		all cell lines	Gibco-Invitrogen (Karlsruhe)

Table 3.9: Media and additives used for cell culture experiments II

3.7 Chemicals

The chemicals used for this work are listed below and were purchased from the indicated companies:

Acetic Acid   Roth (Karlsruhe)

Acrylamid/Bisacrylamid-Solution (29:1)   Serva (Heidelberg)

Adenosine 5´-Triphosphat   Roth (Karlsruhe)

Agarose SeaKem   Biozym (Oldendorf)

Agar-Agar   Roth (Karlsruhe)

Akt Inhibitor VIII   Calbiochem (San Diego, CA, USA)

Ammonium peroxodisulfate   Roth (Karlsruhe)

Materials

Ampicillin	Roth (Karlsruhe)
AMP-PNP (Adenylyl-imidodiphosphate)	Sigma-Aldrich (St. Louis, MO, USA)
Antascomicin B	Stephen Ley (Cambridge University, UK) [141]
Anti-FLAG M2 Magnetic beads	Sigma-Aldrich (St. Louis, MO, USA)
Anti-FLAG M2 affinity resin	Sigma-Aldrich (St. Louis, MO, USA)
AT7867	SelleckChem (Houston, TX, USA)
Biricodar	Dr. S. Gaali, (MPI of Psychiatry, Munich)
Boric acid	Calbiochem (San Diego, CA, USA)
Brilliant Blue R250	Roth (Karlsruhe)
Bovine Serum Albumine (BSA)	Roth (Karlsruhe)
Bromophenol Blue	Merck (Darmstadt)
Calciumchloride	Roth (Karlsruhe)
p-Coumaric acid	Sigma-Aldrich (St. Louis, MO, USA)
cmpd44=GR591	Dr. R. Gopalakrishnan, [148]
Desoxynucleotide mix	NEB (Frankfurt am Main)
Dimethyl sulfoxide (DMSO)	Roth (Karlsruhe)
1,4-Dithiotreitole	Roth (Karlsruhe)
EDTA (Titriplex III)	Merck (Darmstadt)
Ethidium bromide	Roth (Karlsruhe)
EZview Red Anti-HA Affinity Gel	Sigma-Aldrich (St.Louis, MO, USA))
FK1706	Astellas Pharma Inc. (Tokyo, Japan)
FK506 (Tacrolimus)	Sigma-Aldrich (St. Louis, MO, USA))
FLAG peptide	Sigma-Aldrich (St. Louis, MO, USA))
GC-buffer	NEB (Frankfurt am Main)
Gemcitabine hydrochloride	Molekula (Nienburg/Weser)
Glutathion Pro Catch Sepharose	Miltenyi Biotech (Bergisch Gladbach)
Glycine	Roth (Karlsruhe)
Glycerine (86-88% (v/v))	Roth (Karlsruhe)
Glycerophosphate	Roth (Karlsruhe)
HA peptide	Sigma-Aldrich (St. Louis, MO, USA))
Hepes	Biomol (Hamburg)
Immobilon Western Chemiluminescent HRP Substrate (ECL)	Merck-Millipore (Billerica, MA, USA)
Imidazole	Roth (Karlsruhe)
Inhibitor VIII	Merck (Darmstadt)
Isopropyl-beta-D-thiogalactopyranoside (IPTG)	Roth (Karlsruhe)

40

Materials

LB medium (Luria/Miller)	Roth (Karlsruhe)
Lipofectamine 2000	Invitrogen (Karlsruhe)
Lipofectamine LTX	Invitrogen (Karlsruhe)
Luminol	Roth (Karlsruhe)
Magnesium chloride	Merck (Darmstadt)
2-Mercaptoethanol	Merck (Darmstadt)
Milk powder	Roth (Karlsruhe)
Ni-NTA agarose	Qiagen (Hilden)
Phenylmethylsulfonyl fluoride (PMSF)	Molekula (Nienburg/Weser)
Ponceau S	Roth (Karlsruhe)
Protease inhibitor cocktail	Sigma-Aldrich (St. Louis, MO, USA))
Protein A resin	GenScript (Piscataway, USA)
Rapamycin (Lot #R020)	Cfm (Marktredwitz)
SG537	Dr. S. Gaali (MPI of Psychiatry, Munich)
Sodium chloride (NaCl)	Roth (Karlsruhe)
Sodium desoxycholate	Roth (Karlsruhe)
Sodium dihydrogenphosphat	Roth (Karlsruhe)
Sodium dodecylsulfat (SDS)	Merck-Millipore (Billerica, MA, USA)
Sodium flouride	Roth(Karlsruhe)
Sodium dihydrogen orthovanadate	Fluka Sigma-Aldrich (St.Louis, MO, USA)
Sodium pyrophosphate dibasic	Fluka Sigma-Aldrich (St.Louis, MO, USA)
N,N,N',N'-Tetramethylethylenediamine (TEMED)	Roth (Karlsruhe)
Torin-1	provided by D. Sabatini
Tris(hydroxymethyl)-aminomethane	Merck (Darmstadt)
Triton X-100	Roth (Karlsruhe)
Tween 20	Bio-Rad (München)
Wortmannin	Merck (Darmstadt)
YW644	Dr. Y. Wang (MPI of Psychiatry, Munich)
YW648	Dr. Y. Wang (MPI of Psychiatry, Munich)
YW649	Dr. Y. Wang (MPI of Psychiatry, Munich)
YW703	Dr. Y. Wang (MPI of Psychiatry, Munich)

3.8 Enzymes and Proteins

The enzyms that were used for different assays are listed below:

Akt1/PKB$_\alpha$ (inactive) #14-279	Merck-Millipore (Billerica, MA, USA)
Akt1/PKB$_\alpha$ (active) #14-276	Merck-Millipore (Billerica, MA, USA)
Antarctic Phosphatase	NEB (Frankfurt am Main)
GST protein #SCM-G52-30U	Biozol (Eching)
Insulin solution, human	Sigma-Aldrich (St. Louis, MO, USA)
Lysozyme	Roth (Karlsruhe)
Phusion High Fidelity Taq Polymerase	NEB (Frankfurt am Main)
Restriction endonucleases	NEB (Frankfurt am Main)
T4-DNA Ligase	NEB (Frankfurt am Main)
Taq Polymerase	NEB (Frankfurt am Main)

3.9 Kits

The following kits were used for DNA purification and FRET assays according to the manufacturer's recommendations:

BCA Protein Assay	Thermo Fisher Scientific (Schwerte)
CellTiter-Fluor Cell Viability Assay	Promega (Mannheim)
High Yield PCR Clean-up/Gel Extraction Kit	SLG (Gauting)
High Yield Plasmid Mini Kit	SLG (Gauting)
HTRF Phospho Akt (S473)	Cisbio (Codolet, France)
HTRF Phospho Akt (T308)	Cisbio (Codolet, France)
HTRF Phospho mTOR (S2448)	Cisbio (Codolet, France)
Qiagen Plasmid Midi Kit	Qiagen (Hilden)

3.10 Markers

For size quantification of protein and DNA samples, the following standards were used:

1 kb DNA Ladder	NEB (Frankfurt am Main)
Fermentas Page Ruler Plus	Thermo Fisher Scientific (Schwerte)
Prestained Protein Ladder	Merck-Millipore (Billerica, MA, USA)

3.11 Equipment

The following machines and lab items were utilized:

Centrifuge 6K15	Sigma (Osterode)
Centrifuge Megafuge 1.OR	Thermo Fisher Scientific (Schwerte)
Centrifuge Avanti J-25, Rotor JA-20	Beckman (Krefeld)
Centrifuge Biofuge pico	Heraeus (Mannheim)
Centrifuge Universal 30 F	Hettich (Tuttlingen)
ChemiDoc MP	Bio Rad (München)
CO_2 incubator HeraCell	Fischer Thermo Scientific (Schwerte)
Developer machine	3M (Neuss)
Electrophoresis power supply	Pharmacia/GE Healthcare (München)
Gel electrophoresis chambers	PeqLab GmbH (Erlangen)
Gel electrophoresis system XCell SureLock	Invitrogen (Karlsruhe)
Ice machine ZBE 150-MT	Ziegra (Isernhagen)
Incubation shaker Innova 4000	New Brunswick (Edison, NJ, USA)
Magnet stirer R1000	Carl Roth (Karlsruhe)
Magnetight Separation Stand	Merck Millipore (Billerica, MA, USA)
MicroCal iTC200	GE Healthcare (Chalfont St Giles, GB)
Microscope DM IL	Leica (Wetzlar)
Mixer Reax 2	Heidolph Instruments (Schwalbach)
Multichannel Pipette Research Pro	Eppendorf (Hamburg)
Forma Orbital shaker	Thermo Fisher Scientific (Schwerte)
PCR cycler Gene Amp 9700	Applied Biosystems (Darmstadt)
pH meter WTW 538	WTW (Weilheim)
PIPETMAN Pipetten	Gilson (Middleton, WI, USA)

Pipettor Pipetus akku	Hirschmann Laborgeräte (Eberstadt)
Power Supply Power Pac 3000	Bio Rad (München)
Precisa 40SM-200A	Precisa (Dietikon, Switzerland)
Precision scalesMaster Pro LP4200S	Sartorius (Göttingen)
Reader Tecan GENios Pro	Tecan (Crailsheim)
Refrigerator	Liebherr (Biberach)
Shaking table SM25A	Edmund Bühler (Hechingen)
Thermomixer comfort	Eppendorf (Hamburg)
Ultrapure water dispenser PureLab ultra	Elga Lab Water (Celle)
Ultrasound Sonifier 450	Branson (Dietzenbach-Steinberg)
UV transilluminator	Faust (Meckenheim)
UV/VIS spectrophotometer DU 530	Beckman (Krefeld)
Vortexer Mini-Shaker MS2	IKA Labortechnik (Staufen)
Water bath GfL 1002	GfL (Burgwedel)
Work bench LaminAir HB2448	Heraeus (Mannheim)

3.12 Consumables

384-well plates, white	Corning (Kaiserslautern), #3572
384-well plates, low binding surface, black	Corning (Kaiserslautern), #3575
96-well plates, low binding surface, white	Corning (Kaiserslautern), #3605
96-well plates, transparent	Carl Roth (Karlsruhe), #9291.1
96-well plates, transparent	Carl Roth (Karlsruhe), #9293.1
Cell scraper 25 cm	Sarstedt (Nümbrecht)
Cellstar serological pipettes	Greiner Bio-One (Kremsmünster, AT)
Chromatography column 5 ml	Bio Rad (München)
Falcon 6-well plates	BectonDickinson (Franklin Lakes,USA)
96 well plates (cell culture)	Corning (Kaiserslautern) #3879
Falcon 10 cm dish	BectonDickinson (Franklin Lakes,USA)
Tissue culture flasks	BectonDickinson (Franklin Lakes,USA)
Medical X-Ray film Super RX	Fujifilm Corporation (Düsseldorf)
Millex Stringe Filter 0.22 µm	Merck-Millipore (Billerica, MA, USA)
Nucleobond AX2000	Machery-Nagel (Düren)
Nunclon Surface cell culture dishes	Nunc A/S (Roskilde, DK)
Pipette tips	Corning (Kaiserslautern)
Protran BA 83 Nitrocellulose	Whatman (Dassel)

Rotilabo Blotting paper	Carl Roth (Karlsruhe)
SDS Mini gel cassettes	Invitrogen (Karlsruhe)
Slide-A-Lyzer Dialysis units	Pierce/Fisher Thermo Scientific (Bonn)
Test tubes	Sarstedt (Nürnbrecht)
Test tubes (low binding)	Eppendorf (Hamburg)

3.13 Software and databases

For data collection and analysis, the following PC programs were used

Endscript 1.1	Laboratoire de BioChristallographie, Institut de Biologie et Chimie des Protéines; (Lyon, France)
Endnote X5	Thomson Reuters (New York, NY, USA)
Gimp 2.6	Spencer Kimball, Peter Mattis
Human protein reference database (hrpd)	http://www.hprd.org
ImageLab 4.1	Bio-Rad (München)
Multialin Interface	[268]
RCSB Protein Data Bank (PDB)	http://www.rcsb.org
PyMol 0.99	DeLano Scientific
SigmaPlot 11	Systat Software (Erkrath)
SPSS 19	IBM (Ehningen)
PRALINE	[269]
Protein Calculator v3.3	Scripps Research Institute (La Jolla, CA, USA)
ORIGIN 7.0	Microcal (Northhampton, MA, USA)
Word, Excel 2010	Microsoft (München)

Materials

4. Methods

4.1 Molecular biological methods

4.1.1 Preparation of competent *E. coli*

To prepare transformation-competent *E. coli* cells, 50 ml of sterile LB medium were inoculated with a small amount of glycerol stock and incubated over night at 37°C on a shaking platform (200 rpm). 25 ml of this over-night culture were used to inoculate 500 ml of sterile LB medium. This culture was grown at 37°C until an OD_{600} of 0.3 was reached.

Cells were harvested by centrifugation for 15 min at 5000 x g and 4°C. The pellet was resuspended slowly and gently in 125 ml of a cold, sterile 100 mM $MgCl_2$ solution. After another centrifugation step (5000 x g, 4°C, 15 min), the bacteria were resuspended in 25 ml of a sterile 100 mM $CaCl_2$ solution before another 200 ml of a 100 mM $CaCl_2$ solution were added. The mixture was incubated on ice for 20 min. The cells were harvested again (4000 x g, 4°C, 10 min) and resuspended in 10 ml of a 100 mM $CaCl_2$ solution with 10% glycerin (w/w). Finally, 100µl aliquots of the cell suspension were shock-frozen in liquid nitrogen and stored at -80°C until usage.

4.1.2 Transformation

50 µl of competent *E. coli* were thawed on ice and 1-5 ng or 50 ng (for ligation) plasmid DNA was added and mixed carefully. After 30 min incubation on ice they were exposed to heat shock of 42°C for 45 s. After 2 min incubation on ice 900 µl LB medium were added and the transformation mixture was grown at 37°C for 30 min on a shaking platform. Finally, the cells were harvested by brief centrifugation, plated on LB agar plates containing antibiotics (100 µg/ml of ampicillin) and incubated over night at 37°C. The next day single colonies were picked and further analyzed.

4.1.3 Bacterial culture

The required amount of sterile LB medium containing the selection antibiotics was inoculated with a single colony from an LB agar plate or glycerol culture and cultivated with agitation over night at 37°C. For preparation of the glycerol stocks 1 ml of the overnight culture was added to 500 µl of sterile 45 % glycerol solution, mixed carefully and kept at -80°C.

_____

4.1.4 DNA preparation and quantification

DNA was prepared and purified with either High Yield Plasmid Mini Kit, Nucleobond AX Mega columns or Qiagen Plasmid Midi Kit according to manufacturer's protocols. DNA concentration was estimated by measuring the extinction at 260nm after dilution to the linear range (0.1-1) in a quartz cuvette (d=1 cm).

According to Lambert-Beers Law absorption is proportional to DNA concentration:

$A= \varepsilon *c*d$

A=absorption

ε=molar extinction coefficient [L mol^{-1} cm^{-1}]

d=path length of the cuvette [1cm]

Using this law an optical density (OD=1) at 260 nm corresponds to 50 µg/ml double stranded DNA at a pH 7.0.

In addition to the concentration of the DNA measured at 260 nm, the ratio A_{260}/A_{280} was calculated as a measurement for protein contamination and should ideally range from 1.8-2.0.
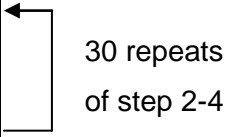
4.1.5 Standard polymerase chain reaction (PCR)

PCR is used to amplify defined DNA-fragments and to insert new restriction sites at 5' or 3'-ends by using specific primers [270, 271]. Additionally it is possible to test if bacteria carry a certain DNA sequence, as with the "colony PCR". For a standard PCR reaction the following components were combined in a 0.2 ml PCR tube and a total volume of 50 µl:

250 µM	dNTP mix (stock: 25 mM)
100 nM	primer forward (Sigma-Aldrich (St. Louis, MO, USA))
100 nM	primer reverse
100 ng	plasmid DNA template
1 U	Phusion "High Fidelity" Taq polymerase
5 µl	10x Phusion High-Fidelity buffer

The polymerase chain reaction was performed in a thermo cycler following a defined time and temperature profile. Per 1 kb of polymerization, 1 minute elongation time was scheduled. Annealing temperature was chosen according to primer melting temperature.

_____

step	temperature	duration	purpose
1	94°C	5 min	initial denaturation of DNA
2	94°C	60 s	denaturation of DNA
3	50-65°C	60 s	annealing of primers
4	72°C	90 s	elongation
5	72°C	10 min	final elongation
6	4°C	hold	protection from degradation

30 repeats
of step 2-4

The chosen annealing temperature was 5-10 °C lower than the melting temperature of the primer. Between step 2 and 4 a loop was programmed, which was repeated 30 times.

4.1.6 Analysis and purification of PCR products:

4.1.6.1 Agarose gel electrophoresis

TBE buffer: 90 mM boric acid; 2.5mM EDTA; 90 mM Tris/HCl, pH 8.3

DNA sample buffer: 40% (w/v) saccharose; 0.25% (w/v) bromophenol blue

                     20 mM EDTA, pH 8.0

To prepare an agarose gel, an appropriate amount of agarose (normally: 0.5 to 1.5 grams to yield 0.5 – 1.5% gels) was mixed with 100 ml TBE buffer and boiled in a microwave oven until it had dissolved completely. After the solution had cooled down to 60°C, 3 µl of ethidium bromide solution were added and mixed thoroughly. Then, the solution was poured into a gel tray. Air bubbles were removed, and the comb was put in place. After 30 min, the gel had solidified and was transferred to a gel chamber containing TBE buffer. The DNA samples (normally: 5 µl of a 100 ng/µl solution) were mixed with an equal amount of DNA sample buffer and were filled into the gel wells. Separation of DNA was performed by applying a current of 200 mA for 30 min (or until desired separation was achieved).

4.1.6.2 Isolation of DNA fragments from agarose gels

The PCR products were visualized using an UV transilluminator and documented photographically, before the bands were excised with a scalpel. The „High Yield PCR and Gel Extraction Kit" was used according to the manufacturer's recommendations to isolate DNA from the gel slices. Usually concentrations of 30 – 50 µg DNA / ml were obtained, determined by standard UV measurement.

_____

4.1.6.3 DNA restriction

For restriction of vector DNA and PCR products, the following components were combined:

1 µg	vector DNA (100 µg/ml)	
2 U	restriction enzyme 1 (20 U/ml)	
2 U	restriction enzyme 2 (20 U/ml)	
2 µl	BSA solution (10 x Stock) if needed	
2 µl	10x restriction buffer	
	bidest. H_2O	ad 20 µl

Alternatively:

1 µg	PCR product (50 µg/ml)	
4 U	restriction enzyme 1 (20 U/ml)	
4 U	restriction enzyme 2 (20 U/ml)	
2 µl	BSA solution (10 x Stock) if needed	
4 µl	10x restriction buffer	
	bidest. H_2O	ad 40 µl

For the enzyme combination *EcoR*I/*BamHI*, the buffer NEB buffer III was used. For *KpNI/EcoRI* NEB buffer I was utilized. The restriction mixtures of PCR products were incubated for 3 h at 37°C.

To avoid re-ligation of single-cut vector, the vector restriction mixtures were supplemented with 1 µl of Antarctic Phosphatase (1 U/µl) and 2 µl of the corresponding 10x AP buffer. After 30 min of incubation at 37°C the samples were subjected to DNA purification using the „Gel Extraction Kit". DNA concentrations of approximately 25 µg/ml were obtained.

5 µl of the purified DNA samples were separated by gel electrophoresis (1.0% agarose gel) to check for contamination and yield.

4.1.6.4 DNA ligation:

For ligation, the digested vector DNA and the digested PCR product were combined in a 1:6 ratio. A typical ligation mixture contained the following components:

50-200 ng	vector DNA (25 µg/ml)
250 ng-1 µg	PCR product (25 µg/ml)
1 U	T4 DNA ligase (20 U/µl)

_____

1 mM	ATP
1 µl	10x ligation buffer
	bidest. H$_2$O

(bidest. H$_2$O ... ad 10 µl)

The mixture was incubated over night at 16°C. If an optimization of the reaction was necessary, a higher amount of PCR product was used. Alternatively, the concentration of ligase and/or the incubation time was increased.

Ligation was further processed as described in 4.1.2.

4.1.6.5 Restriction control

To verify successful cloning, plasmid DNA was subjected to enzymatic restriction. During this control assay the same restriction enzymes are used as for cloning; therefore the insert is cut out of the vector.

The digestion mixtures contained the following components:

1 µg	plasmid DNA (100 µg/ml)
2 U	restriction enzyme 1 (20 U/µl)
2 U	restriction enzyme 2 (20 U/µl)
2 µl	BSA solution (10 x Stock) if needed
	2 µl 10x restriction buffer
	bidest. H$_2$O ad 20 µl

The restriction mixtures were incubated at 37°C for 60 min and analyzed on a 1.5% agarose gel. Preparations of plasmid DNA with insert were saved while plasmids without inserts were discarded.

4.1.6.6 DNA sequencing

For final approval of positive clones the plasmid DNA was sequenced using the chain termination sequencing technique and standard vector-specific primers. This service was provided by the "Microchemistry Core Facility" at the MPI of Biochemistry in Martinsried. The obtained sequences were compared to corresponding references in order to exclude base pair deletions and point mutations.

4.1.6.7 Site directed mutagenesis by PCR

Site directed mutagenesis allows inserting point mutations in plasmids. First a PCR with primers containing the mutation was performed (see section 3.1)

_____

500 µM	dNTP mix (stock: 25 mM)
100 nM	primer forward Sigma-Aldrich (St. Louis, MO, USA)
100 nM	primer reverse
100 ng	plasmid DNA template
1 U	Phusion "High Fidelity" Taq polymerase
2mM	$MgCl_2$
5 µl	5x GC buffer (NEB)

The polymerase chain reaction was performed in a thermo cycler with the following time and temperature profile:

step	temperature	duration	purpose
1	98°C	30 s	initial denaturation of DNA
2	98°C	30 s	denaturation of DNA
3	55°C	60 s	annealing of primers
4	72°C	8.5 min	elongation
5	72°C	10 min	final elongation
6	4°C	hold	protection from degradation

18 repeats of step 2-4 (between step 2 and step 4)

Between step 2 and 4 a loop was programmed, which was repeated 18 times.

After PCR the newly synthesized plasmids contain the mutation. The host plasmids, which originated from methylation competent bacteria needed to be digested. Digestion was performed with the methylation-dependent restriction endonuclease DpnI. Every PCR product was treated with 1 µl DpnI for 1h at 37°C, followed by heat inactivation for 10 min at 80°C. Finally the mutated plasmids were transformed into competent *E. coli* and plated on LB agar as described in section 4.1.2 and incubated at 37°C overnight. The next day colonies were picked, the plasmids were isolated (section 4.1.3 and 4.1.4) and sequenced (section 4.1.6.6)

_____

4.2 **Protein biochemical methods**

4.2.1 **Expression and purification of proteins with a hexahistidin tag**

4.2.1.1 **Induction of *E. coli* with IPTG**

Plasmid DNA encoding a specific hexahistidin tagged protein was transformed into the expression strain *E. coli* BL21 (section 3.4). 3 l of sterile LB medium, supplemented with the appropriate antibiotics, were inoculated with an overnight culture (maximal OD_{600}: 0.1) and incubated at 37°C on a shaking platform. As soon as an optical density of 0.5 was reached, protein expression was induced by addition of 1.8 ml 1 M IPTG (final concentration: 600 µM). After 3 h of additional incubation, the bacteria were harvested by centrifugation in a Sigma centrifuge at 4400 x g and 4°C for 15 min.

4.2.1.2 **Cell lysis**

Lysis buffer: 50 mM Hepes; pH 8.0; 300 mM NaCl; 40 mM imidazole; 1 mM PMSF; 1 mg/ml lysozyme

All further purification steps were carried out at 4°C or on ice.
The bacteria pellet was resuspended in 50 ml lysis buffer and rotated for 30 minute at 4°C. Treatment with an ultrasound sonifier was performed to complete cell lysis (15 cycles: 12 s ultrasound impulses, 18 s break; intensity 4 (output control 80%). To remove insoluble material, the lysate was centrifuged for 40 min at 4°C and 15000 x g in a Beckman centrifuge.

4.2.1.3 **Purification on Ni-NTA sepharose**

Washing buffer: 20 mM Hepes, pH 8.0; 300 mM NaCl; 40 mM imidazole; 5% glycerin (v/v)
Elution buffer: 20 mM Hepes, pH 8.0; 20 mM NaCl; 300 mM imidazole; 5% glycerin (v/v)

5 ml Ni-NTA resin were resuspended in 50 ml water and pelleted again by 5 min of centrifugation at 700 x g. Washing was repeated twice with each 50 ml lysis buffer.
The cleared lysate was added to the resin and incubated for 2 h with agitation at 4°C. Afterwards, the beads were pelleted by centrifugation (700 x g, 4°C), and the supernatant was

_____

discarded. The resin was resuspended in 50 ml washing buffer, incubated shortly and pelleted by centrifugation. This washing step was repeated twice.

Next, the resin was resuspended in 5 ml washing buffer and transferred into a 5-ml chromatography column. As soon as the washing buffer had drained, 5 ml elution buffer were added. The elution was collected in 0.5 ml fractions and controlled for protein content by BCA assay (section 4.2.4.2). Clean elutions with the highest protein concentrations were pooled, aliquoted and stored at -80°C. For FKBP51, analysis of elution fractions revealed an insufficient purity of the preparation. Therefore additional purification steps were needed. Dependent on the amount and concentration of FKBP51 needed, in our lab either ion-exchange chromatography followed by size-exclusion chromatography or affinity chromatography by a FLAG tag is used.

4.2.1.4   Purification by anti-FLAG affinity resin

TBS: 50 mM Tris; 150 mM NaCl; pH 7.5
Elution buffer: 100 µg/ml FLAG peptide in TBS

FKBP51 used throughout this work was purified taking advantage of the C-terminally fused FLAG peptide. This peptide (sequence: DYKDDDDK) binds with high affinity to FLAG antibodies which are covalently bound to a sepharose matrix.

1 ml of resuspended "anti-FLAG immuno-affinity resin" was transferred to a 5-ml plastic column and washed with 10 ml TBS. Then the pooled protein-containing fractions of the Ni-NTA purification were loaded onto the column (in a 1/10 dilution with TBS). After the flow through was completed, the resin material was washed with TBS until no protein could be detected any more in the washing buffer by BCA assay. By addition of elution buffer the FKBP51_FLAG protein was released from the resin and collected in different fractions. Once again, protein content was quantified by a BCA assay, and protein-containing fractions were pooled and stored at -80°C.

4.2.1.5   Dialysis of purified proteins

In case it was necessary proteins were dialyzed into the needed buffer overnight under gentle stirring, using the Slide-A-Lyzer device. The next morning the buffer was changed and the procedure was repeated.

_____

4.2.2 Expression of GST fusion proteins

GST_Akt1 and GST_SGK fusion proteins (expressed and purified from HEK cells) were provided by Dr. Sonja Neimanis (University hospital, Frankfurt (Main)).

4.2.3 Analysis of purified proteins by SDS gel electrophoresis

4.2.3.1 Casting SDS gels

SDS running buffer: 25 mM Tris/HCl, pH 8.3; 250 mM glycine; 0.1% (w/v) SDS

SDS sample buffer 2x: 125 mM Tris/HCl; 10% (v/v) 2-mercaptoethanol;"Lämmli buffer"
                             [272]: 4% (w/v) SDS; 0.004% (w/v) bromophenol Blue

Resolving gel: 380 mM Tris/HCl, pH 8.8; 0.1% (w/v) sodium dodecylsulfate;
                             10-16% (w/v) acryl amid; 0.2 – 0.3% (w/v) bisacryl amid;
                             0.12% (v/v) TEMED; 0.06% (w/v) ammonium peroxydisulfate

Stacking gel: 375 mM Tris/HCl, pH 6.8; 0.1% (w/v) sodium dodeclysulfate
                             5% (w/v) acryl amid; 0.2 – 0.3% (w/v) bisacryl amid
                             0.2% (v/v) TEMED; 0,06% (w/v) ammonium peroxydisulfate

For two mini gels of the indicated acryl amid concentration, following components were combined:

final concentration	acryl amid mix	H_2O bidest.	TEMED	1 M Tris, pH 8.8	10% (w/v) SDS	10 % (w/v) APS
10%	4.7 ml	3.9 ml	17 µl	5.4 ml	140 µl	85 µl
12%	5.7 ml	3.0 ml	17 µl	5.4 ml	140 µl	85 µl
16%	7.6 ml	1 ml	17 µl	5.4 ml	140 µl	85 µl

Table 4.1: Components and necessary amounts for 2 "mini" SDS gels

Ammonium peroxodisulfate and TEMED were added last because they induce radical formation and start the polymerization. The gel solution was filled into a commercially available mini gel cassette and was covered carefully with water. After the polymerization was completed, water was removed, and the gel cassettes were filled with stacking gel solution. Finally, 12 or 15-well combs were inserted.

_____

4.2.3.2   Preparation of samples and gel run

Coomassie staining solution: 40% (v/v) ethanol, 10% (v/v) acetic acid, 0.01% (w/v)
                                                  coommassie brilliant blue

Coomassie destaining solution: 40% (v/v) ethanol, 10% (v/v) acetic acid

Samples of the protein-containing fractions were diluted in SDS sample buffer and incubated at 95°C for 5 min to achieve denaturation. The samples were then loaded into the gel wells and separated using a current of 25 mA in the "XCell SureLock Gel System" for approximately 60 min. Protein patterns were visualized by treatment with Coomassie staining solution for 30 min, followed by destaining in Coomassie destaining solution under mild agitation.

The gel was put on a sheet of blotting paper and was conserved using a gel dryer. Finally, it was digitalized on a flatbed scanner.

Alternatively, the gel was subjected to immunoblotting procedure (section 4.3.7).

4.2.4   Determination of protein concentration

4.2.4.1   UV absorption

Because of the presence of aromatic amino acids (tyrosine, phenylalanine, tryptophan) protein solutions display absorption of ultra-violet light. The maximum of absorption is usually at 280 nm. The Law of Lambert-Beer provides a connection between protein concentration and its UV absorption value:

$A = \varepsilon * c * d$ A=absorption
                                    ε=molar extinction coefficient [L mol^{-1} cm^{-1}]
                                    d=path length of the cuvette [1cm]

The absorption coefficient of a protein can be deduced from its amino acid sequence as it depends mainly on the number of aromatic amino acids. The values for purified proteins can be found in the appendix. Values were calculated using Protein calculator v3.3. provided by Scripps Research institute (CA, USA) with the amino acid sequence as input.

Determination of UV absorption was performed in a Beckman photometer. For calibration the quartz cuvette was filled with 100 µl of elution buffer, and a blank value was recorded. Afterwards, the protein samples were measured in the same manner. If necessary the samples

_____

were diluted in elution buffer to give A_{280} values between 0.1 and 1.0. Protein concentration can be calculated using the formula   c = A / (ε*d), being d = 1 cm.

4.2.4.2   BCA assay

In order to determine protein concentrations, the colorimetry based bicinchoninic acid assay (BCA assay) was used routinely. Peptide bonds in proteins reduce Cu^{2+} ions from the cupric sulfate to Cu^+ (a temperature dependent reaction). The amount of Cu^{2+} reduced is proportional to the amount of protein present in the solution. Next, two molecules of bicinchoninic acid chelate with each Cu^{2+} ion, forming a purple-colored product, which strongly absorbs light at a wavelength of 562 nm.

The assay was performed in transparent 96-well plates (flat bottom). Each well was filled with 200 µl of BCA working solution as described by the manufacturer. For a reference array 10 µl BSA standard solutions from 2000 µg/ml–0 µg/ml were added and mixed thoroughly. The actual protein samples were diluted 1:10 or 1: 100 in water. 10 µl of the dilution were added to each well and mixed thoroughly.

After 30 min of incubation at 37°C all wells were read out in a Tecan GENios Pro reader with standard settings:

> Measurement mode: Absorbance, endpoint
>
> Wavelength: 595 nm
>
> Number of reads: 10 reads
>
> 3 s of orbital shaking before measurement.

The optical density at 595 nm was plotted against the known protein concentration of the references, and a trend line was fitted. Using the linear equation of this trend line in Excel, the concentrations of the protein samples could be determined taking the corresponding dilution factors into account.

4.2.4.3   Determination of active FKBP protein by the Fluorescence polarization assay (FP assay)

Assay buffer: 20 mM Hepes, pH 8; 0.01% (v/v) Triton X-100

As determination of protein concentration by UV/VIS spectroscopy and colorimetric based methods includes misfolded proteins and protein contaminations, "active site titration" leads to the portion of active protein in a protein solution. Therefore the fluorescein coupled FKBP ligand CK97 (derivate of rapamycin, [264]) was titrated in different concentrations against FKBP protein. As free tracer molecules possess a smaller molecular weight it can tumble more easi-

_____

ly compared to tracer molecule bound to an FKBP. This restriction of tumbling leads to a weaker depolarization of polarized monochromatic light, which can be detected by measuring the emission intensities.
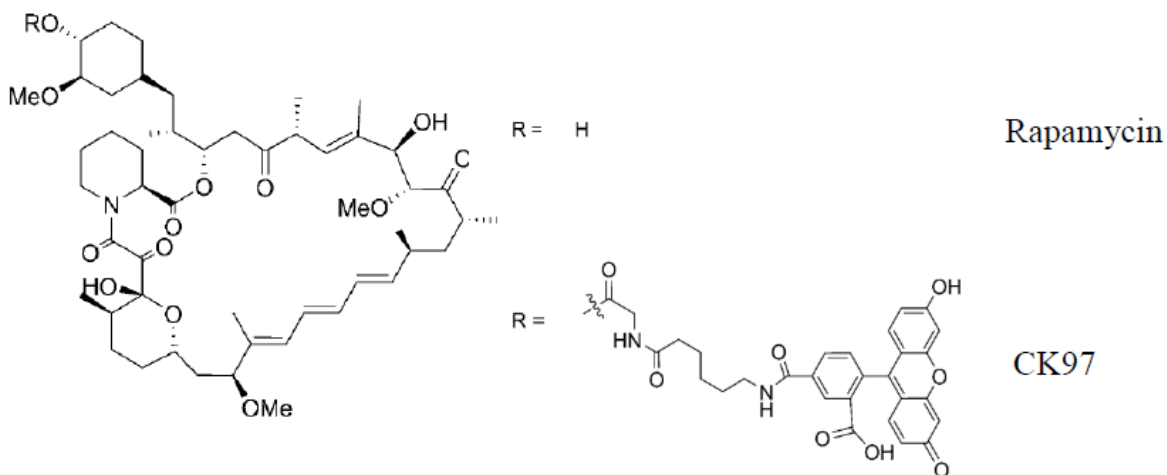
Because one CK97 binds with nanomolar affinity (Kd=0.11$\pm$0.03 nM) to exact one FK1 domain of FKBP51, one can state a 1:1 ratio of CK97 tracer molecule binding to FKBPs [264]. By adding a known concentration of CK97 to proteins of a dilution series which contains a correctly folded FK1 domain, the concentration of the protein solution can be estimated.

The assay was performed as following: In a 96-well low-binding Corning plate 16 wells in two rows were filled with each 50 µl of assay buffer. Another well contained 100 µl of a 20 µM dilution of the respective FKBP protein in assay buffer. From this well, 50 µl were transferred to the first well containing 50 µl of buffer and mixed well. Again, 50 µl were transferred to the next well. This transfer was repeated until the 1:1 dilution series of the protein was completed. The last well contained pure buffer.

Afterwards 25 µl of these dilutions were pipetted into a 384-well low-binding plate before 25 µl of a CK97 dilution (dependent of the FKBP51 usually between 1-200nM final concentration) in assay buffer were added (double final concentration). After 30 min of incubation at room temperature, a Tecan GENios Pro reader was used to determine fluorescence polarization values. The following settings were used:

> Mode: Fluorescence Polarization, end point
> Wavelengths: Excitation: 485 nm; Emission: 535 nm
> Number of reads: 10; Integration time: 100 µs
> T: 25°C

_____

The depolarization (P) of linear polarized light was measured by the emission intensities (I) of parallel (par) and perpendicular (per) light in μsec range after excitation:

$P = ((I_{parallel} - I_{perpendicular}) / (I_{parallel} + I_{perpendicular}))x100$

A plot of mP units against the protein concentration created a dose-response curve that could be analyzed by "Four-Parameter-logistic-curve" fitting in SigmaPlot. This analysis also revealed EC_{50} values that represent a protein concentration at which half of the protein is bound to ligand. The formula is depicted as follows:

$$y = min + \frac{(max - min)}{1 + (^x/_{EC_{50}})^{-Hill\ slope}}$$

min = minimum mP value

max = maximum mP value

The concentration of FKBPs was determined by either multiplication of the calculated EC50 value with the concentration of 50% of the CK97 tracer molecule in nM or, which is exacter, by generation of several curves as exemplified in section 8.2 for FKBP52.

Table 4.2 summarizes used FKBP proteins and their concentrations. Where indicated proteins were purified and characterized by Christian Kozany*, Veronika Kupfer**, Andreas März# or Alexander Kirschner~.

_____

Protein	concentration (µM)	determined by
FKBP12*	600	active site titration
FKBP12.6#	100	active site titration
FKBP13#	20	active site titration
FKBP25#	20	active site titration
FKBP51_FLAG	15.2	active site titration
FKBP52_FLAG	116	active site titration
Cyp40_FLAG*	60	active site titration
FKBP51FK1**	583	active site titration
FKBP51FK1 (ITC experiments)	848	active site titration
FKBP51ΔFK1_FLAG	19.7	UV spectroscopy
FKBP51TPR# (FKBP51ΔFK1FK2)	-	inactive, as determined by active site titration
FKBP51FK1F67V**	150	active site titration
FKBP51FK1F67I**	292	active site titration
FKBP51FK1F67L**	176	active site titration
FKBP51FK1F67M**	442	active site titration
FKBP51FK1F67A**	189	active site titration
FKBP51FK1F67G**	135	active site titration
FKBP51FK1F67S**	136	active site titration
FKBP51FK1F67T**	148.3	active site titration
FKBP51FK1F130Y**	79	active site titration
FKBP51FK1F122V**	302	active site titration
FKBP51F67V_FLAG*	167	active site titration
FKBP51FD67DV_FLAG*	9.9	active site titration
smFKBP51_FLAG~	4.9	active site titration

Table 4.2 Table of purified proteins used in different assays

_____

4.2.5   Determination of protein-protein interactions *in vitro*

4.2.5.1   GST pulldown assay

Pulldown assays are *in vitro* methods used to determine a physical interaction between two or more proteins. For this procedure a tagged protein can be captured on resin material, forming a complex that allows simple fishing of interacting proteins. The assays were performed in 500 µl final volume in NETN buffer + 1 mM DTT.

NETN buffer :   20 mM Tris-HCl [pH 8.0], 100 mM NaCl, 1 mM EDTA, 0.5% igepal, 50mM glycerophosphate and 10 mM NaF, 0.5 mM sodium dihydrogen orthovanadate

20 µl resin solution (50%) were incubated and thereby saturated with 22 µM GST tagged protein. Afterwards the resin was washed 3 times with NETN buffer + 1mM DTT. 15.2 µM FKBP were added followed by 3 h of incubation at 4°C under rotation.

Finally the resin was collected by centrifugation, washed 5 times with each 1 ml NETN buffer + 1mM DTT and boiled in 20 µl SDS sample buffer. The supernatant was subjected to SDS gel electrophoresis and immunoblotting.

4.2.5.2   FLAG pulldown assay

In principle the FLAG pulldown assay was performed as the GST pulldown assay. 20 µl FLAG M2 magnetic column (50%) saturated with FKBP_FLAG proteins were incubated with 50 nM Akt protein (active or inactive) in 500 µl NETN buffer + 1mM DTT at 4°C. The next day the resin was collected, washed 5 times with NETN buffer + 1mM DTT and eluted with FLAG peptide according to manufacturer's instruction. The elution was subjected to SDS-PAGE and immunoblotting.

_____

4.3   Cell biological methods and cell based assays

4.3.1   Cell lines and growth conditions

All human or mouse cell-lines were generally cultured at 37°C and 5% CO_2 in a humidified incubator. Cell growth occurred as adherent culture in standard 125 cm^2 cell culture bottles. For HeLa, HEK293T, SU.86.86 standard DMEM containing phenol red was supplemented with 10% fetal calf serum and 1% penicillin/streptomycin solution. For MEF, MEF51-/- and MEF52-/- cells standard DMEM without phenol red was supplemented as described. As for SH-SY5Y cells DMEM+GLUTAMAX was supplemented with 10% FCS, 1% non-essential aminoacids and 50 µg/ml gentamycin. For selection of SH-SY5Y-shFKBP12 100 µg/ ml hygromycin was added.

4.3.2   Maintenance of cells

When cell density at the bottom of the cell culture bottles was too high for further cell division, the cell culture was split.

During this procedure, DMEM medium was removed, and the cells were washed with approximately 10 ml of PBS under mild agitation. After the PBS was removed, 500 µl of trypsin/EDTA dilution was added and distributed evenly. Cells were incubated for 5 min at 37°C (or until all cells detached from the plastic surface), resuspended in 10 ml DMEM medium and singularized by pipetting up and down. To get rid of residual trypsin, the suspension was centrifuged for 5 min at 1000 g, and the cell pellet was resuspended in fresh supplemented DMEM. The cell suspension was then distributed into several bottles, culture dishes or 6-well plates. Finally, the original volume was re-established by filling up with supplemented DMEM.

4.3.3   Cell transfection

4.3.3.1   Transfection with Lipofectamine 2000 reagent

For transient protein expression in eukaryotic cells, lipofection is widely used as a convenient method to insert a plasmid. An advantage compared to transfection with Calcium phosphate is the higher transfection efficiency.

Transfections were performed as recommended by the manufacturer. Most transfections were performed in a 6-well plate format. Cells were transfected as soon as they reached 80 % confluency. Plasmid DNA and Lipofectamine 2000 for 1 well were prepared as following:

_____

2.5 µg plasmid DNA (Midi-Prep or Mega Prep)	in 250 µl DMEM medium
10 µl Lipofectamine 2000	in 250 µl DMEM medium

After 5 min of incubation at room temperature, the two components were combined and mixed thoroughly. During the following 20 min of incubation time, formation of DNA lipid vesicles occurred.

The cells were prepared for transfection by washing them with PBS and supplying them with 7 ml DMEM/ 10 % FCS. 500 µl of the transfection mixture were added drop wise and carefully to the cells. The dishes were swayed mildly and incubated at 37°C and 5% CO_2 in the incubator. After one day the medium was changed and the cells were cultivated for another 24 h. Thereafter the cells were harvested or treated as indicated.

4.3.3.2   Transfection with Lipofectamine LTX reagent

For transfection of SH-SY5Y-shFKBP12 cells with pcDNA3_FLAG_FKBP12_mut_siRNA Lipofectamine LTX was used due to its lower toxicity compared to Lipofectamine 2000. By using Lipofectamine LTX the Plasmid/Lipofectamine complex can incubate for a longer time. Medium was not changed for 48 h which lead to higher transfection efficiency. This experiment was performed in a 96-well plate format. For each well the following amounts were used:

0.1 µg plasmid DNA (Midi-Prep oder Mega Prep) and 0.1 µl PLUS reagent in 5 µl Opti-MEM	
0.5 µl Lipofectamine 2000	in 5 µl Opti-MEM

After 10 min of incubation time the solutions were mixed and incubated for another 30 min. Finally the mixture was added to the cells supplied with 100 µl DMEM/ 10%FCS.

4.3.3.3   Transfection using calcium phosphate $Ca_3(PO_4)_2$

2xHBS buffer:	0.1 M Hepes, 0.56 M NaCl, 3 mM Na_2HPO_4, pH 7.0

This is a cheap alternative to transfection with commercially available transfection reagents. However one has to be aware that the efficiency is less. Density of the cells should be 60-70%. For transfection of a 10 cm dish in an reaction tube 20-25 µg plasmid DNA and 74 µl sterile 2M $CaCl_2$ solution were filled up to 600 µl total volume with sterile water. While this solution was gently mixed, 600 µl of 2 x HBS were added drop wise. Immediately after, the whole mixture was given directly and drop wise to the cells. After an incubation of 24 h at 37°C and 5% CO_2 in an incubator, the medium was removed. The cells were washed with

_____

PBS, supplied with DMEM/10% FCS and incubated for another 24 h. Then cells were harvested or used in other assays.

4.3.4 Starvation, stimulation and treatment of cells

In order to investigate the influence of stimulation of Akt/mTOR pathway by growth factors transfected or untreated cells were starved. For this purpose, normal medium was removed, cells were washed once with PBS and fed with starvation medium (DMEM with 1% antibiotics) for at least 16 h. Afterwards, cells were kept in DMEM with 10% FCS and/or 100nM insulin. Simultaneously, compounds were added to the wells when indicated. After the indicated amount of incubation time at 37°C and 5% CO_2, the cells were washed twice with PBS and harvested. As starvation did not influence the FKBP/Akt interaction cells were not starved if not otherwise stated but only supplemented with 10% FCS for stimulation.

4.3.5 Lysis of eukaryotic cells

NETN Lysis buffer: 20 mM Tris-HCl, pH 8.0; 100 mM NaCl; 1 mM EDTA; 50mM glycerol
                       phosphate; 10 mM NaF; 0.5 mM sodium dihydrogen orthovanadat;
                       0.5% igepal; 1 % (v/v) protease inhibitor cocktail;
                       1 mM PMSF
                       and 1mM DTT, always freshly added

Desoxycholate buffer: 20 mM Tris-HCl, pH 8.0; 100 mM NaCl; 1 mM EDTA; 50mM glycerol
                       phosphate; 10 mM NaF; 0.5 mM sodium dihydrogen orthovanadat;
                       1% (w/v) sodium desoxycholate; 1% (v/v) protease inhibitor cocktail;
                       1 mM PMSF

In order to harvest transfected cells, the plate was put on ice and washed three times with ice-cold PBS. All liquid was drained as thoroughly as possible before 60 µl of lysis buffer were added. The cells were removed from the surface using a cell scraper and the suspension was transferred to a pre-cooled reaction tube. This lysis mixture was then incubated for 20 min at 4°C with vigorous shaking (1200 rpm) before it was cleared by 20 min of centrifugation at 13000 g and 4°C in a tabletop centrifuge. The supernatant was transferred to another tube and analyzed for total protein concentration by BCA assay.

_____

4.3.6 Co-Immunoprecipitation (Co-IP) with FLAG/HA affinity resin

IP elution buffer: 150 µg/ml FLAG peptide in TBS

                            100 µg/ml HA in TBS

Co-Immunoprecipitation is a method to investigate physical interaction of proteins. In contrast to pulldown assays this interaction can occur directly as well as mediated by a part of a hetero-complex. Anti-FLAG/HA affinity resin contains the corresponding antibody covalently linked to the resin material. Tagged proteins can be captured easily from lysates. As the binding does not depend on quality or quantity of a primary antibody, yields are optimized, and handling is much easier. To prepare the material for use, the affinity resin was washed two times with TBS. A third washing step was used for equilibration with NETN buffer + 1 mM DTT or desoxycholate buffer. 1 mg of total protein in cell lysate were combined with 25 µl of 50% resin suspension, filled up to a volume of 500 µl and incubated for at least 2 h at 4°C under mild agitation. Afterwards the supernatant was removed, the pelleted resin was washed carefully up to 6 times with each 1 ml lysis buffer. For elution of bound proteins, the resin was resuspended in 30 µl FLAG/HA buffer and incubated for 10 min at 4°C under agitation. The beads were collected by the magnet (Flag beads) or the mixture was shortly centrifuged to pellet the beads. The supernatant was supplemented with an equal volume of 2xSDS sample buffer and incubated at 95°C for 5 min. 20 µl of this mixture were separated on a SDS gel.

4.3.7 Immunoblotting

Blotting buffer: 20 mM Tris; 150 mM glycine; 0.02% (w/v) SDS; 20% (v/v) methanol

Ponceau S: 0.5% (w/v) Ponceau S; 3% (v/v) acetic acid

TBS-T: TBS; 0.05% (v/v) Tween 20

5% milk powder: TBS-T; 5% (w/v) skimmed milk powder

10% milk powder: TBS-T; 10% (w/v) skimmed milk powder

Primary antibody: 2 µg antibody in 2 ml 5% milk powder (1:1000)

Secondary antibody: 1 µg antibody in 5 ml 10% milk powder (1:5000)

ECL1:   100 mM Tris/HCl, pH 8.5; 440 mg/l luminol,

                       150 mg/l p-coumaric acid

ECL2:   100 mM Tris/HCl, pH 8.5; 30% (v/v) H_2O_2

or commercial ECL solutions (Millipore)

_____

The immunoblotting procedure was performed according to recommendations of Invitrogen:

After protein separation on a SDS gel (section 4.2.3.2) the proteins were transferred to the nitrocellulose membrane Protran BA 83 in the blotting chamber "XCell II Blot Module". The chamber was filled with blotting buffer before protein transfer was started by applying a current of 400 mA for 60-70 min.

Afterwards, the membrane was stained in Ponceau S solution for 2 min and then destained in water to an appropriate degree. Successful blotting was confirmed by complete transfer of all pre-stained molecular marker bands. Well positions were marked before the membrane was destained completely in distilled water.

Membranes were blocked in 5% skimmed milk powder solution for 30 min at room temperature. After a short washing step with TBS-T, the membrane was kept overnight at 4°C with mild agitation in a dilution of the primary antibody. Membranes were washed three times for 5 min with large volumes of TBS-T. Next, the membrane was incubated in a dilution of the secondary antibody for 60 min at room temperature. Finally the blots were washed again (3 x5 min) with TBS-T.

The luminescence reaction was started by combining 2 ml ECL1 and 2 ml ECL2, and adding the mixture immediately to the membrane. After 1 minute of incubation the blot was developed with the ChemiDoc MP developing machine. Pictures were taken and the optimal exposure time was saved and analyzed by ImageLab 4.0. Some of the Western blots were developed using medical X-ray films.

4.3.8 Cell viability assay

Cell viability was assessed using the CellTiter-Fluor Cell Viability assay from Promega according to manufacturer's protocol. Briefly, cells were plated into a 96-well plate in Dulbecco's Modified Eagle Medium without phenol red and treated for 48-72 h with the in each section indicated compounds. Thereafter, CellTiter-Fluor reagent was added and cells were incubated at 37°C for 30 min. Fluorescence was measured at an excitation of 370 nm and an emission of 520 nm using a Tecan GENios Pro reader. DMSO treated cells served as control and were correlated with treated cells.

4.3.9 Cell based phosphorylation assays for Akt and mTOR

Cells were plated one day before the phosphorylation assay was performed. To prevent cell loss during the assay procedure, plates were coated with Poly-D-Lysine (10 µg/cm^2) for 1h Thereafter, the Poly-D-Lysine was removed and the plate was washed with sterile water. The cells were plated in 96-well plates in DMEM containing 10%FCS and cultivated overnight.

Methods

_____

Phosphorylation at Akt(S473), Akt(T308) and mTOR(S2448) was assessed using a homoge-
neous time-resolved fluorescence assay (Cisbio, Codolet, France) according to the manufac-
turer's recommendations. Briefly, cells were incubated with 10 µM FKBP ligand or 100 nM
torin-1 for 60 min. Cells were lysed and the lysates were transferred to a white 384-well
plate. After addition of d2-labelled anti-Akt or anti-mTOR antibody and K-labeled anti-
phospho-Akt or anti-phospho-mTOR antibody, the mixtures were incubated at room tempera-
ture for 4 h or overnight. FRET efficiency was determined by the emission ratios
665nm/620nm after excitation at 320 nm using a Tecan GENios Pro reader. The data were
normalized to the results for Torin-1 (0 %) and DMSO (100%).

_____

4.4 Physicochemical methods

4.4.1 Isothermal Titration Calorimetry (ITC)

Bacterially expressed, affinity purified human HisFKBP51FK1 (aa 1-140) (see section 4.2.1) was dialyzed against ITC buffer (20 mM HEPES pH= 8, 150 mM NaCl, 5% DMSO). The activity was confirmed by active site titration in an FP assay (see section 4.2.4.3) The pH of protein was determined and ligand solutions were degassed and matched within 0.02 pH units. All experiments were conducted at 20°C. Compound YW 703 (1 mM) was measured by injection into the measurement cell containing the protein (89 μM).

Due to the limiting solubility compounds YW644 and YW703 were measured in a reverse setup injecting the protein (0.5 mM and 0.16 mM, respectively) into a solution of the ligand (40 μM for YW644, 15 μM for YW691). Heats of dilution were measured in blank titrations and subtracted from the binding heat values. ORIGIN software (version 7.0 Microcal) was used for data collection and analysis.

5. Results

5.1 Interactions with FKBPs

5.1.1 The FKBP51/Akt/PHLPP complex in HEK293T cells

To confirm the findings by Pei *et al.* [75] HEK293T cells were co-transfected with FKBP51_FLAG and HA_Akt1. After controlling the input a co-immunoprecipitation was performed. Anti-FLAG M2 beads were used as bait as well as anti-HA agarose. Additionally two buffer systems were used to reduce the background signal:
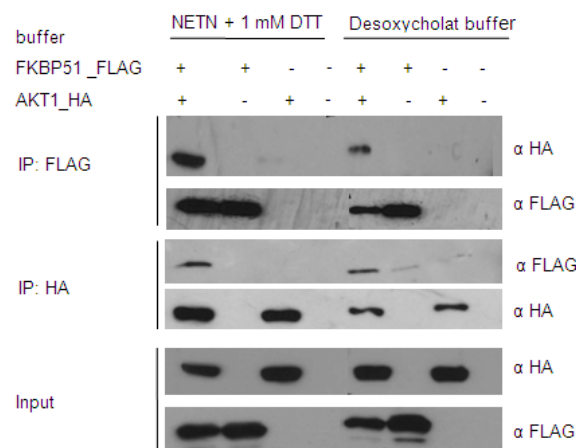
Figure 5.1: FKBP51 and Akt1 can be co-immunoprecipitated.
HEK293T were transfected with HA_Akt1 and the FKBP51_FLAG. After two days the lysates were co-immunoprecipitated (Co-IP) and analyzed by Western blotting.

A clear interaction of FKBP51 and Akt1 (lane 1 and 5) could be detected independent of the used detergents. The immunoprecipitation was possible with both, the HA tagged Akt1 and the FLAG tagged FKBP51 as bait. In order to control for unspecific binding, FLAG or HA beads were incubated with lysates containing the prey but not the bait protein.

Since the obtained co-immunoprecipitation signal was stronger with NETN buffer this buffer was used for further experiments, if not otherwise stated.

As members of the FKBP family are highly homologous to each other we asked if other FKBPs are able to bind to Akt1. Therefore, HEK293T cells were co-transfected with different FKBP subtypes fused to an N-terminal FLAG tag and HA_Akt1.
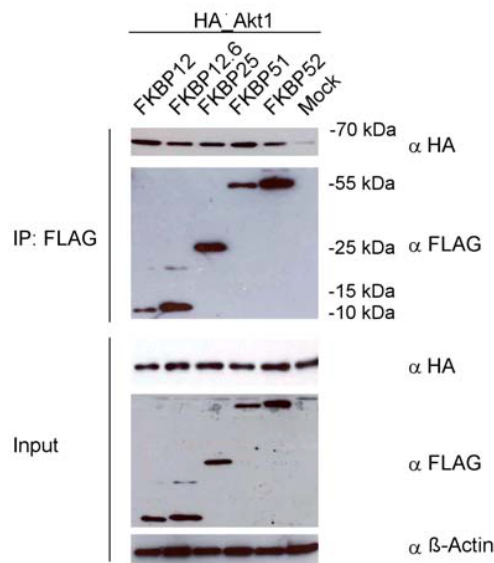
Figure 5.2: FKBP subtypes can be co-immunoprecipitated with Akt1
HEK293T were transfected with HA_Akt1 and FLAG tagged FKBP subtypes. After two days the cells were lysed in NETN buffer, co-immunoprecipitated (Co-IP) and analyzed by Western blotting.

Surprisingly, Akt1 also co-immunoprecipitated with FKBP52, FKBP25 and even with the smaller FKBP12 and 12.6, which consist only of the FK506-binding domain [22, 43].

According to Pei *et al.* [75] the phosphatase PHLPP can also be found in complex with FKBP51, which could be generally confirmed. Figure 5.3A shows a clear co-immunoprecipitation signal when HA_PHLPP1 and FKBP51_FLAG are overexpressed. The amount of co-immunoprecipitated PHLPP2 (Figure 5.3B) is not as high, nevertheless the signal is still slightly above background intensity. This interaction was repeatedly observed as can be seen in Figure 5.5, lane 1 and 2.
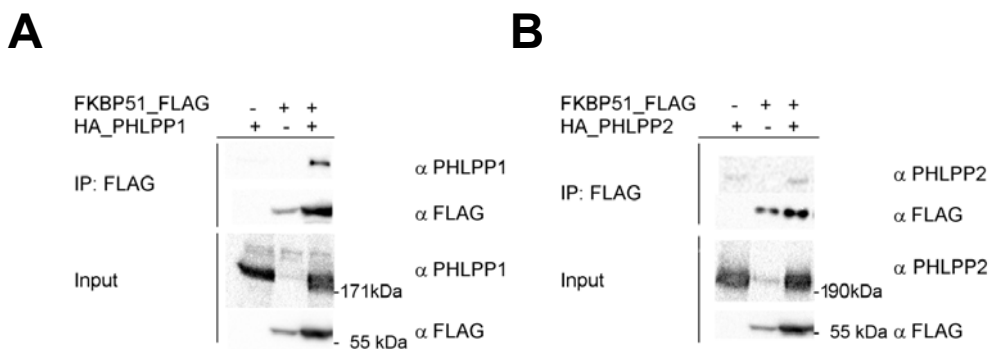
Figure 5.3: FKBP51 can be co-immunoprecipitated with PHLPP1 and PHLPP2
HEK293T were transfected with HA-tagged PHLPP and FLAG tagged FKBP subtypes. After two days the lysates were co-immunoprecipitated (Co-IP) and analyzed by Western blotting.

The detection level for endogenous Akt was too low, therefore, HEK293T cells were transfected with PHLPP1, Akt2 and FKBP51 and FLAG immunoprecipitation was performed (Figure 5.4). PHLPP1 is the specific phosphatase of Akt2 [171]. By immunoprecipitating FKBP51_FLAG from the lysate we could also isolate the Akt2/PHLPP1 complex. However the overexpression of Akt does not seem to influence Akt2/PHLPP1 interaction (compare lanes 1 and 2 with lanes 5 and 6) as similar amounts of PHLPP are co-immunoprecipitated.
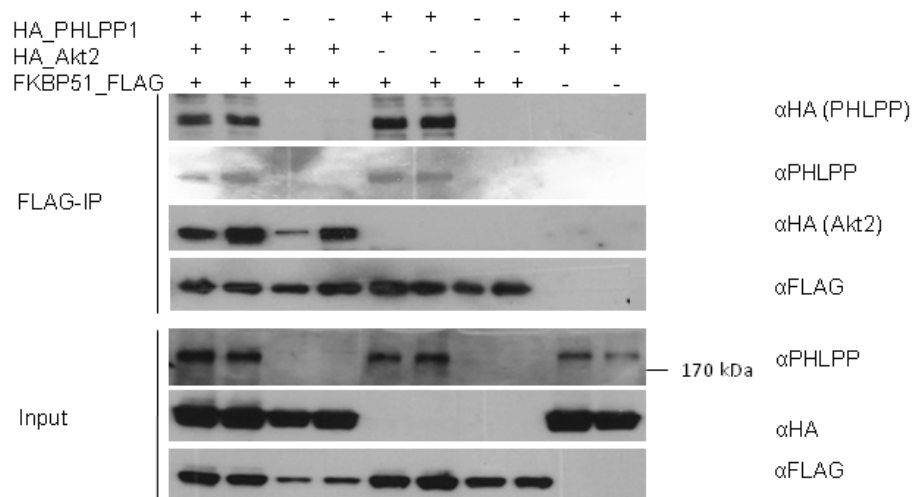
Figure 5.4: FKBP51, Akt2 and PHLPP1 form a complex
HEK293T were transfected with HA-tagged PHLPP1, FLAG tagged FKBP51 and HA tagged Akt2. After two days, the lysates (NETN-buffer) were FLAG co-immunoprecipitated (FLAG-Co-IP) and analyzed by Western blotting.

To explore the potential influence of regulatory regions of PHLPP on the FKBP/PHLPP interaction, HEK293T cells were transfected with PHLPP2, PHLPP1 or the deletion mutants PHLPP1ΔN (aa127-aa1205) and PHLPP1ΔC (aa1-aa1202) [170]. Western blot analysis revealed that PHLPP1 and all modified PHLPP2 proteins can co-immunoprecipitate with FKBP51. At least for FKBP51/PHLPP1 interaction neither the N-terminus nor the very C-terminus containing a PDZ binding motif are important.
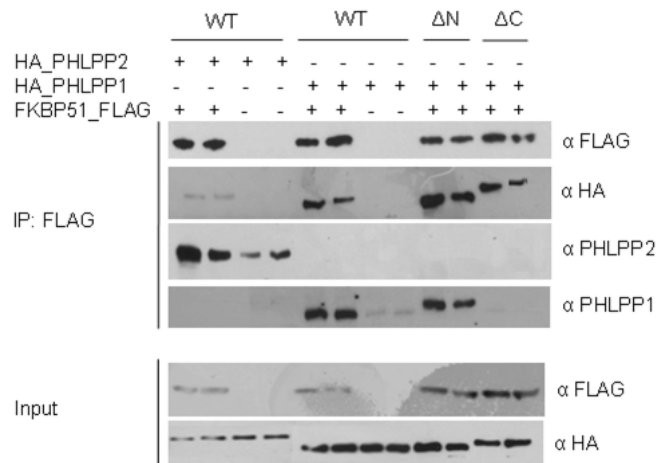
Figure 5.5: The PDZ binding motif of PHLPP1 and the N terminus are not important for FKBP51 binding

HEK293T were transfected with FLAG-tagged FKBP51, HA-tagged PHLPP1, HA-tagged PHLPP2 or two PHLPP1 mutants missing either the N-terminus (aa 1-126) or the three last aminoacids (aa 1203- aa 1205). After two days the lysates (NETN buffer) were FLAG co-immunoprecipitated (FLAG-Co-IP) and analyzed by Western blotting.

5.1.2 The interaction between Akt and FKBP is direct

Direct protein-protein interactions can be tested by pulldown assays. To do so, the proteins were incubated together for a certain amount of time in an appropriate assay buffer. Afterwards the proteins are pulled from the solution using antibody-coupled beads. In addition to the interaction partner, which binds directly to the antibody coupled beads (for example via a FLAG tag) one can find binding partners of the precipitated protein. After elution potential interaction partners can be analyzed on a SDS gel. To analyze the interaction of FKBP51 with Akt1, FKBP51 was purified as described (section 4.2.1.). Protein concentration was 15.2 µM as determined by active site titration.
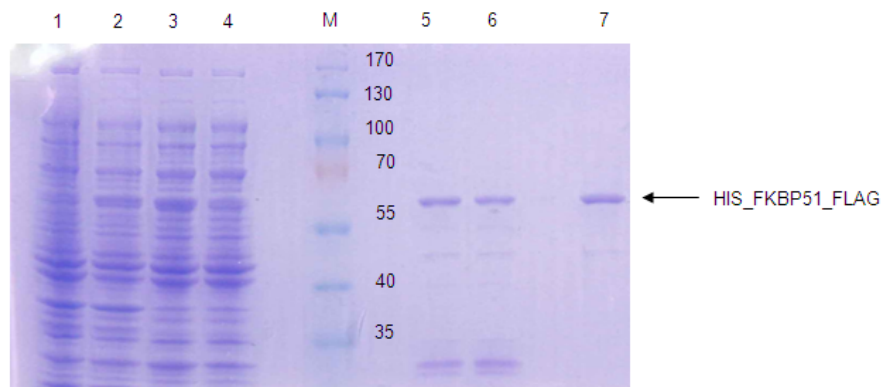
Figure 5.6: Recombinantly expressed FKBP51 is sufficiently pure

Each step was loaded to a SDS protein gel. After separation the gel was stained with Coomassie Brilliant Blue. 1: lysed bacteria before induction with IPTG, 2: lysed bacteria after IPTG induction, 3: protein solution loaded to the nickel column, 4: flowthrough of the nickel column, M: protein marker (in kDa), 5: load of the FLAG column (1:10 diluted), 6: flowthrough of the FLAG column, 7: elution after the FLAG column=purified protein.

As interaction partner commercially available inactive Akt protein was used.

For estimation of the quantity of Akt protein, which would still be detectable different amounts of protein were loaded to a SDS gel and a Western blot analysis was performed. Dependent on exposure time 0.4 ng of Akt protein are still detectable, if exposed long enough.

With this result the appropriate amounts of protein needed for a pulldown assay were determined (Figure 5.7).
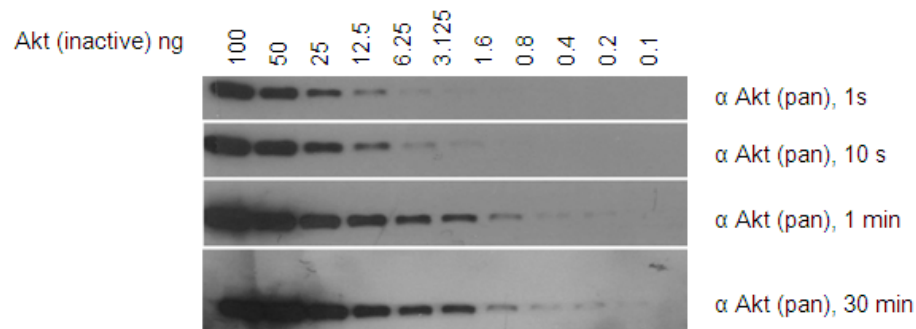
Figure 5.7: With 30 min exposure time 0.4 ng of inactive Akt are still detectable by western blot analysis
0.2-100 ng Akt (inactive) were loaded to a SDS gel. After separation the gel was blotted and the bands were analyzed.

Finally, a direct interaction of Akt/FKBP51 could be shown by a pulldown assay (Figure 5.8). Inactive Akt1 and FKBP51 can be found in complex (lane 2). To control for unspecific signals controls were prepared, which miss either of the two proteins. The most critical control is the one for unspecific binding to the beads (lane one). Intense washing procedures were necessary to reduce background binding.
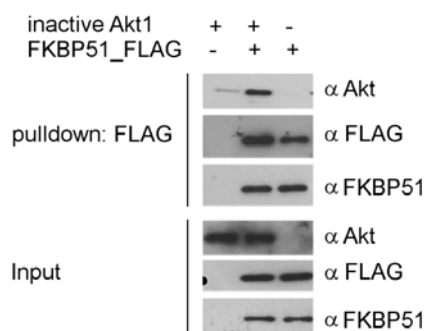
Figure 5.8: In FLAG pulldown assays inactive Ak1 and FKBP51 form a complex
Purified FLAG-tagged FKBP51 and purified inactive Akt were mixed, subjected to a FLAG pulldown and analyzed by Western blotting.

5.1.3 Numerous FKBPs can bind directly to Akt

For further confirmation and to test if other closely related FKBP family members would also form a complex with Akt1 a reversed pulldown assay was performed, using purified GST_Akt1^{S473D} [267], a GST-tagged constitutively active Akt mutant, as well as purified FKBP protein. FKBPs were purified using a protocol established in our lab [264]. Because FKBP13 is located in the lumen of the endoplasmatic reticulum [27] and thus unable to interact with cytoplasmic Akt, we didn't include it in further analysis.
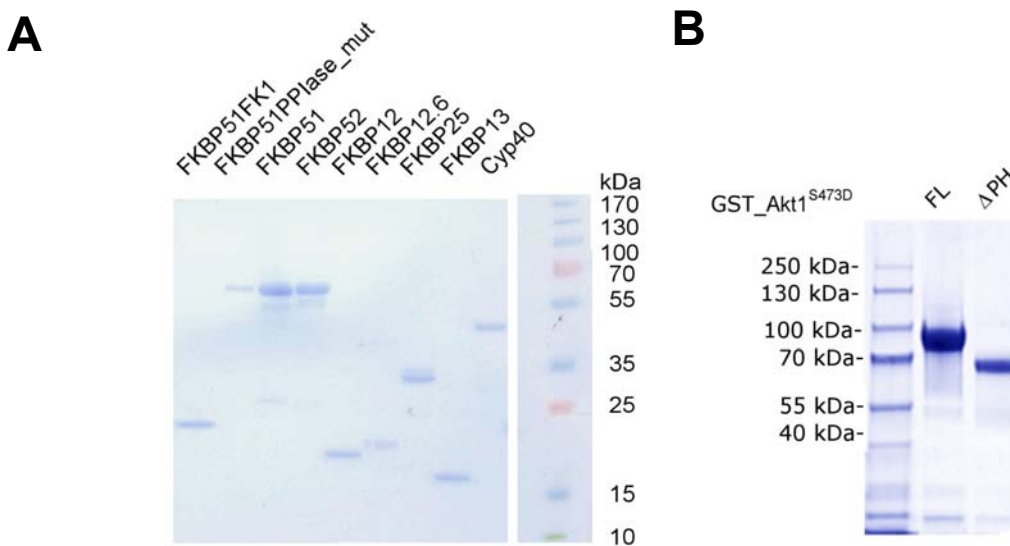
Figure 5.9: Recombinantly expressed FKBPs and a constitutively active Akt1 mutant are pure
Proteins were loaded to SDS protein gels, separated and the gels were stained with coomassie blue. **A** FKBP proteins were pure and active, as tested in FP assays **B** GST_Akt^{S473D} full length and a mutant missing the PH domain, which attaches Akt to the cell membrane for activation, were purified for further assays (courtesy of S. Neimanis)

Afterwards the pull down experiment was performed. Indeed all tested FKBPs bound to Akt1^{S473D} -loaded beads (Figure 5.10A) but not to empty beads or beads loaded with GST alone (B). No interaction was observed with purified Cyp40 [265], a closely related immunophilin.

A
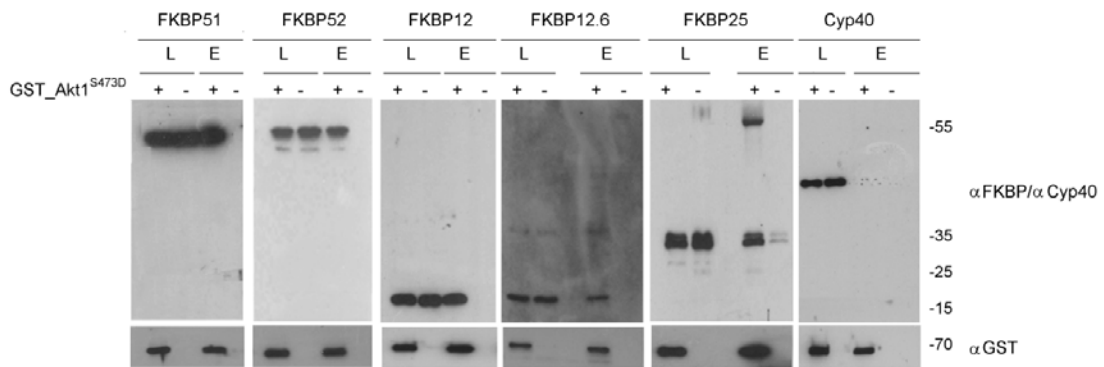
B
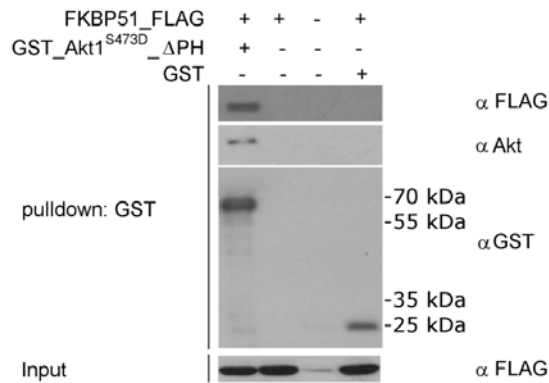
Figure 5.10: Akt1 binds to several FKBPs and this interaction is direct
A Purified FKBPs and purified GST-tagged Akt1S473D (mimicking an active conformation) were subjected to a GST-pulldown followed by Western blotting. Cyclophilin40, which also harbors a TPR domain, but no FK domains, was used as a negative control (Ld = load (0,8%), E = elution (100%)). **B** To test for unspecific GST binding to FKBP51_FLAG a pulldown assay was performed: purified GST or GST_Akt1[S473D] were incubated with purified FKBP51_FLAG.

5.1.4 Squirrel monkey FKBP binds stronger to Akt compared to human FKBP51

Over 30 years ago high circulating cortisol levels were described in squirrel monkeys *(Saimiri boliviensis)*, leading to the concept of cortisol resistance of the glucocorticoid receptor (GR) in New World primates [51, 52]. Glucocorticoid receptor binding is generally negatively regulated by FKBP51 (compare section 1.1.2), which is overexpressed in *Saimiri boliviensis* [48, 55]. Human FKBP51 (hsFKBP51) and squirrel monkey FKBP51 (smFKBP51) are highly homologous (94% protein sequence homology) but individual amino acids differences that contribute to the altered effect on glucocorticoid receptor (GR) inhibition could not be identified [55].

Having the importance of smFKBP51 in mind pulldown experiments with smFKBP51 and hmFKBP51 were performed.

A coomassie stained SDS gel of the purified protein can be seen in Figure 5.14. Figure 5.11. shows the interaction between hsFKBP51 and GST_Akt^{S473D}_ΔPH and smFKBP51 and GST_Akt^{S473D}_ΔPH.
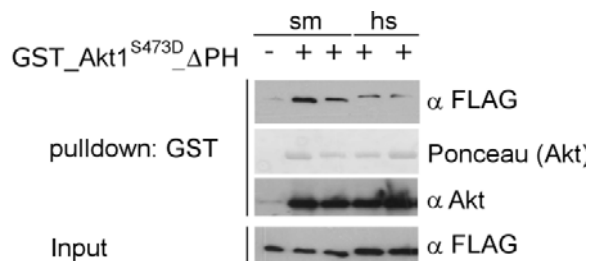
Figure 5.11: The interaction between smFKBP51 and Akt is more pronounced than the interaction between hsFKBP51 and Akt
GST_Akt1^{S473D} missing the PH domain was coupled to Glutathione-beads and the beads were incubated with either smFKBP51 or hsFKBP51 in duplicates. Elutions were loaded to SDS gels and Western blot analysis was performed.

smFKBP51 leads to a stronger signal in Western blot analysis indicating a tighter or less transient interaction.

5.1.5 FK1 domain mutations do not influence Akt/FKBP interaction in pull-down assays

The FK1 domain of FKBP51 was shown to be the crucial domains for the inhibitory activity on GR, while the PPIase activity was dispensable [55]. To investigate the role of the FK1 domain or the PPIase activity of FKBP51 on the interaction with Akt we used a panel of isolated FKBP51FK1 mutants and performed pulldown assays with GST_Akt1^{S473D}. The functionality of the FKBP51 proteins (with exception of the FKBP51 ΔFK1 construct) was verified by active site titration for the FK506-binding pocket ([264] and section 4.2.4).

A
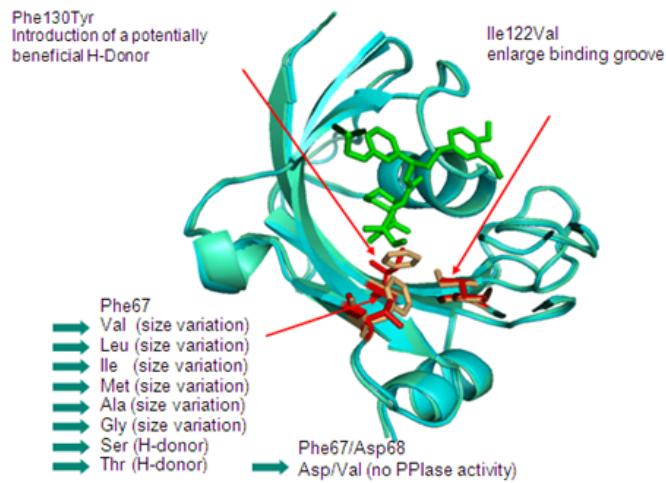
B
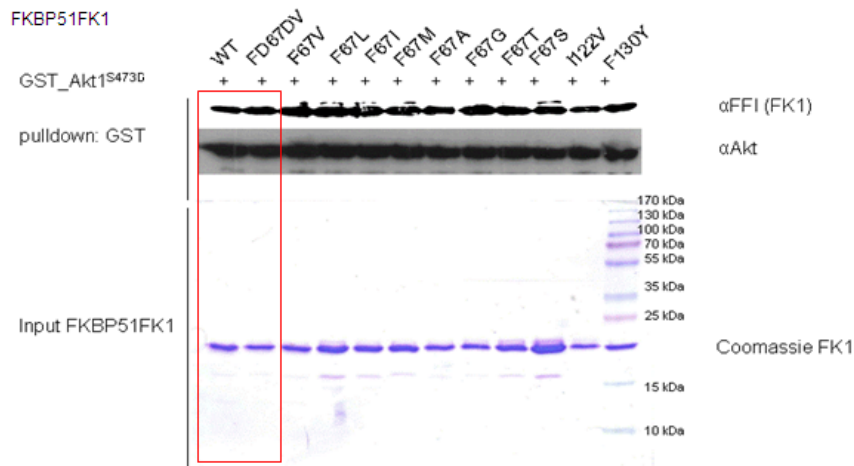
Figure 5.12: FKBP51FK1 mutants can interact with GST_Akt1[S473D]

A Three aminoacids of the endogenous FKBP51FK1 domain (ochre) were mutated (red) to smaller aminoacids to enlarge the binding groove or to introduce potentially beneficial H-donors (modified after C. Kozany).

B GSH beads loaded with purified GST-tagged Akt1[S473D] were incubated with the indicated FLAG-tagged FKBP51FK1 constructs for 3 h. After elution a Western blot analysis was performed and detected with an antibody which detects the FK1 domain of FKBP51 (αFFI). The independency of the PPIase activity is highlighted (red box).

None of the tested FKBP51FK1 mutants showed an altered binding mode to GST_Akt1[S473D].

Importantly the FKBP51FK1 domain alone is able to bind Akt1.

5.1.6 Multiple domains of FKBP51 contribute to the binding to Akt1

We next aimed to further map the domains of FKBP51 that interact with Akt. Figure 5.13. shows the different modifications applied to FKBP51.
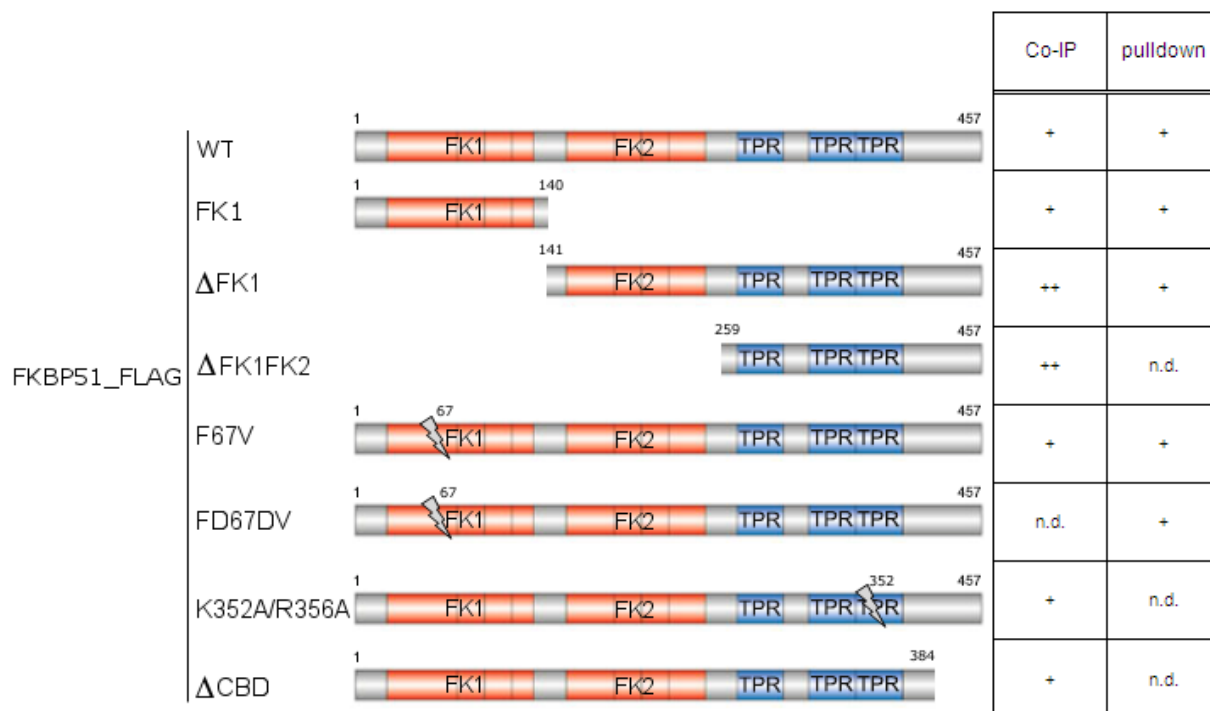
Figure 5.13: Left: Overview of the constructs used to map the FKBP51/Akt interaction.
Right: Summary of the Akt interactions of FKBP domains investigated in HEK293T cells by immunoprecipitation or by pulldown with purified proteins (WT= wildtype, n.d. = not determined).

To test the capacity of multiple domains of FKBP51 to interact with Akt we continued with pulldown assays using purified proteins. A coomassie stained gel depicting purified FKBP51 FK1 domains can be seen in Figure 5.12. Figure 5.14 shows additional constructs tested in pulldown assays (except FKBP51TPR which is also named FKBP51ΔFK1FK2). The functionality of the FKBP51 proteins (with exception of the FKBP51ΔFK1 construct) was verified by active site titration for the FK506-binding pocket ([264] and section 4.2.4.3).
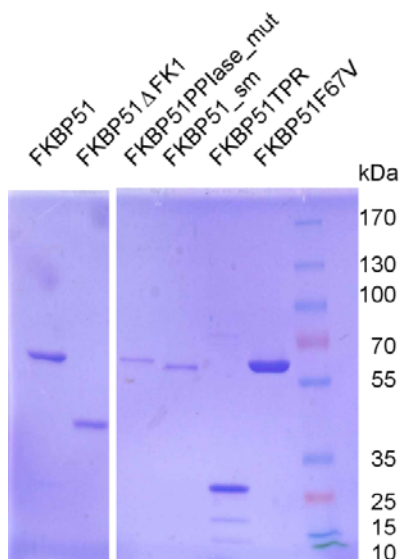
Figure 5.14: Recombinantly expressed hsFKBP51, hsFKBP51 containing various mutations and smFKBP51
Proteins were loaded to SDS protein gels, separated and the gels were stained with coomassie blue.

Again, all FKBP51 constructs were retained by Akt1 to a similar extent. Here, especially the interaction of GST_Akt1^{S473D} with an FKBP51 mutant lacking the FK1 domain should be pointed out.
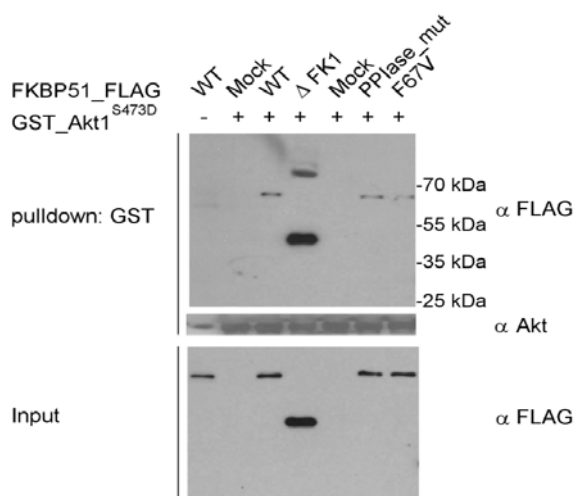
Figure 5.15: Pulldown assays demonstrate the contribution of different protein structures to FKBP51/Akt interaction
A GSH beads loaded with purified GST-tagged Akt1^{S473D} were incubated with the indicated purified FLAG-tagged FKBP51 mutants for 3 h. After elution a Western blot analysis was performed.

For verification of these results under more physiological conditions experiments with HEK293Tcells were performed. First, mutants with truncated FK506-binding domain (ΔFK1) and the FK1-like domain (ΔFK1FK2) were tested. Both deletion constructs co-immunoprecipitated with overexpressed Akt1 (Figure 5.16A). We also co-expressed Akt1 with two FKBP51 mutants where the PPIase activity of the FK1 domain or the Hsp90-binding

capacity of the TPR domain was abolished. Furthermore a construct lacking the putative C-terminal calmodulin binding site and the isolated FK506-binding domain (FK1) were tested.
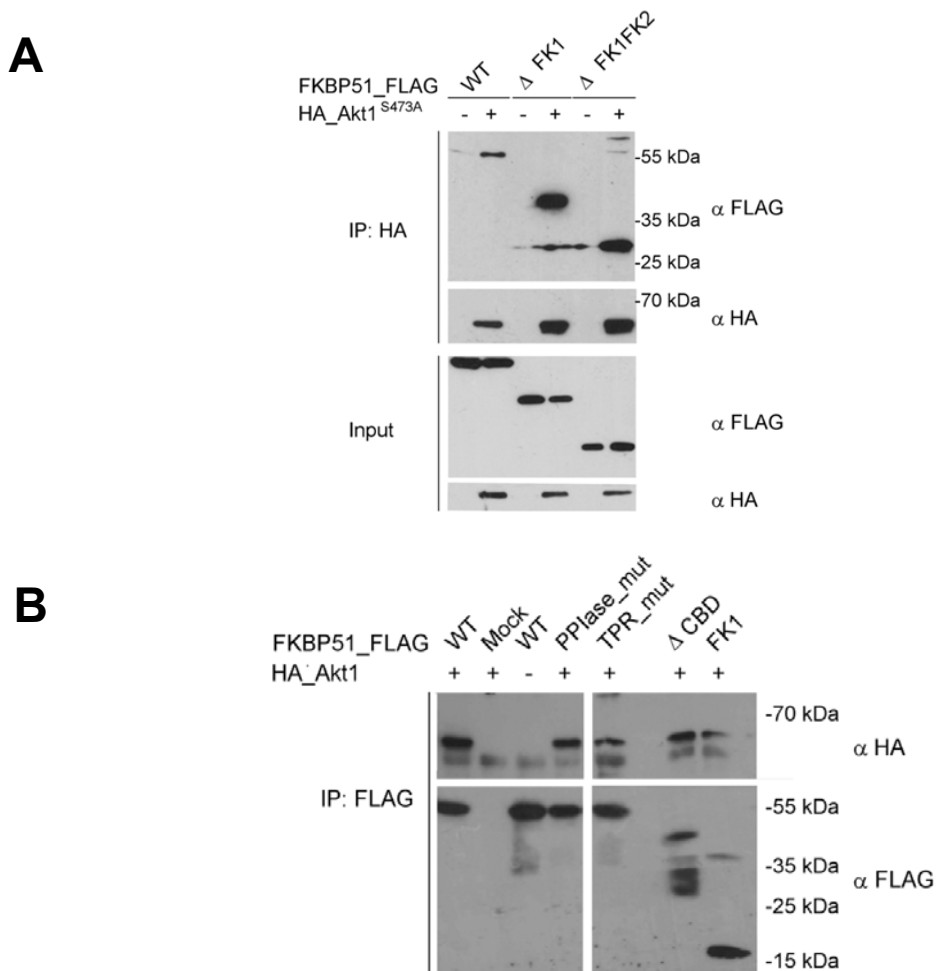
Figure 5.16: In HEK293T cells multiple domains of FKBP51 contribute to FKBP51/Akt1 interaction
HEK293T cells were transfected with the indicated constructs. **A+B** After 48 h lysates were prepared and HA- or FLAG-immunoprecipitation was performed, followed by Western blotting.

Again, in all cases, Akt1 co-immunoprecipitated with the FKBP51 constructs, although with slightly reduced efficiency for the mutants (Figure 5.16B).

5.1.7 FKBP51 can bind to multiple AGC kinases

It was shown that FKBP51 binds to the highly homologous proteins Akt1 and Akt2 but not to Akt3 [75]. Binding to Akt2 could be confirmed after FLAG co-immunoprecipitation from HA_Akt1 and FKBP51_FLAG co-transfected HEK293T cells. Cells only transfected with HA-Akt2 but not with FKBP51_FLAG was used to rule out unspecific binding to the beads.
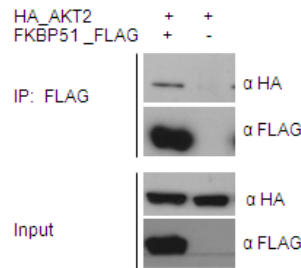
Figure 5.17: FKBP51 can be co-immunoprecipitated in HEK293T cells with overexpressed Akt2
HEK293T cells were co-transfected with FKBP51_FLAG and HA_Akt2. Cells were harvested after 48 h of growth, the input was controlled and co-immunoprecipitation was applied. Finally, the elutions were loaded on a SDS gel, blotted and incubated with the indicated antibodies.

Akt1 and Akt2 and Akt3 belong to the kinase subgroup containing PKA, PKG and PKC (AGC kinases). As depicted in the alignment of representative examples of this kinase group in Figure 5.18 the kinase motif (Akt1: aa149-aa408 according to human protein reference database) is highly conserved. The protein sequence identity of the kinase domains of the Akt homologs SGK1, p70S6K and PKA-C$_{beta}$ calculated by PRALINE [269] was 57%.

Results by A. März [14] showing p70S6K to co-immunoprecipitate with FKBP51 implicated to investigate a possible glucocorticoid kinase (SGK) /FKBP51 complex. Therefore HEK293T cells were co-transfected with GST_ΔN SGK_wildtype or GST_ΔN SGK^{S422D}, which harbors an activating S422D mutation and FKBP51_FLAG.
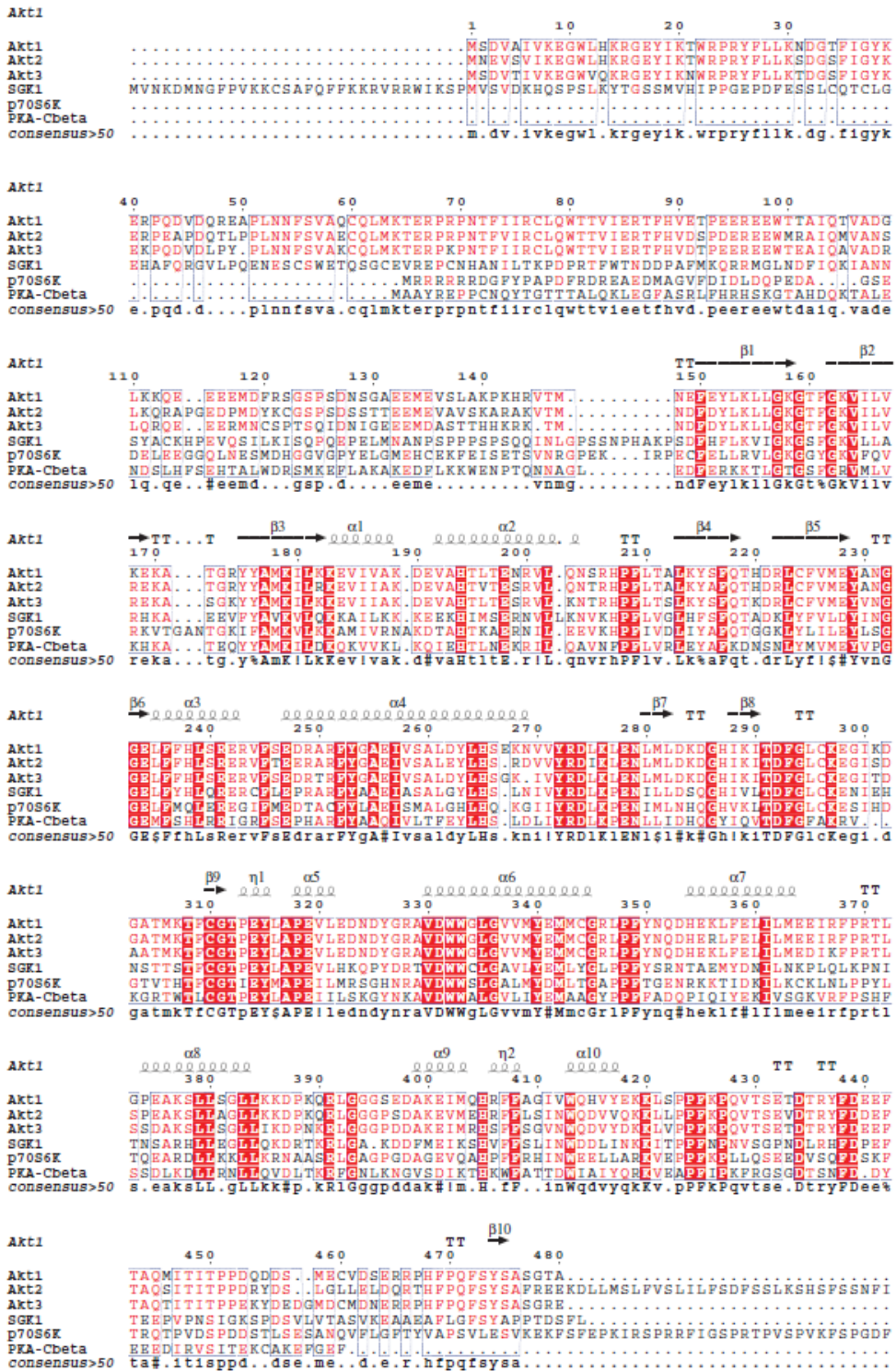
Figure 5.18: The kinase domain of AGC kinases is highly conserved

Sequence alignment of the AGC kinases Akt1, Akt2, Akt3, SGK1, p70S6K, PKA-C$_{beta}$: aminoacid sequences were aligned using Multialin interface [268].

Secondary-structure elements (PDB code: 4EKK) of the kinase domain and numbering for Akt1 are indicated above the sequences. Similar residues are shown in red and identical residues are shown in bold lettering on a red background. Frames indicate homologous regions. The consensus sequence is shown at the bottom (Endscript 1.1).

Figure 5.19 shows that both, wildtype SGK1 and SGK1^{S422D}, clearly co-immunoprecipitate with FKBP51 to a similar extent as GST-tagged Akt1. The detected interaction is clearly higher than the background seen in the control lanes (lanes 7-12).
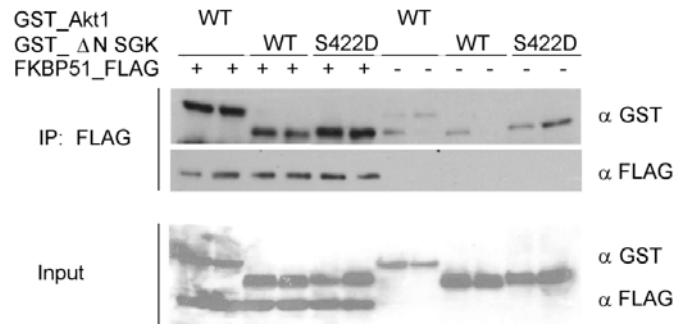
Figure 5.19: In HEK293T cells SGK1 and FKBP51 can be found in complex
HEK293T cells were co-transfected with either GST_ΔN SGK_wildtype or GST_ΔN SGK^{S422D}, which harbors an activating S422D mutation and FKBP51_FLAG or the SGK constructs alone. After 48 h the cells were lysed. FLAG beads were used to fish for FKBP51. By analyzing the co-immunoprecipitated proteins GST_ΔN SGK or GST_ΔN SGK^{S422D} can be clearly detected.

5.1.8 Influence of the PH domain of Akt and its phosphorylation status on the interaction with FKBP51

As wildtype SGK and putative active SGK were found to co-immunoprecipitate with FKBP51 to the same extend we focused on activation status of Akt. Therefore, pull-down assays with full length Akt and with an Akt construct lacking the PH domain were performed. Unspecific binding was controlled by incubating GST tagged Akt constructs with empty beads (Figure 5.20).
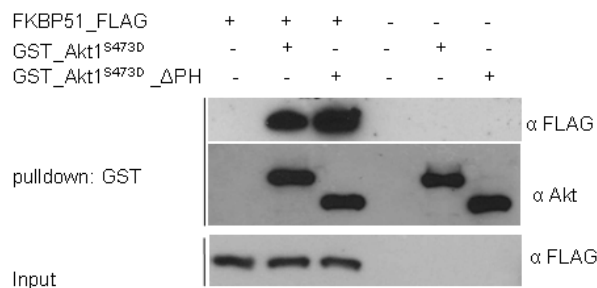
Figure 5.20: For Akt1/FKBP51 interaction the PH domain is not obligatory
Purified GST-tagged active Akt or a mutant, lacking the PH domain, was incubated with purified FLAG-tagged FKBP51. Lane 4-6 served as controls. After 3 h, the interaction was tested by GST pulldown and Western blotting.

HEK293T cells transfected with GST_Akt1^{S473D}_ΔPH and FKBP51$^{K352A/R356A}$ (TPR_mut) were analyzed for the influence of the PH domain. Again, no importance of the PH domain on Akt1/FKBP interaction was observed.
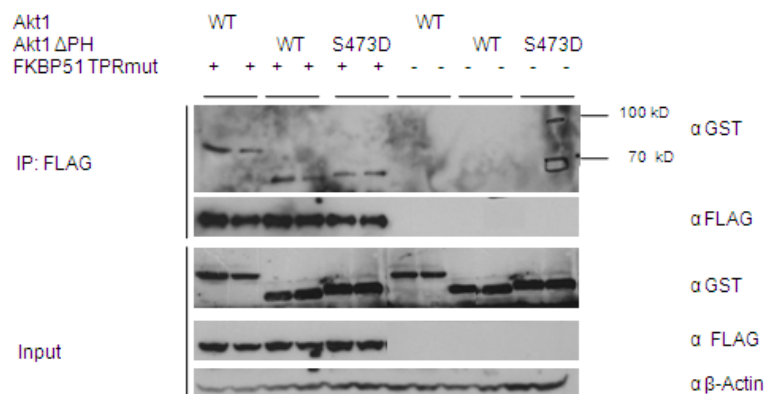

**Figure 5.21: In HEK293T cells the PH domain is not mandatory necessary for FKBP51/Akt interaction.**
HEK293T cells were co-transfected with either GST_Akt1 or GST_Akt1_ΔPH and FKBP51TPR_mut (prevents interaction with Hsp90). After 48 h the cells were lysed. FLAG beads were used to immunoprecipitate FKBP51.

Both constructs interacted identically with FKBP51 indicating that the PH domain is not necessary (lane 1 and 2 and lane 3 and 4). This is consistent with the observed S6K/Akt and SGK/Akt interaction, two kinases which are lacking the PH domain. The conformation and activity of Akt1 is regulated by phosphorylation at T308 and S473. To investigate the influence of these important sites immunoprecipitation assays with HEK273T cells co-expressing FKBP51 (containing a TPR-mutation to exclude confounding influences of Hsp90) were immunoprecipitated together with Akt1 containing a series of phosphorylation-resistant (alanine) or Phospho-mimetic (aspartate) substitutions at T308 and/or S473. In addition, a mutant, where threonine in position 450 (turn motif) was substituted by alanine, was included. This mimics a missing phosphorylation of the turn motif which is necessary for Akt stability [273].
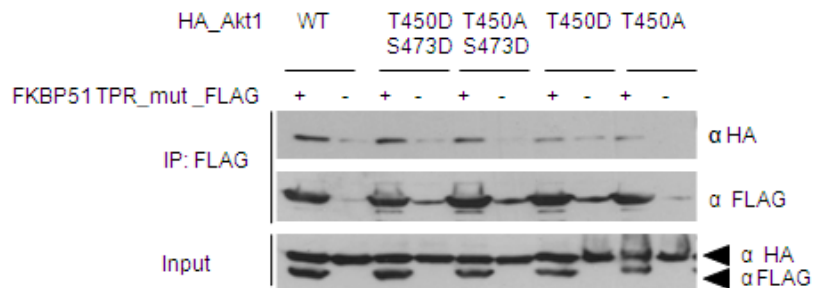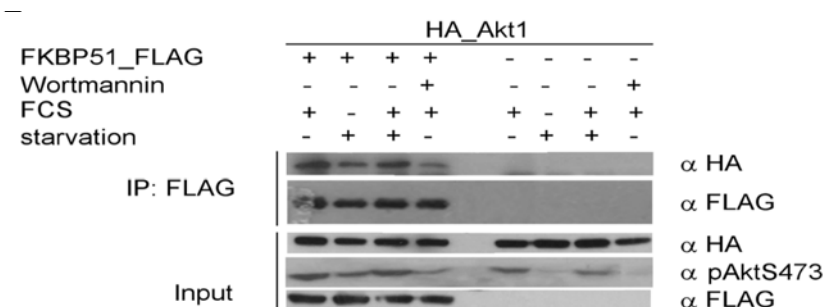
A
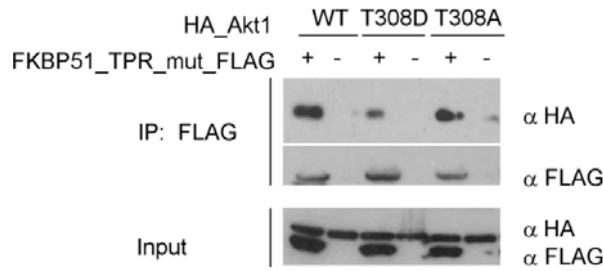
B
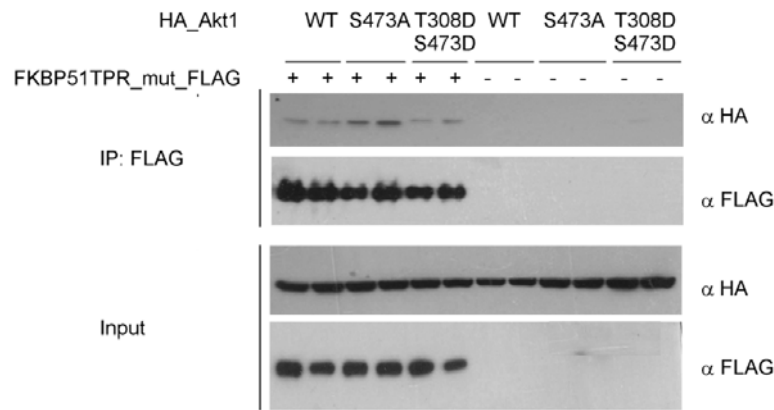
C

Figure 5.22: Phosphorylation status is not important for the Akt1/FKBP51 interaction – Mutational analysis of the influence of phosphorylation sites on FKBP51/Akt interaction

HEK293T cells were transfected with the indicated HA-tagged Akt1 phosphorylation site mutants (alanine mimics the phosphorylation resistant state and aspartate the phosphorylated state) with or without co-transfected FLAG-tagged FKBP51$^{K352A/R356A}$ (TPR_mut). After 2 days cells were collected, lysed, immunoprecipitated and analyzed by Western blotting. **A** Investigation of position T308 within the activation loop **B** Investigation of position S473 within the hydrophobic motif (duplicates were analyzed) **C** Analysis of the influence of pT450 (turn motif)

All tested Akt constructs co-immunoprecipitated specifically with FKBP51 but not with the mock-transfected controls. The phosphorylation status of T308 in the activation loop of Akt and T450 within the turn motif was not important for the interaction with FKBP51 under these

cellular conditions whereas the phosphor-resistant mutation S473A (Figure 5.22B) slightly increased binding of FKBP51.

Next the Akt activation status was controlled by stimulating or starving the cells or by inhibition of the PI3K pathway using wortmannin (Figure 5.23.).

As expected starvation (lane 2) and wortmannin treatment (lane 4) reduced phosphorylation of Akt at S473 and correlated with a slightly reduced binding to FKBP51. The underlying reasons for the discrepancy to the results observed with the S473A mutant remain to be established. Contrary to the findings by Pei *et al.* [75], we observed an increase –not a reduction– in Akt S473 phosphorylation upon co-expression of FKBP51.

Figure 5.23: Phosphorylation status is not important for the Akt1/FKBP51 interaction – Pharmacological analysis of the influence of import phosphorylation sites on FKBP51/Akt interaction

HEK293T cells were starved for 16 h, stimulated with FCS for 45 min or treated with wortmannin. Controls were incubated in the presence of 10% FCS and treated with DMSO. Cells were lysed, immunoprecipitated and analyzed by Western blotting.
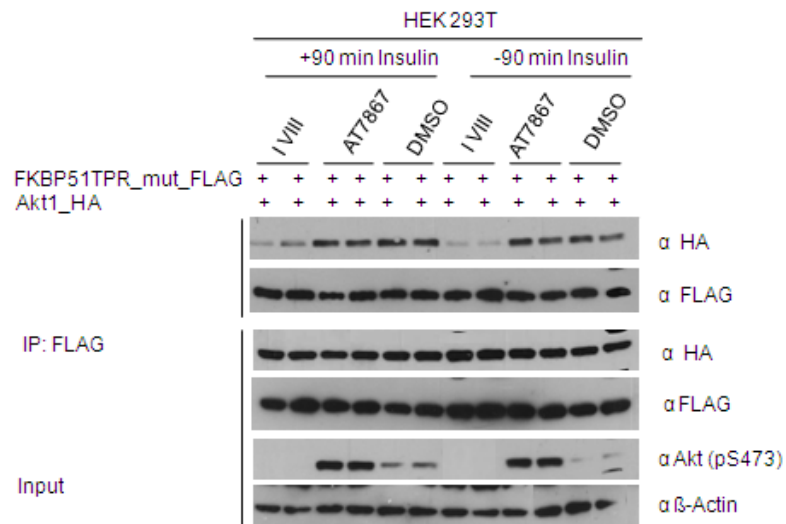
5.1.9   The FKBP51/Akt interaction depends on the conformation of Akt

As demonstrated in section 5.1.8 the Akt1/FKBP51interaction doesn't seem to be mediated by a single site. Therefore the conformation of Akt was sought to be controlled more directly using Akt conformation-specific inhibitors (see section 1.5.2). The classical ATP-competitive inhibitor AT7867 (Figure 5.24A - lanes 3, 4 and 9,10) binds and stabilizes the activated 'PH out' conformation of Akt (PDB code 2UW9) [255] and thereby prevents access of phosphatases [258]. In contrast the allosteric inhibitor VIII (lanes 1,2 and 7,8) intercalates between the PH and the kinase domain of Akt and locks the latter in a closed inactive conformation (PDB code 3O96) [261]. These two inhibitors were used to stabilize the conformation of Akt in cells. As expected, the ATP-competitive inhibitor (AT7867) led to Akt hyperphosphorylation [257, 258] but it did not affect the interaction with FKBP51. Stimulation didn't seem to have an influence at all and the results were identical (compare Figure 5.24A - left and right). This was confirmed *in vitro* by pulldown assays using the non-hydrolysable ATP analog AMP-PNP (Figure 5.24B). As described, the allosteric inhibitor completely abolished cellular Akt S473 phosphorylation [260]. Interestingly, this compound substantially reduced binding of Akt to

FKBP51. This suggests that in the conformation stabilized by inhibitor VIII the binding site with FKBP51 might be masked. It was not possible to study the AktΔPH, because the allosteric inhibitor VIII does not bind to Akt missing the PH domain.
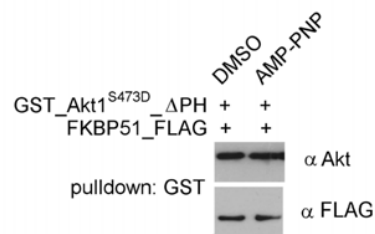
A

B

Figure 5.24: The FKBP51/Akt interaction depends on the conformation of Akt

A HEK293T cells were transfected with FLAG-tagged FKBP51[K352A/R356A] (TPR_mut) and HA-tagged Akt1. After 2 days one part of the cells was stimulated with insulin for 90 min. Additional cells were treated with 10 µM Inhibitor VIII, AT7867 or DMSO for 1h. Cell lysates and immunoprecipitated proteins were analyzed in duplicates by Western blotting. **B** GSH beads loaded with purified activated GST_Akt1ΔPH were incubated with FKBP51 with or without AMP-PNP. Elutions were analyzed by Western blotting.

5.2 Investigation of possible side effects of FKBP inhibitors with regard to the Akt/mTOR pathway

5.2.1 Gemcitabine's toxic effects on cell viability are not reduced by FKBP inhibitor FK1706

Since our group is especially interested in the synthesis of selective FKBP51 inhibitors to treat mental disorders, we were curious about the finding that FKBP51 could lead to a sensitization of pancreatic tumors to the nucleoside analogue gemcitabine, which is a clinically used chemotherapeutic agent [76]. If we could generally confirm this hypothesis, blocking FKBP51 in cancerous tissue would cause resistance to some chemotherapeutic treatments, which would not be tolerable.

Therefore the cell viability of SU.86.86 cells was examined by titration of gemcitabine together with FK1706 (10 µM), an FKBP inhibitor without immunosuppressive properties (see section 1.2.2, [142]). After 72 h gemcitabine dose-dependently reduced cell viability but this was not substantially altered by the presence of FK1706 (Figure 5.25A). Importantly, 10 µM of FK1706 alone did not affect the cell viability (Figure 5.25B).
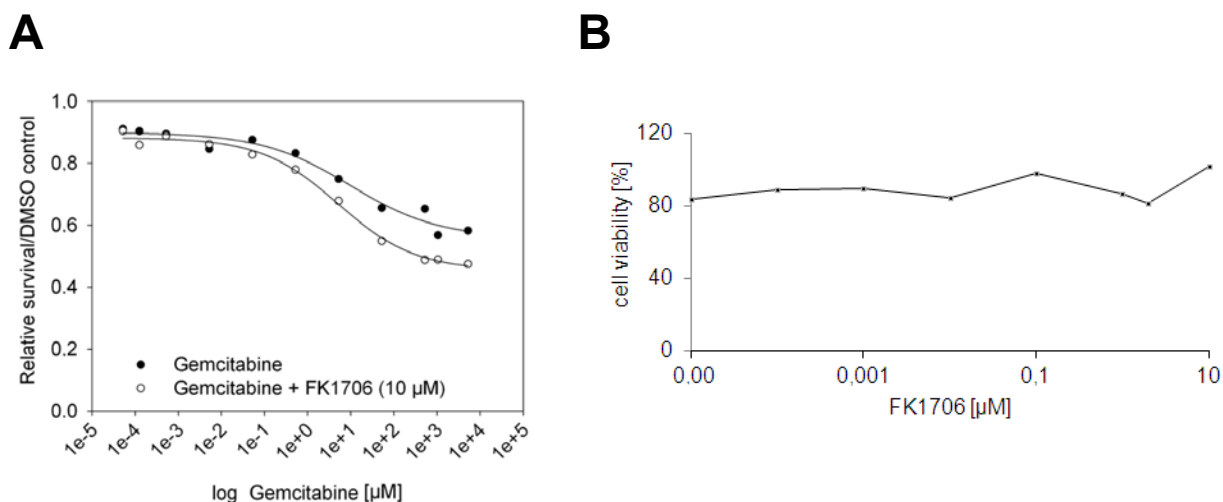

Figure 5.25: FK1706 does not influence gemcitabine's toxic effects on cell viability
A SU.86.86 cells were plated, cultivated for 3 h and afterwards treated with gemcitabine. After 24h FK1706 or DMSO were added. After altogether 72 h the cell survival relative to DMSO treated controls was determined. **B** SU.86.86 cells were plated to 10000 cells per well. Cells were incubated with increasing FK1706 concentrations after 24 h. After altogether 72 h cell a viability assay was performed using the CellTiter-Fluor Cell Viability assay (Promega).

5.2.2 Tested FKBP inhibitors do not influence Akt and Akt target phosphorylation

To further investigate an effect of FKBP inhibition on the Akt/mTOR signaling pathway it was tested, whether cellular Akt or mTOR phosphorylation would be affected by FKBP inhibitors (see section 1.2). Neither the Akt phosphorylation at T308 nor S473 (mTOR phosphorylation site) was affected in HEK293T cells treated with high concentrations of FK1706 (Figure 5.26A). Under equal conditions Akt phosphorylation at both sites was reduced by the highly potent and selective ATP-competitive mTOR inhibitor Torin-1 [274], while phosphorylation was enhanced by the ATP-competitive Akt inhibitor AT7867 (see section 1.5.2). This demonstrates that the assay was able to detect the dynamically regulation of Akt in these cells. Similar results were obtained for Akt (pS473) in FK1706- or FK506-treated SH-SY5Y (Figure 5.26B) and HeLa cells (Figure 5.26C). mTOR (S2448) phosphorylation was not altered after treatment in most samples as well. However, with compound FK1706 a significant reduction of mTOR phosphorylation was observed in HeLa cells, which could be due to a small sample size for this condition. In a similar experiment no effect was observed in FK1706 treated HeLa cells (Figure 5.47). Rapamycin, which served as control, showed the expected effects.

In addition the in-house synthesized FKBP inhibitors YW648, cmpd44 [148] and SG537 were tested (Figure 5.26D). Compound YW648 is a small molecule non-specific FKBP inhibtor, while the synthetic FKBP ligand cmpd 44 is more selective for FKBP12 compared to larger FKBPs. SG537 has an increased selectivity for FKBP51 compared to FKBP52.

In all experiments no significant influence on Akt phosphorylation at position T308 and S473 was observed. Furthermore, no changes in the mTOR phosphorylation status were observed.

These types of experiments were repeated and the results can be found in section 5.4.2.
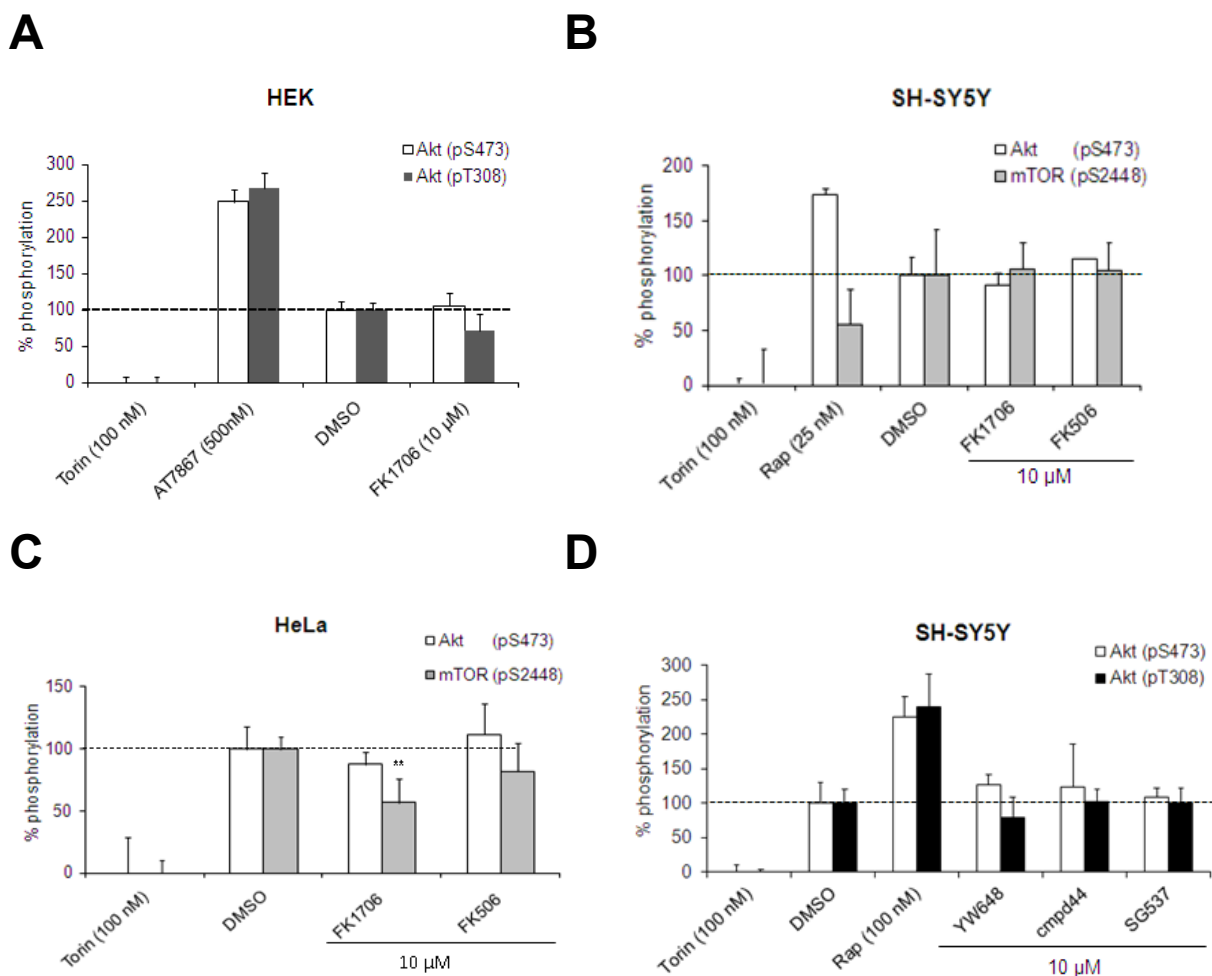
A

B

C

D

Figure 5.26: No influence of FKBP inhibitors on Akt or mTOR phosphorylation was seen in a homogeneous time re-solved FRET assay

A-D HEK293T, SH-SY5Y or HeLa cells were stimulated with FCS for 1 h in the presence of the indicated compounds. After cell lysis, cellular Akt- and mTOR phosphorylation was determined using a homogeneous time resolved FRET assay. For all experiments mean values of at least 2-3 data points ($\pm$ SD) are shown. Results were normalized to those of dimethyl sulfoxide (DMSO)-treated controls (100%) and torin-1 (0%) treated cells.

The values are presented as mean $\pm$ SD. Two-way analysis of variance (ANOVA) and a priori testing were used for statistical analysis. Compared with DMSO treatment: ** $p<.01$

With the exception of FK1706 mTOR phosphorylation in HeLa none of the FKBP ligand altered Akt (pS473), Akt (pT308) or mTOR (pS2448) significantly.

5.2.3 FKBP inhibitors do not disrupt the integrity of the FKBP51/Akt or of the FKBP51/PHLPP complex

The ability of several FKBP members to bind to Akt (section 5.1.3) suggested the FK506-binding pocket common to all of these proteins as an interaction site. Therefore it was tested if FKBP ligands blocking the PPIase domain could reduce binding of Akt to FKBP51. First, pulldown experiments were performed using purified FKBP51 and purified Akt^{S473D} as bait in the absence and presence of the high-affinity ligand rapamycin. The amount of FKBP51 that was specifically retained by Akt was not affected by an excess of rapamycin (Figure 5.27A).

Next, Akt was co-immunoprecipitated with FKBP51 or its TPR-mutant in the presence or absence of the non-immunosuppressive FK506 analogue FK1706 [142]. Binding of Akt was slightly reduced for the TPR-mutant but it was still significantly retained compared to background (Figure 5.27B). Treatment with FK1706 did not affect HA_Akt1 interaction with neither of the FKBP51 constructs. Similar results were obtained in cells treated with FK506 or rapamycin (Figure 5.27C).
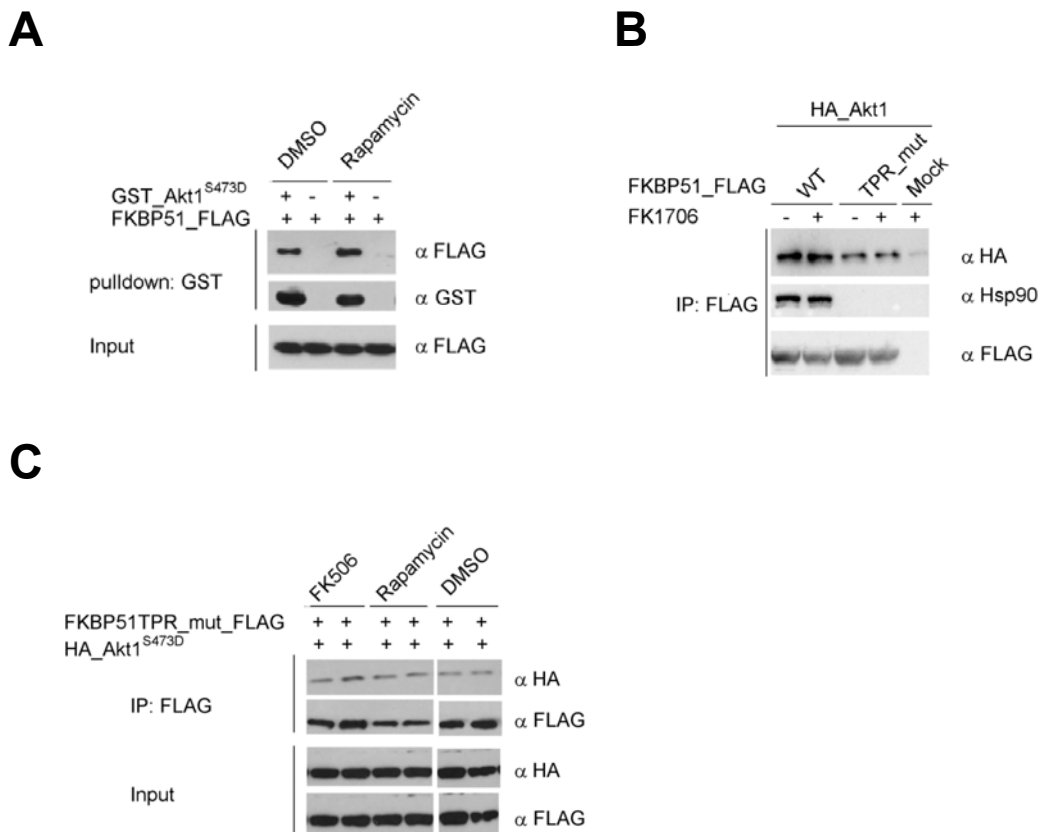

Figure 5.27: FKBP inhibitors do not disrupt FKBP/Akt interaction
A Purified proteins were mixed and treated with DMSO or Rapamycin (1µM). After 3h a GST-pulldown was performed followed by Western blotting. **B** HEK293T cells were transfected with the indicated constructs. After 48 h 1 µM FK1706 was added for 1 h. The lysates were immunoprecipitated and a Western blot was performed. **C** HEK293T transfected with the indicated constructs were treated with or without 1 µM FK506 or rapamycin 1 µM for 1 h followed by immunoprecipitation and Western blotting.

Since PHLPP is regulating Akt phosphorylation and is proposed to be part of the Akt/FKBP51/PHLPP complex [75] it was explored if FKBP inhibitors affected the FKBP51/PHLPP complex. As shown in Figure 5.28 FKBP inhibitors had no effect on the integrity of the complex of FKBP51 with PHLPP1 or PHLPP2.
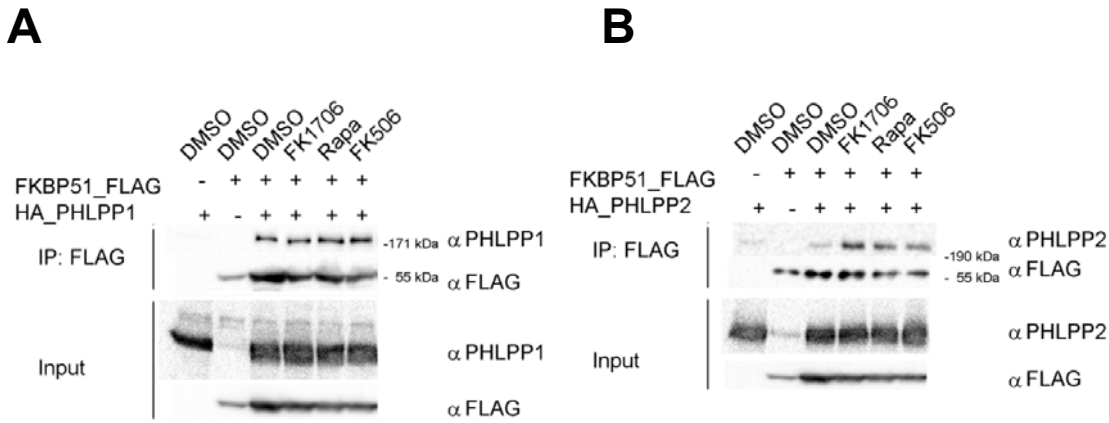
A   **B**

Figure 5.28: FKBP51/PHLPP interaction is not impaired by FKBP inhibitors
A and B HEK293T cells were transfected with FLAG_FKBP51 and HA-tagged PHLPP1 or HA-tagged PHLPP2. After 48 h FKBP inhibitors (10 µM) or DMSO were added for 1h. Lysates were immunoprecipitated and analyzed by Western blotting.

5.3 A chemical inducer of the FKBP51/Akt complex

5.3.1 Testing FKBP inhibitors for induction of the FKBP51/Akt complex

As stated in section 5.2 the tested FKBP inhibitors do not affect FKBP/Akt interaction. This is an important observation in order to evaluate possible side effects of these inhibitors. However, immunoprecipitation experiments with available FKBP inhibitors consistently revealed an enhancement of the Akt1/FKBP interaction by the natural product Antascomicin B (see section 1.2.2 [141]). For these experiments HEK293T cells were transfected with HA_Akt^{S473D} and FKBP51TPR_mut_FLAG, in order to exclude confounding influences caused by the Hsp90/FKBP interaction. After two days cells were treated for 60 min with 1µM of Antascomicin B or of the FKBP ligands FK506 and rapamycin (Figure 5.29).

After treatment cells were harvested, FLAG immunoprecipitation was performed and the immunoprecipitates were analyzed by Western blotting. Addition of Antascomicin B gives a unique and interesting result: Antascomicin B is the only compound that increases the FKBP51/Akt interaction. None of the other compounds shows a strong enhancement or decline in the FKBP51/Akt interaction.
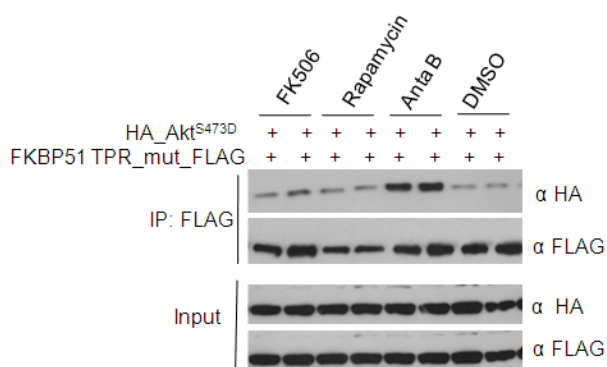

Figure 5.29: Antascomicin B enhances FKBP51/Akt1 interaction

HEK293T cells were transfected with the indicated constructs. After 48 h they were treated with 1 µM of FK506, Rapamycin, Antascomicin B (Anta B) or DMSO for 1h. After cell lysis a FLAG immunoprecipitation was performed, followed by protein separation on SDS gel and Western blotting.

5.3.2 Verification of induction of FKBP51/Akt interaction

To evaluate and further specify the newly discovered property of Antascomicin B a few control experiments were performed. Theoretically a stronger interaction between FKBP51 and Akt1 by Antascomicin B could be due to enhanced unspecific adsorption of Akt or FKBP51 alone to the beads due to changes in pH, charge or other influences by the compound. To

control for this, HEK293T cells were transfected in duplicates with FKBP51_FLAG and HA_Akt1. Before harvesting Antascomicin B was added for 60 min. Thereafter, the lysates were FLAG co-immunoprecipitated and analyzed by Western blotting. No Antascomicin B-induced signal was observed, neither in cells transfected with FKBP51 (Figure 5.30, lane 3, 9) or Akt1 (lane 5, 11) alone. The signal intensity was clearly enhanced when both proteins were transfected together and Antascomicin was added (compare lane 1 with lane 2 and lane 7 with lane 8).
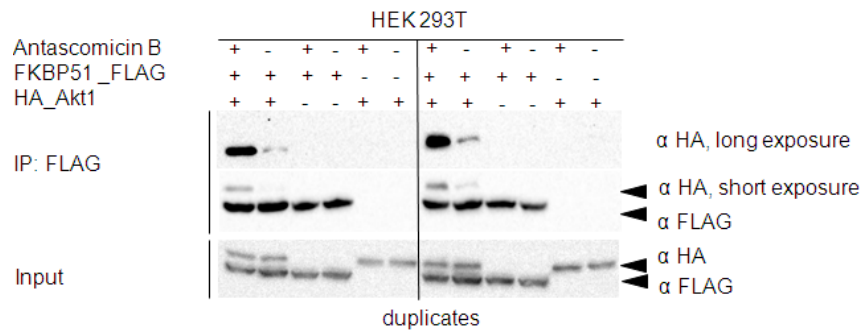

Figure 5.30: Induction of FKBP51/Akt1 interaction by Antascomicin B seems to be specific
HEK239T cells were transfected with FKBP51_FLAG and HA_Akt1. Cells were treated with 1 µM Antascomicin B for 60 min. After 48 h cells were harvested and FLAG co-immunoprecipitated.

To determine the potency of Antascomicin B for induction of the FKBP51/Akt complex HEK293T cells were double transfected with the indicated constructs and treated for 60 min with increasing concentrations of Antascomicin B (0 nM, 0,1 nM, 1 nM, 10 nM, 100 nM, 1000 nM). Duplicates were tested. After FLAG co-immunoprecipitation and Western blotting a clear dependency on titrated Antascomicin B could be seen. A concentration of 1 µM leads to the most intense effects. Therefore all subsequent experiments were performed with 1 µM Antascomicin B if not otherwise stated.
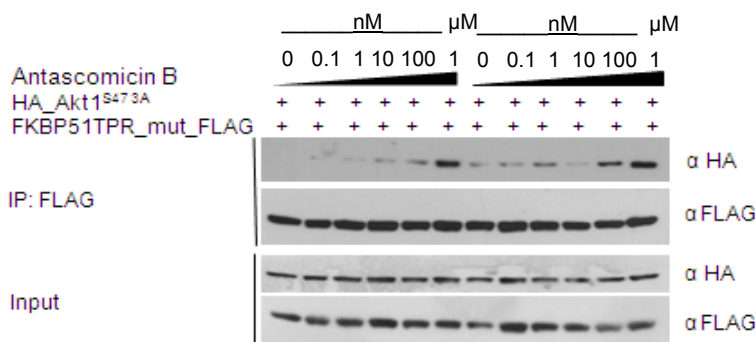

Figure 5.31: Antascomicin B mediated enhancement of the Akt1/FKBP51 interaction is concentration dependent
HEK293T cells were transfected with the indicated constructs. After growth for 48 h cells were treated with increasing concentrations of Antascomicin B from 0 nM-1000 nM in duplicate for 60 min. After cell lysis a FLAG immunoprecipitation was performed, followed by protein separation on SDS gel and Western blotting.

Pulldown assays revealed that the Antascomicin B enhanced FKBP51/Akt1 interaction is direct and the presence of only these two proteins is sufficient.
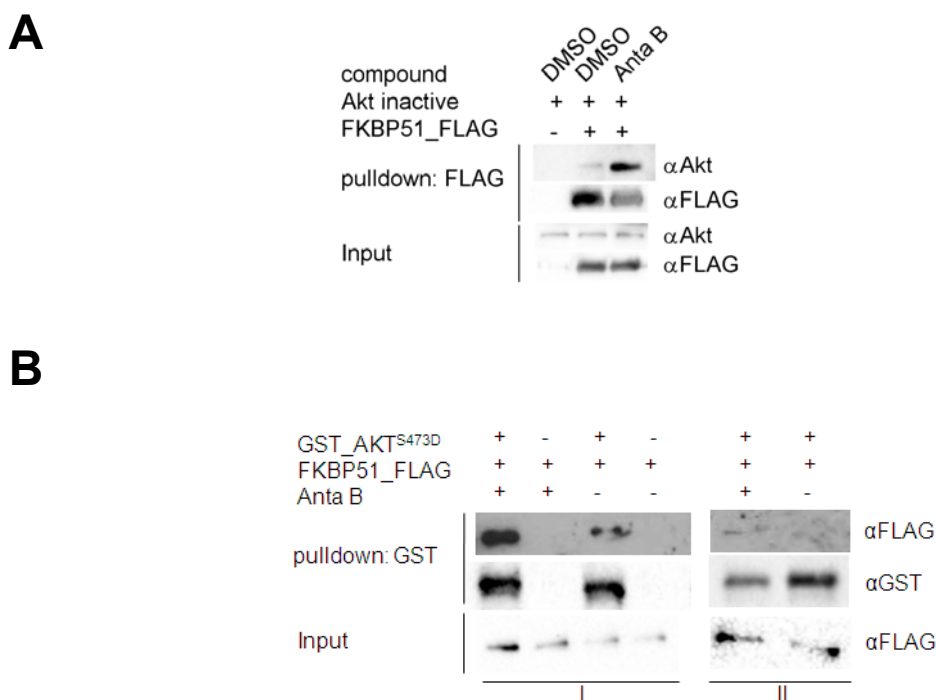

Figure 5.32: In pulldown assays Antascomicin B enhances the Akt1/FKBP51 interaction
A Purified FLAG-tagged FKBP51 and purified inactive Akt1 were mixed in the presence of DMSO or 1 µM of Antascomicin B, subjected to a FLAG pulldown and analyzed by Western blotting. **B** Purified FLAG-tagged FKBP51 and purified active Akt were mixed in the presence of DMSO or 1 µM of Antascomicin B, subjected to a GST pulldown and analyzed by Western blotting. Controls were missing the according bait protein. I+II are replicates

5.3.3 Antascomicin B as inducer of FKBP/Akt1 complexes

In order to get deeper insight in the specificity of the induction of FKBP51/Akt1 interaction our FKBP portfolio was tested. To do so we overexpressed HA_Akt1^{S473A} with four FLAG tagged FKBP homologs, namely FKBP12, FKBP12.6, FKBP51 and FKBP52, and performed co-immunoprecipitation experiments. A general interaction of these FKBPs with Akt1 could be demonstrated in pulldown assays and Co-IP experiments (compare section 5.1). However, 1 µM Antascomicin B clearly enhanced Akt interaction compared to DMSO treatment with all tested FKBPs, as depicted in Figure 5.33.

The effect was most pronounced for FKBP12.6, followed by FKBP52 and FKBP51 and FKBP12. The latter one shows already a rather strong basal FKBP12/Akt1 interaction, which is only slightly enhanced by Antascomicin B. To emphasize the difference between Antascomicin B and DMSO treated samples the depicted X-ray film of the Western blot showing the co-immunoprecipitated FKBP proteins was exposed for a short time. This ex-plains the absent bands even when both binding partners were transfected.
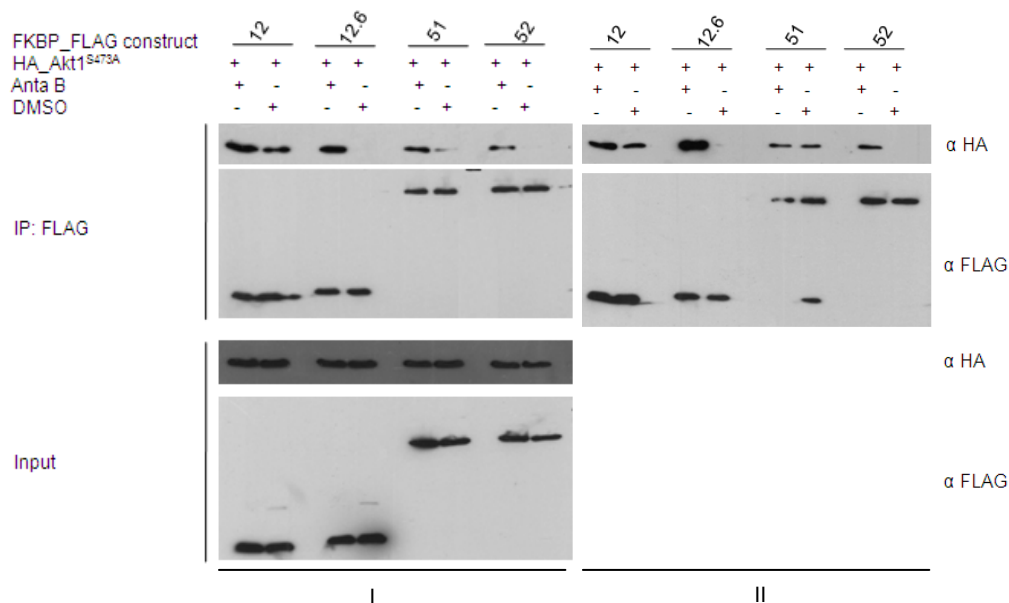
Figure 5.33: Antascomicin B (Anta B) induces FKBP/Akt1 interaction in double transfected cells

HEK293T cells were transfected in duplicates with the indicated constructs. After growth for 48 h cells were treated with 1 µM Antascomicin B for 60 min. Cells were lysed and a FLAG co-immunoprecipitation was performed, followed by protein separation on SDS gel and Western blotting. I+II are replicates, as I+II were treated identically the load was only controlled for I

In order to mimic conditions, which might be closer to in vivo conditions than double transfections we performed an HA-co-immunoprecipitation experiment in HeLa cells containing over-expressed HA-tagged Akt1 (Figure 5.34). After Antascomicin B administration interaction with endogenous FKBP12, FKBP51 and FKBP52 was observed, although for the latter there was a high background.

Of note, reverse co-immunoprecipitation (here the HA-Co-IP) leads to the same Antascomicin B induced effects as observed in Flag-IPs (as for example in the double over-expressing samples in section 5.3.2.).
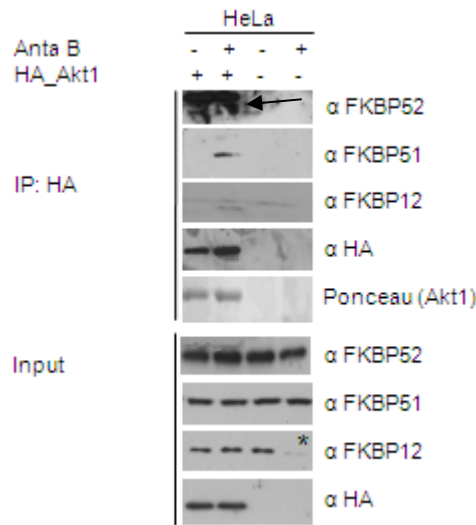
Figure 5.34: Antascomicin B (Anta B) induces FKBP/Akt1 interaction
HeLa cells were transfected with HA-tagged Akt1. After 48 h cells were treated with 1 µM Antascomicin B for 60 min. Cells were lysed and a HA co-immunoprecipitation was performed, followed by protein separation on SDS gel and Western blotting. (*weak signal due to edge effect)

5.3.4 Antascomicin B as inducer of FKBP51/AGC kinase complexes

In order to test if the more intense binding of FKBPs after Antascomicin B treatment is unique to Akt1 the property of Antascomicin B to enhance FKBP51 interaction with other AGC kinases was investigated. For this purpose HEK293T cells were transfected with FKBP51TPR_mut_FLAG and HA-tagged Akt1, Akt2, S6K or GST-tagged SGK. All tested AGC kinases displayed stronger binding to FKBP51 after Antascomicin B administration (compare also section 5.1.7). In principle the strongest increase of FKBP51/AGC kinase interaction after Antascomicin B treatment was observed for Akt2. As for Akt1, S6K and SGK the Antascomicin B mediated increase was similar. For better clarity the X-ray films showing the co-immunoprecipitated AGC kinases were exposed for a shorter time compared to the Western blots in section 5.1.7. The results are shown in Figure 5.35.
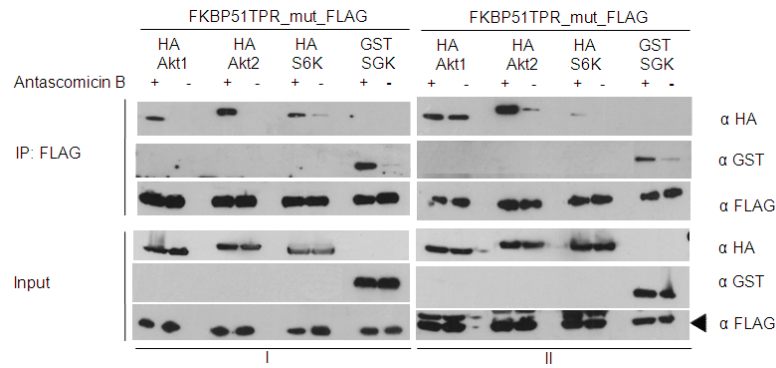
Results

Figure 5.35: Antascomicin B induces FKBP51/AGC kinase interaction
HEK293T cells were transfected in duplicates (I+II) with the indicated constructs. After growth for 48 h cells were treated with 1 µM Antascomicin B for 60 min. Cells were lysed and a FLAG co-immunoprecipitation was performed, followed by protein separation on SDS gel and Western blotting.

5.3.5 Insight into the mode of induction of the FKBP51/Akt1 interaction by Antascomicin B

To dissect the mode of action of Antascomicin B on the Akt1/FKBP51 interaction the Antascomicin B was competed with several ligands known to interact with either of the two proteins. In the first experiment of these series, double transfected HEK293T cells were treated with 1 µM Antascomicin B and 10 µM of the ATP-competing Akt inhibitor AT7867. After 60min cells were harvested, FLAG immunoprecipitated and analyzed by Western blotting (Figure 5.36A). The signal intensity of co-immunoprecipitated HA_Akt1 for each condition is shown in Figure 5.36B. Antascomicin B clearly enhanced interaction of FKBP51 and Akt1. AT7867 was not able to disturb this interaction.
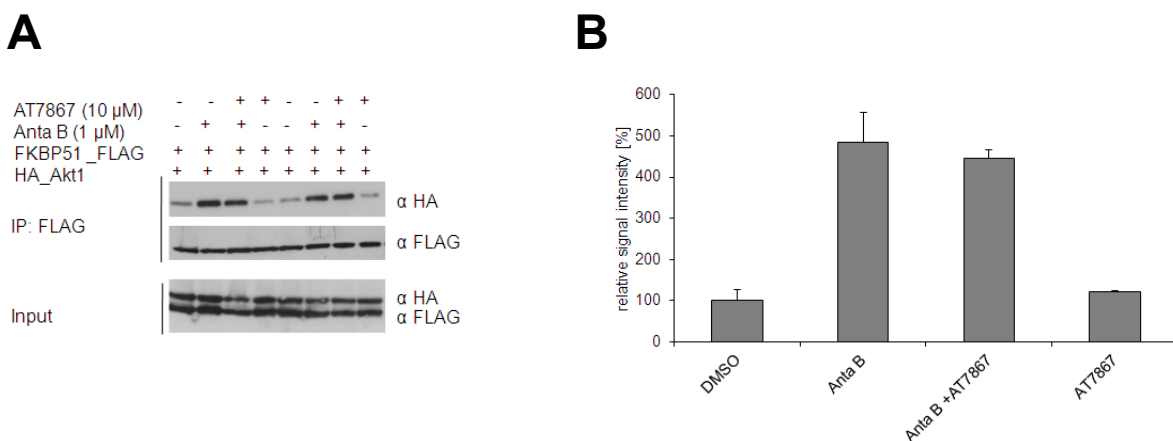

Figure 5.36: AT7867 does not diminish the Antascomicin B-induced Akt/FKBP51 interaction
HEK293T cells were transfected in duplicates with FKBP51_FLAG and HA_Akt1. After 48 h cells were treated for 60 min with Antascomicin B and 10 µM of the Akt inhibitor AT7867 or Antascomicin B or AT7867 alone. **A** Cells were lysed and a FLAG immunoprecipitation was performed, followed by protein separation on SDS gel and Western blotting. **B** Signal intensities were determined using Biorad image software. Results were normalized to those of dimethyl sulfoxide (DMSO)-treated cells, where each DMSO treated sample was set 100% ± SD.

98

Next ,10 µM of the allosteric Akt inhibitor VIII [260] were administered (Figure 5.37A). Inhibitor VIII was shown to abolish Akt phosphorylation [260] which we also observed (lane 3 and 4 and Figure 5.24A). Furthermore, Inhibitor VIII reduced the interaction between Akt and FKBP51, similar to previous results but it did not block the capability of Antascomicin B to enhance the interaction between FKBP51 and Akt. The Akt phosphorylation in the hydrophobic motif (S473) seems to be independent of Antascomicin B treatment (compare Western blot showing Akt (pS473), lane 1 and 2 with lane 3 and 4; and lane 4 and 5 with lane 6 and 7). The amount of co-immunoprecipitated HA_Akt1 is depicted in Figure 5.37B.
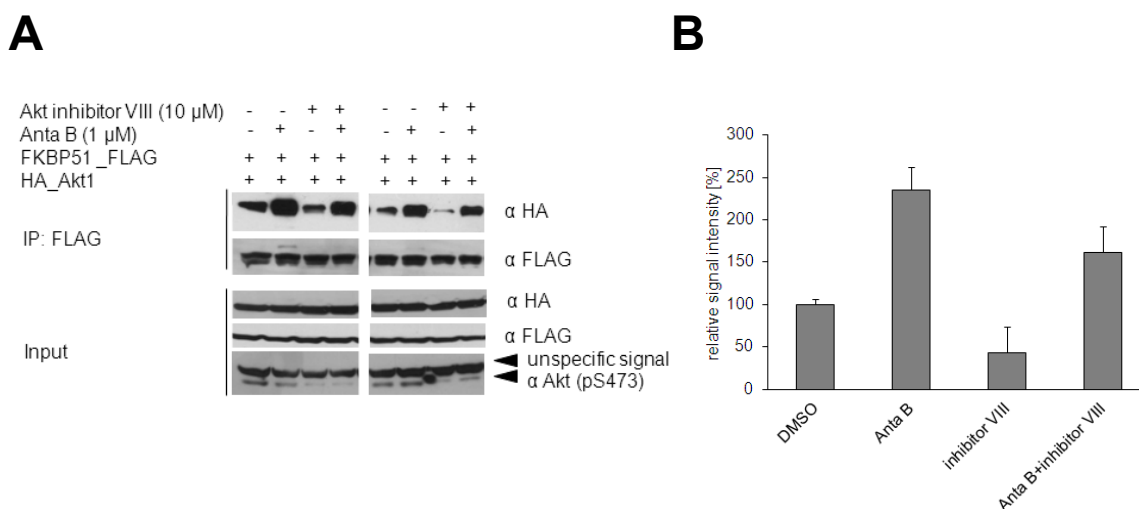

Figure 5.37: Inhibitor VIII does not diminish the Antascomicin B induced Akt/FKBP51 interaction
HEK293T cells were transfected in duplicates with FKBP51_FLAG and HA_Akt1. After 48 h cells were treated for 60 min with Antascomicin B and 10 µM of the Akt inhibitor VIII or Antascomicin B or inhibitor VIII alone. **A** Cells were lysed and a FLAG immunoprecipitation was performed, followed by protein separation on SDS gel and Western blotting. **B** Signal intensities were determined using Biorad image software. Results were normalized to those of dimethyl sulfoxide (DMSO)-treated cells, where each DMSO treated sample was set 100% ± SD.

Furthermore, we applied 10 µM of the FKBP inhibitor FK506 (Figure 5.38). Interestingly we observed that in the presence of FK506 Antascomicin B did not enhance binding of FKBP51 to Akt (compare lane 2 and 8 with boxed lanes).
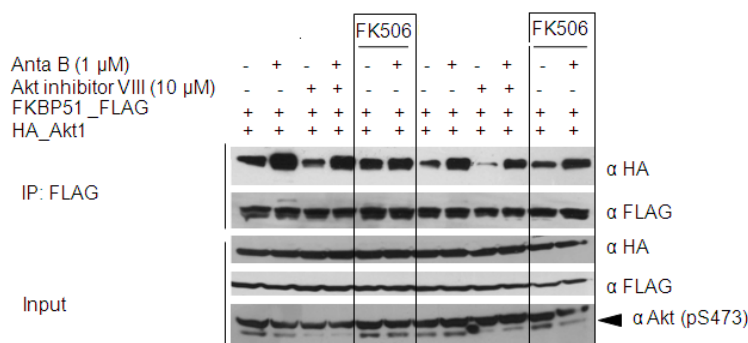
Figure 5.38: The FKBP inhibitor FK506 abolishes the stronger interaction of Akt/FKBP51 caused by Antascomicin
HEK293T cells were transfected in duplicates with FKBP51_FLAG and HA_Akt1. After 48 h cells were treated for 60 min with Antascomicin B and 10 µM of the FKBP ligand FK506 or Antascomicin B or FK506 alone (for explanations regarding Akt inhibitor VIII compare Figure 5.37). Cells were lysed and a FLAG immunoprecipitation was performed, followed by protein separation on SDS gel and Western blotting.

Encouraged by this finding the FKBP inhibitor FK1706 (50 µM) was applied together with Antascomicin B (1 µM). Antascomicin B enhanced FKBP51/Akt interaction as expected. Application of FK1706 prevented the increase of Antascomicin mediated FKBP51/Akt interaction (compare lane 3 to lane 2, lane 6 to lane 5 and lane 11 to lane 10).
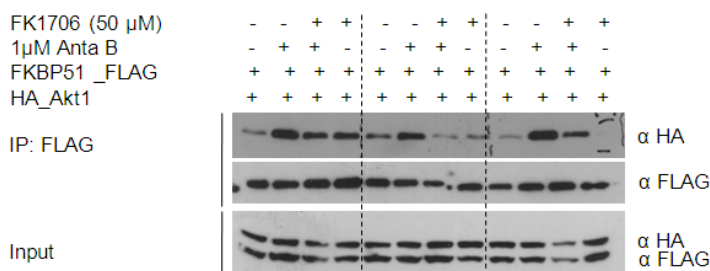

Figure 5.39: The FKBP inhibitor FK1706 abolishes the stronger interaction of Akt/FKBP51 caused by Antascomicin
HEK293T cells were transfected in triplicates with FKBP51_FLAG and HA_Akt1. After 48 h cells were treated for 60 min with Antascomicin B and 50 µM of the FKBP ligand FK1706 or Antascomicin B or FK1706. Cells were lysed and a FLAG immunoprecipitation was performed, followed by protein separation on SDS gel and Western blotting. (The missing band (α HA) in lane 12 could be due to an edge effect)

5.3.6 Influence of Antascomicin B on Akt phosphorylation and downstream targets

Having the findings of Pei [75] in mind, where FKBP51 serves as a scaffold protein to bring the phosphatase PHLPP and Akt in close proximity for Akt dephosphorylation, one could imagine that enhanced binding of Akt and FKBP could lead to less phosphorylated Akt. As initially indicated in section 5.3.5 this does not seem to be the case in HEK293T cells. No influence on Akt phosphorylation in the position S473 could be observed by Western blot

analysis after Antascomicin B treatment for 60 min (Figure 5.37). Treatment of HeLa cells with 0-10 mM Antascomicin B for 24 h revealed (Figure 5.40): First, stimulation with FCS (10%) or insulin (100 nM) enhanced Akt phosphorylation at S473 or T308 as expected. The effects observed after stimulation could also be seen in Antascomicin treated cells. Therefore the following experiments were performed in medium containing 10% FCS.

Second, a slight increase in Akt phosphorylation at both positions (S473 and T308) was observed after treatment with 0.1 and 1 µM Antascomicin B.

Third, a clear reduction of the Akt phosphorylation signal was caused by 10 µM of Antascomicin B. To clarify weather this was due to a loss of viable cells cell viability assays were performed, here in SH-SY5Y neuroblastoma cells (Figure 5.40).

A
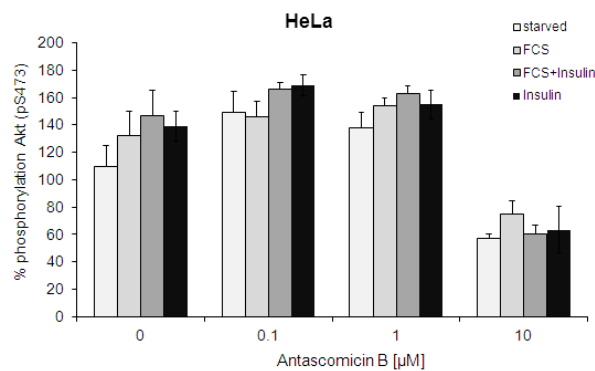
B
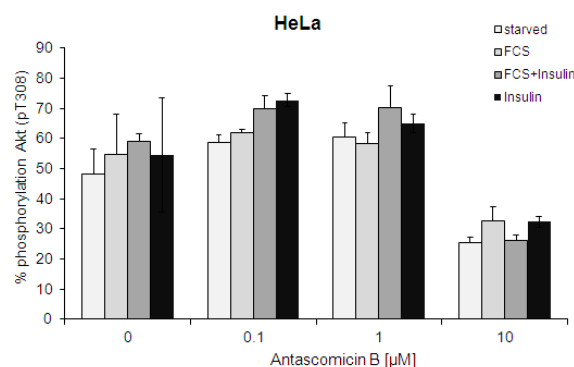
Figure 5.40: Stimulation of cells does not influence the effects of Antascomicin B

HeLa cells were plated and cultured for 48 h. Cells were incubated with increasing concentrations of Antascomicin B for 24 h. Additionally cells were either starved or stimulated with FCS (10%) , insulin (10 nM) or both for 45 min before cell lysis. Cellular Akt phosphorylation was determined using a homogeneous time resolved FRET assay. Results are displayed as standard deviations from the mean. **A** Phosphorylation status of Akt (pS473) was determined **B** Phosphorylation status of Akt (pT308)

In SH-SY5Y neuroblastoma cells toxicity of Antascomicin concentrations above 0.1 µM could be observed in a cell viability assay (Figure 5.41).

A

B

Figure 5.41: Antascomicin B long term-treatment becomes toxic in neuroblastoma SH-SY5Y cells
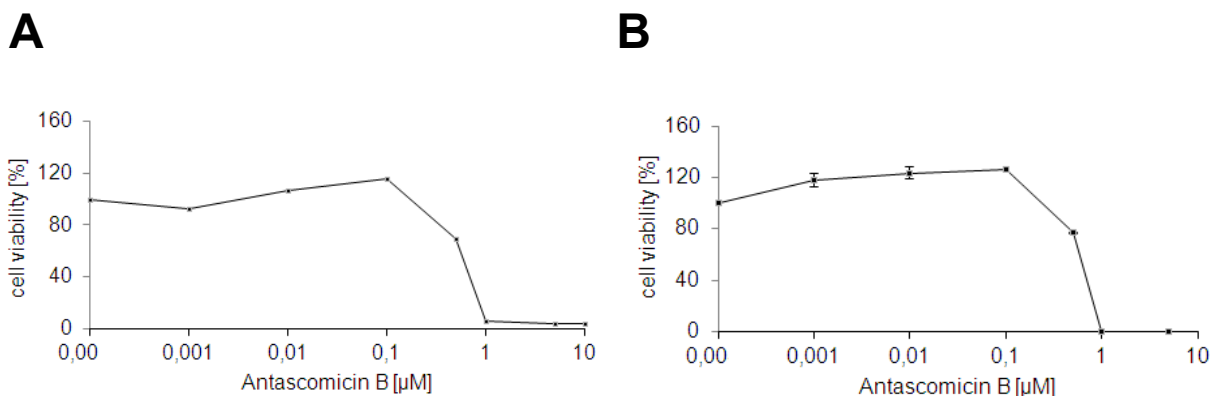10000 SH-SY5Y cells per well (supported with medium + 10% FCS) were plated in a 96 well plate. **A** After 4 h Antascomicin B was added and after 48 h cell viability was analyzed using the CellTiter-Fluor Cell Viability assay Kit (Promega) **B** After 4h Antascomicin B was added for 96 h and cell viability was assessed using the CellTiter-Fluor Cell Viability assay Kit (Promega).

Next the influences on Akt (S473) and Akt (T308) phosphorylation were tested in SH-SY5Y cells. Because of the toxic effects after 24 h or 48 h or 96 h we continued using a short term Antascomicin B treatment for 60 min. Interestingly, as in HeLa cells (Figure 5.40A and Figure 5.40B) an increased phosphorylation status was observed after Antascomicin B administration in SH-SY5Y (Figure 5.42). This increased phosphorylation was concentration-dependent.

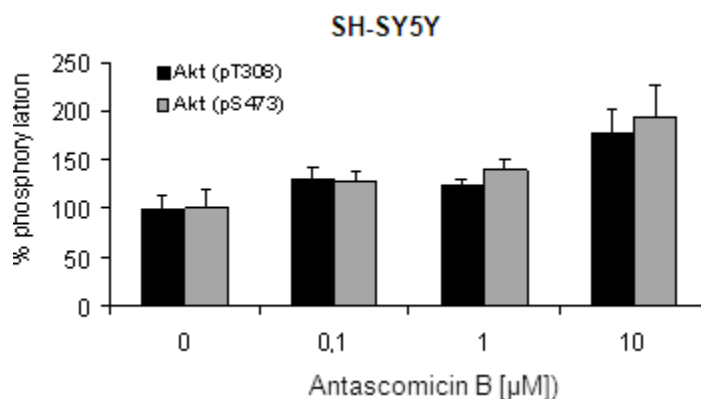**Figure 5.42: Antascomicin B enhances Akt phosphorylation in SH-SY5Y neuroblastoma cells**
SH-SY5Y cells were supplied with FCS and were incubated with Antascomicin B for 60 min. After cell lysis, cellular Akt phosphorylation was determined using a homogeneous time resolved FRET assay.
Results were normalized to those of dimethyl sulfoxide (DMSO)-treated cells (100%) for each phosphorylation site $\pm$ SD.

The phosphorylated and thereby activated Akt enzyme is able to phosphorylate downstream targets. Akt target phosphorylation triggers survival, growth, migration, proliferation, polarity, metabolism, cell cycle progression, muscle and cardiomyozyte contractility as well as angio-genesis [275]. To investigate functional consequences of the Antascomicin enhanced FKBP51/Akt1 interaction HeLa cells were cultured for 48 h, followed by 1h in the presence of Antascomicin B. Here we focused on FoxO1 (pS256) and GSK-3ß (pS9). Additionally, Akt activity status was controlled (Akt (pS473)).

A
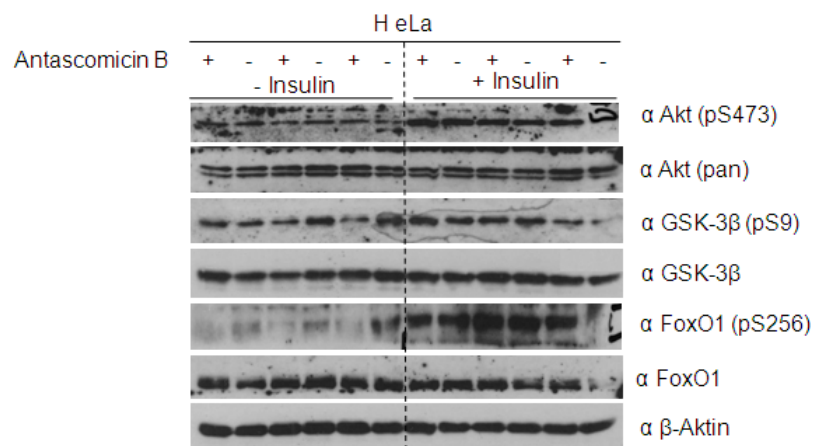
B
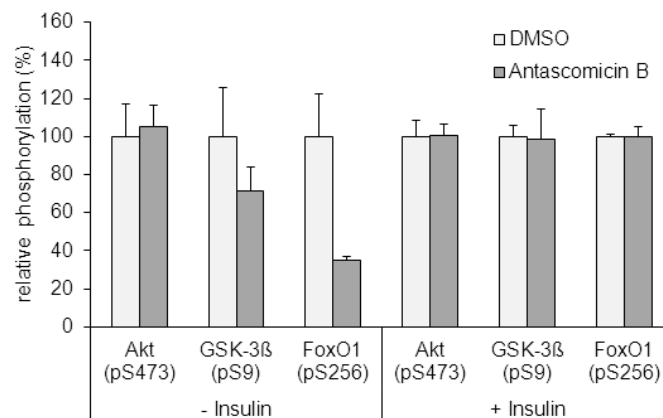
Figure 5.43: Antascomicin influences Akt target phosphorylation
A HeLa cells were cultivated for 48 h. Medium was changed (10% FCS) and 1 µM Antascomicin B was applied for 1 h with or without Insulin (10 nM, 45 min). Cells were harvested and Western blot analysis was performed using the indicated antibodies. **B** Band intensity was analyzed and results were normalized to those of dimethyl sulfoxide (DMSO)-treated cells (100%) for each protein $\pm$ SD. Lane 12 was not analyzed due to edge effects.

In these triplicate experiments an influence of Antascomicin B on Akt phosphorylation could not be detected. However, FoxO1 and GSK-3β phosphorylation were decreased in the samples lacking insulin.

5.3.7 Antascomicin B enhances the interaction between FKBP51_FLAG and HA_PHLPP2

To get a deeper understanding of the involvement of PHLPP in the Akt/FKBP51/PHLPP complex it should be investigated if the binding between FKBP51 and PHLPP1 or PHLPP2 is also enhanced by Antascomicin B. To do so HEK293T cells were transfected with FKBP51_FLAG and HA_PHLPP1 or HA_PHLPP2. Cells were treated for 60 min with 10 µM of the indicated compounds. Afterwards cells were lysed, FLAG co-immunoprecipitated and Western blot analysis was performed. Antascomicin was the only tested compound able to enhance FKBP51/PHLPP interaction. It should be pointed out, that rapamycin is the only FKBP inhibitor able to increase Akt phosphorylation at S473. PHLPP overexpression does not decrease Akt phosphorylation under these conditions which supports our results described in section 5.1.8, but contradicts the findings of Pei [75].
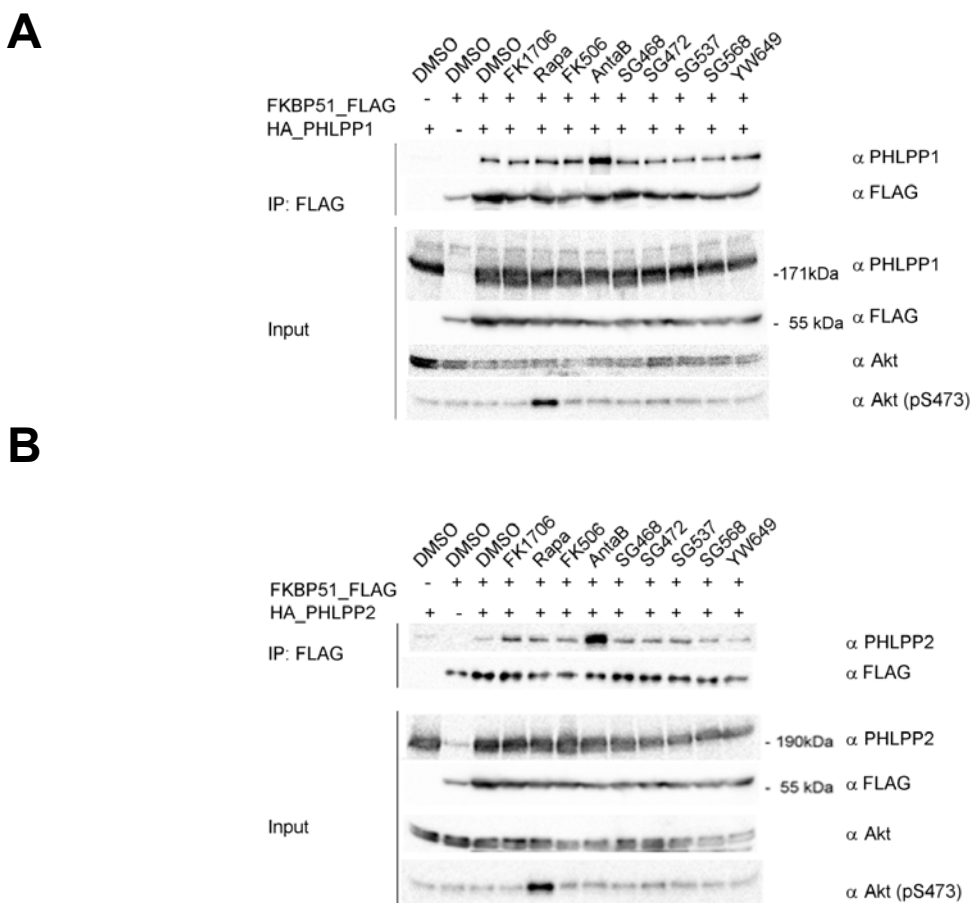
Figure 5.44: Antascomicin B induces interaction between FKBP51 and PHLPP
HEK293T cells were transfected with FLAG_FKBP51 and HA-tagged PHLPP1 or HA-tagged PHLPP2. After 47 h FKBP inhibitors (10 µM) or DMSO were added for 1h. Lysates were immunoprecipitated and analyzed by Western blotting. **A** Antascomicin B enhances the interaction between FKBP51 and PHLPP1 **B** Antascomicin B enhances the interaction between FKBP51 and PHLPP2

5.3.8 Investigation of toxicity effects of Antascomicin B

Some cells seem to be more sensitive to Antascomicin B than others. Antascomicin B as an inducer of FKBP51/Akt1/PHLPP interaction might act synergistic to the chemotherapeutically used compound Gemcitabine, even so FKBP51 effects on Akt S473 phosphorylation could not be generally confirmed in our hands. To investigate this further the pancreas cancer cell line SU.86.86, which was shown to be sensitive to FKBP51 overexpression [76], was used. First, the effects of Antascomicin B on the general cell viability of SU.86.86 cells were tested (Figure 5.45A). Concentrations of up to 10 µM Antascomicin B were well tolerated when administered for 24 h. Thereafter SU.86.86 cells were treated with increasing concentrations of gemcitabine in the presence of 10 µM of Antascomicin B. After 72h gemcitabine dose-dependently reduced cell viability, however no synergistic effect of Antascomicin B was observed (Figure 5.45B).

A

B
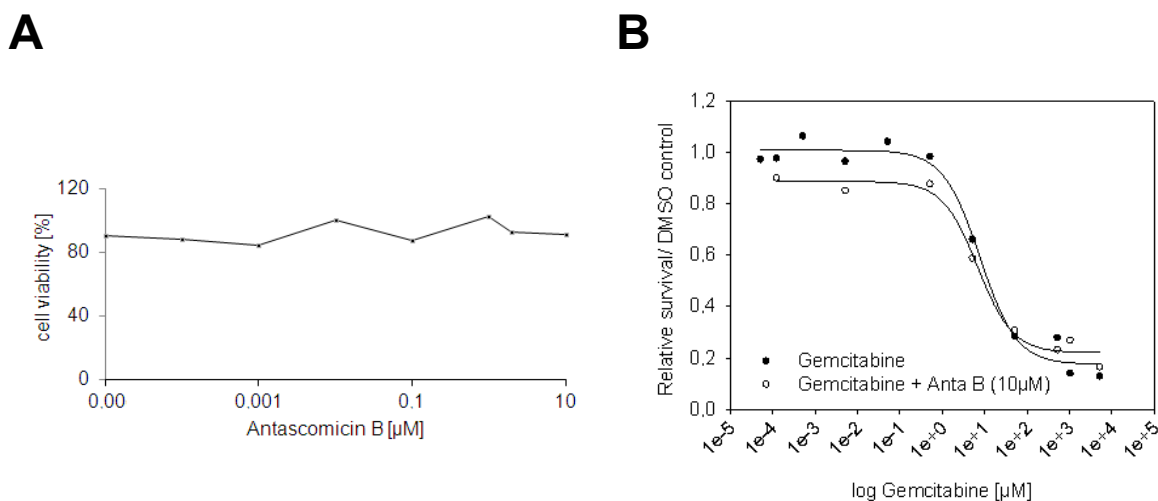
Figure 5.45: Antascomicin B does not enhance cell toxicity of Gemcitabine
A To test the effect of Antascomicin without gemcitabine 10000 SU.86.86 cells per well were plated and let attach for 48 h. Cells were incubated with increasing Antascomicin B concentrations for 24 h. After altogether 72 h cell a viability assay was performed using the CellTiter-Fluor Cell Viability assay (Promega). **B** 10000 cells were plated and cells were incubated with increasing Gemcitabine concentrations for 72 h. 24 h before cell viability was assessed Antascomicin B (10 µM) was added.

5.4 Contribution of FKBPs to the cellular action of rapamycin

So far the drug rapamycin, which is FDA-approved for prevention of graft-versus-host dis-
ease and as an anti-cancer agent (see section 1.2.1), is almost exclusively interpreted and
discussed in the context of a complex with the prototypical FKBP12. However, our group
could demonstrate, that rapamycin does not exclusively interact with FKBP12 but rather
binds with high affinity to most members of the F506-binding-protein family [264]. Additional
data by Andreas März revealed that larger FKBP homologs like FKBP51 contribute substan-
tially in mediating the effects of rapamycin [14]. The following data supports this postulate
with additional findings.

5.4.1 Modulation of mTOR (pS2448) by rapamycin is cell type dependent

The anti-proliferate efficiency of rapamycin has been modest for many cancer cell types
[276]. Therefore it was essential to select a cell line which would respond to rapamycin in
order to study the effect of rapamycin and specific FKBP inhibitors in more detail. Rapamycin
was titrated in several concentrations leading to dose-response curves (Figure 5.46). mTOR
(pS2448) measured by a time resolved FRET assay was used as a read out.
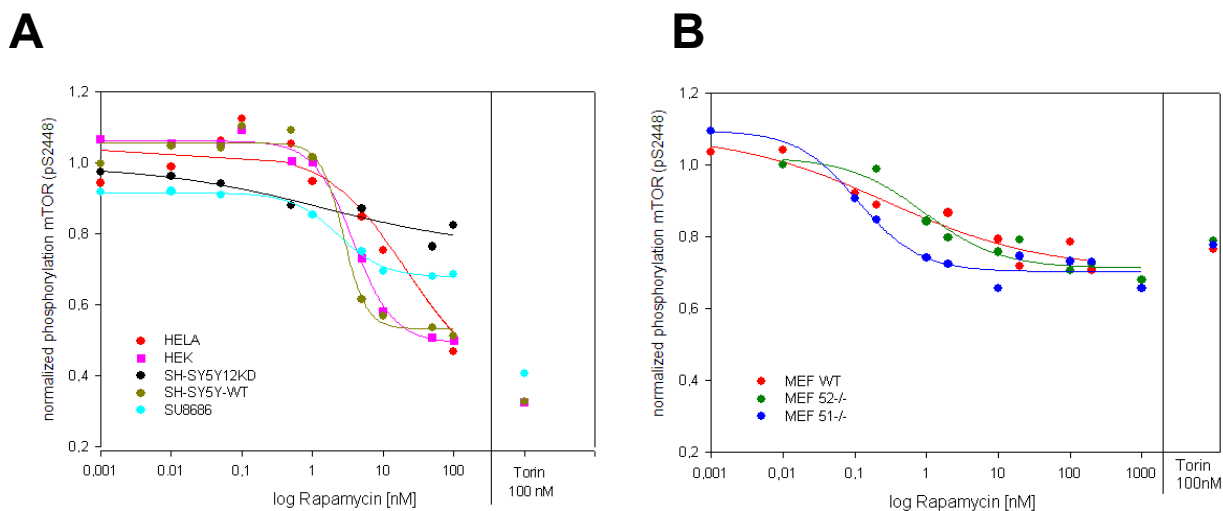
Figure 5.46: Modulation of mTOR (pS2448) by Rapamycin is cell type dependent
A HEK, HeLa, SH-SY5Y wildtype , SH-SY5Y-shFKBP12 and SU.86.86 cells were treated with increasing concentrations of
rapamycin or DMSO for 60 min. mTOR (pS2448) was assessed using a time resolved FRET assay. Results of rapamycin
treatment were normalized to the DMSO control of each cell type. Torin-1 (100 nM) was used as positive control **B** MEF, MEF
52-/- and MEF 51-/- were treated with increasing concentrations of rapamycin or DMSO for 60 min. mTOR (pS2448) was as-
sessed using a time resolved FRET assay. Results of rapamycin treatment were normalized to the DMSO control of each cell
type.

In HeLa, HEK and SH-SY5Y-WT cells the mTOR phosphorylation at position S2448 started to decrease at rapamycin concentrations below 1 nM. Rapamycin concentration up to 100 nM could not decrease phosphorylation any further and a plateau was reached in the latter ones. In contrast there was no plateau reached in HEK cells with the used concentrations, indicating that mTOR phosphorylation could still be decreased with higher rapamycin concentrations. The ductal carcinoma cell line SU.86.86 showed a response at concentrations below 1 nM but even with high rapamycin concentrations mTOR (pS2248) could not be decreased which limits their response to rapamycin. Interestingly a difference between SH-SY5Y-WT and SH-SY5Y_12KD cells was observed: With decreased FKBP12 expression rapamycin reduced mTOR (pS2448) to a much lower extend. Finally MEF WT cells showed the fastest response to rapamycin treatment. To decrease phosphorylation of mTOR (S2448) in MEF52-/- rapamycin concentrations higher than 0.1 nM were necessary. However, knockout of FKBP51 or FKBP52 in MEF cells did not change the reached minimal phosphorylation. Taken together FKBP knockout or knockdown alters the response to rapamycin.

Table 5.1 summarizes the dose-response curves.

	Torin-1	Minimum	Maximum	EC50 [nM]
HeLa	0.3	0.36±0.50	1.04±0.05	21.2±49.1
HEK	0.3	0.50±0.02	1.06±0.01	3.8±0.4
SH-SY5Y_12KD	0.3	0.76±0.17	0.9±0.09	1.3±4.9
SH-SY5Y	0.3	0.53±0.02	1.06±0.02	2.7±0.6
SU.86.86	0.4	0.68±0.01	0.92±0.01	2.3±0.3
MEF	0.8	0.7±0.07	1.09±0.10	0.3±0.4
MEF52-/-	0.8	0.71±0.02	1.02±0.05	0.9±0.6
MEF51-/-	0.8	0.70±0.02	1.10±0.04	0.1±0.0

Table 5.1: Summary of the resulting curves
In grey are calculated values which can't be considered as right due to missing plateau in HeLa cells and no typical dose response curve in SH-SY5Y_12KD cells.

Since HeLa, HEK and SH-SY5Y cells showed maximal response to rapamycin, we decided to continue with HeLa or/and SH-SY5Y cells to distinguish between the contribution of FKBP12 and other members of the FKBP family to the functional effects of rapamycin in human cells.

5.4.2 FKBP12-selective ligands do not block the cellular effects of rapamycin

To explore the FKBP-subtype involved in the action of rapamycin a pharmacological approach in which rapamycin was administered together with non-selective FKBP inhibitors (FK1706, FK506, YW649) and FKBP12 selective-inhibitors (Biricodar and cmpd 44) was used. As a pre-experiment it was verified that FKBP ligands alone do not affect Akt phosphorylation at S473 or mTOR phosphorylation at S2448 (see section 5.2.2 and Figure 5.47).
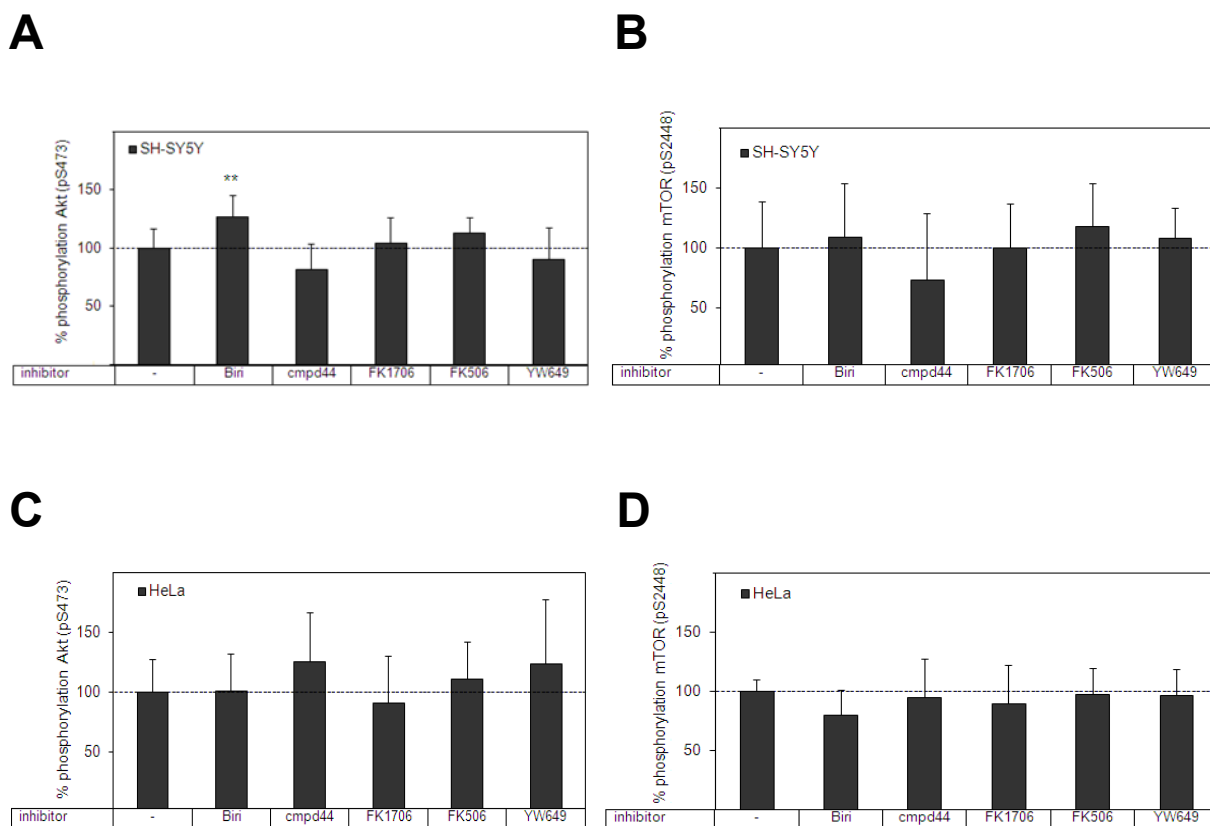
Figure 5.47: FKBP inhibitors alone do not affect Akt or mTOR phosphorylation in SH-SY5Y neuroblastoma cells and HeLa cells

SH-SY5Y neuroblastoma or HeLa cells were treated with DMSO, 10 µM of FKBP12-selective inhibitors Biricodar (Biri) [145], compound 44 [148], the non-selective FKBP inhibitors FK1706 [142], FK506 [264] or YW649 [144]. After 60 min cellular Akt phosphorylation **(A and C)** and cellular mTOR phosphorylation **(B and D)** were determined using a homogenous time resolved FRET assay.

For all experiments mean values from at least 3 data points are shown. DMSO control was set to 100% phosphorylation while Torin-1 was defined as 0 % phosphorylation.

The values are presented as mean $\pm$ SD. Two-way analysis of variance (ANOVA) and a priori testing were used for statistical analysis. Compared with DMSO treatment: ** $p<.01$

Except for Biricodar which induced increase in Akt phosphorylation in SH-SY5Y cells, none of the FKBP ligands altered Akt (pS473) or mTOR (pS2448) significantly.

Afterwards the effects of FKBP ligands on rapamycin induced Akt hyperphosphorylation and the inhibition of mTOR auto-phosphorylation was determined. In SH-SY5Y neuroblastoma cells the rapamycin-induced effects were blocked or significantly reduced by the pan-

selective FKBP ligand FK506, which potently binds to all cytosolic FKBPs (Figure 5.48). FK1706, a non-immunosuppressive analogue of FK506, which tightly binds to FKBP12 as well as to FKBP51 (K_I=50 nM) and to FKBP52 (K_I=20 nM), likewise blocked the effects of rapamycin [142, 264]. The same could be observed for the small molecule non-immunosuppressive unselective FKBP ligand YW649. Biricodar [145] and compound 44 [148] are two structurally different substances, which bind to FKBP12 almost as tightly as FK506 and FK1706 but which more strongly discriminate against the larger FKBP51 and FKBP52 (> 500 fold selectivity for FKBP12). In contrast to FK506, FK1706 or YW649 none of the FKBP12-specific inhibitors affected the effects of rapamycin on mTOR auto-phosphorylation or Akt hyperphosphorylation, even at concentrations 3-10-fold higher compared to FK506, FK1706 and YW649.

Figure 5.48: In SH-SY5Y neuroblastoma cells FKBP12 selective ligands do not block the cellular effects of rapamycin
SH-SY5Y cells were treated with DMSO, rapamycin or Torin-1 (100 nM) in the absence or presence of the FKBP12-selective inhibitors Biricodar (Biri) [145] or compound 44 [148] or the non-selective FKBP inhibitors FK1706 [142], FK506 [264] or YW649 [144] at the indicated concentrations. After 60 min cellular Akt phosphorylation **(A)** and cellular mTOR phosphorylation **(B and C)** were determined using a homogenous time resolved FRET assay. The pan-selective FKBP inhibitors, but not the FKBP12-selective inhibitors, blocked the effect of rapamycin.
For all experiments mean values from at least 3 data points are shown. DMSO control was set to 100% phosphorylation while Torin-1 was defined as 0 % phosphorylation.
The values are presented as mean $\pm$ SD. Two-way analysis of variance (ANOVA) and a priori testing were used for statistical analysis. Compared with DMSO treatment: *** $p<.001$, ** $p<.01$, * $p<.05$; compared with treatment of rapamycin alone: +++ $p<.001$, ++$p<.01$, + $p<.05$

Almost identical results were obtained in HeLa cells as shown in Figure 5.49.

A

B

C

D

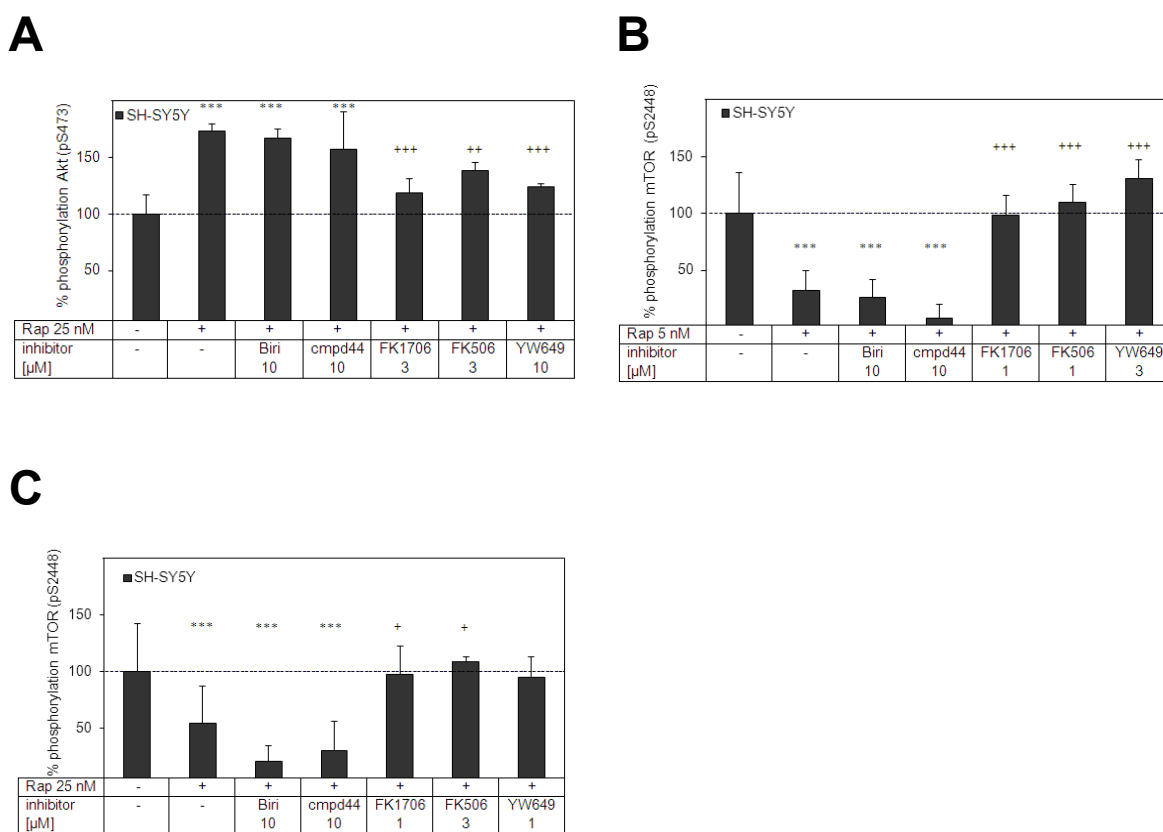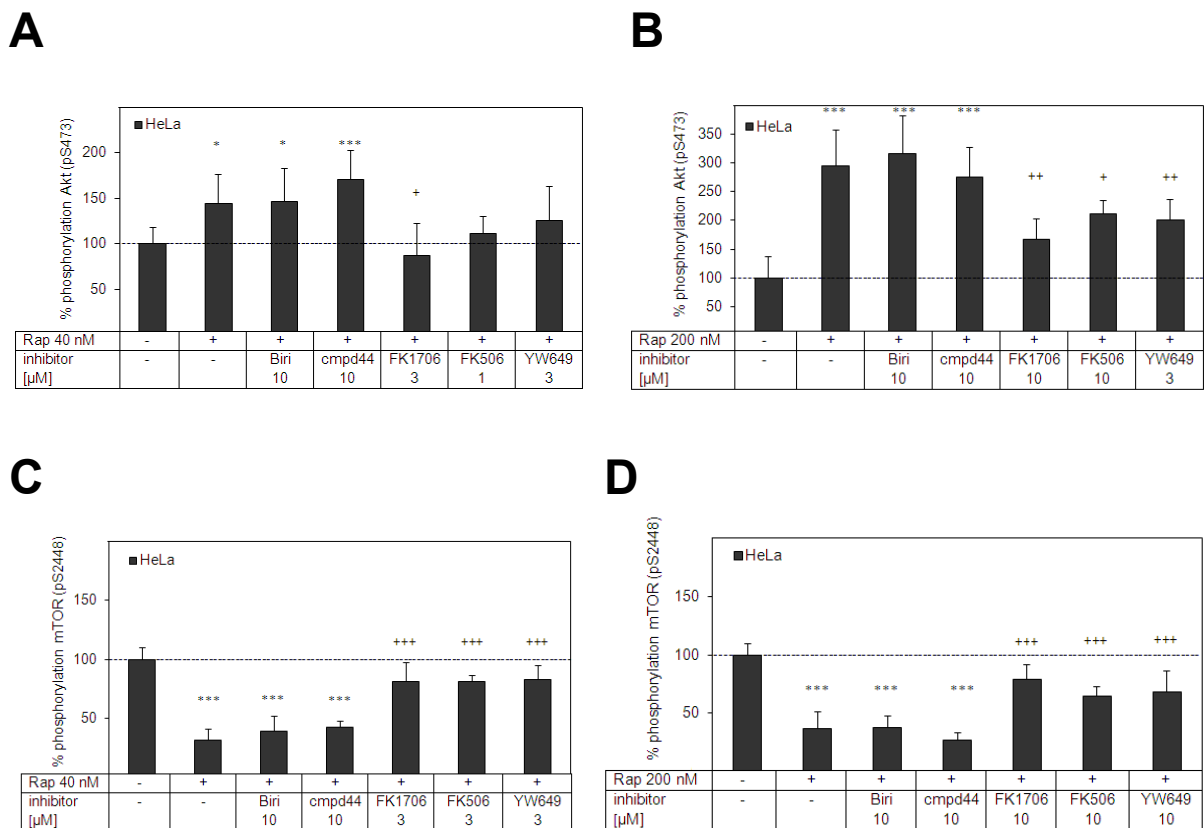**Figure 5.49: In HeLa cells FKBP12 selective ligands do not block the cellular effects of rapamycin**

Hela cells were treated with DMSO, rapamycin or Torin-1 (100 nM) in the absence or presence of the FKBP12-selective inhibitors Biricodar (Biri) [145] or compound 44 [148] or the non-selective FKBP inhibitors FK1706 [142] and FK506 [264] or YW649 [144] at the indicated concentrations. After 60 min cellular Akt phosphorylation **(A and B)** and cellular mTOR phosphorylation **(C and D)** were determined using a homogenous time resolved FRET assay. The pan-selective FKBP inhibitors, but not the FKBP12-selective inhibitors, blocked the effect of rapamycin.

For all experiments mean values from at least 3 data points are shown. DMSO control was set to 100% phosphorylation while Torin-1 was defined as 0 % phosphorylation.

The values are presented as mean $\pm$ SD. Two-way analysis of variance (ANOVA) and a priori testing were used for statistical analysis. Compared with DMSO treatment: *** $p \leq .001$, ** $p \leq .01$, * $p \leq .05$; compared with treatment of rapamycin alone: +++ $p \leq .001$, ++$p \leq .01$, + $p \leq .05$

5.4.3 FKBP12 is necessary for rapamycin mediated effects

The neuroblastoma SH-SY5Y and FKBP12-knockdown SH-SY5Y [20] cell lines turned out to be appropriate model systems to study rapamycins effects. In wild type SH-SY5Y cells, rapamycin potently and dose-dependently reduced mTOR auto-phosphorylation and induced Akt hyperphosphorylation, whereas these effects were blunted in FKBP12-knockdown SH-SY5Y cells (Figure 5.50A and B). Even very high rapamycin concentrations did not induce Akt hyperphosphorylation in the FKBP12-depleted cells (Figure 5.50A).

A
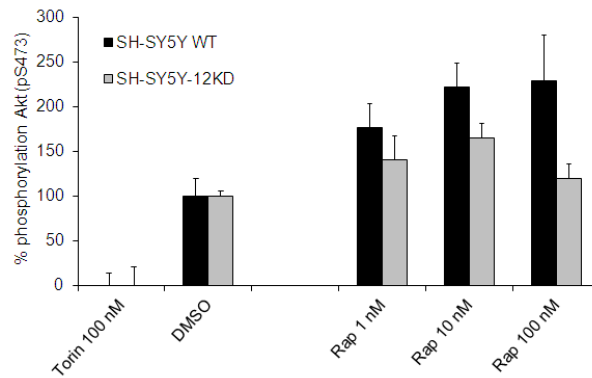
B
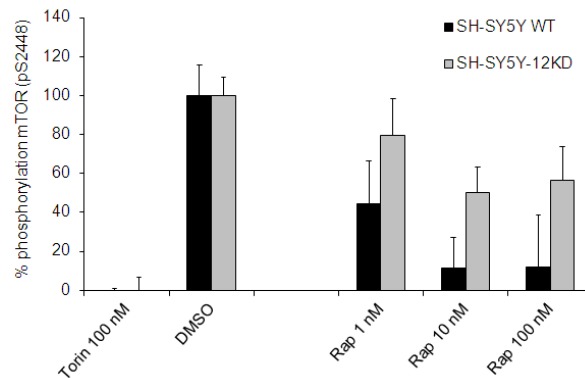
Figure 5.50: FKBP12 is necessary for rapamycin-induced feedback on mTOR phosphorylation and Akt hyperphosphorylation

SH-SY5Y neuroblastoma cells (wild type and FKBP12-knockdown) in medium supplemented with FCS (10%) were incubated for 60 min with 0-100 nM rapamycin or 100 nM Torin-1. Cells were lysed and Akt S473 **(A)** or mTOR S2448 phosphorylation **(B)** were assessed using a phosphor-antibody based FRET assay. Mean values of four independent samples are shown. Values were normalized to 0 % phosphorylation for Torin-1 and 100% phosphorylation for DMSO treated cells.

5.4.4 FKBP12, but also FKBP51 expression restores rapamycin's effect on Akt phosphorylation but not on mTOR phosphorylation

Re-expression of FKBP12 restored the inducibility of Akt S473 phosphorylation by rapamycin in these cells. Importantly, FKBP51 was almost as efficient as FKBP12 to enable the rapamycin-induced Akt S473 hyperphosphorylation, suggesting that FKBP51 can functionally replace FKBP12. However rapamycin's effect on mTOR could not be restored, neither by FKBP12 nor by FKBP51. The Western blots at the bottom (Figure 5.51C) confirm overexpression of FKBP12 and FKBP51, respectively.

A
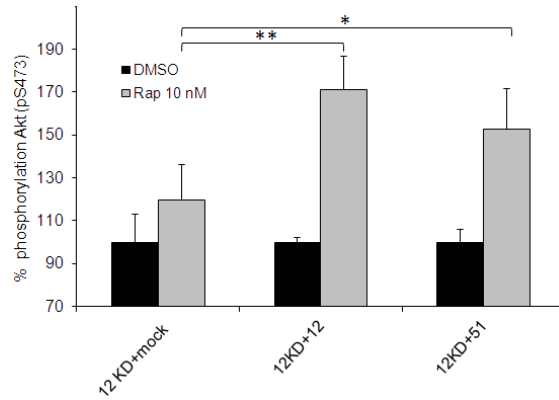
B
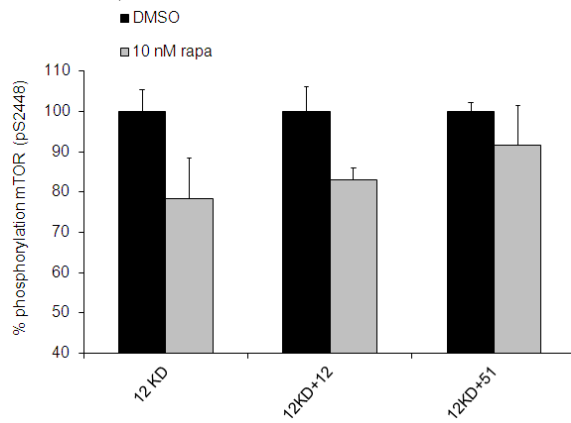
C
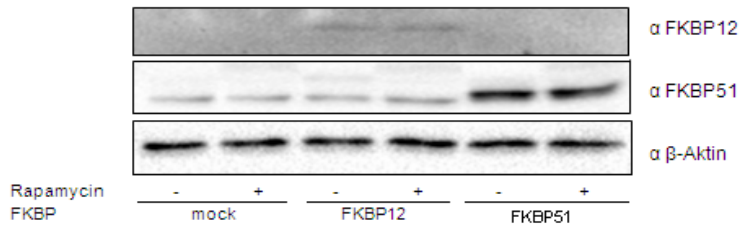
Figure 5.51: FKBP12 can be replaced by FKBP51 in mediating the effects of rapamycin

A+B FKBP12-knockdown SH-SY5Y cells were transfected with FKBP12, FKBP51 or a control plasmid. After 24 h the cells were treated with 10 nM rapamycin or 100 nM Torin-1 for 60 min. Cellular Akt (pS473) and mTOR (pS2448) were assessed using a homogeneous time resolved FRET assay. Mean values of three independent data points are shown. Results were normalized to DMSO-treated controls (100%) for each transfection condition. $**p<.002$, $*p<.05$ **C** Western Blot analysis was used for control of expression of FKBP12 and FKBP12 respectively.

5.5 Bicyclic FKBP ligands and the energetic characterization of their binding

Based on structure based rational ligand design Y. Wang of our research group synthesized FKBP51 ligands with reduced flexibility to improve ligand affinities and efficiencies [144]. He was able to improve the ligand efficiency (LE) of FKBP51 ligands. LE is an important metric tool as LE values ≥ 0.3 are considered as promising candidates for the development of orally available drugs [277-281]. The [4.3.1] scaffold was shown to have higher affinity compared to the [3.3.1] or monocyclic scaffold (Table 5.2).
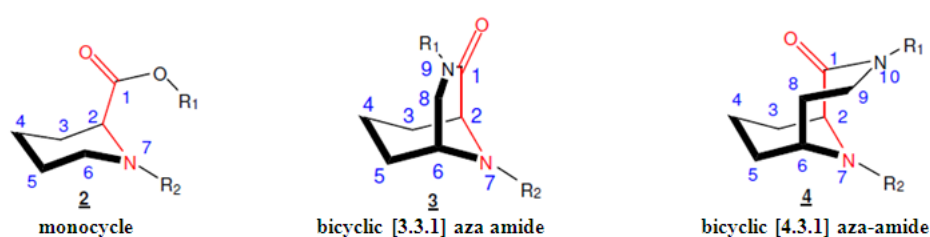
Compound	Scaffold	R$_1$	R$_2$	K$_i$ [µM][a]	LE[b]
FK506	2	d	d	0.08± 0.01[c]	0.17
Rapamycin	2	d	d	0.003± 0.0003[c]	0.18
YW644	2			7.6± 0.5	0.20
YW703	3			13.9± 0.9	0.19
YW691	4			0.3± 0.02	0.24

Table 5.2: Structures and binding affinities of lead-like monocyclic or conformationally constrained FKBP ligands for FKBP51 (courtesy of Y. Wang)

a) affinities were measured by fluorescence polarization assay using the purified FK506-Binding domain of human FKBP51 (see section 4.2.4.3 and [264]) **b)** Ligand efficiency (LE) is defined as ratio of Gibbs free energy (ΔG) to the number of non-hydrogen atoms of the compound: LE = (ΔG/N), where ΔG = -RTlnKi with RT equal to 0,6 and N is the number of non-hydrogen atoms. **c)** Binding affinities as reported before [264] **d)** for substructures compare section 1.2.1

Classically, higher affinities of rigid scaffolds are attributed to an entropic advantage compared to flexible analogs. To elucidate the origin of the additional binding energy in more detail isothermal titration calorimetry measurements (ITC) were performed as depicted in Figure 5.52A.

All three curves were fitted according to a one site binding model (0.8<n<1.2). While the ITC

data for compound YW691 is very robust, the data for YW644 and YW703 are less so. In the titration curve of compound YW644 and YW703 no plateau was reached which makes exact data-analysis difficult. Thermodynamic characteristics are summarized in Figure 5.52B.

A

compound	ΔH (KCal/mole)	ΔS (KCal/mole/K)	TΔS (KCal/mole)	ΔG (KCal/mole)	Ki (μM)	n	Chi²/DoF
YW644	-4.48±0.14	0.01	2.88	-7.36	3.26±0.48	0.72±0.02	16870
YW703	-2.99±0.08	0.01	3.69	-6.68	10.49±2.3	0.90±0.02	6484
YW691	-13.57±0.18	-0.02	-4.92	-8.65	0.36±0.1	0.86±0.01	79440
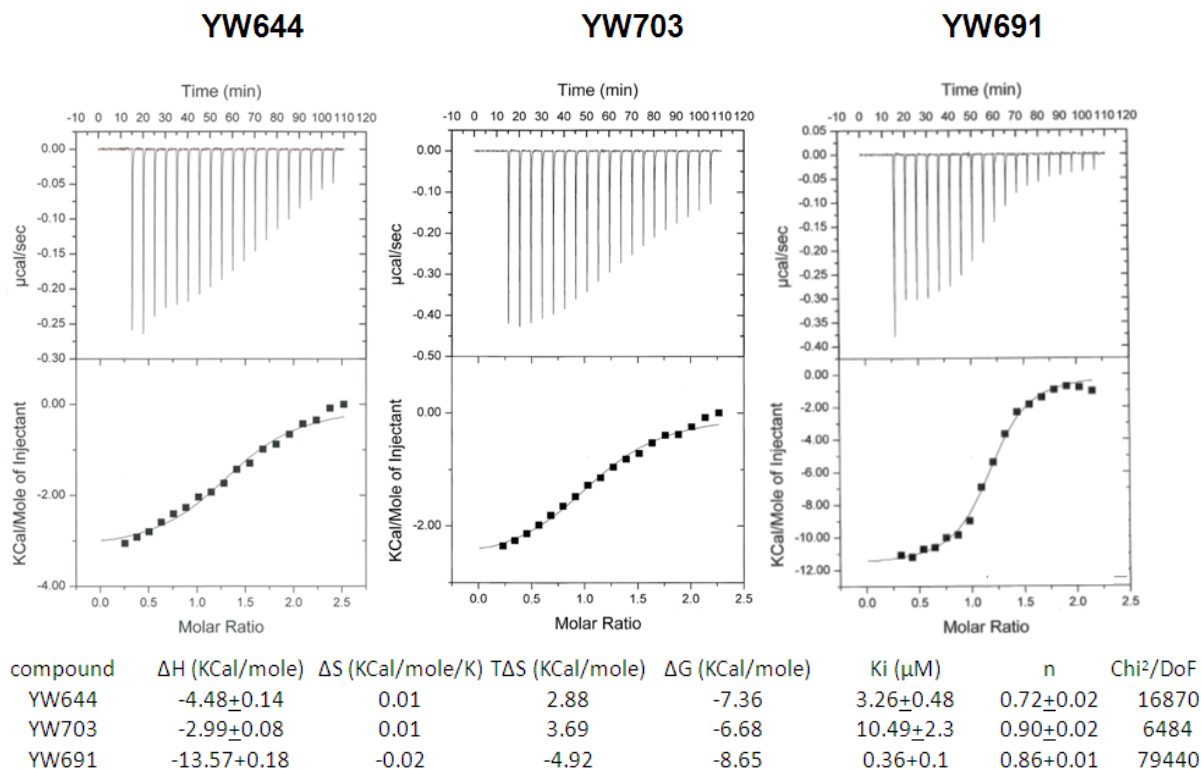
B
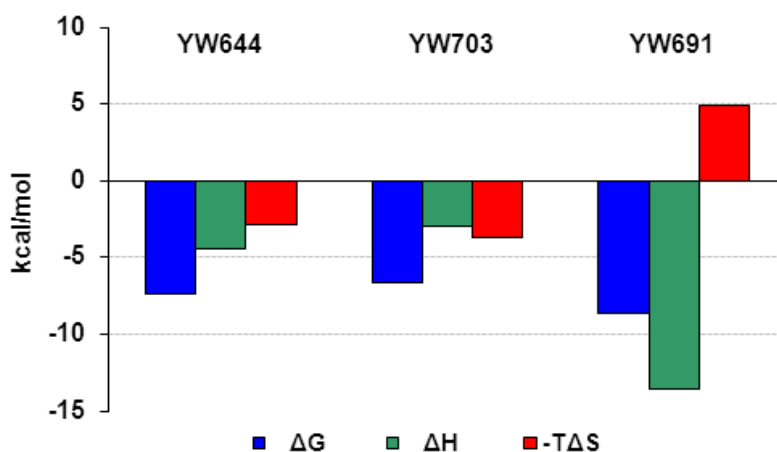
Figure 5.52: A Thermodynamic parameters for binding of YW644, YW703 and YW691 to the FK506 binding domain of FKBP51
B Overview of thermodynamic signatures of YW644, YW703 and YW691 upon binding to the FK506 binding domain of FKBP51

For FKBP51FK1 the [4.3.1]-bicyclization contributed $\Delta G > 2$ kcal/mol to the binding energy. The Kd values obtained (3.3 µM, 10.5 µM and 0.36 µM, respectively) were in excellent agreement with the fluorescence polarization assay results (Table 5.2). Compound YW644 and YW703 showed a very similar thermodynamic profile. The binding was driven enthalpically and entropically. Surprisingly a strong increase in binding enthalpy was observed for the [4.3.1] bicycle YW691 compared to YW703 and YW644 ($\Delta H = -13.6$ kcal/mol vs. -3.0 and -4.5 kcal/mol, respectively). This indicates that the interactions between FKBP51FK1 and YW691 were even stronger than hypothesized by the affinity data (i.e, ΔG). The enhanced binding enthalpy was, however, largely counterbalanced by an opposing negative change in entropy.

6. Discussion

6.1 Akt1 and FKBP51 – only the tip of the iceberg

6.1.1 Expanding interactions

The presented data support a robust FKBP51/Akt1 interaction as it was proposed by Pei *et al*. [75]. According to the results presented here, the interaction of Akt with FKBP51 might be more complex than previously thought. Importantly, the interaction is direct and not restricted to FKBP51 since Akt can bind several FKBPs. Whether different FKBPs can compete for a similar binding site on Akt and whether this could be important for the effect of individual FKBPs on Akt remains to be established. For example, other FKBPs such as FKBP52, FKBP25 or the smaller FKBPs FKBP12 and FKBP12.6 could displace FKBP51 from the Akt/PHLPP complex in a way reminiscent of the opposing effects of FKBP51 and FKBP52 on steroid hormone receptors [112].

It is also interesting that squirrel monkey FKBP51 seems to interact more strongly with Akt than human FKBP51 as shown in section 5.1.4. The amino acid identity between the squirrel monkey FKBP51 and the human FKBP51 protein is 94%. 28 amino acids deviate between the two species, whereas 15 are within the FK1 domain, five are within the FK2 domain and eight amino acids differ within the TPR domain (Figure 6.1). More than 50 % of the amino acid deviation between human FKBP51 and squirrel monkey FKBP51 are consequently located at the FK1 domain. In glucocorticoid signaling the monkey version of the protein displays stronger inhibitory effects than human FKBP51. However, this effect could not be explained by structural differences so far [55].

Chimeric mutants of human FKBP51 and squirrel monkey FKBP51, which were generated in our group, could serve as a valuable tool to investigate the reason for the enhanced interaction displayed by squirrel monkey FKBP51.
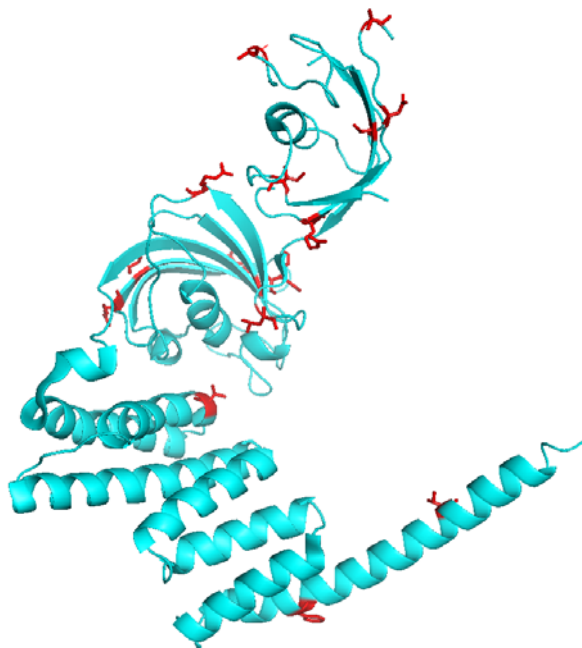
Figure 6.1: Crystal structure of human FKBP51

Amino acid deviations between the squirrel monkey FKBP51 and human FKBP51 are highlighted as red sticks. Amino acids were mapped on the human FKBP51 wildtype sequence (PDB code 1KT0).

Additionally our findings support an interaction between closely related AGC kinases and at least FKBP51. As FKBPs can compete for their binding partners so might do the highly homologous AGC kinases Akt, S6K and SGK. The finding that FKBPs can bind to several kinases is consistent with data from previous studies [67, 282] showing an interaction of FKBP51 with other kinases such as IKKα, IKKε, TAK1 and MEKK1. It should be mentioned that SGK shares downstream targets and upstream effectors of Akt and provides a potential parallel pathway to PI3K/Akt signaling. Thereby SGK represents a novel player in PI3K oncogenic signaling [283]. Similarly S6K signaling is highly interconnected with Akt and SGK signaling. Any effects observed on the PI3K/Akt/mTOR pathway after FKBP51 overexpression or down regulation are thus not necessarily being mediated via Akt but could be due to modulation of any of those kinases. Whether the binding to SGK or S6K is direct or via a third partner (e.g. Hsp90) is currently unclear.

6.1.2 PHLPP – another interaction partner of FKBP51

The phosphatase PHLPP (PH domain leucine-rich repeat protein phosphatase) dephosphorylates and thereby inactivates Akt (S473) [170] and p70SK [284]. It is likely that the closely related SGK and p90S6K, which possess a hydrophobic phosphorylation motif as well are substrates of PHLPP. However, experimental evidence is missing so far.

Mechanistically FKBP51 was suggested to act as a scaffolding protein thereby helping to switch off the Akt pathway [75].

The presented study supports an interaction between FKBP/Akt and PHLPP (see section 5.1.1). While the PDZ binding motif consisting of the amino acid sequence DTLP (PHLPP1) and DTAL (PHLPP2) of PHLPP was shown to be important for Akt regulation [170] it is dispensable for PHLPP/FKBP interaction. The FKBP51/Akt interaction is independent of PHLPP as demonstrated in several biochemical experiments throughout this thesis as the FKBP51/PHLPP interaction is independent of the presence of Akt. The lacking PHLPP1 signal in lane 11 an12 (Figure 5.5) is due to the PDZ binding motif being the target for the antibody against PHLPP1. Therefore in addition the HA signal was detected.

PHLPP's N-terminus is not important for AKT/PHLPP/FKBP51 interaction as well. Since there were no pulldown assays performed it is not known if the interactions between FKBP51 and PHLPP are direct.

We were unable to observe enhanced dephosphorylation induced by FKBP51 as Pei *et al*. [75]. In contrast, we detected an even stronger Akt phosphorylation in HEK293T cells upon overexpression of FKBP51 (Figure 5.23).

This might be due to PHLPP not being the rate-limiting phosphatase for Akt in our cells or under our cell culture conditions.

6.1.3 Akt1 binds FKBP51 via the FK domain

Since the small FKBPs, which only contain the highly conserved FK506-binding domain interact with FKBP51 this domain seems to be sufficient for a direct Akt/FKBP interaction. The FK506-binding domain displays its well-characterized PPIase activity but can also mediate protein-protein interactions [285]. The finding that all FKBPs, but not Cyp40, bound to Akt suggested the common and highly conserved FK506-binding site being the connector to Akt. However, binding of FKBP51 to Akt was not affected by several high-affinity ligands, neither in purified systems nor in cells (Figure 5.27). Likewise, mutations in the FK506-binding site, which abolish the PPIase activity, did not affect binding to Akt (see section 5.1.6). Additional mutations within the binding pocket did not alter Akt/FKBP51 interaction as well (Figure 5.12).

Since the FK506-binding pocket is not the interaction site for Akt other highly conserved parts of the FK506-binding domain must interact with Akt. As depicted in Figure 6.2 several residues can be considered. For example the conserved structures within the 50S loop could serve as a starting point for mutational analysis (compare also [286]). However, several ami-

Discussion

no acid mutations might be necessary in order to abolish the FKBP/Akt interaction completely.

A
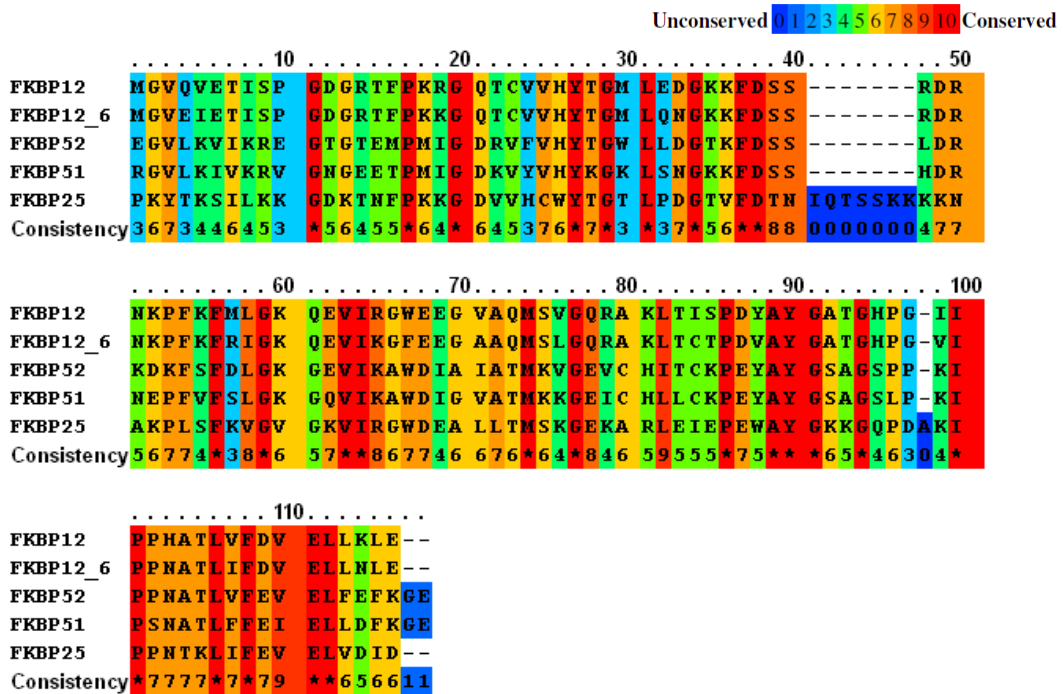
B
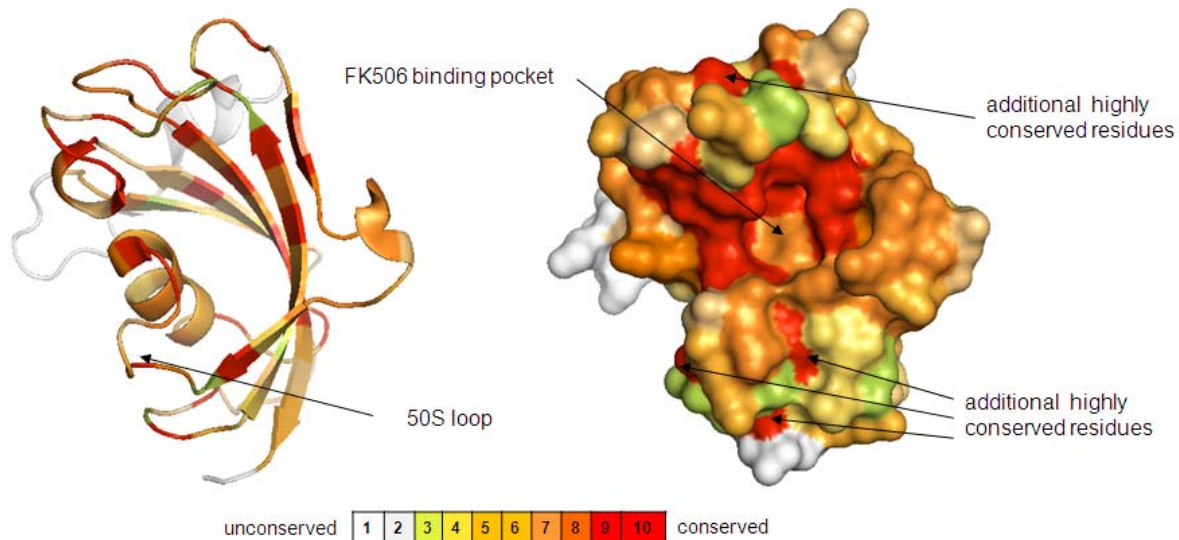
Figure 6.2: Conserved regions within the FK1 domain

A PRALINE representation of the multiple sequence alignment [269] of FKBP12 (PDB code 2PPN) with FKBP12.6 (PDB code 1PBK), and the FK binding domains of FKBP25 (PDB code 3KZ7), FKBP51 (PDB code 3O5E) and FKBP52 (PDB code 1Q1C) **B** Cartoon (left side) and surface representation (right side) of FKBP51FK1 (PDB code 3O5E) colored according to sequence conservation, ranging from (white (variable residues) through yellow to red (conserved residues). Sequence conservation corresponds to the PRALINE calculations depicted in A.

6.1.4 The conformation of Akt is important for interaction but not necessarily the phosphorylation

Mutational analysis of important phosphorylation sites did not substantially affect the FKBP51/Akt interaction although Akt1 containing the phosphorylation-resistant (alanine) S473 mutation interacted slightly less compared to the wildtype (Figure 5.22).

In our mapping studies regarding the Akt/FKBP51 interaction we found the PH domain itself not being required for the FKBP51/Akt interaction. This is consistent with the finding that AGC kinases missing a PH domain can also interact with FKBP51 (e.g. S6K and SGK). The best indication where FKBP51 binds on the Akt surface was obtained using conformation-specific Akt inhibitors. The structures of Akt in complex with AT7867 and inhibitor VIII show that most of the core C- and N-lobes are structurally conserved, indicating that most regions of the conserved kinase domain may not provide the key interaction sites with FKBP51.

The most prominent difference in the conformations of Akt stabilized by AT7867 and by inhibitor VIII is the rearrangement of the αC-helix (residues 185-205), which is stabilized in the presence of AT7867 allowing the binding of the HM to the PIF-pocket and which is destabilized in complex with inhibitor VIII. In addition, the activation loop (residues 292-313) is completely occluded by the PH domain in the presence of inhibitor VIII (Figure 6.3).
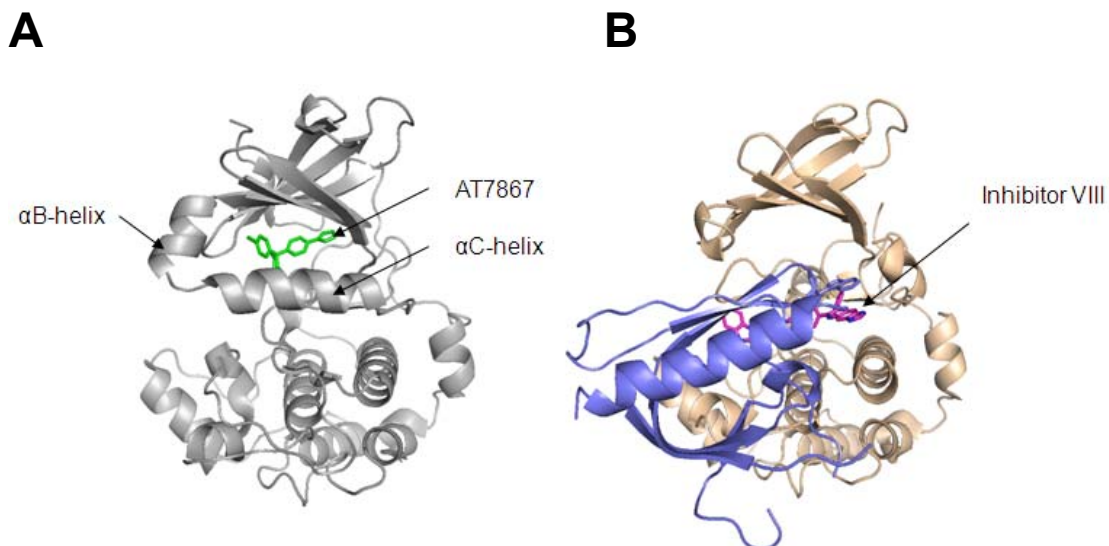
C
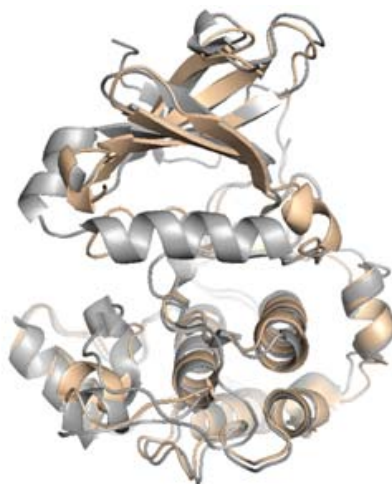
Figure 6.3: The ATP-competitive inhibitor AT7867 stabilizes the αC-helix of Akt

A Cartoon representation of the Akt2 core structure (grey) complexed with AT7867 (green). Ordered structural domains like the αB-helix and the αC-helix are are specified (PDB code 2UW9). **B** Cartoon representation of the Akt1 core structure (wheat) and PH domain (lavender) complexed with inhibitor VIII (pink) (PDB code 3O96) **C** Overlay of the core structures of Akt complexed with AT7867 (grey) or inhibitor VIII (wheat)

Interestingly, the attachment of the PH domain to the catalytic domain of Akt occluding the activation loop, as observed in complex with inhibitor VIII, is thought to occur in the inactive conformation of Akt [287, 288], to which FKBP51 also binds. Therefore, a key binding site for FKBP51 is unlikely to lie within the PH-domain interaction site on the catalytic domain. Rather, the interaction site may exist at or within the proximity of the actual site where inhibitor VIII binds on the catalytic domain or at allosteric sites affected by the interaction with inhibitor VIII. Interestingly, the binding of inhibitor VIII to Akt completely disrupts the formation of the αC-helix highlighting this region, which appears highly flexible in AGC kinases in solution, as the potential common recognition site for kinases by FKBPs.

In contrast the stabilization of the αC-helix is observed with the non-hydrolyzable ATP analog AMP-PNP which did not affect the Akt/FKBP51 interaction, similar to the observations made with inhibitor AT7867 (Figure 6.4).
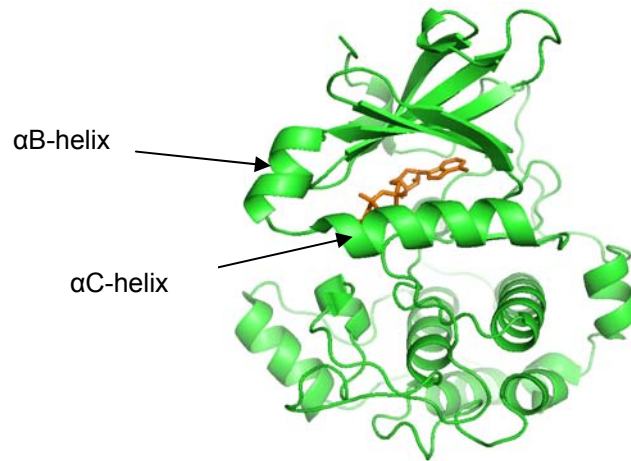
Figure 6.4: AMP-PNP complexed with Akt2

A Cartoon representation of the Akt2 core structure (green) complexed with AMP-PNP (orange).
Ordered structures such as the αB-helix and the αC-helix are specified (PDB code 1O6K).

6.1.5   Introducing Hsp90 – boosting complexity

Since binding of Akt to FKBP51 is partially affected by Hsp90-disrupting mutations (see Figure 5.16 and Figure 5.27) we suggest that the Akt/FKBP51 interaction is mediated in part by Hsp90. Based on the presented results a model is proposed, in which the Akt/FKBP51 interaction is probably bimodal at the biochemical level (Figure 6.5C).

This is consistent with the domain mapping of FKBP51, where all constructs that contained either a functional TPR domain or the FK1 domain (see section 5.1.6) were able to bind to Akt. The only exception is the pull-down of purified FKBP51ΔFK1_FLAG, where FKBP51 lacks the FK1 domain and cannot bind via Hsp90 since the latter is lacking in the purified reconstituted system. This may indicate that FKBP51 can bind to Akt also via the FK2 domain or it could be due to misfolding of this construct and spurious binding of Akt (FKBP51Δ FK1_FLAG was the only construct that could not be checked by active site titration prior to the pull-down assays).

This two-domain interaction model also raises the possibility that FKBP51 might use both interaction sites to regulate Akt within a FKBP51/Hsp90/Akt complex, similar to the putative regulation of steroid hormone receptors by FKBP51.

A

B

C
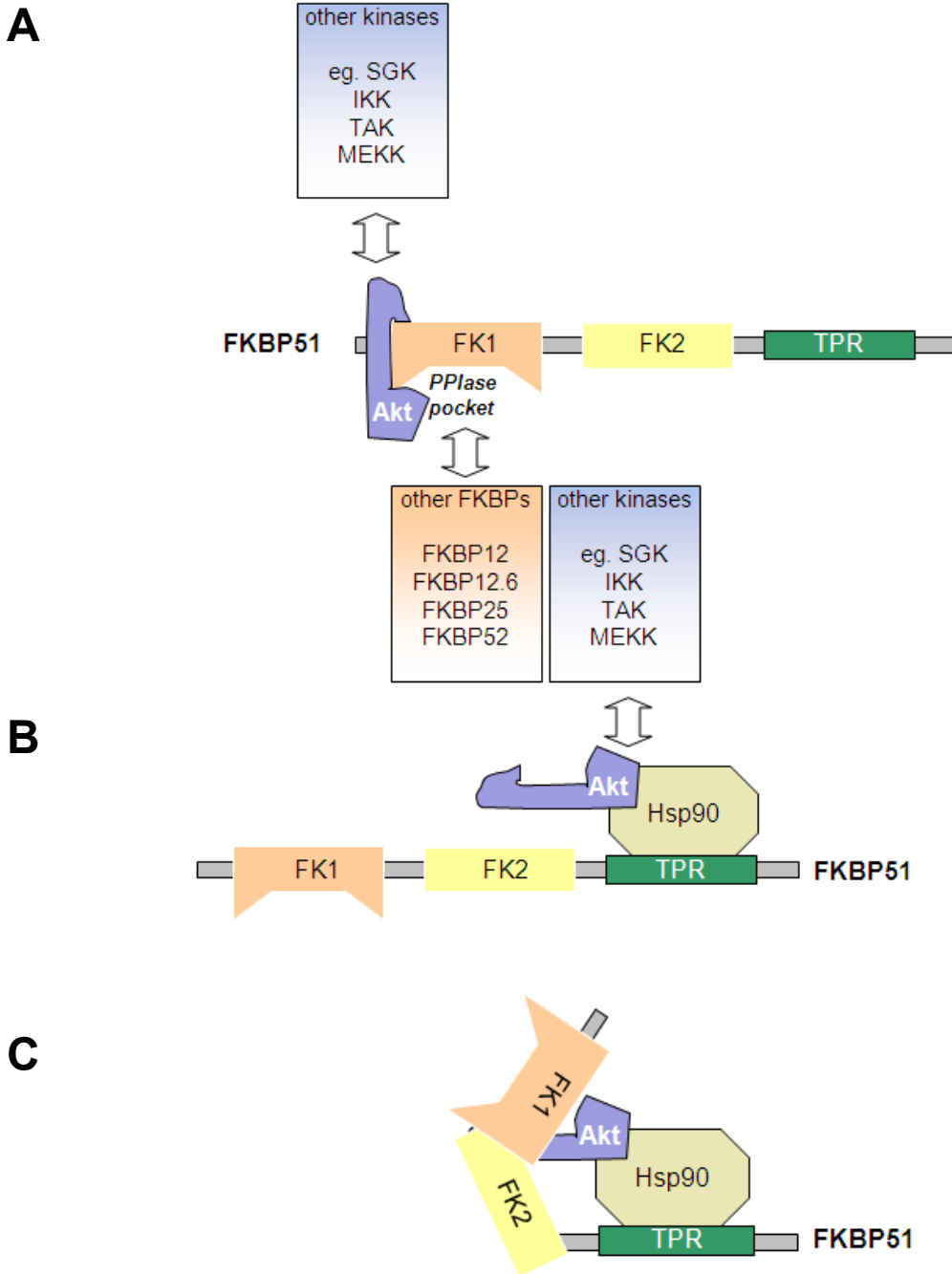
Figure 6.5: Schematic model of possible Hsp90/Akt/FKBP51 complexes
A FKBP51 can bind directly to Akt via its FK1 domain, but not with its FK506-binding pocket. Several other FK1-possessing FKBP homologs may bind to Akt in a similar mode. **B** Akt and several other kinases can bind to FKBP51 indirectly via Hsp90. **C** FKBP51 could assist the chaperoning of Akt by binding to Hsp90 via its TPR domain and by interacting with Akt via its FK1 domain.

6.2   Large FKBPs mediate the effects of rapamycin

The primary effect of rapamycin is its ternary complex formation with FKBP12 and the FRB (**F**KBP12-**r**apamycin-**b**inding) domain of mTOR, thereby inhibiting mTOR kinase activity. Mechanistically, the allosterically restrained access of substrates (e.g. S6K) to the kinase active site or interference with the mTOR complex integrity [289] or assembly [254] are discussed.

So far the pharmacological effects of rapamycin are almost exclusively interpreted and discussed in the context of a complex with the prototypical FKBP12, although there is little experimental evidence for this exclusive role in mammals. In several fungi, knockout of the respective homolog of FKBP12 was shown to abolish sensitivity to rapamycin [290-293].

However, the FKBP repertoire in fungi is much smaller than in mammals and fungal FKBP12 is the only well-established ortholog of human FKBPs [294]. In addition, fungal FKBP12 is usually the only cytoplasmatic FKBP expressed, explaining the strict FKBP12 dependence of rapamycin in these organisms. Indeed, A. März [14] could demonstrate that overexpression of large FKBPs restores rapamycin sensitivity in a FKBP12 deficient yeast strain.

In mammalian cells FKBP12.6, a highly related homolog to FKBP12 was found to form a ternary complex with rapamycin and FRB-TOR [295]. However, in FKBP12.6 deficient mice it was shown that FKBP12.6 can be redundant for the action of rapamycin [296]. Moreover, FKBP38 has been proposed as a player in mTOR inhibition, but this effect was largely rapamycin independent and might be indirect [297]. In addition other groups argued against a role of FKBP38 in mTORC1 signaling [298, 299].

The complex-forming FK506-binding domains are highly homologues and it was shown that rapamycin does not exclusively interact with FKBP12 but rather binds with high affinity to most members of the FKBP family [264]. Our group therefore set out to investigate, whether the pharmacology of rapamycin is indeed restricted to FKBP12.

In his studies A. März [14] observed downstream effects mediated by complexes of larger FKBPs with mTOR/rapamycin. Inhibition of mTOR by larger FKBPs appeared to be even more pronounced than those mediated by FKBP12. März argues that FKBP51 might be the main mediator of rapamycin action in some tissues in vivo. Despite the rapamycin-dependent interaction of small and large FKBPs with mTOR he observed a rapamycin independent binding, especially in the case of FKBP51. This was discussed as the mTOR complexes being multi-protein complexes, where interactions can occur outside of the FRB (**F**KBP12-**r**apamycin-**b**inding) domain of mTOR. These interactions do not have to be necessarily direct, rather adapter proteins (substrate recruiters such as Raptor or Rictor) or even mTOR substrates like S6Kinase or Akt could be involved.

Discussion

The data presented herein consolidate the finding that several FKBPs, especially the large FKBP51, contribute to the action of rapamycin (see section 5.4).

Of note, in our cellular experiments the response to short term rapamycin treatment (60 min) was clearly cell type dependent (Figure 5.46). The mTOR (S2448) phosphorylation as assessed by a time resolved FRET assay was efficiently reduced in HEK and SH-SY5Y cells with an EC_{50} of 3.8$\pm$0.4 nM and 2.7$\pm$0.6 nM respectively. In HeLa cells increasing rapamycin concentrations also lead to a reduced mTOR phosphorylation, even though higher rapamycin concentrations were necessary. Of note, the comparison between the neuroblastoma cell line SH-SY5Y and the SH-SY5Y_FKBP12 knockdown version revealed an impaired response of SH-SY5Y_FKBP12 knockdown to rapamycin concentrations higher than 1 nM. Rapamycin in principle exerts its inhibitory effects in a concentration range below 5 nM as found in an in vitro mTOR assay [14]. A small fraction of FKBP12/rapamycin which could still be available in FKB12 knockdown cells (a knockdown is never 100%) and/or a substitution by other FKBPs could mediate the rapamycin effect at lower rapamycin concentrations in these cells.

Mouse embryo fibroblast (MEF) cells showed a generally lower response to rapamycin. However there was not much difference in MEF cells lacking FKBP51 or FKBP52 compared to wildtype cells. Here the remaining FKBPs might be sufficient to mediate the effects of rapamycin. The pancreatic ductal carcinoma cell line SU.86.86 partially inhibited mTOR phosphorylation with an EC_{50} of 2.3$\pm$0.3 nM but higher concentrations could not further reduce the phosphorylation status, indicating an overall reduced response to short term rapamycin treatment.

It is indeed known that the efficiency of rapamycin can be disappointingly modest for several cancer cell types. This can be in part attributed to a counterproductive repression of a negative feedback on Akt that increases the PI3K/Akt pathway. This feedback mechanism can be exerted either via Grb10 or S6Kinase (Figure 1.8), the insulin receptor substrates [246, 300] or at least in some cells via an enhanced degradation of PHLPP by ubiquitination or reduction of PHLPP expression [248]. However the cellular factors involved in partial rapamycin resistance are not well understood.

As shown by the above described experiment mTOR phosphorylation measured by a time-resolved FRET assay can serve as a valuable readout for the effects of rapamycin, a method that was used in our inhibition studies and reconstitution experiments.

Based on the initial experiments we performed our inhibition studies in SH-SY5Y- and HeLa cells. In order to block rapamycin-induced inhibition of mTOR auto-phosphorylation and Akt hyperphosphorylation the inhibition of all cytosolic FKBPs by the pan-selective FKBP inhibitors FK1706 and FK506 was necessary (Figure 5.48 and Figure 5.49).

The inhibition of FKBP12 by FKBP12-selective FKBP inhibitors (compound 44 or Biricodar) alone was insufficient even in concentrations 3-10 x higher than the pan-selective inhibitors. The FKBP12-selective inhibitors compound 44 and Biricodar are highly lipophilic substances and several close analogs easily permeate cells. The inability of these compounds to block the effect of rapamycin is therefore unlikely to be due to insufficient cell penetration. Taken together larger FKBP homologs seem to substitute for FKBP12 in mediating the effects of rapamycin.

Intriguingly it was repeatedly shown that inhibition of mTOR auto-phosphorylation and the hyperphosphorylation of Akt by rapamycin depend on the availability of higher FKBP levels in SH-SY5Y cells ([14] and Figure 5.50). It was demonstrated by Tang *et al.* that rapamycin inhibits the late phases of neuronal long-term potentiation (LTP), an adaptive process contributing to synaptic plasticity and memory consolidation [301]. In FKBP12-deficient neurons rapamycin induced LTP inhibition was reduced and this was interpreted as FKBP12 being necessary for the effects of rapamycin on mTOR [40]. An additional explanation for the functional alteration in neurons lacking FKBP12 could be, based on our result, that low FKBP12 levels reduce the rapamycin induced activation of the PI3K/Akt pathway per se.

In order to investigate if FKBP51 could rescue rapamycin induced Akt (S473) phosphorylation and inhibition of mTOR auto-phosphorylation we used SH-SY5Y_12 knockdown cells and reconstituted FKBP12 or FKBP51. We could clearly show that both FKBP12 and the larger FKBP51 protein could enable the effect of rapamycin.

The identity of specific FKBP homologs in rapamycin-mTOR complexes will be functionally important when they add novel functionalities to the ternary complexes. As mTOR complexes have been shown to depend on the Hsp90 machinery [302] and to be sensitive to rapamycin only in certain cell types one could imagine that the identity of specific FKBP homolgs in rapamycin-mTOR complexes will be functionally highly important. In this context, FKBP51 or FKBP52-rapamycin complexes, both co-chaperones of Hsp90, could be more effective than the smaller single-domain homolog FKBP12.

It is important to note that most FKBP family members bind to rapamycin with comparably high affinity [264]. Consequently, a mixture of different FKBP proteins will bind to rapamycin, when the compound is administered. At the level of a whole animal/human the action of the relevant FKBP homologs will also depend on their tissue distributions. For the cytosolic FKBPs, the contributions of each particular FKBP homolog might be largely dictated by their relative cellular abundance. Baughman *et al.* characterized the tissue distribution and cellular concentration of FKBP51 and directly compared it to FKBP12 [30]. They found that FKBP51 was more abundant in 11 of 17 tissues with up to a 12-fold molar excess in the liver. Fur-

thermore, mRNA quantification suggests that FKBP51 is highly over-expressed especially in adipocytes and in skeletal muscle cells, compared to median expression [303]. These tissues are extremely important for the metabolic (side)-effects of rapamycin and FKBP51 might be the most relevant FKBP subtype for the inhibition of mTOR by rapamycin in these tissues.

Besides immunomodulation, rapamycin treatment has been suggested for several other indications including type II diabetes, neurodegenerative diseases [127], or even life span extension [132, 304], but the prolonged systemic use of rapamycin is hampered by unacceptable side effects [305]. For these indications, a tissue-selective mTOR inhibition would be very advantageous. Our results suggest a mechanistic rationale how tissue or cell type-biased mTOR inhibition might be realized, namely by engaging specific FKBP homologs dominating the FKBP pool in the desired cell types. This could be accomplished by blocking undesired FKBPs with non-immunosuppressive, FKBP-subselective FKBP ligands such as Biricodar or cmpd44, which leave other FKBPs like FKBP51 or FKBP52 as the mediators of rapamycin's action. A more direct way would be tailoring rapalogs for the desired FKBP homologs. Such FKBP subtype-selective rapamycin analogs can be expected to be active primarily in those cells where their cognate FKBP is highly expressed, e.g. liver, skeletal muscle or adipocytes in the case of FKBP51 [30, 303]. Conversely, rapalogs devoid of FKBP51 binding might be less active in these compared to other tissues.

Taken together, the presented results call for expanding the customary focus on FKBP12-rapamycin and for considering additional FKBP/rapamycin/mTOR complexes to comprehensively understand and optimally exploit the action of rapamycin.

6.3 Antascomicin B – mediation of a new functional ternary complex?

In search for novel materials that might elicit similar biological effects to rapamycin and FK506 Sandoz discovered the novel Antascomicin family, which was isolated from a *Micromonospora* strain from a soil sample collected in china [140]. The most abundant derivative Antascomicin B potently binds to FKBP12 with an IC_{50} of 0.7 nM [140], which is in the same range as rapamycin and FK506. However, Antascomicin B lacks their immunosuppressive properties as the effector region is structurally different (Figure 1.4).

Several groups engaged in the total synthesis of Antascomicin B and in 2005 the Ley group reported the completed total synthesis [141]. However, to our knowledge nothing is known about biological effects of Antascomicin B. Here we unambitiously show that Antascomicin B can enhance protein-protein interactions leading to new biological effects.

We discovered that Antascomicin B is the only tested FKBP ligand exclusively able to enhance the interaction between FKBP51 and Akt1 (Figure 5.29 and Figure 5.34). This enhancement of the interaction between FKBP51/Akt by Antascomicin B seems to be direct, as it was confirmed in pulldown experiments (Figure 5.32).

Of note by titrating Antascomicin B in HEK293T cells the strongest interaction of Akt1 with FKBP51TPR_mut was observed with concentrations above 1 µM. The FKBP51TPR mutant was used to prevent confounding influences of interaction with Hsp90 (see section 6.1.5). This concentration is at least 200 times higher than the binding affinity of Antascomicin B to FKBP51 as obtained in a fluorescence polarization assay (see section 4.2.4.3) (unpublished results by A. März, labbook IV, p. 16/17, 17.2.2009). Therefore we conclude that FKBP51 first binds to Antascomicin. This complex then binds to Akt, whether allosteric or otherwise, leading to a weak interaction. We suggest a scenario where the other FKBPs have to be saturated before FKBP51/Akt gets sufficiently accumulated. Indeed, A. März obtained for FKBP/Antascomicin B interaction IC_{50} values FKBP12<FKBP52<FKBP51<FKBP25, with 0.03 nM, 0.5 nM, 2.2 nM and 4 nM, respectively (unpublished results by A. März, labbook IV, p. 16 ff., 02/2009). Our co-immunoprecipitation experiments in HEK293T cells showed the strongest increase of Akt interaction for FKBP12.6/Anta B, followed by FKBP52/Anta B and FKBP51/Anta B while for FKBP12/Anta B the enhancement of interaction was very little in comparison with samples lacking Antascomicin B. Different H-bonds or electrostatic interactions might be responsible for these differences together with possible multiple complex formations which could favor or discriminate an enhancement of interaction. For quantitative analysis of co-immunoprecipitated protein it is important to compare staining with the same

antibody (e.g. α-FLAG), therefore only qualitative conclusions can be obtained from Figure 5.34.

All formed FKBP/Antascomicin B complexes will then compete for Akt, SGK or S6K as we found an enhancement of the interaction between AGC kinases and at least FKBP51TPR_mut. Here, Akt2 seems to be favored, followed by Akt1, S6K and SGK, indicating some degree of selectivity. The preference for certain FKBPs or certain AGC kinases could be further analyzed in competition experiments.

Our competition experiments performed in HEK293T cells (section 5.3.5) revealed that the ATP competitive Akt- (IC_{50} = 32 nM for Akt1) [255] and p70S6K- (IC_{50} = 85 nM) [256] inhibitor AT7867 is unable to abolish the stronger interaction of FKBP51 with Akt even in concentrations 20 times higher than the one of Antascomicin B. Therefore additional interactions which contribute to the enhanced binding of FKBP51 and Akt are unlikely to be mediated by amino acids within the ATP binding domain. Inhibitor VIII (IC_{50} = 58 nM for Akt1) [259] did not abolish the enhancement of Antascomicin B (Figure 5.37) but it did reduce the overall binding (Figure 5.24 and Figure 5.37) suggesting an impairment of the FKBP51/Akt interaction by inhibitor VIII, which is stabilized again by Antascomicin B.

In contrast FKBP inhibitors such as FK506 and FK1706 counteracted the Antascomicin B mediated effect pointing to a clear structural dependency on the FK506-binding domain of FKBP51 (Figure 5.38 and Figure 5.39).

Recently Pei *et al*. [75] found FKBP51 acting as a scaffold protein mediating the dephosphorylation of Akt by PHLPP. According to this mechanism an enhancer of the FKBP51/Akt interaction as Antascomicin B would theoretically reduce Akt phosphorylation. However, instead we found a slight increase, not a decrease, in Akt phosphorylation at both position T308 and S473 in HeLa cells by Antascomicin B treatment after 24 h (Figure 5.40). This supports our initial finding in HEK293T cells where FKBP51 overexpression induced Akt phosphorylation (Figure 5.23). Activation of Akt is not necessary for Antascomicin B-enhanced Akt1/FKBP51 interaction as Akt (S473A), an inactivating mutant of Akt, can also serve as an interaction partner in the ternary complex formation (Figure 5.31 and Figure 5.33).The clear reduction of phosphorylation caused by Antascomicin B concentration higher than 1-10 µM after 24 h can simply be explained by reduced cell viability (Figure 5.41).

As long term treatment of concentration higher than 1 µM impaired cell viability we set out to focus more on short term effects. Therefore we controlled for the Antascomicin B phosphorylation in SH-SY5Y neuroblastoma cells. Here we could repeatedly observe a slight increase in Akt phosphorylation at both positions (T308 and S473) after administration of increasing Antascomicin B concentrations. One possible explanation for this could be that Antascomicin

B in complex with FKBP51 and Akt favors and stabilizes the active conformation of Akt, similar to AT7867, which then blocks the access of phosphatases. Furthermore one could imagine an enhanced phosphorylation by mTORC2 due to feedback mechanisms other than p70S6K since this is blocked by AT7867 as well. A third possibility is based on alternative FKBP51/Antascomicin B/Akt complexes which block the enhancement of dephosphorylation by PHLPP mediated by uncomplexed FKBP51.

An increased Akt phosphorylation is indicative of more active Akt kinase and should lead to effects on at least some targets of Akt. We focused on GSK-3β and FoxO1 phosphorylation (see section 1.3.2.). Surprisingly, we observed a decreased phosphorylation upon short term Antascomicin B treatment in HeLa cells (Figure 5.43). Therefore we propose an inhibiting effect of FKBP51/Antascomicin B on the Akt downstream targets GSK-3β and FoxO1. However, since the above results are cell based the decreased phosphorylation of GSK-3β and FoxO1 might be indirect. Therefore these data of downstream effects should be consolidated with biochemical and in vitro analysis and evaluated carefully due to complexity and involvement of possible feedback mechanisms.

Antascomicin B is not only able to enhance the interaction between AGC kinases and FKBPs but also between FKBP51 and the Akt phosphatase PHLPP (Figure 5.44). However, as this was only tested in a cell based assay this could be indirect, for example via Akt. Future experiments will elucidate the biological relevance of this finding.

Wang and colleagues found FKBP51 to enhance the response to chemotherapeutics, such as Gemcitabine in pancreatic and breast cancer cell lines [75, 76]. Mechanistically, the latter effect was attributed to the scaffolding function of FKBP51, which could promote dephosphorylation of Akt by the phosphatase PHLPP. However, in a cell viability assay the toxic effects of Gemcitabine on the pancreatic cancer cell line SU.86.86 were observed as expected but there was no prominent effect of Antascomicin B when given in combination with Gemcitabine. For us there was no indication of a possible role of FKBP51 being a tumor suppressor in these cells.

Taken together the experiments of this section point towards the discovery of a new "gain-of-function" ternary complex. Such complexes are very rare in pharmacologic intervention strategies since it is more straightforward to design ligands for inhibition of biological processes. The most prominent examples of gain-of-function formation complexes necessary for pharmacological actions are the inhibition of mTOR by rapamycin and the inhibition of calcineurin by FK506 and Cyclosporine A [112] (Figure 6.6).
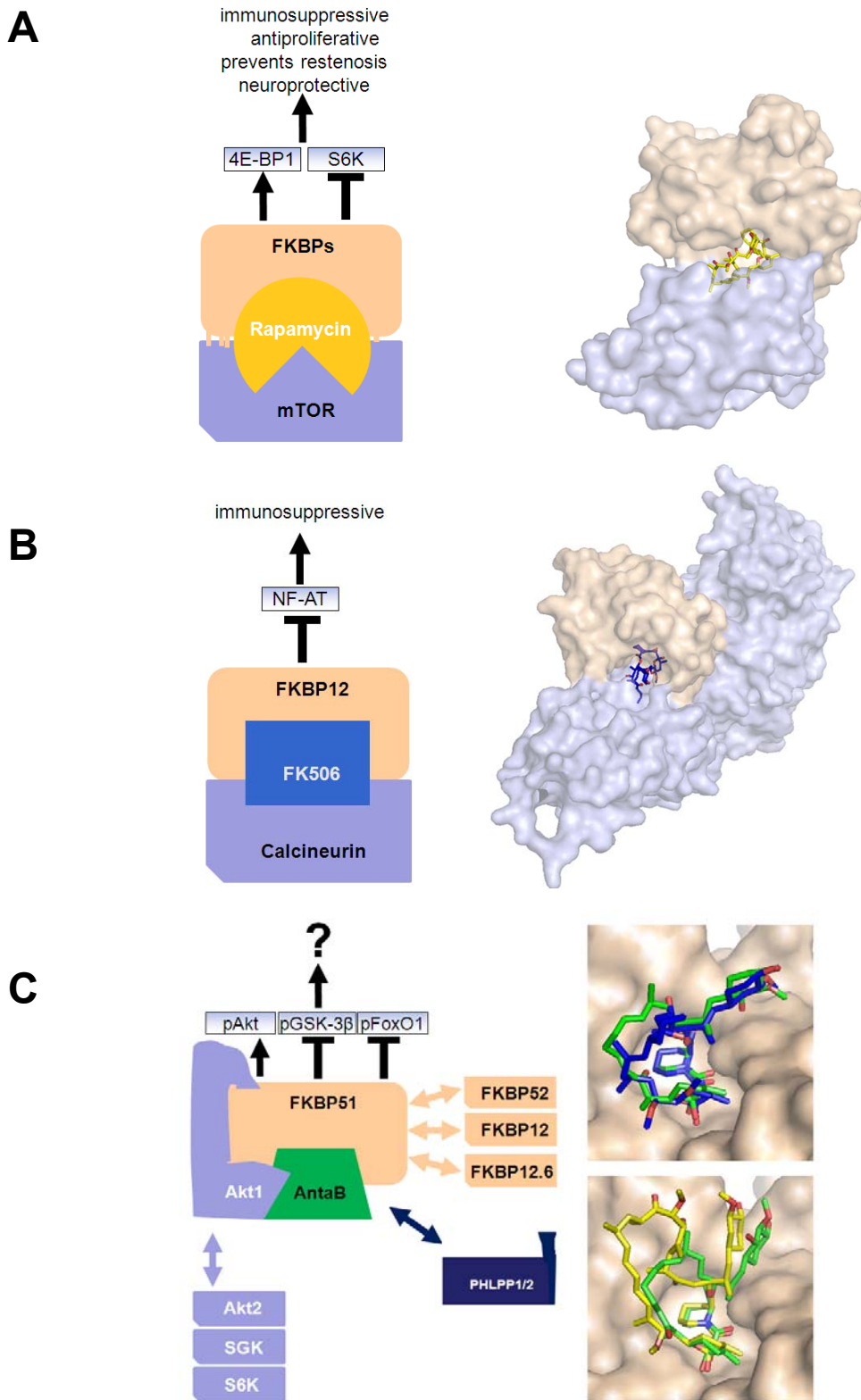
Figure 6.6: Antascomicin B forms functional ternary complexes

A The ternary complex formed by mTOR/rapamycin/FKBPs: schematic (left side), crystal structure of mTOR FRB/rapamycin/FKBP51 (PDB code 4DRI) (right side)

B The ternary complex formed by Calcineurin/FK506/FKBP12: schematic (left side), crystal structure of the calcineurin A fragment, calcineurin B/FK506/FKBP12 (PDB code 1TCO) (right side)

C schematic model of a ternary complex possibly formed by AGC kinases/Antascomicin B/FKBPs and/or PHLPP (left side)
Model of Antascomicin B (green) in the FK506 binding pocket (wheat) together with FK506 (blue) or Rapamycin (yellow)

Discussion

The differences of the structure of C_{16}-C_{25} of Antascomicin B compared to rapamycin is most likely to be responsible for the observed exclusive effects of Antascomicin B as the modelling of Antascomicin B into the FK506-binding pocket of FKBP12 reveales. In contrast the additional OH-group at the top group (cyclohexan) is unlikely to contribute to interactions due to missing H-donors in close proximity.

The exploration of FKBP/Antascomicin/AGC kinases or FKBP/Antascomicin B/PHLPP complexes could bear a completely new therapeutic strategy. Therefore it is important to clarify if the observed dephosphorylation caused by Antascomicin B is a direct effect, for example in in vitro kinase assays. Competition experiments with FK506 or rapamycin where the effects caused by Antascomicin B are rescued in vitro and in cell based systems could further specify its action. Furthermore the different Akt inhibitors might be able to compete with Antascomicin B providing additional insights in structural requirements. It will be interesting to examine the effects of Antascomicin on FKBPs of other species, such as squirrel monkey.

It is important to understand the reason for the reduced cell viability of Antascomicin B after long term treatment in some cell types. Reduced cell viability might be based on reduced cell growth, e.g. caused by the observed reduction of the phosphorylation status of GSK-3β, which in principle could lead to a reduced transcription activity of pro-survival proteins. On the other hand cells could be lost by apoptosis. With the observed decreased FoxO1 phosphorylation one would expect enhanced transcription of pro-apoptotic proteins. These predictions need to be tested experimentally and it should be elucidated which of these effects is more pronounced in which cell types.

Additional direct or indirect downstream effects of Antascomicin B might be seen in antibody phospho proteomic screens (for example PhosphoScan™ Kit from Cell Signaling Technology). By the approach used so far differential expression patterns after Antascomicin B treatment might be missed even though they are likely due to the observed changes in phosphorylation of FoxO1 or GSK-3β. Microarrays and SILAC based methods could serve as a starting point to elucidate the biological meaning of the FKBP/AGC kinase complexes, which are enhanced by Antascomicin B and its enigmatic pharmacological applications.

Since Antascomicin B enhances FKBP51/Akt interaction it could further serve as a tool to solve the crystal structure of the complex in order to locate residues important for interaction. Thus Antascomicin B serves as an innovative lead structure to manipulate the FKBP/AGC kinase or the FKBP/AGC kinase/PHLPP complex formation.

6.4 Towards selective FKBP inhibitors

6.4.1 FKBP selective inhibitors against psychiatric disorders

An imbalanced stress hormone system, the deregulation of the hypothalamus pituitary adrenal (HPA) axis (see Figure 6.7), is correlated with the risk and course of psychiatric diseases such as major depression, bipolar disorder, post-traumatic stress disorder (PTSD), schizophrenia and anxiety disorders [90]. A crucial characteristic of the HPA axis is a negative feedback exerted by cortisol via the glucocorticoid receptor (GR), thus keeping the stress reaction in balance, a process found to be impaired in depressed patients [58].
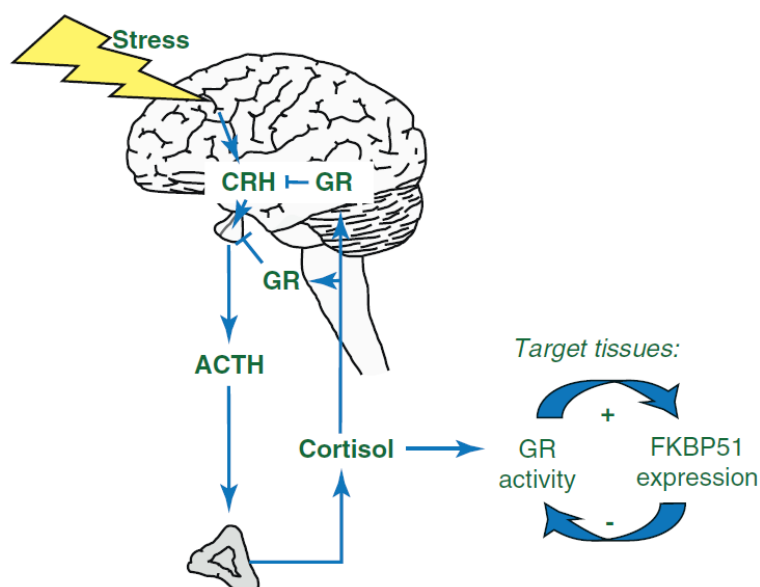
Figure 6.7: FKBP51 decreases HPA axis reactivity after stress or a glucocorticoid challenge [90].
Upon perception of stress, CRH (corticocotropin-releasing-hormone) is released from the hypothalamus, thus promoting synthesis and release of ACTH from the pituitary. ACTH in turn increases release of cortisol from the adrenal glands. In a negative feedback loop, glucocorticoids down-regulate the HPA axis. Decreased sensitivity of this feedback loop and glucocorticoid hyposensitivity were repeatedly observed in depressed patients.

The expression of FKBP51 is strongly increased by corticosteroids [56] indicating that FKBP51 attenuates cortisol responses in hormone-conditioned tissues as part of the mentioned feedback mechanism [53, 57]. High circulating FKBP51 levels lead to reduced hormone binding affinity as observed in squirrel monkeys [48-50]. Results from animal studies show a protective effect of FKBP51 knockout or knockdown on stress endocrinology and stress-coping behavior [62-64]. Finally, human genetic studies correlate polymorphisms within the FKBP51 encoding gene *FKBP5,* with increased recurrence of depressive episodes and improvement of patient's response to antidepressive treatment [59-61]. All this culminates in

_____

an important role of FKBP51 in HPA axis deregulation. Pharmacological targeting of this protein by FKBP51 inhibitors might be beneficial for treatment of patients suffering from depression and anxiety disorders.

As FKBP52 has an opposite function on the GR and as the FKBPs are highly homologues in structure but different in function, which could lead to severe side effects (for example concerning the reproductive system), there is a high need for selective FKBP51 inhibitors.

As current pharmacotherapeutic options for mood disorders leave substantial unmet medical needs, tailoring selective FKBP51 inhibitors is an innovative strategy to correct disturbances of the HPA axis and a main aim pursued in our group.

6.4.2 Improving the ligand efficiency for FKBP51

All known FKBP51 ligands, including the natural products rapamycin and FK506, suffer from a very low ligand efficiency (<0.18) [145, 148].

Increasing ligand efficiency, here defined as ligand free binding energy normalized to the number of non-hydrogen atoms [306], is an attractive conceptual framework for guiding drug discovery as it balances the potency of ligands against undesired properties such as increasing molecular weight [278, 280, 307-310]. Ligand efficiency has been firmly linked to the quality of lead compounds but also to the druggability of the individual protein target classes [278, 279, 308, 310-312]. Notably, shallow binding sites such as those mediating protein-protein interactions have an intrinsically limited contact surface and these targets are notoriously difficult for the development of efficient ligands or drugs [313].

Flexible ligands are thought to suffer an entropic penalty upon binding due to the freezing of rotatable bonds [314, 315]. In turn, reducing ligand flexibility is an appealing concept to improve potency [316-319]. It is also well known that flexible ligands often adopt higher energy conformations upon binding to fine-tune ligand-protein interactions [320-323]. Thus, in principle, additional binding energy could be gained by pre-organizing or stabilizing these high-energy active conformations.

A higher affinity of rigid ligands such as compounds YW703 and YW691 (see Table 5.2, section 5.5) is commonly attributed to entropic advantages. In our isothermal calorimetric experiments (section 5.5) the opposite was observed when comparing YW691 to YW644. While we cannot exclude that the rigidification in ligand YW691 was entropically advantageous *per se* – e.g. compared to a hypothetical unconstrained analog of equal binding enthalpy – this was masked compared to YW644 by a dominating enthalpy-entropy compensation, a common phenomenon in ligand-protein interactions [324], which was also observed for FKBP12

_____

and the high affinity ligands FK506 and rapamycin [325]. Negative changes in binding entropy upon ligand rigidification have recently been observed by several groups [326-330]. In one case, the counterproductive entropic change was shown to be caused by a stronger ordering of the protein by the more rigid ligands [329].

The differences between the monocycle YW644 and the more rigid bicycles YW691 and YW703 could be explained, first by better hydrogen bond acceptor properties of the C_1-amide compared to the C_1-ester and second by stabilization of the conformation of O_1-C_1-C_2-N_7. In addition the C_8-methylene could mediate additional van-der-Waals contacts. The enhanced binding enthalpy of YW691 (ΔH=-13.6 kcal/mole) is surprising, given the minimal differences in the binding mode compared to YW703 (ΔH=-3 kcal/mole). The direct comparison reveals the strong orientation dependence of the hydrogen bond and dipolar contact network around the C_1=O carbonyl which could account for a substantial amount of the additional binding entropy of YW691.

The binding affinities of YW644, YW703 and YW691 measured by ITC (3.3 µM, 10.5 µM and 0.36 µM, respectively) were in excellent agreement with the fluorescence polarization assay results (Table 5.2).

It should be noted that 5% DMSO, as used for solubility reasons throughout the measurements is a high amount and even careful preparation of controls that contain the same amount of DMSO can't fully exclude mistakes by buffer mismatches. Therefore it is recommended either to use smaller fractions of DMSO or prepare the ligand and the protein solution from the same diluted DMSO stock solutions.

Altogether the bicyclic [4.3.1] aza-amide scaffold was identified as a privileged substructure for FK506-binding proteins (FKBPs) and serves as a valuable starting point for the synthesis of efficient FKBP51 ligands [144].

6.4.3 Selective FKBP inhibitors – will they be safe?

The multitude of functions known for FKBP51 (co-chaperone, involvement in glucocorticoid receptor- , NF-κB- signaling, PPIase – see section 1.1.2) carries the inherent danger of side effects when blocking FKBP51.

However, no target specific side effects became apparent from studies on FKBP51 knockout mice [62-64]. A phase I clinical trial with the pan-specific FKBP ligand FK1706 suggested that the blockage of FKBPs (including FKBP51 and FKBP52) are tolerated in humans for prolonged times [143].

_____

In contrast Hou *et al.* [76] found that the down regulation of FKBP51 in shFKBP51 xenograft mice promotes tumor growth and resistance to gemcitabine, a phenomenon consistent with their previous findings in pancreatic cell lines [75]. This raises the possibility that the blockage of FKBP51 might promote cell growth in cancerous tissue or at least promotes resistance to certain therapies in some types of cancer. This was attributed to increased Akt hyperphosphorylation and activation caused by a reduction of FKBP51-facilitated action of the phosphatase PHLPP. Using the pancreatic cancer cell line SU.86.86, which was also used in the above publication we could demonstrate that the pan-specific FKBP inhibitor FK1706 did not alter cell viability alone (Figure 5.25B). When administered together with the nucleoside analog gemcitabine, gemcitabine's ability to reduce cell viability was not impaired even by 10 µM of FK1706 (Figure 5.25A).

Consistent with this finding FKBP51 ligands did not disrupt the FKBP51/Akt interaction (Figure 5.27) or FKBP51/PHLPP interaction (Figure 5.28) suggesting that the clinically used FKBP ligands are unlikely to affect the regulation of Akt by FKBP51. This coincides with the lack of an effect of the high-affinity ligands FK506 or FK1706 and YW648 but also the FKBP-subgroup specific inhibitors cmpd 44 (FKBP12-selective) and SG537 (FKBP51 selective) on the Akt/mTOR pathway in several studied cell types (Figure 5.26).

However, FK1706 showed a significant reduction on mTOR phosphorylation in HeLa cells in one experiment (Figure 5.26). In general this study can only serve as a starting point since statistical analysis with such a small sample size (2-3 samples) is very critical.

At the biochemical level, however, parts of the FK1 domain, which must be in the vicinity of the FK506-binding site, seem to be important for the interaction with Akt. This raises the possibility to develop ligands for the FK506-binding site that might be able to allosterically modulate the FKBP51/Akt interaction. The feasibility of this hypothesis will require a better understanding of the parts of FKBP51 that bind to Akt. Here the further exploration of the enhancement of Akt1/FKBP51 interaction by Antascomicin B could provide a first starting point (see section 6.3).

Moreover, the safety of future medication has to be discussed not only from the pharmacodynamic point of view but also pharmacokinetic properties have to be taken into account. For example FK506 was shown to inhibit the drug efflux pump Pgp1, leading to increased glucocorticoid levels [331]. The inhibition of drug efflux pumps also has to be considered when additional medication occurs since it can strengthen toxic side effects.

6.5 The possible role of FKBP51 in cancer aethology

The kinase Akt is a key signaling node which is essential for many adaptive processes (e.g. neuroregeneration [332]), but detrimental when overactive like in many cancers. In turn, the activity of Akt is tightly regulated under normal conditions. Recently, FKBP51 emerged as a new regulator of Akt. FKBP51 is a target of the clinically used immunosuppressants or anti-cancer-drugs FK506 and rapamycin. While the role of protein kinases in cancer development is well established, the influence of FKBP51 on malignancy is contradictory. Several studies have shown that FKBP51 is up-regulated in several cancers and that it can promote the pro-liferation of many cancer cell lines [69, 72, 74, 77, 333]. Interestingly A. März [14] found a rapamycin dependent increase of Akt (S473) phosphorylation up to 30% upon overexpression of FKBP51 compared to mock transfected cells.

In contrast, Wang and colleagues found FKBP51 to enhance the response to chemothera-peutics, such as Gemcitabine in pancreatic and breast cancer cell lines [75, 76]. Mechanisti-cally, the latter effect was attributed to a scaffolding function of FKBP51, which could pro-mote dephosphorylation of Akt by the phosphatase PHLPP. The presented results support a role of FKBP51 in Akt phosphorylation, however we observed an increase not a decrease in Akt phosphorylation. A reason for this discrepancy could be that PHLPP is not the limiting phosphatase in HEK293T cells or under our cell culture conditions. Recently deficiency of diacylglycerol kinase δ (DGK δ) was found to be connected to an activation of protein kinase C α (PKCα) which via reduced epidermal growth factor led to the dephosphorylation of Akt. Since depletion of PHLPP2 exclusively rescued Akt phosphorylation in DGK δ deficient cells it was argued that β-arrestin 1 might function as a scaffolding protein which mediates specific interaction of PHLPP2 with Akt [334]. It is likely that the regulation, composition and interplay of scaffolding proteins contribute to the outcome of signalling pathways.

We believe in a connection of FKBP51 expression levels and the promotion of cancer. Since the effects of FKBP expression seem to be highly context and cell type dependent immuno-histochemical expression studies in human malignancies will help to understand the role of FKBP51 levels in abnormal cell growth of cancers, and this could be considered as a promis-ing new marker of tumor progression and response to radio/chemotherapy [77, 335].

6.6 Possible effects of Akt/FKBP51 interaction on other pathways

A cell is immersed in an ocean of growth factors and signaling molecules integrate these multiple cues. The integration of signaling pathways is only marginally understood. Feedforward and feedback loops embracing interacting pathways make the input-output response of one pathway dependent of the activity of another. Therefore, by focussing on just one pathway like the Akt/mTOR pathway it is difficult to understand the effects of a newly found interaction such as FKBP51 and Akt. The following table summarizes important pathways that could be affected by Akt/FKBP51 interaction (Table 6.1).

Protein involved	Pathway/mechanism	Involved signaling nodes	literature
Akt	Ras/MAPK	PI3K, GRB2, E3-ubiquitin ligase, p70S6K, TSC2 etc.	[336, 337]
	glycolysis	AMPK, glucose transporter, hexokinase. PFK	[201]
	autophagy	AMPK, mTORC1	[165]
	Pentose phosphate pathway	Prolipogenic factor SREBP1	[338]
	lipogenesis	DEPTOR, Prolipogenic factor SREBP1	[218, 339]
	JAK/STAT	PI3K	[340]
	IKK/NF-κB	mTOR	[341]
	angiogenesis	HIF1α	[342]
	Wnt signaling	GSK3	[343]
	Cytoskeletal organization	mTORC2	[165]
	Hsp90	mTORC1	[302]

Protein involved	Pathway/mechanism	Involved signaling nodes	literature
FKBP51	Hsp90/glucocorticoid receptor signaling	Hsp90	[344]
	apoptosis	Calcineurin, NFAT	[66]
	NF-κB		[67, 345]
	Hsp90	mTOR	[302]
	Akt/PHLPP	scaffolding protein	[75]

Table 6.1: Akt and FKBP51 can be involved and are interconnected in several pathways

Furthermore, if other AGC kinases such as SGK or S6K could substitute for Akt in some point and certain FKBPs could take over the role of others the complexity will even raise. Indeed it was shown, that tumor cells, which are resistant to Akt inhibitors exhibit higher levels of SGK [D. Alessi, personal communication]. One has to consider that these pathways are highly cell- and context dependent [218].

Due to detection purposes and protein stability we decided to overexpress Akt, FKBP and/or PHLPP. We are aware that is at the same time a limitation. When overexpressed we observed a stable interaction of Akt1 and FKBP51 and influences on downstream targets. Nevertheless, it must be considered that the plasmid-based overexpression of proteins may alter protein compositions which might change the outcome of experiments. In addition one signaling pathway cannot be favored against others; thus most probably one observes a combination of different effects on several pathways. Some of them may amplify each other, some of them may extinguish each other. In addition compensatory signaling can be involved. In order to study single pathways others could be blocked by inhibitors or mutations as for example achieved by the FKBP51TPR_mut, which rules out effects of the Hsp90 pathway. In addition expression levels of recombinant proteins were only moderately higher than endogenous proteins.

Altogether overexpression of proteins serves as a valuable tool when protein-protein interactions are very weak or intermediate. In order to observe maturation processes or transition states one could apply pulse-chase techniques to monitor protein-protein interactions.

7. Summary

The immunosuppressant and anti-cancer drug rapamycin works by a ternary gain-of-function mechanism that enables cytosolic proteins to inhibit the kinase mTOR. The obligatory accessory partner of rapamycin was thought to be FKBP12. Here it is demonstrated that the pan-selective FKBP inhibitors but not FKBP12-specific inhibitors can block the effects of rapamycin. In addition, we show that at least the large Hsp90 co-chaperone FKBP51 can reconstitute the effects of FKBP12 in FKBP12-knockdown cells. Our findings call for a broader interpretation of the actions of rapamycin. Moreover, they provide a rationale for FKBP subtype-selective rapamycin analogs, which could specifically target tissues that express a certain FKBP subtype.

FKBP51 was shown to be involved in several cancers, both as an oncogenic- or tumor suppressing protein. Here we clearly demonstrate that FKBP51 directly interacts with the kinase Akt. This kinase constitutes an important signaling node as it plays a crucial role in several pathways, which are frequently deregulated in a wide variety of cancers. In addition to Akt we found other AGC kinases to form complexes with FKBP51. In turn, paralogs and orthologs of FKBP51 were involved in complex formation with Akt. Our mapping studies revealed that FKBP51 interacts with Akt via multiple domains independent of their activation or phosphorylation status. We present a model where FKBP51 binds directly to Akt as well as via Hsp90.

The FKBP51/Akt1 interaction was not affected by FK506 analogs or Akt active site inhibitors, but was diminished by the allosteric Akt inhibitor VIII. None of the FKBP51 inhibitors affected Akt (S473) or Akt (T308) phosphorylation or downstream targets of Akt. The FKBP51/Akt interaction is sensitive to the conformation of Akt1, but does not depend on the FK506-binding pocket of FKBP51. Thus we found FKBP inhibitors unlikely to inhibit the Akt/FKBP/PHLPP network.

In the search for modulators of the Akt/FKBP51 complex we serendipitously identified Antascomicin B, which forms a ternary complex with FKBP51/Akt and FKBP51/PHLPP respectively. The FKBP51/Antascomicin B/Akt complex does not depend on additional proteins as shown in our pulldown experiments. Furthermore, several AGC kinases and different FKBP homologs can substitute each other in an enhanced interaction mediated by Antascomicin B. We further observed downstream effects on Akt phosphorylation and downstream targets such as GSK3β and FoxO1, providing for the first time experimental data for

biological effects of Antascomicin B. Antascomicin B constitutes a valuable tool for the investigation of FKBP51/Akt interaction and more importantly a starting point for chemical dimerizers of FKBPs and AGC kinases.

_____

8. Appendix

8.1 Extinction coefficients for purified proteins

The protein concentrations were determined using extinction coefficients which were calculated based on the protein sequence. A web-based application was used:

Proteincalculator v3.3: http://www.scripps.edu/~cdputnam/protcalc.html

Protein	Molecular weight [kDa]	Molar extinction coefficient [L*mol^{-1}*cm^{-1}]	Specific extinction coefficient [L*g^{-1}*cm^{-1}]
HisFKBP51_FLAG	55.5	46200	0.8317
HisFKBP52_FLAG	56.1	51800	0.9227
HisFKBP51ΔFK1	36.8	28000	0.7862
HisFKBP51FK1	18.7	16800	0.9007

Table 8.1: Extinction coefficients used to calculate protein concentrations

8.2 Active site titration of FKBP52

As the purification process can diminish the functionality of expressed purified proteins, the activity was checked before proceed with the functional assays. Therefore "active site" titrations with the synthetic fluorescein-labeled FKBP ligand CK97 ("tracer") were carried out [264]. "Active site titrations" offer valuable clues if the concentration, determined by UV measurement corresponds to the concentration of active protein. Where indicated in Table 4.2 (see section 4.2.4.3) this procedure was used. As an example FKBP52 titration curves are depicted in Figure 8.1. Here, FKBP52 is titrated against a fixed concentration of labeled ligand. The experiment was performed several times with different concentrations of constant CK97 (Figure 8.1A). For each binding curve the EC$_{50}$ values were extracted and plotted against the corresponding ligand concentration (Figure 8.1B). By linear curve fitting and extrapolation the intersection with the y-axis is determined which leads to a Kd like value. This value was examined by [264] to be 1.4±0.1 nM and found throughout this experiment to be 3.4 (bold letters in the regression formula). The value herein measured is also in the low nanomolar range and the slight difference could be based on pipetting or technical differences.

A
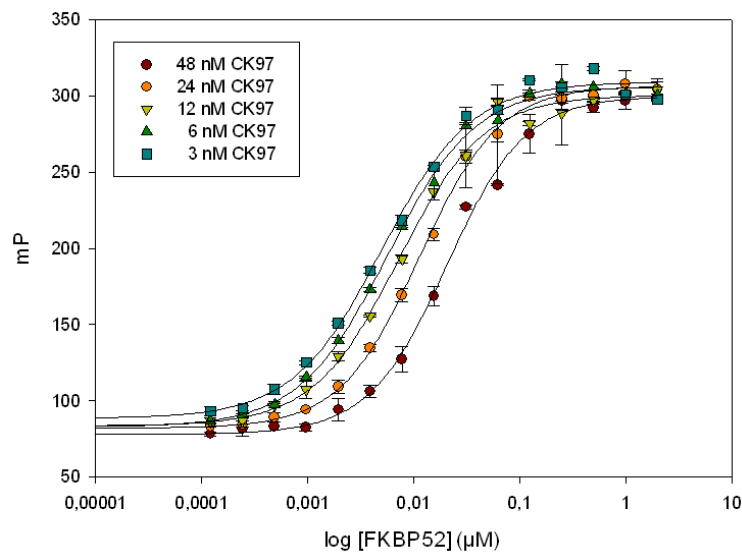
B
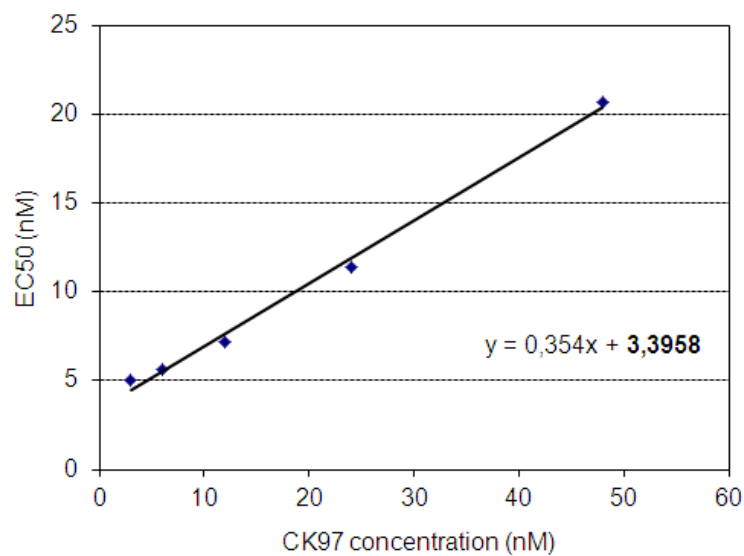
Figure 8.1: Determination of the concentration of FKBP52 by active site titration
A Binding curved of the titration of FKBP52 against 3-48 nM CK97, half-logarithmic plot
B Plot of calculated EC_{50} values against the actual tracer concentration, the linear equation is depicted and the intersection with the y-axis is printed in bold

The slope value shows the portion of active FKBP52 being underestimated. The correction factor which should be used for correction of the UV values determined can be calculated by forming the quotient of 0.5 and the slope value. Multiplication of the concentration deter-

mined by UV measurement multiplied with the factor leads to the correct value as exemplified here for FKBP52 (Table 8.2).

Protein	Slope	Correction Faktor	Kd	Protein concentration, UV determined (µM)	Protein concentration corrected (µM)
FKBP52	0.354	1.4	3.4	83	116

Table 8.2: Protein concentrations must be corrected corresponding to results of active site titration

8.3 Abbreviations

AP	Alkaline Phosphatase
APS	ammonium peroxodisulfate
aa	amino acid
AGC kinases	cAMP-dependent, cGMP-dependent and PKC (protein kinase C) kinase
Anta B	Antascomicin B
ATP	adenosine-5'-triphosphate
bp	base pair(s)
BCA	bicinchoninic acid
BSA	bovine serum albumin
CIP	calf intestine phosphatase
CV	column volume
d	day
Da	Dalton
bidest. H2O	double distilled water
DMSO	dimethyl sulfoxide
DNA	deoxyribonucleic acid
dNTP	2'-deoxynucleoside 5'-triphosphate
dsDNA	double strand DNA
E. coli	*Escherichia coli*
EDTA	ethylendiamine-tetraacetic acid
EMA	European Medicines Agency
EtOH	ethanol
FCS	fetal calf serum
FDA	Food and Drug Administration
g	gram(s)
GSK-3	glycogen synthase kinase 3
h	hour(s)
Hepes	4-(2-hydroxyethyl)-1-piperazineethanesulfonic acid
HRP	horseradish peroxidase
Hs	Homo sapiens
IP	Immunoprecipitation
IPTG	Isopropyl-β-D-1-thiogalactopyranoside

IRS	insulin receptor substrate
ITC	isothermal titration calorimetry
kb	kilo base pair(s)
kDa	kilo Dalton
l	litre
LB Medium	lysogeny broth
M	molar (mol/l)
m	metre(s)
mA	milliAmpere(s)
MAPK	mitogen-activated protein kinase
min	minute(s)
ml	millilitre(s)
mM	millimolar
MW	molecular weight
nM	nanomolar
NF-AT	nuclear factor of activated T cells
OD	optical density
ORF	open reading frame
PCR	polymerase chain reaction
PFK	phospho-fructokinase
pM	picomolar
RNase A	Ribonuclease A
rpm	round(s) per minute
Rap	Rapamycin
RT	room temperature
S6K	ribosomal S6 kinase
SD	standard deviation
SDS	sodium dodecyl sulfate
SGK	serum/glucocorticoid-inducible kinase
SHR	steroid hormone receptor
s	second(s)
sm	squirrel monkey
ssDNA	single strand DNA
Tris	tris(hydroxymethyl)aminomethane
Triton X-100	polyethylene glycol p-(tetramethylbutyl)-phenyl ether
U	enzymatic unit(s)
UV	ultraviolet

V	Volt
v/v	volume per volume
w/v	weight per volume
wt	wild type
µl	microlitre(s)
µM	micromolar

9. Bibliography

1. Siekierka, J.J., et al., *A cytosolic binding protein for the immunosuppressant FK506 has peptidyl-prolyl isomerase activity but is distinct from cyclophilin.* Nature. 1989 Oct 26;341(6244):755-7., 1989.
2. Siekierka, J.J., et al., *The cytosolic-binding protein for the immunosuppressant FK-506 is both a ubiquitous and highly conserved peptidyl-prolyl cis-trans isomerase.* J Biol Chem, 1990. **265**(34): p. 21011-5.
3. Fischer, G., H. Bang, and C. Mech, *Determination of enzymatic catalysis for the cis-trans-isomerization of peptide binding in proline-containing peptides.* Biomed Biochim Acta, 1984. **43**(10): p. 1101-11.
4. Fischer, G., et al., *Cyclophilin and peptidyl-prolyl cis-trans isomerase are probably identical proteins.* Nature, 1989. **337**(6206): p. 476-8.
5. Harding, M.W., et al., *A receptor for the immunosuppressant FK506 is a cis-trans peptidyl-prolyl isomerase.* Nature, 1989. **341**(6244): p. 758-60.
6. Fischer, S., S. Michnick, and M. Karplus, *A mechanism for rotamase catalysis by the FK506 binding protein (FKBP).* Biochemistry, 1993. **32**(50): p. 13830-7.
7. Galat, A., *Peptidylproline cis-trans-isomerases: immunophilins.* Eur J Biochem, 1993. **216**(3): p. 689-707.
8. Liu, J., et al., *Calcineurin is a common target of cyclophilin-cyclosporin A and FKBP-FK506 complexes.* Cell, 1991. **66**(4): p. 807-15.
9. Mukai, H., et al., *FKBP12-FK506 complex inhibits phosphatase activity of two mammalian isoforms of calcineurin irrespective of their substrates or activation mechanisms.* J Biochem, 1993. **113**(3): p. 292-8.
10. Liu, J., et al., *Inhibition of T cell signaling by immunophilin-ligand complexes correlates with loss of calcineurin phosphatase activity.* Biochemistry, 1992. **31**(16): p. 3896-901.
11. Sabatini, D.M., et al., *RAFT1: a mammalian protein that binds to FKBP12 in a rapamycin-dependent fashion and is homologous to yeast TORs.* Cell, 1994. **78**(1): p. 35-43.
12. Chung, J., et al., *Rapamycin-FKBP specifically blocks growth-dependent activation of and signaling by the 70 kd S6 protein kinases.* Cell, 1992. **69**(7): p. 1227-36.
13. Burnett, P.E., et al., *RAFT1 phosphorylation of the translational regulators p70 S6 kinase and 4E-BP1.* Proc Natl Acad Sci U S A, 1998. **95**(4): p. 1432-7.
14. März, A., *A New Player in mTOR Regulation: Introducing FKBP51.* PhD thesis, 2011.
15. Lyons, W.E., et al., *Immunosuppressant FK506 promotes neurite outgrowth in cultures of PC12 cells and sensory ganglia.* Proceedings of the National Academy of Sciences, 1994. **91**(8): p. 3191-3195.
16. Steiner, J.P., et al., *Neurotrophic actions of nonimmunosuppressive analogues of immunosuppressive drugs FK506, rapamycin and cyclosporin A.* Nat Med, 1997. **3**(4): p. 421-428.
17. Gold, B.G., et al., *Immunophilin FK506-Binding Protein 52 (Not FK506-Binding Protein 12) Mediates the Neurotrophic Action of FK506.* Journal of Pharmacology and Experimental Therapeutics, 1999. **289**(3): p. 1202-1210.
18. Edlich, F., et al., *The Specific FKBP38 Inhibitor N-(N',N'-Dimethylcarboxamidomethyl)cycloheximide Has Potent Neuroprotective and Neurotrophic Properties in Brain Ischemia.* Journal of Biological Chemistry, 2006. **281**(21): p. 14961-14970.
19. Pong, K. and M.M. Zaleska, *Therapeutic implications for immunophilin ligands in the treatment of neurodegenerative diseases.* Curr Drug Targets CNS Neurol Disord, 2003. **2**(6): p. 349-56.

20.   Gerard, M., et al., *Unraveling the role of peptidyl-prolyl isomerases in neurodegeneration.* Mol Neurobiol. 2011 Aug;44(1):13-27. Epub 2011 May 7., 2011.

21.   Schiene-Fischer, C., T. Aumuller, and G. Fischer, *Peptide Bond cis/trans Isomerases: A Biocatalysis Perspective of Conformational Dynamics in Proteins.* Top Curr Chem, 2013. **328**: p. 35-67.

22.   Michnick, S., et al., *Solution structure of FKBP, a rotamase enzyme and receptor for FK506 and rapamycin.* Science, 1991. **252**(5007): p. 836-839.

23.   Young, J.C., W.M. Obermann, and F.U. Hartl, *Specific binding of tetratricopeptide repeat proteins to the C-terminal 12-kDa domain of hsp90.* J Biol Chem, 1998. **273**(29): p. 18007-10.

24.   Wu, B., et al., *3D structure of human FK506-binding protein 52: implications for the assembly of the glucocorticoid receptor/Hsp90/immunophilin heterocomplex.* Proc Natl Acad Sci U S A, 2004. **101**(22): p. 8348-53.

25.   Van Duyne , G.D., Standaert, Robert F., Karplus Andrew, Schreiber, Stuart L., Clardy, John, *Atomic Structure of FKBP-FK506, an immunophilin-immunosuppressant complex.* Science, 1991. **252**(5007): p. 4.

26.   Jin, Y.J., et al., *Molecular cloning of a membrane-associated human FK506- and rapamycin-binding protein, FKBP-13.* Proceedings of the National Academy of Sciences, 1991. **88**(15): p. 6677-6681.

27.   Nigam, S.K., et al., *Localization of the FK506-binding protein, FKBP 13, to the lumen of the endoplasmic reticulum.* Biochem. J., 1993. **294**(2): p. 511-515.

28.   Sinars, C.R., et al., *Structure of the large FK506-binding protein FKBP51, an Hsp90-binding protein and a component of steroid receptor complexes.* Proc Natl Acad Sci U S A, 2003. **100**(3): p. 868-73.

29.   Lam, E., M. Martin, and G. Wiederrecht, *Isolation of a cDNA encoding a novel human FK506-binding protein homolog containing leucine zipper and tetratricopeptide repeat motifs.* Gene, 1995. **160**(2): p. 297-302.

30.   Baughman, G., et al., *Tissue distribution and abundance of human FKBP51, and FK506-binding protein that can mediate calcineurin inhibition.* Biochem Biophys Res Commun, 1997. **232**(2): p. 437-43.

31.   Bierer, B.E., et al., *Two distinct signal transmission pathways in T lymphocytes are inhibited by complexes formed between an immunophilin and either FK506 or rapamycin.* Proc Natl Acad Sci U S A, 1990. **87**(23): p. 9231-5.

32.   Chen, J., et al., *Identification of an 11-kDa FKBP12-rapamycin-binding domain within the 289-kDa FKBP12-rapamycin-associated protein and characterization of a critical serine residue.* Proc Natl Acad Sci U S A, 1995. **92**(11): p. 4947-51.

33.   MacMillan, D. and J.G. McCarron, *Regulation by FK506 and rapamycin of Ca2+ release from the sarcoplasmic reticulum in vascular smooth muscle: the role of FK506 binding proteins and mTOR.* Br J Pharmacol, 2009. **158**(4): p. 1112-20.

34.   Jayaraman, T., et al., *FK506 binding protein associated with the calcium release channel (ryanodine receptor).* J Biol Chem, 1992. **267**(14): p. 9474-7.

35.   Ahern, G.P., P.R. Junankar, and A.F. Dulhunty, *Single channel activity of the ryanodine receptor calcium release channel is modulated by FK-506.* FEBS Lett, 1994. **352**(3): p. 369-74.

36.   Okadome, T., et al., *Characterization of the interaction of FKBP12 with the transforming growth factor-beta type I receptor in vivo.* J Biol Chem, 1996. **271**(36): p. 21687-90.

37.   Mathea, S., et al., *Suppression of EGFR autophosphorylation by FKBP12.* Biochemistry, 2011. **50**(50): p. 10844-50.

38.   Sugata, H., et al., *A peptidyl-prolyl isomerase, FKBP12, accumulates in Alzheimer neurofibrillary tangles.* Neurosci Lett, 2009. **459**(2): p. 96-9.

39.   Liu, F.L., et al., *The intracellular domain of amyloid precursor protein interacts with FKBP12.* Biochem Biophys Res Commun, 2006. **350**(2): p. 472-7.

40.   Hoeffer, C.A., et al., *Removal of FKBP12 enhances mTOR-Raptor interactions, LTP, memory, and perseverative/repetitive behavior.* Neuron, 2008. **60**(5): p. 832-45.

41. Ma, T., et al., *Dysregulation of the mTOR pathway mediates impairment of synaptic plasticity in a mouse model of Alzheimer's disease.* PLoS One, 2010. **5**(9): p. 0012845.

42. Deleersnijder, A., et al., *Comparative analysis of different peptidyl-prolyl isomerases reveals FK506-binding protein 12 as the most potent enhancer of alpha-synuclein aggregation.* J Biol Chem, 2011. **286**(30): p. 26687-701.

43. Sewell, T.J., et al., *Inhibition of calcineurin by a novel FK-506-binding protein.* J Biol Chem, 1994. **269**(33): p. 21094-102.

44. Li, B.-Y., et al., *The Role of FK506-Binding Proteins 12 and 12.6 in Regulating Cardiac Function.* Pediatric Cardiology, 2012. **33**(6): p. 988-994.

45. Baughman, G., et al., *FKBP51, a novel T-cell-specific immunophilin capable of calcineurin inhibition.* Mol Cell Biol, 1995. **15**(8): p. 4395-402.

46. Yeh, W.C., et al., *Identification and characterization of an immunophilin expressed during the clonal expansion phase of adipocyte differentiation.* Proc Natl Acad Sci U S A, 1995. **92**(24): p. 11081-5.

47. Barent, R.L., et al., *Analysis of FKBP51/FKBP52 chimeras and mutants for Hsp90 binding and association with progesterone receptor complexes.* Mol Endocrinol, 1998. **12**(3): p. 342-54.

48. Denny, W.B., et al., *Squirrel monkey immunophilin FKBP51 is a potent inhibitor of glucocorticoid receptor binding.* Endocrinology, 2000. **141**(11): p. 4107-13.

49. Scammell, J.G., et al., *Overexpression of the FK506-Binding Immunophilin FKBP51 Is the Common Cause of Glucocorticoid Resistance in Three New World Primates.* General and Comparative Endocrinology, 2001. **124**(2): p. 152-165.

50. Reynolds, P.D., et al., *Glucocorticoid resistance in the squirrel monkey is associated with overexpression of the immunophilin FKBP51.* J Clin Endocrinol Metab, 1999. **84**(2): p. 663-9.

51. Brown, G.M., et al., *Pituitary-Adrenal Function in the Squirrel Monkey.* Endocrinology, 1970. **86**(3): p. 519-529.

52. Chrousos, G.P., et al., *Glucocorticoid hormone resistance during primate evolution: receptor-mediated mechanisms.* Proc Natl Acad Sci U S A, 1982. **79**(6): p. 2036-40.

53. Hubler, T.R., et al., *The FK506-binding immunophilin FKBP51 is transcriptionally regulated by progestin and attenuates progestin responsiveness.* Endocrinology, 2003. **144**(6): p. 2380-7.

54. Wochnik, G.M., et al., *FK506-binding proteins 51 and 52 differentially regulate dynein interaction and nuclear translocation of the glucocorticoid receptor in mammalian cells.* J Biol Chem, 2005. **280**(6): p. 4609-16.

55. Denny, W.B., et al., *Structure-function analysis of squirrel monkey FK506-binding protein 51, a potent inhibitor of glucocorticoid receptor activity.* Endocrinology, 2005. **146**(7): p. 3194-201.

56. Vermeer, H., et al., *An in vitro bioassay to determine individual sensitivity to glucocorticoids: induction of FKBP51 mRNA in peripheral blood mononuclear cells.* Mol Cell Endocrinol, 2004. **218**(1-2): p. 49-55.

57. Cheung, J. and D.F. Smith, *Molecular chaperone interactions with steroid receptors: an update.* Mol Endocrinol, 2000. **14**(7): p. 939-46.

58. Holsboer, F., *The corticosteroid receptor hypothesis of depression.* Neuropsychopharmacology, 2000. **23**(5): p. 477-501.

59. Binder, E.B., et al., *Polymorphisms in FKBP5 are associated with increased recurrence of depressive episodes and rapid response to antidepressant treatment.* Nat Genet. 2004 Dec;36(12):1319-25. Epub 2004 Nov 21., 2004.

60. Zou, Y.F., et al., *Meta-analysis of FKBP5 gene polymorphisms association with treatment response in patients with mood disorders.* Neurosci Lett, 2010. **484**(1): p. 56-61.

61. Ellsworth, K.A., et al., *FKBP5 genetic variation: association with selective serotonin reuptake inhibitor treatment outcomes in major depressive disorder.* Pharmacogenet Genomics, 2013. **23**(3): p. 156-66.

62.   Touma, C., et al., *FK506 Binding Protein 5 Shapes Stress Responsiveness: Modulation of Neuroendocrine Reactivity and Coping Behavior.* Biological Psychiatry, 2011. **70**(10): p. 928-936.

63.   Hartmann, J., et al., *The involvement of FK506-binding protein 51 (FKBP5) in the behavioral and neuroendocrine effects of chronic social defeat stress.* Neuropharmacology, 2012. **62**(1): p. 332-9.

64.   O'Leary, J.C., 3rd, et al., *A new anti-depressive strategy for the elderly: ablation of FKBP5/FKBP51.* PLoS One, 2011. **6**(9): p. 15.

65.   Jinwal, U.K., et al., *The Hsp90 cochaperone, FKBP51, increases Tau stability and polymerizes microtubules.* J Neurosci, 2010. **30**(2): p. 591-9.

66.   Giraudier, S., et al., *Overexpression of FKBP51 in idiopathic myelofibrosis regulates the growth factor independence of megakaryocyte progenitors.* Blood, 2002. **100**(8): p. 2932-40.

67.   Bouwmeester, T., et al., *A physical and functional map of the human TNF-alpha/NF-kappa B signal transduction pathway.* Nat Cell Biol. 2004 Feb;6(2):97-105. Epub 2004 Jan 25., 2004.

68.   Avellino, R., et al., *Rapamycin stimulates apoptosis of childhood acute lymphoblastic leukemia cells.* Blood, 2005. **106**(4): p. 1400-6.

69.   Jiang, W., et al., *FK506 binding protein mediates glioma cell growth and sensitivity to rapamycin treatment by regulating NF-kappaB signaling pathway.* Neoplasia, 2008. **10**(3): p. 235-43.

70.   Romano, M.F., et al., *Rapamycin inhibits doxorubicin-induced NF-kappaB/Rel nuclear activity and enhances the apoptosis of melanoma cells.* Eur J Cancer. 2004 Dec;40(18):2829-36., 2004.

71.   Romano, S., et al., *Role of FK506-binding protein 51 in the control of apoptosis of irradiated melanoma cells.* Cell Death Differ. 2010 Jan;17(1):145-57. Epub . 2010.

72.   Periyasamy, S., et al., *The immunophilin ligands cyclosporin A and FK506 suppress prostate cancer cell growth by androgen receptor-dependent and -independent mechanisms.* Endocrinology, 2007. **148**(10): p. 4716-26.

73.   Periyasamy, S., et al., *FKBP51 and Cyp40 are positive regulators of androgen-dependent prostate cancer cell growth and the targets of FK506 and cyclosporin A.* Oncogene, 2010. **29**(11): p. 1691-701.

74.   Ni, L., et al., *FKBP51 promotes assembly of the Hsp90 chaperone complex and regulates androgen receptor signaling in prostate cancer cells.* Mol Cell Biol, 2010. **30**(5): p. 1243-53.

75.   Pei, H., et al., *FKBP51 affects cancer cell response to chemotherapy by negatively regulating Akt.* Cancer Cell, 2009. **16**(3): p. 259-66.

76.   Hou, J. and L. Wang, *FKBP5 as a selection biomarker for gemcitabine and Akt inhibitors in treatment of pancreatic cancer.* PLoS One, 2012. **7**(5): p. e36252.

77.   Romano, S., et al., *FK506-binding protein 51 is a possible novel tumoral marker.* Cell Death Dis, 2010. **1**: p. e55.

78.   Wiederrecht, G., et al., *Characterization of high molecular weight FK-506 binding activities reveals a novel FK-506-binding protein as well as a protein complex.* J Biol Chem. 1992 Oct 25;267(30):21753-60., 1992.

79.   Lebeau, M.C., et al., *P59, an hsp 90-binding protein. Cloning and sequencing of its cDNA and preparation of a peptide-directed polyclonal antibody.* J Biol Chem, 1992. **267**(7): p. 4281-4.

80.   Peattie, D.A., et al., *Expression and characterization of human FKBP52, an immunophilin that associates with the 90-kDa heat shock protein and is a component of steroid receptor complexes.* Proc Natl Acad Sci U S A, 1992. **89**(22): p. 10974-8.

81.   Riggs, D.L., et al., *The Hsp90-binding peptidylprolyl isomerase FKBP52 potentiates glucocorticoid signaling in vivo.* EMBO J, 2003. **22**(5): p. 1158-67.

82.   Tranguch, S., et al., *Cochaperone immunophilin FKBP52 is critical to uterine receptivity for embryo implantation.* Proc Natl Acad Sci U S A, 2005. **102**(40): p. 14326-31.

83. Cheung-Flynn, J., et al., *Physiological role for the cochaperone FKBP52 in androgen receptor signaling.* Mol Endocrinol, 2005. **19**(6): p. 1654-66.

84. Riggs, D.L., et al., *Noncatalytic role of the FKBP52 peptidyl-prolyl isomerase domain in the regulation of steroid hormone signaling.* Mol Cell Biol, 2007. **27**(24): p. 8658-69.

85. Davies, T.H., Y.M. Ning, and E.R. Sanchez, *A new first step in activation of steroid receptors: hormone-induced switching of FKBP51 and FKBP52 immunophilins.* J Biol Chem, 2002. **277**(7): p. 4597-600.

86. Davies, T.H., Y.M. Ning, and E.R. Sanchez, *Differential control of glucocorticoid receptor hormone-binding function by tetratricopeptide repeat (TPR) proteins and the immunosuppressive ligand FK506.* Biochemistry, 2005. **44**(6): p. 2030-8.

87. Galigniana, M.D., et al., *The hsp90-FKBP52 complex links the mineralocorticoid receptor to motor proteins and persists bound to the receptor in early nuclear events.* Mol Cell Biol, 2010. **30**(5): p. 1285-98.

88. Galigniana, M.D., et al., *Evidence that the peptidylprolyl isomerase domain of the hsp90-binding immunophilin FKBP52 is involved in both dynein interaction and glucocorticoid receptor movement to the nucleus.* J Biol Chem, 2001. **276**(18): p. 14884-9.

89. Galigniana, M.D., et al., *Binding of hsp90-associated immunophilins to cytoplasmic dynein: direct binding and in vivo evidence that the peptidylprolyl isomerase domain is a dynein interaction domain.* Biochemistry, 2002. **41**(46): p. 13602-10.

90. Storer, C.L., et al., *FKBP51 and FKBP52 in signaling and disease.* Trends Endocrinol Metab, 2011. **22**(12): p. 481-90.

91. Yong, W., et al., *Essential role for Co-chaperone Fkbp52 but not Fkbp51 in androgen receptor-mediated signaling and physiology.* J Biol Chem, 2007. **282**(7): p. 5026-36.

92. Yang, Z., et al., *FK506-binding protein 52 is essential to uterine reproductive physiology controlled by the progesterone receptor A isoform.* Mol Endocrinol, 2006. **20**(11): p. 2682-94.

93. Tranguch, S., et al., *FKBP52 deficiency-conferred uterine progesterone resistance is genetic background and pregnancy stage specific.* J Clin Invest, 2007. **117**(7): p. 1824-34.

94. Hirota, Y., et al., *Deficiency of immunophilin FKBP52 promotes endometriosis.* Am J Pathol, 2008. **173**(6): p. 1747-57.

95. Warrier, M., et al., *Susceptibility to diet-induced hepatic steatosis and glucocorticoid resistance in FK506-binding protein 52-deficient mice.* Endocrinology, 2010. **151**(7): p. 3225-36.

96. Kraemer, B.C., et al., *Molecular pathways that influence human tau-induced pathology in Caenorhabditis elegans.* Hum Mol Genet, 2006. **15**(9): p. 1483-96.

97. Chambraud, B., et al., *A role for FKBP52 in Tau protein function.* Proc Natl Acad Sci U S A, 2010. **107**(6): p. 2658-63.

98. Giustiniani, J., et al., *Decrease of the immunophilin FKBP52 accumulation in human brains of Alzheimer's disease and FTDP-17.* J Alzheimers Dis, 2012. **29**(2): p. 471-83.

99. Salminen, A., et al., *Hsp90 regulates tau pathology through co-chaperone complexes in Alzheimer's disease.* Prog Neurobiol, 2011. **93**(1): p. 99-110.

100. Gold, B.G., et al., *Immunophilin FK506-binding protein 52 (not FK506-binding protein 12) mediates the neurotrophic action of FK506.* J Pharmacol Exp Ther, 1999. **289**(3): p. 1202-10.

101. Quinta, H.R., et al., *Subcellular rearrangement of hsp90-binding immunophilins accompanies neuronal differentiation and neurite outgrowth.* J Neurochem, 2010. **115**(3): p. 716-34.

102. Galat, A., et al., *A rapamycin-selective 25-kDa immunophilin.* Biochemistry, 1992. **31**(8): p. 2427-34.

103. Jin, Y.J., S.J. Burakoff, and B.E. Bierer, *Molecular cloning of a 25-kDa high affinity rapamycin binding protein, FKBP25.* J Biol Chem, 1992. **267**(16): p. 10942-5.

104. Liang, J., Hung D. T.; Schreiber S. L.; Clardy, J., *Structure of the Human 25 kDa FK506 Binding Protein Complexed with Rapamycin.* J. Am. Chem. Soc., 1996. **118**: p. 1231-1232.

105. Hung, D.T. and S.L. Schreiber, *cDNA cloning of a human 25 kDa FK506 and rapamycin binding protein.* Biochem Biophys Res Commun, 1992. **184**(2): p. 733-8.

106. Riviere, S., A. Menez, and A. Galat, *On the localization of FKBP25 in T-lymphocytes.* FEBS Lett, 1993. **315**(3): p. 247-51.

107. Jin, Y.J. and S.J. Burakoff, *The 25-kDa FK506-binding protein is localized in the nucleus and associates with casein kinase II and nucleolin.* Proc Natl Acad Sci U S A, 1993. **90**(16): p. 7769-73.

108. Yang, W.M., Y.L. Yao, and E. Seto, *The FK506-binding protein 25 functionally associates with histone deacetylases and with transcription factor YY1.* Embo J, 2001. **20**(17): p. 4814-25.

109. Leclercq, M., F. Vinci, and A. Galat, *Mammalian FKBP-25 and its associated proteins.* Arch Biochem Biophys, 2000. **380**(1): p. 20-8.

110. Ahn, J., et al., *Down-regulation of the stathmin/Op18 and FKBP25 genes following p53 induction.* Oncogene, 1999. **18**(43): p. 5954-8.

111. Ochocka, A.M., et al., *FKBP25, a novel regulator of the p53 pathway, induces the degradation of MDM2 and activation of p53.* FEBS Lett, 2009. **583**(4): p. 621-6.

112. Gaali, S., et al., *The chemical biology of immunophilin ligands.* Curr Med Chem, 2011. **18**(35): p. 5355-79.

113. Crabtree, G.R. and S.L. Schreiber, *SnapShot: Ca2+-calcineurin-NFAT signaling.* Cell, 2009. **138**(1): p. 026.

114. Thomson, A.W., ed. *Cyclosprin A-Mode of Action and Clinical application.* 1989, Klumer Academic Press: London.

115. Xu, X., et al., *FKBP12 is the only FK506 binding protein mediating T-cell inhibition by the immunosuppressant FK506.* Transplantation, 2002. **73**(11): p. 1835-8.

116. Weiwad, M., et al., *Comparative analysis of calcineurin inhibition by complexes of immunosuppressive drugs with human FK506 binding proteins.* Biochemistry, 2006. **45**(51): p. 15776-84.

117. Luger, T. and C. Paul, *Potential new indications of topical calcineurin inhibitors.* Dermatology, 2007. **1**: p. 45-54.

118. Vezina, C., A. Kudelski, and S.N. Sehgal, *Rapamycin (AY-22,989), a new antifungal antibiotic. I. Taxonomy of the producing streptomycete and isolation of the active principle.* J Antibiot, 1975. **28**(10): p. 721-6.

119. Sehgal, S.N., H. Baker, and C. Vezina, *Rapamycin (AY-22,989), a new antifungal antibiotic. II. Fermentation, isolation and characterization.* J Antibiot, 1975. **28**(10): p. 727-32.

120. Singh, K., S. Sun, and C. Vezina, *Rapamycin (AY-22,989), a new antifungal antibiotic. IV. Mechanism of action.* J Antibiot, 1979. **32**(6): p. 630-45.

121. Baker, H., et al., *Rapamycin (AY-22,989), a new antifungal antibiotic. III. In vitro and in vivo evaluation.* J Antibiot, 1978. **31**(6): p. 539-45.

122. Houchens, D.P., et al., *Human brain tumor xenografts in nude mice as a chemotherapy model.* Eur J Cancer Clin Oncol, 1983. **19**(6): p. 799-805.

123. Martel, R.R., J. Klicius, and S. Galet, *Inhibition of the immune response by rapamycin, a new antifungal antibiotic.* Can J Physiol Pharmacol, 1977. **55**(1): p. 48-51.

124. Collier, D.S., et al., *Rapamycin in experimental renal allografts in dogs and pigs.* Transplant Proc, 1990. **22**(4): p. 1674-5.

125. Doggrell, S.A., *Sirolimus- or paclitaxel-eluting stents to prevent coronary artery restenosis.* Expert Opin Pharmacother, 2004. **5**(11): p. 2209-20.

126. Soulard, A., et al., *The rapamycin-sensitive phosphoproteome reveals that TOR controls protein kinase A toward some but not all substrates.* Mol Biol Cell, 2010. **21**(19): p. 3475-86.

127. Zoncu, R., A. Efeyan, and D.M. Sabatini, *mTOR: from growth signal integration to cancer, diabetes and ageing.* Nat Rev Mol Cell Biol, 2011. **12**(1): p. 21-35.

128. Zhou, H.Y. and S.L. Huang, *Current development of the second generation of mTOR inhibitors as anticancer agents.* Chin J Cancer, 2012. **31**(1): p. 8-18.

129. Baxi, S.M., et al., *Targeting the mTOR pathway in tumor malignancy.* Curr Cancer Drug Targets, 2013. **2**: p. 2.

130. Powers, R.W., et al., *Extension of chronological life span in yeast by decreased TOR pathway signaling.* Genes & Development, 2006. **20**(2): p. 174-184.

131. Chen, C., Y. Liu, and P. Zheng, *mTOR regulation and therapeutic rejuvenation of aging hematopoietic stem cells.* Sci Signal, 2009. **2**(98): p. 2000559.

132. Harrison, D.E., et al., *Rapamycin fed late in life extends lifespan in genetically heterogeneous mice.* Nature, 2009. **460**(7253): p. 392-5.

133. Sharp, Z.D. and R. Strong, *The role of mTOR signaling in controlling mammalian life span: what a fungicide teaches us about longevity.* J Gerontol A Biol Sci Med Sci, 2010. **65**(6): p. 580-9.

134. Bjedov, I. and L. Partridge, *A longer and healthier life with TOR down-regulation: genetics and drugs.* Biochem Soc Trans, 2011. **39**(2): p. 460-5.

135. Ravikumar, B., et al., *Inhibition of mTOR induces autophagy and reduces toxicity of polyglutamine expansions in fly and mouse models of Huntington disease.* Nat Genet, 2004. **36**(6): p. 585-95.

136. Caccamo, A., et al., *Molecular interplay between mammalian target of rapamycin (mTOR), amyloid-beta, and Tau: effects on cognitive impairments.* J Biol Chem, 2010. **285**(17): p. 13107-20.

137. Malagelada, C., Jin, Z. H., Jackson-Lewis, V., Przedborski, S., Greene L. A., , *Rapamycin protects against Neuron Death in In vitro and In vivo Models of Parkinson's disease.* Journal of Neuroscience, 2010. **30**(3): p. 1166-1175.

138. Spilman, P., et al., *Inhibition of mTOR by rapamycin abolishes cognitive deficits and reduces amyloid-beta levels in a mouse model of Alzheimer's disease.* PLoS One, 2010. **5**(4): p. 0009979.

139. Liu, Y., et al., *Rapamycin Decreases Tau Phosphorylation at Ser214 through Regulation of cAMP-Dependent Kinase.* Neurochem Int, 2013. **25**(13): p. 014.

140. Fehr, T., et al., *Antascomicins A, B, C, D and E. Novel FKBP12 binding compounds from a Micromonospora strain.* J Antibiot, 1996. **49**(3): p. 230-3.

141. Brittain, D.E.A., et al., *Total Synthesis of Antascomicin B.* Angewandte Chemie International Edition, 2005. **44**(18): p. 2732-2737.

142. Price, R.D., et al., *FK1706, a novel non-immunosuppressive immunophilin: neurotrophic activity and mechanism of action.* Eur J Pharmacol, 2005. **509**(1): p. 11-9.

143. Minematsu, T., et al., *Time-dependent inhibitory effects of (1R,9S,12S,13R,14S,17R,18E,21S,23S,24R,25S,27R)-1,14-dihydroxy-12-(E)-2-[(1R,3R,4 R)-4-hydroxy-3-methoxycyclohexyl]-1-methylvinyl-23,25-dimethoxy-13,19,21,27-tetra methyl-17-(2-oxopropyl)-11,28-dioxa-4-azatricyclo[22.3.1.0(4.9)]octacos-18-ene-2, 3,10,16-tetrone (FK1706), a novel nonimmunosuppressive immunophilin ligand, on CYP3A4/5 activity in humans in vivo and in vitro.* Drug Metab Dispos, 2010. **38**(2): p. 249-59.

144. Wang, Y., *Design and Synthesis of bicyclic ligands for the FK506-Binding Protein 51 and 52.* PdD thesis, 2012.

145. Gopalakrishnan, R., et al., *Evaluation of synthetic FK506 analogues as ligands for the FK506-binding proteins 51 and 52.* J Med Chem, 2012. **55**(9): p. 4114-22.

146. Germann, U.A., et al., *Cellular and biochemical characterization of VX-710 as a chemosensitizer: reversal of P-glycoprotein-mediated multidrug resistance in vitro.* Anticancer Drugs, 1997. **8**(2): p. 125-40.

147. Dey, S., *Biricodar. Vertex Pharmaceuticals.* Curr Opin Investig Drugs, 2002. **3**(5): p. 818-23.

148. Gopalakrishnan, R., et al., *Exploration of pipecolate sulfonamides as binders of the FK506-binding proteins 51 and 52.* J Med Chem, 2012. **55**(9): p. 4123-31.

149. Gaali, S., *Design and Synthesis of Selective Ligands for the FK506-binding Protein 51.* PhD thesis, 2012.

150. Staal, S.P., *Molecular cloning of the akt oncogene and its human homologues AKT1 and AKT2: amplification of AKT1 in a primary human gastric adenocarcinoma.* Proc Natl Acad Sci U S A, 1987. **84**(14): p. 5034-7.

151. Jones, P.F., et al., *Molecular cloning and identification of a serine/threonine protein kinase of the second-messenger subfamily.* Proc Natl Acad Sci U S A, 1991. **88**(10): p. 4171-5.

152. Bellacosa, A., et al., *A retroviral oncogene, akt, encoding a serine-threonine kinase containing an SH2-like region.* Science, 1991. **254**(5029): p. 274-7.

153. Coffer, P.J. and J.R. Woodgett, *Molecular cloning and characterisation of a novel putative protein-serine kinase related to the cAMP-dependent and protein kinase C families*1992: Eur J Biochem. 1992 May 1;205(3):1217.

154. Manning, G., et al., *The protein kinase complement of the human genome.* Science, 2002. **298**(5600): p. 1912-34.

155. Vanhaesebroeck, B. and D.R. Alessi, *The PI3K-PDK1 connection: more than just a road to PKB.* Biochem J, 2000. **3**: p. 561-76.

156. Altomare, D.A., et al., *Cloning, chromosomal localization and expression analysis of the mouse Akt2 oncogene.* Oncogene, 1995. **11**(6): p. 1055-60.

157. Altomare, D.A., et al., *Akt2 mRNA is highly expressed in embryonic brown fat and the AKT2 kinase is activated by insulin.* Oncogene, 1998. **16**(18): p. 2407-11.

158. Brodbeck, D., P. Cron, and B.A. Hemmings, *A human protein kinase Bgamma with regulatory phosphorylation sites in the activation loop and in the C-terminal hydrophobic domain.* J Biol Chem, 1999. **274**(14): p. 9133-6.

159. Nakatani, K., et al., *Identification of a human Akt3 (protein kinase B gamma) which contains the regulatory serine phosphorylation site.* Biochem Biophys Res Commun, 1999. **257**(3): p. 906-10.

160. Pearce, L.R., D. Komander, and D.R. Alessi, *The nuts and bolts of AGC protein kinases.* Nat Rev Mol Cell Biol, 2010. **11**(1): p. 9-22.

161. Bellacosa, A., et al., *Akt activation by growth factors is a multiple-step process: the role of the PH domain.* Oncogene, 1998. **17**(3): p. 313-25.

162. Alessi, D.R., et al., *Characterization of a 3-phosphoinositide-dependent protein kinase which phosphorylates and activates protein kinase Balpha.* Curr Biol, 1997. **7**(4): p. 261-9.

163. Sarbassov, D.D., et al., *Phosphorylation and regulation of Akt/PKB by the rictor-mTOR complex.* Science, 2005. **307**(5712): p. 1098-101.

164. Alessi, D.R., et al., *Mechanism of activation of protein kinase B by insulin and IGF-1.* Embo J, 1996. **15**(23): p. 6541-51.

165. Laplante, M. and D.M. Sabatini, *mTOR signaling at a glance.* J Cell Sci, 2009. **122**(Pt 20): p. 3589-94.

166. Oh, W.J., et al., *mTORC2 can associate with ribosomes to promote cotranslational phosphorylation and stability of nascent Akt polypeptide.* Embo J. **29**(23): p. 3939-51.

167. Kuo, Y.C., et al., *Regulation of phosphorylation of Thr-308 of Akt, cell proliferation, and survival by the B55alpha regulatory subunit targeting of the protein phosphatase 2A holoenzyme to Akt.* J Biol Chem, 2008. **283**(4): p. 1882-92.

168. Padmanabhan, S., et al., *A PP2A regulatory subunit regulates C. elegans insulin/IGF-1 signaling by modulating AKT-1 phosphorylation.* Cell. 2009 Mar 6;136(5):939-51. Epub 2009 Feb 26., 2009.

169. Sato, S., N. Fujita, and T. Tsuruo, *Modulation of Akt kinase activity by binding to Hsp90.* Proc Natl Acad Sci U S A. 2000 Sep 26;97(20):10832-7., 2000.

170. Gao, T., F. Furnari, and A.C. Newton, *PHLPP: a phosphatase that directly dephosphorylates Akt, promotes apoptosis, and suppresses tumor growth.* Mol Cell, 2005. **18**(1): p. 13-24.

171. Brognard, J., et al., *PHLPP and a second isoform, PHLPP2, differentially attenuate the amplitude of Akt signaling by regulating distinct Akt isoforms.* Mol Cell, 2007. **25**(6): p. 917-31.

172. Liao, Y. and M.C. Hung, *Physiological regulation of Akt activity and stability.* Am J Transl Res. **2**(1): p. 19-42.

173. Vanhaesebroeck, B., L. Stephens, and P. Hawkins, *PI3K signalling: the path to discovery and understanding.* Nat Rev Mol Cell Biol, 2012. **13**(3): p. 195-203.

174. Datta, S.R., et al., *Akt phosphorylation of BAD couples survival signals to the cell-intrinsic death machinery.* Cell, 1997. **91**(2): p. 231-41.

175. Tran, H., et al., *The many forks in FOXO's road.* Sci STKE, 2003. **4**(172).

176. Cardone, M.H., et al., *Regulation of cell death protease caspase-9 by phosphorylation.* Science, 1998. **282**(5392): p. 1318-21.

177. Ozes, O.N., et al., *NF-kappaB activation by tumour necrosis factor requires the Akt serine-threonine kinase.* Nature, 1999. **401**(6748): p. 82-5.

178. Mayo, L.D. and D.B. Donner, *A phosphatidylinositol 3-kinase/Akt pathway promotes translocation of Mdm2 from the cytoplasm to the nucleus.* Proc Natl Acad Sci U S A, 2001. **98**(20): p. 11598-603.

179. Manning, B.D., et al., *Identification of the tuberous sclerosis complex-2 tumor suppressor gene product tuberin as a target of the phosphoinositide 3-kinase/akt pathway.* Mol Cell, 2002. **10**(1): p. 151-62.

180. Sancak, Y., et al., *PRAS40 is an insulin-regulated inhibitor of the mTORC1 protein kinase.* Mol Cell, 2007. **25**(6): p. 903-15.

181. Liang, J., et al., *PKB/Akt phosphorylates p27, impairs nuclear import of p27 and opposes p27-mediated G1 arrest.* Nat Med, 2002. **8**(10): p. 1153-60.

182. Okumura, E., et al., *Akt inhibits Myt1 in the signalling pathway that leads to meiotic G2/M-phase transition.* Nat Cell Biol, 2002. **4**(2): p. 111-6.

183. Vivanco, I. and C.L. Sawyers, *The phosphatidylinositol 3-Kinase AKT pathway in human cancer.* Nat Rev Cancer, 2002. **2**(7): p. 489-501.

184. Carpten, J.D., et al., *A transforming mutation in the pleckstrin homology domain of AKT1 in cancer.* Nature, 2007. **448**(7152): p. 439-44.

185. Xue, G. and B.A. Hemmings, *PKB/Akt-Dependent Regulation of Cell Motility.* J Natl Cancer Inst, 2013. **25**: p. 25.

186. Chen, J., et al., *Akt1 regulates pathological angiogenesis, vascular maturation and permeability in vivo.* Nat Med, 2005. **11**(11): p. 1188-96.

187. Somanath, P.R., et al., *Akt1 in endothelial cell and angiogenesis.* Cell Cycle, 2006. **5**(5): p. 512-8.

188. Schultze, S.M., et al., *Promiscuous affairs of PKB/AKT isoforms in metabolism.* Arch Physiol Biochem, 2011. **117**(2): p. 70-7.

189. Cross, D.A., et al., *Inhibition of glycogen synthase kinase-3 by insulin mediated by protein kinase B.* Nature, 1995. **378**(6559): p. 785-9.

190. van Weeren, P.C., et al., *Essential role for protein kinase B (PKB) in insulin-induced glycogen synthase kinase 3 inactivation. Characterization of dominant-negative mutant of PKB.* J Biol Chem, 1998. **273**(21): p. 13150-6.

191. Quevedo, C., A. Alcazar, and M. Salinas, *Two different signal transduction pathways are implicated in the regulation of initiation factor 2B activity in insulin-like growth factor-1-stimulated neuronal cells.* J Biol Chem, 2000. **275**(25): p. 19192-7.

192. Embi, N., D.B. Rylatt, and P. Cohen, *Glycogen synthase kinase-3 from rabbit skeletal muscle. Separation from cyclic-AMP-dependent protein kinase and phosphorylase kinase.* Eur J Biochem, 1980. **107**(2): p. 519-27.

193. Whiteman, E.L., H. Cho, and M.J. Birnbaum, *Role of Akt/protein kinase B in metabolism.* Trends Endocrinol Metab, 2002. **13**(10): p. 444-51.

194. Wieman, H.L., J.A. Wofford, and J.C. Rathmell, *Cytokine stimulation promotes glucose uptake via phosphatidylinositol-3 kinase/Akt regulation of Glut1 activity and trafficking.* Mol Biol Cell, 2007. **18**(4): p. 1437-46.

195. Gottlob, K., et al., *Inhibition of early apoptotic events by Akt/PKB is dependent on the first committed step of glycolysis and mitochondrial hexokinase.* Genes Dev, 2001. **15**(11): p. 1406-18.

196. Majewski, N., et al., *Hexokinase-mitochondria interaction mediated by Akt is required to inhibit apoptosis in the presence or absence of Bax and Bak.* Mol Cell, 2004. **16**(5): p. 819-30.

197. Deprez, J., et al., *Phosphorylation and activation of heart 6-phosphofructo-2-kinase by protein kinase B and other protein kinases of the insulin signaling cascades.* J Biol Chem, 1997. **272**(28): p. 17269-75.

198. Kitamura, T., et al., *Insulin-induced phosphorylation and activation of cyclic nucleotide phosphodiesterase 3B by the serine-threonine kinase Akt.* Mol Cell Biol, 1999. **19**(9): p. 6286-96.

199. Berggreen, C., et al., *Protein kinase B activity is required for the effects of insulin on lipid metabolism in adipocytes.* American Journal of Physiology - Endocrinology And Metabolism, 2009. **296**(4): p. E635-E646.

200. Warburg, O., *On respiratory impairment in cancer cells.* Science, 1956. **124**(3215): p. 269-70.

201. Vander Heiden, M.G., L.C. Cantley, and C.B. Thompson, *Understanding the Warburg effect: the metabolic requirements of cell proliferation.* Science, 2009. **324**(5930): p. 1029-33.

202. Robey, R.B. and N. Hay, *Is Akt the "Warburg kinase"?-Akt-energy metabolism interactions and oncogenesis.* Semin Cancer Biol, 2009. **19**(1): p. 25-31.

203. Read, D.E. and A.M. Gorman, *Involvement of Akt in neurite outgrowth.* Cell Mol Life Sci, 2009. **66**(18): p. 2975-84.

204. Wang, Q., et al., *Control of synaptic strength, a novel function of Akt.* Neuron, 2003. **38**(6): p. 915-28.

205. Humbert, S., et al., *The IGF-1/Akt pathway is neuroprotective in Huntington's disease and involves Huntingtin phosphorylation by Akt.* Dev Cell, 2002. **2**(6): p. 831-7.

206. Chen, H.K., et al., *Interaction of Akt-phosphorylated ataxin-1 with 14-3-3 mediates neurodegeneration in spinocerebellar ataxia type 1.* Cell, 2003. **113**(4): p. 457-68.

207. Griffin, R.J., et al., *Activation of Akt/PKB, increased phosphorylation of Akt substrates and loss and altered distribution of Akt and PTEN are features of Alzheimer's disease pathology.* J Neurochem, 2005. **93**(1): p. 105-17.

208. Emamian, E.S., et al., *Convergent evidence for impaired AKT1-GSK3beta signaling in schizophrenia.* Nat Genet, 2004. **36**(2): p. 131-7.

209. Zheng, W., et al., *The possible role of the Akt signaling pathway in schizophrenia.* Brain Res, 2012. **27**: p. 145-58.

210. Kaspar, B.K., et al., *Retrograde viral delivery of IGF-1 prolongs survival in a mouse ALS model.* Science, 2003. **301**(5634): p. 839-42.

211. Beaulieu, J.M., *A role for Akt and glycogen synthase kinase-3 as integrators of dopamine and serotonin neurotransmission in mental health.* J Psychiatry Neurosci, 2012. **37**(1): p. 7-16.

212. Cho, H., et al., *Insulin resistance and a diabetes mellitus-like syndrome in mice lacking the protein kinase Akt2 (PKB beta).* Science, 2001. **292**(5522): p. 1728-31.

213. Garofalo, R.S., et al., *Severe diabetes, age-dependent loss of adipose tissue, and mild growth deficiency in mice lacking Akt2/PKB beta.* J Clin Invest, 2003. **112**(2): p. 197-208.

214. Cho, H., et al., *Akt1/PKBalpha is required for normal growth but dispensable for maintenance of glucose homeostasis in mice.* J Biol Chem, 2001. **276**(42): p. 38349-52.

215. Chen, W.S., et al., *Growth retardation and increased apoptosis in mice with homozygous disruption of the Akt1 gene.* Genes Dev, 2001. **15**(17): p. 2203-8.

216. Tschopp, O., et al., *Essential role of protein kinase B gamma (PKB gamma/Akt3) in postnatal brain development but not in glucose homeostasis.* Development, 2005. **132**(13): p. 2943-54.

217. Dummler, B., et al., *Life with a single isoform of Akt: mice lacking Akt2 and Akt3 are viable but display impaired glucose homeostasis and growth deficiencies.* Mol Cell Biol, 2006. **26**(21): p. 8042-51.

218. Laplante, M. and D.M. Sabatini, *mTOR signaling in growth control and disease.* Cell, 2012. **149**(2): p. 274-93.

219. Inoki, K., et al., *TSC2 is phosphorylated and inhibited by Akt and suppresses mTOR signalling.* Nat Cell Biol, 2002. **4**(9): p. 648-57.

220. Potter, C.J., L.G. Pedraza, and T. Xu, *Akt regulates growth by directly phosphorylating Tsc2.* Nat Cell Biol, 2002. **4**(9): p. 658-65.

221. Tee, A.R., et al., *Tuberous sclerosis complex-1 and -2 gene products function together to inhibit mammalian target of rapamycin (mTOR)-mediated downstream signaling.* Proc Natl Acad Sci U S A, 2002. **99**(21): p. 13571-6.

222. Tee, A.R., et al., *Tuberous sclerosis complex gene products, Tuberin and Hamartin, control mTOR signaling by acting as a GTPase-activating protein complex toward Rheb.* Curr Biol, 2003. **13**(15): p. 1259-68.

223. Kwiatkowski, D.J., *Tuberous sclerosis: from tubers to mTOR.* Ann Hum Genet, 2003. **67**(Pt 1): p. 87-96.

224. Long, X., et al., *Rheb binds and regulates the mTOR kinase.* Curr Biol, 2005. **15**(8): p. 702-13.

225. Kovacina, K.S., et al., *Identification of a proline-rich Akt substrate as a 14-3-3 binding partner.* J Biol Chem, 2003. **278**(12): p. 10189-94.

226. Vander Haar, E., et al., *Insulin signalling to mTOR mediated by the Akt/PKB substrate PRAS40.* Nat Cell Biol, 2007. **9**(3): p. 316-23.

227. Wang, L., et al., *PRAS40 regulates mTORC1 kinase activity by functioning as a direct inhibitor of substrate binding.* J Biol Chem, 2007. **282**(27): p. 20036-44.

228. Oshiro, N., et al., *The proline-rich Akt substrate of 40 kDa (PRAS40) is a physiological substrate of mammalian target of rapamycin complex 1.* J Biol Chem, 2007. **282**(28): p. 20329-39.

229. Hardie, D.G., *AMP-activated/SNF1 protein kinases: conserved guardians of cellular energy.* Nat Rev Mol Cell Biol, 2007. **8**(10): p. 774-85.

230. Inoki, K., T. Zhu, and K.L. Guan, *TSC2 mediates cellular energy response to control cell growth and survival.* Cell, 2003. **115**(5): p. 577-90.

231. Shaw, R.J., et al., *The LKB1 tumor suppressor negatively regulates mTOR signaling.* Cancer Cell, 2004. **6**(1): p. 91-9.

232. Gwinn, D.M., et al., *AMPK phosphorylation of raptor mediates a metabolic checkpoint.* Mol Cell, 2008. **30**(2): p. 214-26.

233. Pause, A., et al., *Insulin-dependent stimulation of protein synthesis by phosphorylation of a regulator of 5'-cap function.* Nature, 1994. **371**(6500): p. 762-7.

234. Gingras, A.C., et al., *Regulation of 4E-BP1 phosphorylation: a novel two-step mechanism.* Genes Dev, 1999. **13**(11): p. 1422-37.

235. Ayuso, M.I., et al., *New hierarchical phosphorylation pathway of the translational repressor eIF4E-binding protein 1 (4E-BP1) in ischemia-reperfusion stress.* J Biol Chem, 2010. **285**(45): p. 34355-63.

236. Grove, J.R., et al., *Regulation of an epitope-tagged recombinant Rsk-1 S6 kinase by phorbol ester and erk/MAP kinase.* Biochemistry, 1993. **32**(30): p. 7727-38.

237. Reinhard, C., et al., *Nuclear localization of p85s6k: functional requirement for entry into S phase.* Embo J, 1994. **13**(7): p. 1557-65.

238. Shima, H., et al., *Disruption of the p70(s6k)/p85(s6k) gene reveals a small mouse phenotype and a new functional S6 kinase.* Embo J, 1998. **17**(22): p. 6649-59.

239. Frodin, M., et al., *A phosphoserine/threonine-binding pocket in AGC kinases and PDK1 mediates activation by hydrophobic motif phosphorylation.* EMBO J, 2002. **21**(20): p. 5396-407.

240. Panasyuk, G., et al., *Nuclear export of S6K1 II is regulated by protein kinase CK2 phosphorylation at Ser-17.* J Biol Chem, 2006. **281**(42): p. 31188-201.

241. Song, Q. and L.I. Gilbert, *S6 phosphorylation results from prothoracicotropic hormone stimulation of insect prothoracic glands: a role for S6 kinase.* Dev Genet, 1994. **15**(4): p. 332-8.

242. Raught, B., et al., *Phosphorylation of eucaryotic translation initiation factor 4B Ser422 is modulated by S6 kinases.* Embo J, 2004. **23**(8): p. 1761-9.

243. Jastrzebski, K., et al., *Coordinate regulation of ribosome biogenesis and function by the ribosomal protein S6 kinase, a key mediator of mTOR function.* Growth Factors, 2007. **25**(4): p. 209-26.

244. Um, S.H., et al., *Absence of S6K1 protects against age- and diet-induced obesity while enhancing insulin sensitivity.* Nature, 2004. **431**(7005): p. 200-5.

245. Greene, M.W., et al., *Modulation of insulin-stimulated degradation of human insulin receptor substrate-1 by Serine 312 phosphorylation.* J Biol Chem, 2003. **278**(10): p. 8199-211.

246. Hsu, P.P., et al., *The mTOR-regulated phosphoproteome reveals a mechanism of mTORC1-mediated inhibition of growth factor signaling.* Science, 2011. **332**(6035): p. 1317-22.

247. Copps, K.D. and M.F. White, *Regulation of insulin sensitivity by serine/threonine phosphorylation of insulin receptor substrate proteins IRS1 and IRS2.* Diabetologia, 2012. **55**(10): p. 2565-82.

248. Liu, J., P.D. Stevens, and T. Gao, *mTOR-dependent regulation of PHLPP expression controls the rapamycin sensitivity in cancer cells.* J Biol Chem, 2011. **286**(8): p. 6510-20.

249. Yuan, T.L. and L.C. Cantley, *PI3K pathway alterations in cancer: variations on a theme.* Oncogene, 2008. **27**(41): p. 5497-510.

250. Sheppard, K., et al., *Targeting PI3 kinase/AKT/mTOR signaling in cancer.* Crit Rev Oncog, 2012. **17**(1): p. 69-95.

251. Grzmil, M. and B.A. Hemmings, *Overcoming resistance to rapalogs in gliomas by combinatory therapies.* Biochim Biophys Acta, 2013. **7**(13): p. 00060-5.

252. Guba, M., et al., *Rapamycin inhibits primary and metastatic tumor growth by antiangiogenesis: involvement of vascular endothelial growth factor.* Nat Med, 2002. **8**(2): p. 128-35.

253. Loewith, R., et al., *Two TOR complexes, only one of which is rapamycin sensitive, have distinct roles in cell growth control.* Mol Cell, 2002. **10**(3): p. 457-68.

254. Sarbassov, D.D., et al., *Prolonged rapamycin treatment inhibits mTORC2 assembly and Akt/PKB.* Mol Cell. 2006 Apr 21;22(2):159-68. Epub 2006 Apr 6., 2006.

255. Saxty, G., et al., *Identification of inhibitors of protein kinase B using fragment-based lead discovery.* J Med Chem, 2007. **50**(10): p. 2293-6.

256. Grimshaw, K.M., et al., *AT7867 is a potent and oral inhibitor of AKT and p70 S6 kinase that induces pharmacodynamic changes and inhibits human tumor xenograft growth.* Mol Cancer Ther, 2010. **9**(5): p. 1100-10.

257. Okuzumi, T., et al., *Inhibitor hijacking of Akt activation.* Nat Chem Biol, 2009. **5**(7): p. 484-93.

258. Lin, K., et al., *An ATP-site on-off switch that restricts phosphatase accessibility of Akt.* Sci Signal, 2012. **5**(223): p. ra37.

259. Lindsley, C.W., et al., *Allosteric Akt (PKB) inhibitors: discovery and SAR of isozyme selective inhibitors.* Bioorg Med Chem Lett, 2005. **15**(3): p. 761-4.

260. Calleja, V., et al., *Role of a novel PH-kinase domain interface in PKB/Akt regulation: structural mechanism for allosteric inhibition.* PLoS Biol, 2009. **7**(1): p. e17.

261. Wu, W.I., et al., *Crystal structure of human AKT1 with an allosteric inhibitor reveals a new mode of kinase inhibition.* PLoS One, 2010. **5**(9): p. e12913.

262. Richardson, P.G., et al., *Perifosine , an oral, anti-cancer agent and inhibitor of the Akt pathway: mechanistic actions, pharmacodynamics, pharmacokinetics, and clinical activity.* Expert Opin Drug Metab Toxicol, 2012. **8**(5): p. 623-33.

263. van Blitterswijk, W.J., et al., *Fas/CD95 down-regulation in lymphoma cells through acquired alkyllysophospholipid resistance: partial role of associated sphingomyelin deficiency.* Biochem J, 2009. **425**(1): p. 225-34.

264. Kozany, C., et al., *Fluorescent probes to characterise FK506-binding proteins.* Chembiochem, 2009. **10**(8): p. 1402-10.

265. Gaali, S., et al., *Facile Synthesis of a Fluorescent Cyclosporin A Analogue To Study Cyclophilin 40 and Cyclophilin 18 Ligands.* ACS Medicinal Chemistry Letters, 2010. **1**(9): p. 536-539.

266. Wochnik, G.M., *Die Funktion der Cochaperone FKBP51, FKBP52 und p23 bei der Signaltransduktion der Corticoidrezeptoren*
PhD thesis, 2004.

267. Biondi, R.M., et al., *The PIF-binding pocket in PDK1 is essential for activation of S6K and SGK, but not PKB.* EMBO J, 2001. **20**(16): p. 4380-90.

268. Corpet, F., *Multiple sequence alignment with hierarchical clustering.* Nucleic Acids Res, 1988. **16**(22): p. 10881-90.

269. Simossis, V.A. and J. Heringa, *PRALINE: a multiple sequence alignment toolbox that integrates homology-extended and secondary structure information.* Nucleic Acids Res, 2005. **33**(Web Server issue): p. W289-94.

270. Mullis, K.B. and F.A. Faloona, *Specific synthesis of DNA in vitro via a polymerase-catalyzed chain reaction*, in *Methods in Enzymology*, W. Ray, Editor 1987, Academic Press. p. 335-350.

271. Saiki, R.K., et al., *Primer-directed enzymatic amplification of DNA with a thermostable DNA polymerase.* Science, 1988. **239**(4839): p. 487-91.

272. Laemmli, U.K., *Cleavage of structural proteins during the assembly of the head of bacteriophage T4.* Nature, 1970. **227**(5259): p. 680-5.

273. Oh, W.J., et al., *mTORC2 can associate with ribosomes to promote cotranslational phosphorylation and stability of nascent Akt polypeptide.* Embo J, 2010. **29**(23): p. 3939-51.

274. Thoreen, C.C., et al., *An ATP-competitive mammalian target of rapamycin inhibitor reveals rapamycin-resistant functions of mTORC1.* J Biol Chem, 2009. **284**(12): p. 8023-32.

275. Liao, Y. and M.C. Hung, *Physiological regulation of Akt activity and stability.* Am J Transl Res, 2010. **2**(1): p. 19-42.

276. Benjamin, D., et al., *Rapamycin passes the torch: a new generation of mTOR inhibitors.* Nat Rev Drug Discov, 2011. **10**(11): p. 868-80.

277. Hopkins, A.L., C.R. Groom, and A. Alex, *Ligand efficiency: a useful metric for lead selection*2004: Drug Discov Today. 2004 May 15;9(10):430-1.

278. Paolini, G.V., et al., *Global mapping of pharmacological space.* Nat Biotechnol, 2006. **24**(7): p. 805-15.

279. Verdonk, M.L. and D.C. Rees, *Group efficiency: a guideline for hits-to-leads chemistry.* ChemMedChem, 2008. **3**(8): p. 1179-80.

280. Perola, E., *An analysis of the binding efficiencies of drugs and their leads in successful drug discovery programs.* J Med Chem, 2010. **53**(7): p. 2986-97.

281. Hann, M.M. and G.M. Keseru, *Finding the sweet spot: the role of nature and nurture in medicinal chemistry.* Nat Rev Drug Discov, 2012. **11**(5): p. 355-65.

282. Hinz, M., et al., *Signal Responsiveness of I{kappa}B Kinases Is Determined by Cdc37-assisted Transient Interaction with Hsp90.* J. Biol. Chem., 2007. **282**(44): p. 32311-32319.

283. Bruhn, M.A., et al., *Second AKT: the rise of SGK in cancer signalling.* Growth Factors, 2010. **28**(6): p. 394-408.

284. Liu, J., et al., *PHLPP-mediated dephosphorylation of S6K1 inhibits protein translation and cell growth.* Mol Cell Biol, 2011. **31**(24): p. 4917-27.

285. Huse, M., et al., *Crystal structure of the cytoplasmic domain of the type I TGF beta receptor in complex with FKBP12.* Cell, 1999. **96**(3): p. 425-36.

286. Blackburn, E.A. and M.D. Walkinshaw, *Targeting FKBP isoforms with small-molecule ligands.* Curr Opin Pharmacol, 2011. **11**(4): p. 365-71.

287. Yang, J., et al., *Molecular mechanism for the regulation of protein kinase B/Akt by hydrophobic motif phosphorylation.* Mol Cell, 2002. **9**(6): p. 1227-40.

288. Huang, X., et al., *Crystal structure of an inactive Akt2 kinase domain.* Structure, 2003. **11**(1): p. 21-30.

289. Yip, C.K., et al., *Structure of the human mTOR complex I and its implications for rapamycin inhibition.* Mol Cell, 2010. **38**(5): p. 768-74.

290. Heitmann, J.M.N.R.H.M., *Targets for cell cycle arrest by the immunosuppressant rapamycin in yeast.* Science, 1991. **253**: p. 5.

291. Cruz, M.C., et al., *Rapamycin antifungal action is mediated via conserved complexes with FKBP12 and TOR kinase homologs in Cryptococcus neoformans.* Mol Cell Biol, 1999. **19**(6): p. 4101-12.

292. Cruz, M.C., et al., *Rapamycin and less immunosuppressive analogs are toxic to Candida albicans and Cryptococcus neoformans via FKBP12-dependent inhibition of TOR.* Antimicrob Agents Chemother, 2001. **45**(11): p. 3162-70.

293. Bastidas, R.J., et al., *Rapamycin exerts antifungal activity in vitro and in vivo against Mucor circinelloides via FKBP12-dependent inhibition of Tor.* Eukaryot Cell, 2012. **11**(3): p. 270-81.

294. Pemberton, T.J., *Identification and comparative analysis of sixteen fungal peptidyl-prolyl cis/trans isomerase repertoires.* BMC Genomics, 2006. **7**: p. 244.

295. Lam, E., et al., *A novel FK506 binding protein can mediate the immunosuppressive effects of FK506 and is associated with the cardiac ryanodine receptor.* J Biol Chem, 1995. **270**(44): p. 26511-22.

296. Dubois, S., et al., *Distinct pathways involving the FK506-binding proteins 12 and 12.6 underlie IL-2-versus IL-15-mediated proliferation of T cells.* Proc Natl Acad Sci U S A, 2003. **100**(24): p. 14169-74.

297. Bai, X., et al., *Rheb activates mTOR by antagonizing its endogenous inhibitor, FKBP38.* Science, 2007. **318**(5852): p. 977-80.

298. Wang, X., et al., *Re-evaluating the roles of proposed modulators of mammalian target of rapamycin complex 1 (mTORC1) signaling.* J Biol Chem, 2008. **283**(45): p. 30482-92.

299. Uhlenbrock, K., et al., *Reassessment of the role of FKBP38 in the Rheb/mTORC1 pathway.* FEBS Lett, 2009. **583**(6): p. 965-70.

300. Yu, Y., et al., *Phosphoproteomic analysis identifies Grb10 as an mTORC1 substrate that negatively regulates insulin signaling.* Science, 2011. **332**(6035): p. 1322-6.

301. Tang, S.J., et al., *A rapamycin-sensitive signaling pathway contributes to long-term synaptic plasticity in the hippocampus.* Proc Natl Acad Sci U S A, 2002. **99**(1): p. 467-72.

302. Takai, H., et al., *Tel2 structure and function in the Hsp90-dependent maturation of mTOR and ATR complexes.* Genes Dev, 2010. **24**(18): p. 2019-30.

303. Su, A.I., et al., *A gene atlas of the mouse and human protein-encoding transcriptomes.* Proc Natl Acad Sci U S A, 2004. **101**(16): p. 6062-7.

304. Wilkinson, J.E., et al., *Rapamycin slows aging in mice.* Aging Cell, 2012. **11**(4): p. 675-82.

305. Saunders, R.N., M.S. Metcalfe, and M.L. Nicholson, *Rapamycin in transplantation: a review of the evidence.* Kidney Int, 2001. **59**(1): p. 3-16.

306. Kuntz, I.D., et al., *The maximal affinity of ligands.* Proceedings of the National Academy of Sciences of the United States of America, 1999. **96**(18): p. 9997-10002.

307. Abad-Zapatero, C. and J.T. Metz, *Ligand efficiency indices as guideposts for drug discovery.* Drug Discov Today, 2005. **10**(7): p. 464-9.

308. Hajduk, P.J., *Fragment-Based Drug Design: How Big Is Too Big?* Journal of Medicinal Chemistry, 2006. **49**(24): p. 6972-6976.

309. Hopkins, A.L., C.R. Groom, and A. Alex, *Ligand efficiency: a useful metric for lead selection.* Drug Discov Today, 2004. **9**(10): p. 430-1.

310. Orita, M., K. Ohno, and T. Niimi, *Two [`]Golden Ratio' indices in fragment-based drug discovery.* Drug Discovery Today, 2009. **14**(5-6): p. 321-328.

311. Carlson, H.A., et al., *Differences between High- and Low-Affinity Complexes of Enzymes and Nonenzymes.* Journal of Medicinal Chemistry, 2008. **51**(20): p. 6432-6441.

312. Hann, M.M. and G.M. Keserü, *Finding the sweet spot: the role of nature and nurture in medicinal chemistry.* Nat Rev Drug Discov, 2012. **11**(5): p. 355-365.

313. Wells, J.A. and C.L. McClendon, *Reaching for high-hanging fruit in drug discovery at protein-protein interfaces.* Nature, 2007. **450**(7172): p. 1001-1009.

314. Gerhard, U., M.S. Searle, and D.H. Williams, *The free energy change of restricting a bond rotation in the binding of peptide analogues to vancomycin group antibiotics.* Bioorganic & Medicinal Chemistry Letters, 1993. **3**(5): p. 803-808.

315. Klebe, G., F. Dullweber, and H.-J. Böhm, *Thermodynamic Models of Drug-Receptor Interactions: a General Introduction*, in *Drug-Receptor Thermodynamics: Introduction and Applications*2001, John Wiley & Sons. p. 83-104.

316. Abe, H., et al., *Synthesis of conformationally constrained spirodihydrofuropyridine analogues of epibatidine.* Tetrahedron Letters, 2003. **44**(14): p. 2971-2973.

317. Brieaddy, L.E., et al., *Synthesis of bridged analogs of epibatidine. 3-Chloro-5,7,8,9,9a,10-hexahydro-7,10-methanopyrrolo[1,2-b]-2,6-naphthyridine and 2-chloro-5,5a,6,7,8,10-hexahydro-5,8-methanopyrrolo[2,1-b]-1,7-naphthyridine.* Tetrahedron Letters, 2001. **42**(23): p. 3795-3797.

318. Driggers, E.M., et al., *The exploration of macrocycles for drug discovery [mdash] an underexploited structural class.* Nat Rev Drug Discov, 2008. **7**(7): p. 608-624.

319. Boström, J. and A. Grant, *Exploiting Ligand Conformations in Drug Design*, in *Methods and Principles in Medicinal Chemistry*, R. Mannhold, Editor 2007, Wiley-VCH. p. 183-205.

320. Hao, M.H., O. Haq, and I. Muegge, *Torsion angle preference and energetics of small-molecule ligands bound to proteins.* J Chem Inf Model, 2007. **47**(6): p. 2242-52.

321. Perola, E. and P.S. Charifson, *Conformational analysis of drug-like molecules bound to proteins: an extensive study of ligand reorganization upon binding.* J Med Chem, 2004. **47**(10): p. 2499-510.

322. Sitzmann, M., et al., *PDB Ligand Conformational Energies Calculated Quantum-Mechanically.* Journal of Chemical Information and Modeling, 2012. **52**(3): p. 739-756.

323. Tirado-Rives, J. and W.L. Jorgensen, *Contribution of conformer focusing to the uncertainty in predicting free energies for protein-ligand binding.* J Med Chem, 2006. **49**(20): p. 5880-4.

324. Olsson, T.S.G., et al., *Extent of enthalpy–entropy compensation in protein–ligand interactions.* Protein Science, 2011. **20**(9): p. 1607-1618.

325. Connelly, P.R., et al., *Enthalpy of hydrogen bond formation in a protein-ligand binding reaction.* Proc Natl Acad Sci U S A, 1994. **91**(5): p. 1964-8.

326. Benfield, A.P., et al., *Ligand preorganization may be accompanied by entropic penalties in protein-ligand interactions.* Angew Chem Int Ed Engl, 2006. **45**(41): p. 6830-5.

327. de Mol, N.J., et al., *Protein Flexibility and Ligand Rigidity: A Thermodynamic and Kinetic Study of ITAM-Based Ligand Binding to Syk Tandem SH2.* ChemBioChem, 2005. **6**(12): p. 2261-2270.

328. Edwards, A.A., et al., *Altered enthalpy-entropy compensation in picomolar transition state analogues of human purine nucleoside phosphorylase.* Biochemistry, 2009. **48**(23): p. 5226-38.

329. Edwards, A.A., et al., *Conformational states of human purine nucleoside phosphorylase at rest, at work, and with transition state analogues.* Biochemistry, 2010. **49**(9): p. 2058-67.

330. Martin, S.F., *Preorganization in biological systems: Are conformational constraints worth the energy?* Pure Appl. Chem., 2007. **79**(2): p. 193-200.

331. Kralli, A. and K.R. Yamamoto, *An FK506-sensitive transporter selectively decreases intracellular levels and potency of steroid hormones.* J Biol Chem, 1996. **271**(29): p. 17152-6.

332. Jo, H., et al., *Small molecule-induced cytosolic activation of protein kinase Akt rescues ischemia-elicited neuronal death.* Proc Natl Acad Sci U S A, 2012. **109**(26): p. 10581-6.

333. Periyasamy, S., et al., *FKBP51 and Cyp40 are positive regulators of androgen-dependent prostate cancer cell growth and the targets of FK506 and cyclosporin A.* Oncogene. **29**(11): p. 1691-701.

334. Crotty, T.M., et al., *Diacylglycerol kinase delta modulates Akt phosphorylation through pleckstrin homology domain leucine-rich repeat protein phosphatase 2 (PHLPP2).* J Biol Chem, 2013. **288**(3): p. 1439-47.

335. Staibano, S., et al., *Immunohistochemical analysis of FKBP51 in human cancers.* Curr Opin Pharmacol, 2011. **11**(4): p. 338-47.

336. Ma, L., et al., *Phosphorylation and Functional Inactivation of TSC2 by Erk: Implications for Tuberous Sclerosisand Cancer Pathogenesis.* Cell, 2005. **121**(2): p. 179-193.

337. Aksamitiene, E., A. Kiyatkin, and B.N. Kholodenko, *Cross-talk between mitogenic Ras/MAPK and survival PI3K/Akt pathways: a fine balance.* Biochem Soc Trans, 2012. **40**(1): p. 139-46.

338. Düvel, K., et al., *Activation of a metabolic gene regulatory network downstream of mTOR complex 1.* Mol Cell, 2010. **39**(2): p. 171-83.

339. Laplante, M., et al., *DEPTOR cell-autonomously promotes adipogenesis, and its expression is associated with obesity.* Cell Metab, 2012. **16**(2): p. 202-12.

340. Tasian, S.K., et al., *Aberrant STAT5 and PI3K/mTOR pathway signaling occurs in human CRLF2-rearranged B-precursor acute lymphoblastic leukemia.* Blood, 2012. **120**(4): p. 833-42.

341. Dan, H.C., et al., *Akt-dependent regulation of NF-{kappa}B is controlled by mTOR and Raptor in association with IKK.* Genes Dev, 2008. **22**(11): p. 1490-500.

342. Toschi, A., et al., *Differential dependence of hypoxia-inducible factors 1 alpha and 2 alpha on mTORC1 and mTORC2.* J Biol Chem, 2008. **283**(50): p. 34495-9.

343. Gao, C., et al., *GSK3: a key target for the development of novel treatments for type 2 diabetes mellitus and Alzheimer disease.* Rev Neurosci, 2011. **23**(1): p. 1-11.

344. Galigniana, N.M., et al., *Regulation of the glucocorticoid response to stress-related disorders by the Hsp90-binding immunophilin FKBP51.* J Neurochem, 2012. **122**(1): p. 4-18.

345. Romano, S., M. Mallardo, and M.F. Romano, *FKBP51 and the NF-kappaB regulatory pathway in cancer.* Curr Opin Pharmacol, 2011. **11**(4): p. 288-93.

10. Acknowledgement

My personal gratitude goes to my parents Wolfgang and Heidrun Fabian and my sister Stefanie for their continuous support and faith.

Last but not least I thank wholeheartedly my husband Jürgen Brandl for his short introduction into statistics. Furthermore I'm grateful for his optimism, motivation, cooking tasks and for providing me with the best daily "Kraftquellen".